THE INFLUENCE OF MICROSTRUCTURE ON AUTOHESIVE ASPECTS OF RUBBER TACK

A thesis submitted for the degree of Doctor of Philosophy in

The City University, London

by

ROBERT PAGET CAMPION, B.Sc. (Nottingham)

Dunlop Research Centre

December 1977

TABLE OF CONTENTS

CONTENTS (cont.) Page No.

CONTENTS (cont.)

LIST OF TABLES

LIST OF ILLUSTRATIONS

LIST OF ILLUSTRATIONS (cont.)

PREFACE

The work reported in this thesis was performed at Dunlop Research Centre, Birmingham, in association with the Chemistry Department of The City University. I would like to express my gratitude to Dunlop Limited for use of experimental facilities and for permitting the results of the work to be incorporated into this thesis. I also thank The City University for making the association possible.

The advice and help which I have received from my supervisor, Mr. K.W. Allen of the Chemistry Department of The City University, is much appreciated, and I thank my industrial supervisor, Mr. P.J. Corish, for his 'on-the-spot' advice and encouragement.

I am also indebted to [redacted] for discussion of the ideas presented herein, and to [redacted] for performing necessary engineering and electronic work. Thanks are due to [redacted] for their suggestions, to [redacted] for performing the X-ray diffraction studies described in Table 24, and to [redacted] for experimental assistance.

My final thanks are to [redacted] for typing this thesis and for all her help.

ABSTRACT

Autoadhesion (autohesion) is the spontaneous adherence between two unvulcanised surfaces of an elastomer. Autohesive tack can occur between elastomeric compounds. For hydrocarbon elastomers, the accepted autohesion mechanism is the interdiffusion of chain portions across the interface, so that chain packing and molecular weight are significant parameters.

Deficiencies in existing tack tests led to the development of the Dunlop Rotary Tackmeter, which uses a "sun and planet" motion for the continuous peel measurement of the tack between the peripheral surfaces of two squat cylindrical rubber testpieces. The system is in dynamic equilibrium during testing and gives high contact pressures and realistically short contact times. Consequently, tack and bulk strengths can be largely differentiated.

Optimum autohesive strengths have been measured ranging from high magnitudes for natural rubber through intermediate levels for synthetic elastomers to low values for ethylene propylene terpolymer. The use of specially-isomerised natural rubber has shown that stress crystallization is supplementary only. Theories of diffusion suggest that the extreme diffusion coefficients differ by an order of ten and that this difference arises from the influence of chain structure. Space regions "contained" in cavities associated with permanent chain structural features have been defined collectively as "intrachain" free volume. The coincidence of several cavities plus the interchain space causes easier formation of holes. These holes may attain sufficient size during normal chain thermal fluctuations to facilitate forward motion of an incoming chain portion.

The proposed model has been compared with a simple alternative involving interchain free volume only, and has shown better agreement between distributed free volume and autohesive characteristics. Chain structure affects both chain flexibility and the provision of intrachain cavities and therefore provides an explanation of the different autohesive behaviour of various elastomers. The proposed concept is supported by an experiment involving unilateral interfacial diffusion, and its apparent correlation with the diffusion through elastomers of a range of gases and solvents has been considered in detail.

List of Abbreviations and Main Symbols

Abbreviations - elastomers

IR = polyisoprene
NR = natural rubber (a high-cis IR)
BR = polybutadiene
SBR = styrene-butadiene copolymer
SBR 1500 = SBR containing 23.5 weight % styrene moiety
PIB = polyisobutylene
IIR (butyl rubber) = copolymer of isobutylene (99%) and isoprene
EPDM = ethylene propylene diene (ca 2%) terpolymer
EPM = ethylene propylene copolymer
EBM = ethylene butylene-1 copolymer
NBR (or nitrile rubber) = acrylonitrile-butadiene copolymer

Other abbreviations

HAF = high abrasion furnace (carbon black)
BS = butadiene sulphone
TBC = tertiary butyl catechol
EB_u = elongation at tensile break of unvulcanised testpieces
MWD = molecular weight distribution
phr = parts (by weight) per hundred parts of rubber

Symbols

Some of the symbols listed below are occasionally used with additional suffixes for further descriptive purposes.

a = radius (cm) of Rotary Tackmeter planet testpiece
a'' = representative cross-sectional area of 'intrachain' cavity
A = area; in particular (Chap. 10 et seq.), the mean cross-sectional area of interstitial free space distributed amongst polymer chains
A' = mean cross-sectional area of 'interchain' free space similarly distributed
A_o = cross-sectional area of chain
A_c = cross-sectional area of hole between contact-packed chains at the appropriate level of packing
c = concentration
c_o = initial concentration
c'' = representative volume of intrachain cavity
C'' = Σ c'' for 1 g of elastomer = intrachain free volume
d_c = depth of intrachain cavity
d_o = distance travelled radially inwards by Rotary Tackmeter planet testpiece before making contact with sun
D = Diffusion Constant
D_o = pre-exponential frequency factor associated with diffusion
E_d, E_{vis} = activation energies of diffusion and viscoelasticity
E/V = molar cohesive energy, the square of the solubility parameter

Symbols (cont.)

f = percentage ratio for an elastomer of its N_o value relative to that of cis BR (i.e. $100\ N_o/N_{o\ (cis\ BR)}$)
f_B ; see t_B
f_o = segmental friction force
F = Tack Strength
F_R = relative tack (F divided by bulk strength)
F_w = the tack component of F (during Rotary Tackmeter testing) acting in a calibrated direction
H = energy loss component during Rotary Tackmeter testing
k = Boltzmann constant
K = general constant term
K_D = constant related to D
L = length of monomer (or repeating) unit of a polymer chain
m_1 = gradient of direction of tack force
m_2 = gradient of direction of Rotary Tackmeter calibration force
M = molecular weight (general)
$\overline{M}$ = mean or representative molecular weight
M_v = M measured by solution viscosity
M_1 = value of M above which $F_R < 1$
M_M = molecular weight of a chain monomer unit
n = degree or level of chain packing
$\bar{n}$ = average level of chain packing
n' = orbiting rate (rpm) of planet testpiece around sun on Rotary Tackmeter
N_A = Avogadro's number
N_s = number of polymer segments per chain
N_o = number of intrachain cavities for 1 g of elastomer
p = number of branchings on a diffusing chain end
P = yielding stress of stress/strain curve (i.e. frequently the bulk strength)
P_m = minimum magnitude of P for adequate handling
P_i = internal pressure of an elastomer
q = length of the equivalent random link of a chain
Q = overall correction term during Rotary Tackmeter testing
r = radius of molecule or polymer chain
R = radius (cm) of Rotary Tackmeter sun testpiece
R_A = ratio (Σ areas of matter/Σ areas of space)
s ; $2s$ = average distance which might exist between chains in ideal packing array
s_1, s_2 = Rotary Tackmeter leaf-spring displacements for drag and energy loss (2H) respectively
S_n = number of interstitial spaces per circle (chain cross-section) for an ideal packing array
t = time, in particular, contact time
t_B = breaking time under constant load f_B for Skewis tackmeter
T = temperature
T_G = glass transition temperature

Symbols (cont.)

u = speed of separation of testpieces on Rotary Tackmeter ≡ velocity of tearing one chain from polymer bulk

v_1 = peripheral velocity of planet testpiece at the point of separation during Rotary Tackmeter testing

v_2 = the velocity of the point of separation around the sun

v_H = volume of portion of H atom intruding into intrachain cavity

V ; used for volume and free volume terms ($cc.mole^{-1}$) (all defined in section 4.10.1)

w ; $2w$ = width of contact between testpieces on Rotary Tackmeter

x = general distance term, in particular, the distance diffused by a penetrating molecule

$\bar{x}$ = mean square displacement, or distance travelled by diffusant in time t

X = number of intrachain cavities per monomer (repeating)unit

y = power term for speed of separation u

z = power term for contact time t

$\propto$ = "is proportional to"

∞ = infinity

$\alpha, \beta, \Theta, \phi, \xi$ = various angles described in Figures 23 and 25, and discussed in section 6.3

α_L, α_G = volume thermal expansion coefficients above and below $T_G\,^{o}K$ respectively

γ = surface (free) energy, dG/dA,(G is Gibbs free energy), ≡ surface tension

γ_{lv} applies to a liquid-vapour interface, being the 'normal' surface tension of the liquid

γ_c = critical surface tension

δ_j = molecular jump distance during diffusion

δ_1 = depression of planet testpiece after making contact with the sun during Rotary Tackmeter testing

δ_2 = similar depression of sun testpiece

Δ = mutual depression of the two testpieces = $\delta_1 + \delta_2$

ΔG, ΔS, ΔH = changes in Gibbs free energy, entropy and enthalpy respectively

Φ = molecular jump frequency during diffusion

η = viscosity

θ = contact angle made by drop of liquid on solid surface

ν = frequency of impacts of a molecule ≡ frequency of molecular vibrations

ρ = elastomer density

τ = function of D and t (equation 4.21)

φ generally, (cf V); used for specific volume and free volume terms ($cc.g^{-1}$)

φ (per se) = total free volume of polymer at room temperature ($cc.g^{-1}$)

φ' = interchain free volume = φ - C"

Chapter 1 Introduction

The advanced level of technology required by modern civilisation places considerable demands on high polymers, materials which effectively bridge the gap between the liquid and solid states. The technological challenges are met by the existence of numerous polymerisation products derived from many relatively simple monomeric types. The nature of the polymeric product can depend on the original structure and chemistry of the monomer, the mode of polymerisation and the extent to which polymerisation was allowed to continue. The choice of polymer-type for particular applications is governed by the service conditions.

The science of adhesion, which originally evolved in connection with numerous facets of the solid and liquid states, has naturally been also established in the field of high polymers. The present work is concerned with a particular adhesion phenomenon associated with elastomeric high polymers i.e. polymers which are rubbery in nature at normal temperatures. This phenomenon, autoadhesive tack, is of considerable technical value.

As the term 'tack' has been given to several forms of adhesion involving polymers, the autoadhesive phenomenon is best placed in perspective by some discussion on the position of elastomers within a theoretical framework of viscoelasticity.

1.1 Elastomers and viscoelasticity

A body which is not quite rigidly solid at normal temperatures combines characteristics of both liquid and solid. When subjected to

constant stress the body initially deforms and the deformation slowly increases with time: when constrained to constant deformation, the associated stress decreases with time. At sufficiently high temperatures, the stress-induced deformation tends to be flow-like in manner, and some of the energy input is stored instead of being completely dissipated as heat. In addition, on removing the stress, the stored energy can cause an elastic recovery, the extent of the deformation diminishing. Consequently, if the stress is applied as sinusoidal oscillations, a phase difference δ_s exists between the applied stress and the resulting strain. Materials which behave in this manner are termed viscoelastic. When strains and rates of strain are infinitesimal, Newton's Law and Hooke's Law both contribute to give linear viscoelastic behaviour.

Viscoelasticity has been discussed in detail by several workers including Ferry[1] and Tobolsky[2]. For sinusoidal oscillations of frequency ω rad. s^{-1}, the relationship between stress at time t and strain in the direction of applied shear has been shown to be

$$\text{Stress} = \text{Strain}_{max} (G' \sin \omega t + G'' \cos \omega t),$$

the two shear moduli, G' (storage or in phase) and G'' (loss), also being related by

$$G''/G' = \tan \delta_s.$$

Various other relationships exist for these and other modulus terms. However, the present purpose is simply to use G' as a typical modulus term for defining the elastomeric region of high polymers.

A division of the viscoelastic behaviour of an amorphous polymer into five characteristic regions of widely different modulus/temper-

Modulus/temperature data for amorphous polyvinyl n-butyl ether, after Schmieder and Wolf[4].

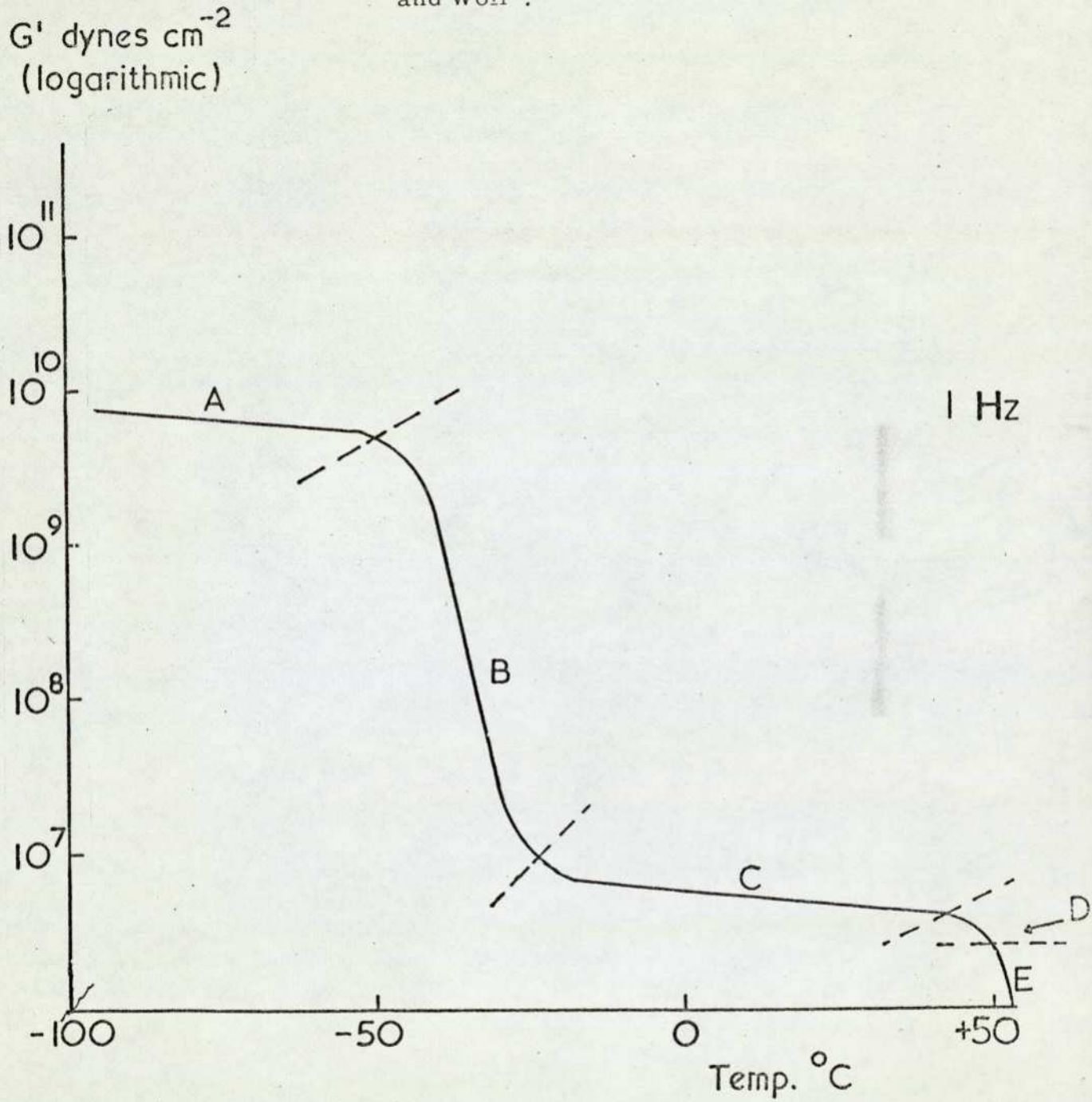

Figure 1 Five characteristic polymeric regions.

ature behaviour was proposed by Tobolsky and McLoughlin[3] utilising a relaxation modulus for characterisation purposes[2]. A similar relationship for temperature T and G' measured at an oscillation frequency of approximately 1 Hz for amorphous polyvinyl n-butyl ether[4,1] is illustrated in Figure 1 and shows the full scope of modulus variations which can occur over a wide temperature range. Similarly-shaped curves are obtained by plotting modulus as a function of time (or reciprocal frequency) at constant temperature. The modulus/temperature plots are the most convenient for the present purpose.

The five regions A to E illustrated by Figure 1 are detailed in Table 1, which also includes general comments on the associated polymer chain motions. The testing of a suitable range of polymers has shown[2] that regions A and B are unaffected by changes in chain length (for sufficiently high chain lengths), whereas varying this parameter markedly affects both the modulus and temperature range of D and E. Only the temperature range of region C depends on chain length. In practice, the transition region B is frequently described simply by a single temperature, T_G, the glass transition temperature. The comments in Table 1 can be compared with those on T_G in section 3.3. However, B strictly applies over a range of temperatures.

Modulus/temperature curves obtained statically or at low frequencies reflect the physical characteristics of the polymer and, when appropriate, its ultimate use. For instance, polymers existing in the glassy (A) region at normal temperatures are thermoplastic and have many applications: on occasions, thermoplastics possess regions of

Table 1

Five Regions of Viscoelastic Behaviour[3]

Region	Physical characteristics of polymer	Modulus G' range (1) (dynes.cm^{-2})	Temperature range (1) (^{o}C)	Associated motions of polymer chains
A (glass)	Hard and brittle	$\sim 10^{10}$	< ca -50	Negligible diffusional molecular motion. Chain segments entwined in fixed positions to give a disordered quasi-lattice structure.
B (transitional)	Leathery	$10^{9.7}$ to $10^{6.9}$	-48 to -24	Some effects from both A and C, these interacting to enhance loss characteristics. The temperature of maximum discontinuity is termed the glass transition temperature T_G(2).
C (rubber)	Rubbery, with some elasticity	$10^{6.9}$ to $10^{6.6}$	-24 to +40	Rapid short-range diffusional segmental motion in company with larger-scale restrictions (chain entanglements). $M_c \sim 10^4$ (3). Chain lattice varying around a mean structure on a time average basis.
D (rubbery flow)	Rubbery, but yielding	$10^{6.6}$ to $10^{6.4}$	+40 to +50	Intermediate effects between C and E.
E (liquid)	Apparent liquid flow	$10^{6.4}$ to < $10^{6.4}$	> +50	Major configurational changes, including the slippage of long-range entanglements, occurring more rapidly than the testing frequency.

Note (1) For the system and conditions considered in Figure 1.
(2) For example, the value of T_G for NR* is -72^{o}C.
(3) Molecular weight between entanglements.

* Natural rubber.

crystallinity, a condition which considerably raises the modulus of region B so that a high modulus region exists throughout the temperature range until the sudden occurrence of flow. In contrast, the use of excessively low molecular weights (short chain lengths) can cause the flow regions D and E to prevail at all temperatures, a phenomenon exploited when using adhesives to obtain intimate interfacial contact prior to a hardening by some other means.

Elastomeric polymers are associated with region C, even at low frequencies, and remain so throughout the several processes which are required to give elastically stable products. The stability of the rubber products occurs after a cross-linking reaction which considerably extends region C. Autoadhesive tack is a phenomenon associated with elastomeric surfaces in the uncured state, i.e. prior to the cross-linking or vulcanising stage.

The relatively high molecular weights necessary to give adequate handling and strength properties to elastomers (i.e. adequately extending region C before crosslinking) cause bulk viscoelastic responses to act more slowly than other responses which can occur at the surface, such as those due to chain diffusion. The autoadhesion phenomenon arises for reasons other than viscoelasticity. The relationship of autoadhesion, chain diffusion and aspects of the microstructural shape of the chain is the main subject of the present work.

1.2 Rubber tack and autohesion - preliminary comments

The formation of cured rubber products involves the vulcanisation of rubber compounds, materials formed by mixing the elastomer with

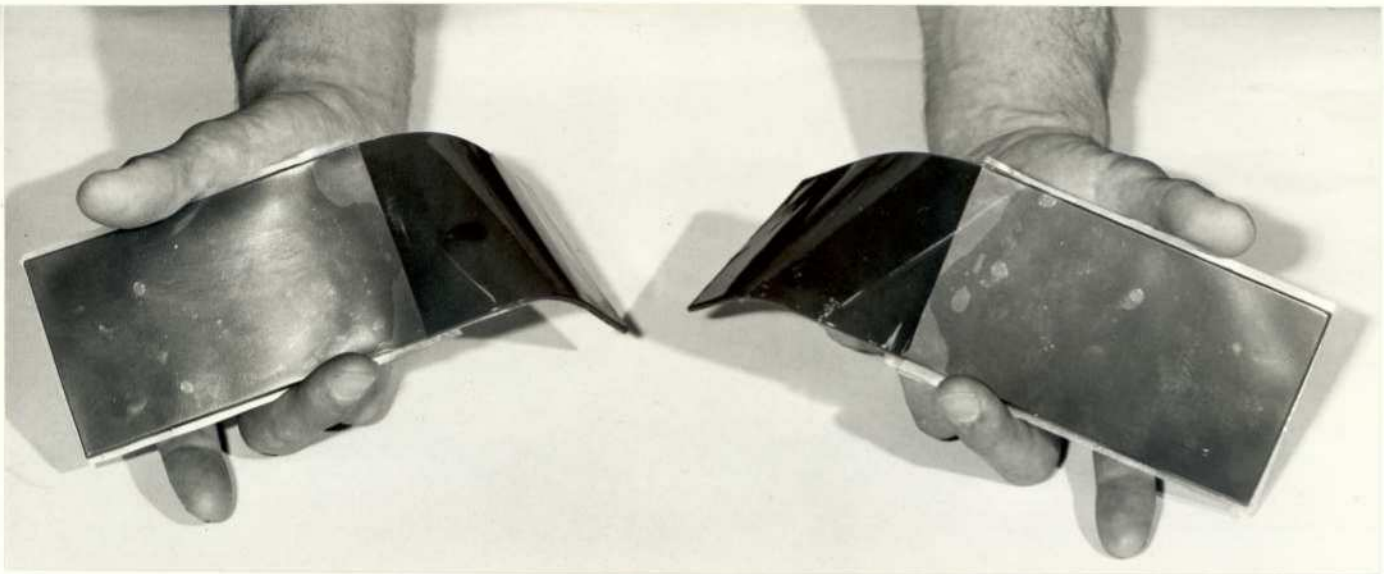

RFU 24490A

Before contact

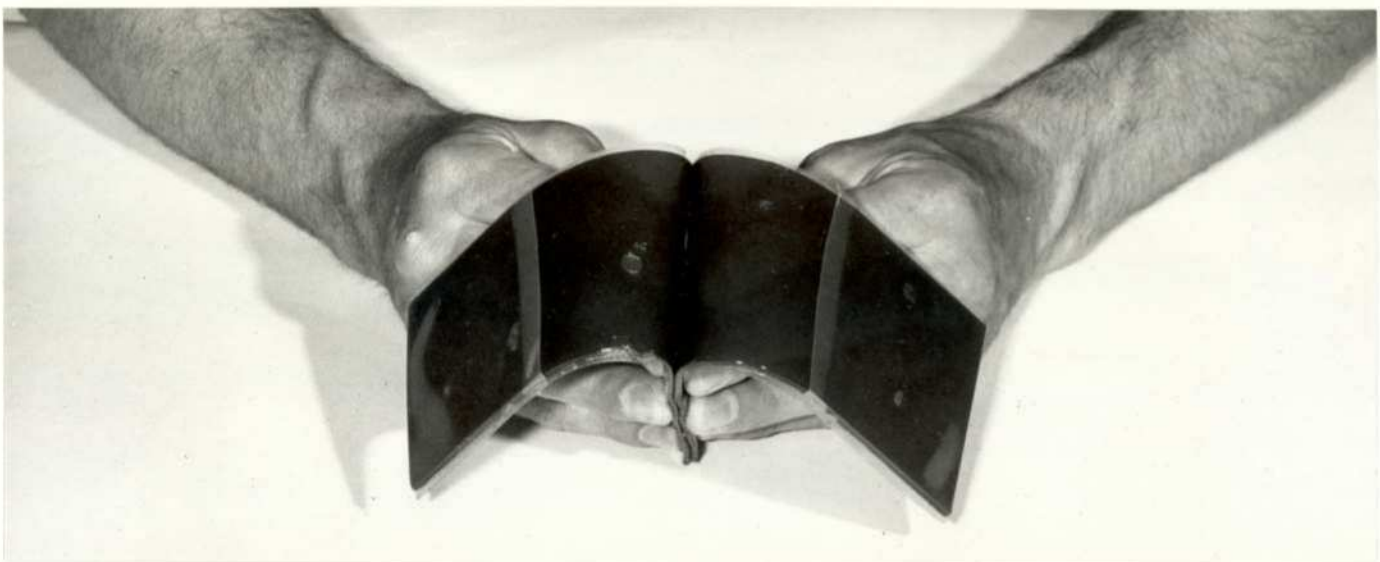

RFU 24490B

Contact under applied pressure

RFU 24490C

Attempted separation

Plate 1. The phenomenon of autohesive tack.

ingredients such as particulate fillers, extender oils(and other processing aids) and reagents which subsequently perform the crosslinking function. If two smooth sheets of certain unvulcanised rubber compounds are pressed together with some force, the sheets adhere. Not only will the sheets remain attached when the compressive force is removed, but also the bond will resist any subsequent attempt of separation (Plate 1). This bonding phenomenon is called "rubber tack". The property (termed "building tack")is widely exploited in technological operations in the tyre and other rubber industries as its existence has enabled the various parts of multi-component rubber articles to be assembled more easily and to remain assembled prior to the curing process.

With conventional compounding methods, those rubber compounds which possess high tack do so because their base polymers display the same phenomenon. The mechanism which applies for the spontaneous bonding between elastomers is effectively extended to apply to tack between their compounds. Hence the basis of tack is autoadhesion or autohesion[5], the spontaneous adherence between two unvulcanised surfaces of the same elastomer. Under optimum conditions, natural rubber (NR) possesses a high degree of autohesion whereas ethylene propylene (EP) elastomers exhibit little autohesion. Consequently, EP compounds are generally not tacky.

Rubber compounds are formulated to specific recipes, and technology has established the formulations most suited to the particular post-cure requirements for each region of the tyre. It has not been possible to formulate one compound suitable for the whole tyre,

although the various compounds may be based on one elastomer. Although the construction of tyres by assembling components comprising suitable compounds of unvulcanised NR or styrene-butadiene copolymer (SBR) is commonplace, similar use of EP compounds is difficult, as the lack of building tack frequently gives rise to component separation. An adequate level of rubber tack is essential to the building of tyres.

At this point, a mention is necessary of the relationship to autohesive tack of the term 'tack' used in two other branches of technology, viz the adhesive and printing ink industries. An adhesive is designed by the choice of appropriate values of mean molecular weight (representing polymer plus resin additive) and molecular weight distribution to deform and flow under the action of a contact force. The property known as adhesive tack[6-9] is assessed by inserting solid probes (of various shapes) into adhesive layers and subsequently measuring (by a variety of methods) the forces required to remove the probes (e.g.[10,11]). This adhesive property has been shown to be completely viscoelastic in nature[6,7,12,13] and best represented as tack energy rather than force[14,15]. In contrast, autohesive bonding does not radically alter the shape of the participating elastomeric sheets, and viscoelastic action is restricted to the attainment of intimate interfacial contact for autohesive tack.

The term 'tack' used in the printing ink industry is even more remote from autohesive tack, having been described[16] as a wholly viscous phenomenon, independent of surfaces or bulk mechanical properties, and relating to the separation force of the Stefan equation.

1.3 Chain structural aspects - the object of the present work

Although the influence of variations in experimental conditions has been frequently discussed[17-21], relatively little attention has been directed to the molecular interpretation of the autohesive phenomenon. Current opinion on the autohesive mechanism favours the interdiffusion of chain molecular segments between surfaces[22,19,23-26], resulting in the intermingling of chain segments and the ultimate disappearance of the interface. Diffusion in high polymers has been considered[27] to occur by the cooperative motion of several neighbouring segments to form a hole of sufficient size to permit the ingress of a chain section: however, correlation between free volume data and autohesive strengths has not been previously demonstrated.

In the present work, a new tackmeter is described which assesses autohesive strengths under conditions conforming with technological and industrial practice, and which provides autohesive magnitudes agreeing with practical experience including the large difference between the NR and EP values. The main object of the work is the proposal of an explanation of this difference in autohesion. Polymer chain structure is suggested as influencing the exact location of the free volume distributed throughout the elastomer by normal micro-Brownian movements of the chains. In this speculative model, the size of holes formed by cooperative motion is increased for certain elastomers by the fine-scale location of free volume (i.e. the free volume in small spaces close between atoms), thereby enhancing autohesive diffusion. A reasonable correlation for several elastomers will be shown between their calculated allocated free space and

their autohesive strength magnitudes. The relationship of the proposed model with chain cooperative motion will be discussed, and an apparent correlation with the diffusion of gases and solvents through polymers will be used as a comment on the validity of the model.

Hence autohesion is considered by the author to be a particular case of a wider field which frequently involves bulk properties and is governed by chain packing criteria. This viewpoint represents a novel approach to the subject.

PART I - THE STATE OF KNOWLEDGE ON AUTOADHESIVE (AUTOHESIVE) TACK BEFORE THE PRESENT WORK

Chapter 2 Theoretical aspects of the interface between elastomeric polymers and between their unvulcanised compounds

Although the most fundamental mechanism of bond formation is the adsorption of one species on to a second surface, some bonding phenomena occur by other mechanisms. For instance, the bonding of certain pressure sensitive adhesive systems is brought about by electrostatic attraction, and chemical links can be formed when adhering rubber to a metal surface (a process which can occur concurrently with vulcanisation). A further exception is the mechanism appropriate to autohesion (discussed later) which is interfacial interdiffusion.

Th- development between polymeric surfaces of bonds approximating in magnitude to the cohesive strength of the polymer is pre-empted by the need for attaining intimate molecular contact. The achievement at a polymeric interface of such contact is subject to thermodynamic and viscoelastic flow criteria. From the nature of viscoelasticity, the application of force causes elastomeric flow (this being a special case of rheological flow). At the interface, the flow of adjacent surface regions causes the contact area to increase continuously (each surface acting as the limiting barrier to the other flowing region) until the surfaces make complete contact after a critical time. When assessing bond strengths, it is desirable that the contact force should be of such a magnitude that the critical time becomes less than the experimental time of contact so that the measured result represents the bonding mechanism alone.

The tangent to the drop at O
describes angle θ with the horizontal.

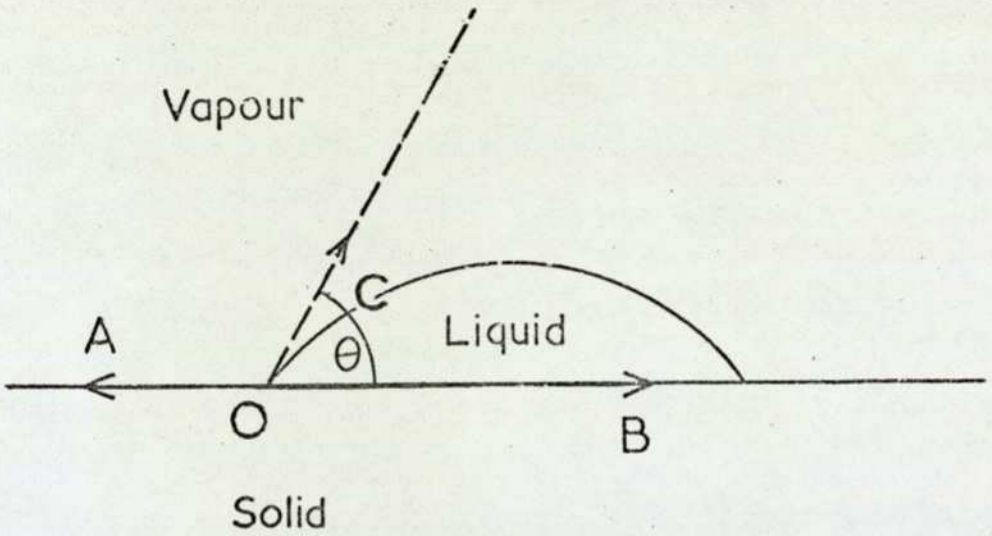

θ, the contact angle, is a function of the balance of the various intermolecular attractions.

Figure 2 Vertical section of a drop of liquid on a solid surface.

To demonstrate the forces involved, the light microscopy work of Bauer[28] showed for a cispolybutadiene elastomer that, even after the application for 60s of a contact pressure of 100kPa, contact was insufficiently intimate for complete interfacial interpenetration to occur. A similar effect has been shown for styrene-butadiene copolymer in a kinetic analysis[29].

An important role of viscoelasticity can be to govern the rate at which processes predicted by thermodynamics take place, high viscosity often prevailing on a practical time-scale. The ultimate validity of the thermodynamic prediction is unquestionable: only the time-scale involved can be manipulated experimentally.

2.1 Contact between dissimilar elastomeric materials

In practice, contact between certain dissimilar elastomers is required in processes used by the tyre and other rubber industries. Finished products are often composite articles comprising a completely-bonded assembly of component rubber compounds based on different elastomers.

Before discussing energetic considerations at the interface between dissimilar elastomers, it is convenient to consider the liquid/solid interface, an area well-documented and rationalised (e.g.[30,31,9]). Consider a drop of liquid placed on a solid surface. At equilibrium (Figure 2) the contact angle θ, or its cosine, describes the extent to which the liquid wets the solid surface: for perfect wetting, θ is zero. The configuration adopted by the drop is governed by the surface free energy, dG/dA or γ, which applies at each interface. For the solid-vapour, solid-liquid and liquid-vapour interfaces at A, B and C in Figure 2, the surface energies are designated γ_{sv}, γ_{sl} and γ_{lv} respectively.

The surface free energy arises from the excess potential possessed by molecules in the surface compared with those in the bulk. γ_{lv} follows from the work done in extending the liquid surface area against a tension (acting at, and parallel to, the surface) resulting from the cohesive forces in the liquid bulk. The surface tension of a liquid (frequently also denoted by γ_{lv}) is numerically identical with the surface free energy. The surface tension of a solid, a more nebulous phenomenon as it relates to a resistance against the stretching of the surface, is greater than the solid surface energy.

The equilibrium system shown in Figure 2 can be represented by the Young equation:-

$$\gamma_{sv} = \gamma_{sl} + \gamma_{lv} \cos \theta.$$

If γ_{lv} etc. refer to surface tensions, the Young equation is a simple statement of the balance of forces (depicted in Figure 2 by vectors) associated with θ. This approach is not universally accepted[9]. An alternative derivation of the equation, considering surface energies, arises from a thermodynamic cycle[32] comprising the hypothetical cleavage of the drop from the solid, the infinitesimal change in its surface area at constant volume and its replacement on to the surface. The measurement of θ therefore provides a means of obtaining surface energy values.

Adhesion considerations require some knowledge of solid surface energetic aspects. The work of adhesion W_A is given by the Dupré equation

$$W_A = \left(\sum \text{Surface free energies of solid \& liquid}\right) - \left(\text{Interfacial energy}\right)$$

so that

$$W_A = (\gamma_s + \gamma_{lv}) - \gamma_{sl}.$$

The surface free energy γ_s of a solid decreases to γ_{sv} when the surface adsorbs a molecular layer of vapour, and $\gamma_s - \gamma_{sv}$ is the spreading pressure Π. Hence from the Young and Dupré equations

$$W_A = \gamma_{lv} (1 + \cos \theta) + \Pi.$$

However the term Π is frequently difficult to determine, limiting the usefulness of this approach.

A more empirical technique has been developed by Zisman[33], who observed an apparently linear relationship between cos θ and γ_{lv} for a series of liquids successively placed in contact with the same solid surface. The extrapolation to unity for cos θ of the line (or, more realistically, the band) drawn through data of γ_{lv} plotted against cos θ yields the surface tension of the liquid (real or hypothetical) which will just spread on the surface area with zero contact angle. Zisman called this limiting value the critical surface tension γ_c, a quasi-thermodynamic term which is nevertheless a most convenient characterisation of the solid surface that has been wetted. Values of γ_c for many polymers are now known (e.g.[34,35]): the values for the main elastomeric polymers are presented in Table 2. A liquid will wet a polymer if γ_{lv} for the liquid is less than γ_c for the polymer.

The elastomers of greatest interest to the tyre industry, and consequently those important to the present study of autohesion, lie in the relatively narrow range of γ_c values of 27 to 33 mNm^{-1}.

Table 2

Critical surface tensions (γ_c) of common elastomers (after Lee[34,35])

Surface	Monomer ratio for copolymers (Weight %)	γ_c (mNm^{-1})
Isobutene-isoprene copolymer (butyl)	99/1	27
Typical ethylene-propylene copolymer	44/56	28
Cis polyisoprene (including NR)	-	31
Polybutadiene* (BR)	-	31
Cis polybutadiene	-	32
Typical styrene-butadiene copolymer (SBR 1500)	23.5/76.5	33
Acrylonitrile-butadiene copolymer	33/67	37
Polychloroprene**	-	38

* Having a cis/trans/vinyl (1,2) ratio of 37/52/11.

** High trans.

A comment on the surface energy conditions which might apply when two dissimilar rubbers attain sufficiently intimate contact for subsequent chain diffusion can arise by analogy with the liquid/solid format. The assumption is made that the two elastomers are of different viscosities, the elastomer of lower viscosity being "liquid" compared with the other. The "liquid" has effectively increased in modulus by several orders from the drop of Figure 2. When the bulk viscosities of the two elastomers are similar, the situation becomes local and determined by temperature and the molecular weight distributions: the liquid phase might exist on either side of the interface, its whereabouts being

governed at any point by the proximate viscosity conditions.

The formation of an interface between two slightly-dissimilar elastomers may occur irrespective of surface energetic aspects because of an overriding bulk flow driven by a sufficiently-large force. However, when the flow finally stops, it can be speculatively argued that the eventual "quality", or degree of intimacy, of contact at such an interface will be somewhat influenced by the surface energies. From the viewpoint of the last paragraph, it is reasonable that a high degree of intimacy should require that γ_c values are similar for the two elastomers. Experience has shown that autohesive-type bonding is easily possible at room temperature between, for instance, uncured compounds separately containing NR and SBR 1500, elastomers having respective γ_c values of 31 and 33 mNm^{-1} (Table 2). In contrast, autohesive-type bonding between NR and acrylonitrile-butadiene copolymer (which differ in γ_c value by $6mNm^{-1}$) is not common.

2.2 Contact between two surfaces of the same elastomeric material

The situation now resolves to an interface at which the quality of contact is governed by viscoelasticity only. Intimate contact at room temperature will be obtained after the required contact time whenever the molecular weights of the elastomeric materials are sufficiently low, or the molecular weight distributions are sufficiently wide, to allow the occurrence of adequate flow on the application of the contact force. When such contact is made, no surface stresses should exist as the two surfaces will possess the same energetic characteristics, so that there should be no problems of wetting. These remarks apply to the occurrence of both autohesion and autohesive tack, the latter involving the bonding of rubber compounds.

Chapter 3 Practical aspects influencing autohesive tack

As explained in section 1.2, the most widely encountered aspect of autohesion is the tack between unvulcanised rubber compounds. Therefore the bond formation mechanism should take into account the various empirical techniques used for improving tack magnitudes (e.g. the mechanical working of the rubber and the incorporation into elastomers of fillers and processing aids such as tackifiers). Naturally, more complex technology is required to improve compounds based on elastomers possessing little autohesion.

The tack/bulk strength relationship which applies when handling rubber compounds in practice is discussed in this chapter. However, the influence on tack magnitudes of rubber viscosity and testing criteria such as temperature, contact time and contact force are best reviewed with the diffusion theory.

3.1 The relationship of tack and autohesion

The superior autohesion of NR over that of synthetic polymers, especially EP co- and terpolymers, is well-known to rubber technologists. Yet, although much evidence has been published about the influence of various testing and material parameters on tack magnitudes, the data do not generally grade elastomeric compounds in a sequence of tack strengths agreeing with technical experience, even when authors have made subjective statements implying the existence of such a sequence. The shortcomings are apparently connected with methods of tack testing (Chapter 5). For this reason, Table 3 shows the conclusions reached after tests made over an extensive period on

several elastomers and their compounds at optimum or near-optimum conditions by the present author using a prototype model of the Dunlop Rotary Tackmeter. The tack rating aligns with practical experience. (The present tackmeter is described in Chapter 6, and many relevant data are provided in Chapter 7.)

Table 3

A grading of tack strengths for several general purpose elastomeric materials

Elastomeric material	Tack rating
NR and cis polyisoprene (IR) elastomers and compounds	Very good
SBR compound	Good
SBR elastomer	Fair
Transpolychloroprene elastomer	
Cis BR elastomers and compounds	
Butyl (IIR) elastomers	
EP elastomers and compounds	Poor

Autohesive tack can well be greater for a compound than for its base elastomer, although the elastomer governs the general tack level. The problem of attaining adequate tack for compounds increases as the base polymer is varied from NR to EP.

3.1.1 The preparation of rubber compounds

Rubber compounds are produced by mechanically incorporating various additive materials into the elastomer; two processes, namely internal-mixing and milling, frequently being used in conjunction.

The high shear forces to which the elastomeric mixture is subjected due to the rotation of twin screw blades in the totally enclosed mixing chamber of e.g. a Banbury internal mixer[36] are particularly suitable for the early stages of mixing. Soluble additives thus dissolved into the elastomeric phase are processing oils (which facilitate subsequent mixing stages), tackifiers, antioxidants and antiozonants, whilst insoluble reinforcing fillers (such as carbon blacks) and other ingredients for use in the later vulcanisation stage are distributed through the rubber by the process. Internal mixing techniques and the effects of fillers in increasing the high shear forces applied have been fully discussed in the literature (e.g.[37-40]), together with the influence of chemical links between rubber chains and carbon black on processibility[41].

However, the final dispersion of fillers through the elastomer is inadequate after internal mixing. Consequently, a second, milling, stage (shown schematically in Figure 3) is performed on the crudely-mixed rubber when curing ingredients are added to the rubber and all additives become completely dispersed or solubilised.

3.1.2 The role of building tack during composite construction

The resulting rubber compound is prepared for technological applications by employing a technique such as calendering (e.g.[43]), a process first used in other industries in the last century. The calender, basically a multi-roll mill (normally three-roll) with rolls mounted vertically, is engineered to produce a continuous thin sheeting of rubber (or rubberised cord fabric) having uniform dimensions: the sheeting is normally wrapped with protective polyethylene layers.

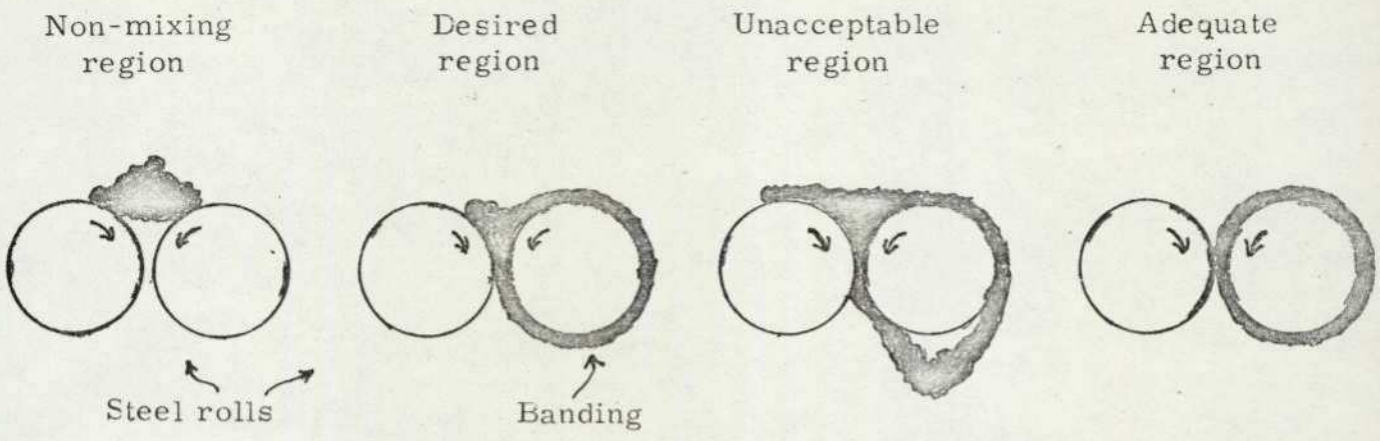

Figure 3 A description of optimum milling behaviour, after Tokita and White[12].

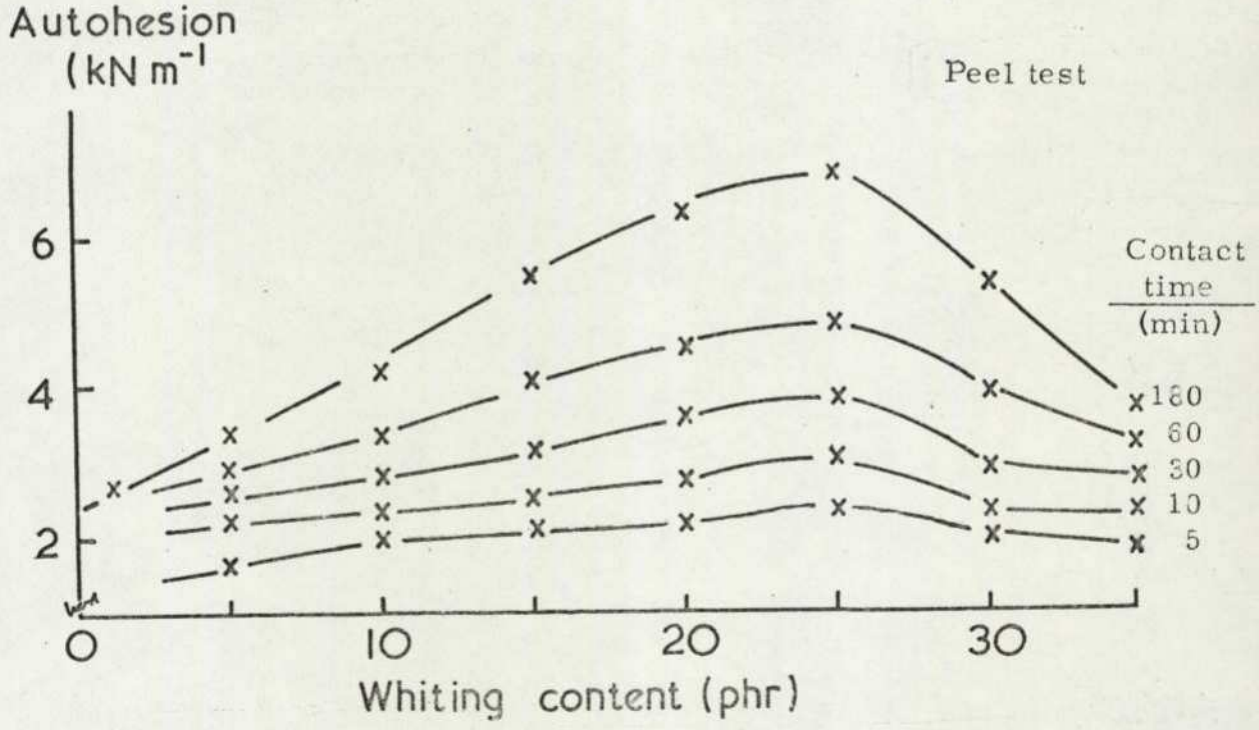

Figure 4 The effect on autohesion of adding whiting to NBR (after Raevskii).

When the polyethylene is removed just before the assembly of the composite article, the rubber surface should be of good appearance and should possess good building tack so that the constructed article will hold together securely until curing is completed.

The formation of crosslinks between the elastomer chains during vulcanisation causes tack ultimately to disappear, as the chains can no longer diffuse. The premature onset of curing ('scorching') during mixing must be avoided (by the correct choice of curing ingredients) in order to retain adequate tack for the assembly stage.

3.1.3 Autohesion and mastication of the elastomer

The effect of mechanically working (masticating) the polymer alone varies for different elastomers. The polymer chains of NR and other cis polyisoprenes are broken by the shear applied during mastication, the molecular weight decreasing considerably, especially as the longest chains are those most prone to rupture[40]. Raw NR elastomer has a molecular weight in the order of 10^6 and is initially too tough to allow the easy incorporation of additives. Hence the mechanically-induced reduction in molecular weight which makes NR pliable has been a vital part of the industry. However, the molecular weights of many synthetic elastomers decrease only slightly with mechanical working: consequently these polymers are produced at lower molecular weights.

The influence of molecular weight and its distribution (MWD) is of paramount importance to autohesion and is to be discussed more fully in sections 4.6 and 8.2. Briefly, an increase in autohesion is

connected with a decrease in molecular weight. Hence mastication considerably enhances the tack of NR but only improves slightly that of SBR and EPDM.

3.1.4 The influence on autohesion of the addition of fillers by mechanical mixing

Because incorporation of fillers into the elastomer stiffens the material, the shear associated with mastication is increased, and the ensuing increases in tack which frequently occur are to be expected from the concomitant decreases in polymer molecular weight[19] and changes in MWD. The molecular weight of the original elastomer is influential in this area. However, this trend does not continue through to higher filler loadings.

The effect on tack of the loading of three fillers, viz carbon black, whiting and kaolin, in two elastomers, NBR and polyisobutylene (PIB), is demonstrated by many data obtained by Voyutskii and colleagues[19,44-46]. Figure 4 shows typical results for the NBR/whiting system[44], a maximum tack strength being associated with an optimum filler loading. Other workers have recorded similar behaviour for black added to NR and cis BR[47,48]. The low tack magnitudes at higher filler-loadings are due to a dilution effect, viz a decrease in rubber contact area at the interface because of displacement by filler[19]: the suggestion is strongly supported by the dry appearance and 'feel' of compounds at very high loadings (e.g. 100phr for carbon black of particle size ca 25nm). The onset of the dilution effect occurs at higher loadings for fillers of small particle size than those for large-particle blacks due to the better packing of the small particles.

Variations in the particle size of the added filler also influence the magnitude of tack[49-51] as shown in Table 4 for black and NR[50] (this table also emphasising the lower value of an unfilled control sample).

Table 4

Effect of Carbon Black particle size on the tack of NR compound (after Baranwal)[50]

	A	B	C	D	E
Loading of NR	100	100	100	100	100
Loading of black (phr)	0	40	40	40	40
Black particle size range (nm)	-	200-500	61-100	49-60	20-30
Tack strength (kPa)	254	400	460	500	627

The tack strength was measured in the tensile mode by placing together two surfaces of the same material and recording the force required for subsequent separation.
Contact pressure 110kPa, contact time 60s, separation speed 0.42 $mm.s^{-1}$.

Control sample A was masticated for same time as the compounded stocks.

As size decreases, the total surface area of filler at constant loading increases to enhance rubber/filler interaction and therefore rubber stiffness. A particular interaction is reinforcement which takes place during mastication if active surface groups on certain fillers (e.g. carbon black) chemically link with the polymeric chains. The degree of reinforcement is given by the bound rubber content (the comparison of the weights of solid matter before and after the swelling of the compounded rubber by solvents, e.g.[41]). Bound rubber formation causes further increases in the severity of shear during mastication so that, for NR, degradation becomes further advanced, especially as

the polymer chains bound to the black are probably those of highest molecular weight[41], the chains most prone to rupture[40]. Even for SBR or cis BR, the removal as bound rubber of the longest chains leaves an elastomeric phase which is now richer in low molecular weight species[41]. The diffusive aspects of tack are assisted in both cases. Not surprisingly, optimum measured tack values have been greater for reinforcing fillers than for the inert type[50], and have depended on the degree of structure possessed by carbon black[48].

Two other suggested factors are that filler-rubber or filler-rubber-filler chemical linkages might occur across the interface to improve tack[50], whilst carbon gel might form in black-filled NBR, to reduce tack[46].

A consideration of section 3.2 is the relationship of tack and the bulk strength of a rubber. Briefly, the presence of filler is a major influence on the strength of the compound. The possibility exists that, for the more tacky rubbers, the long contact times used in tack measurements by most workers could have produced, at least locally, autohesive bonds of magnitude approaching cohesive strength values if the contact forces employed were sufficiently large. Hence the measured values could reflect bulk characteristics rather than an ability to coalesce. However, some data have been published which cannot be considered to represent bulk strength. A 400% increase in tack strength has been found[47] on adding black to NR after a contact time of 6s only. In addition, by studying NBR, Raevskii[44] avoided the potential problem as the rate of diffusion for this polymer is apparently low.

3.1.5 The influence on autohesion of the addition of oils, plasticisers and tackifiers

Most polymers can be handled with greater ease during mixing if some liquid plasticiser is incorporated. Process oils, of molecular weight 10^2 - 10^3, are employed in this way with the non-polar elastomers commonly used in the tyre industry. Although the stiffness of the resulting compound is diminished, the improvement in banding when milling (Figure 3) ensures that high shear conditions prevail. The presence of oil considerably affects tack magnitudes.

Plasticisers are best chosen for use with particular polymers for reasons of compatibility, the molecules of "true" plasticisers[19] completely penetrating individual polymeric chains. The ensuing "loosening" of the high molecular weight structure reasonably enhances flow properties, so that contact between surfaces is improved but bulk strength diminished: in addition, chain interdiffusion at the interface is increased. When the plasticiser and polymer are of limited compatibility, the formation of microcavities and the blooming of plasticiser to the surface (forming a weak boundary) combine to decrease the level of measured tack strengths.

Some early work serves to illustrate these points. The presence of small amounts of true plasticiser in a compound has caused increases in tack levels[17]; however, the addition of excessive quantities of plasticiser eventually caused measured values to reduce. The implication of the reductions is that complete bonding had been reached within the contact times employed so that test measurements now reflected bulk strength values. Later workers[49,18,47] have only observed decreases in tack when

Table 5

An arbitrary classification of typical tackifiers with some examples

Pyrolysis products

Terpenes

Pyrolysate of wood resins and tall oils[52]

Recycling of materials

Scrap tyres (pyrolysate condensed with furfuraldehyde)[53]

Terpene oils and resins

Unmodified[54]

Wood rosin, pine tar

Simply modified

Rosin esters[54], terpene polymers

Isoprenoidal reaction products[55,56]

Phenolic condensate resins

Alkyl (R') phenolic condensation with chemical X'[19,20,57-59]

Koresin (R'=t-butyl, X'=acetylene)

Many other resins with e.g. R'=C_4H_9, C_8H_{17} & C_9H_{19} and X'= acetaldehyde, formaldehyde or novolak: also more complex condensates

Hydrocarbon resins

Unmodified ex coal tar

Indene resin

Unmodified ex petroleum[60]

Derivatives ex coal tar

Coumarone-indene resin[20]

Derivatives ex petroleum aromatics

Esters of diphenyl and polyphenyl compounds (polar)

Liquid elastomers

Liquid polyisobutylene[61]

incorporating various liquids into rubbers, long contact times invariably having been applied. The reasons for the decreases reasonably lie with the bulk strength coupled with a lack of compatibility.

Other compatibility aspects are emphasised in a particular class of liquid processing aid. Tackifiers, unlike the plasticisers discussed to date, are specifically included in rubber compounds to enhance the level of autohesive tack. The materials are frequently resins at normal temperatures although certain viscous oils and low molecular weight polymers also suffice.

Many tackifiers are obtained from abundant natural sources and are consequently relatively cheap, e.g. pine tar and rosin esters (derivatives of abietic acid) which are obtained after the fractionation of wood stumps. The additional pyrolyses of wood rosin and tall oil have given other tackifier types and, in an analogous development, the pyrolysis of scrap tyres followed by a reaction with furfuraldehyde has also produced tackifiers. Other natural sources are coal tar and petroleum. It is therefore not surprising that numerous tackifiers, arbitrarily classified in Table 5, have been listed in the technical and patent literature.

The same tackifiers are often used both in rubber stocks and adhesive formulations. The main difference lies in the loading of tackifier. In rubber compounds, loadings are generally ≤ 10 phr to avoid bulk strength deficiencies. In adhesives, the reinforcing influences of the substrates being bonded overcome such strength deficiencies up to loadings of ca 50 phr, at which stage viscoelastic flow aspects are

considerably enhanced, ie. the tackifier functions also as a plasticiser.

Tackifiers may be used to increase the autohesive tack of all elastomeric compounds. The presence of tackifier in NR compounds obviates the need to continue milling until optimum conditions of molecular weight (M) are attained. SBR elastomer is produced in a suitable M range and the incorporation of tackifier can give adequate tack for practical usage. However, even with the incorporation of tackifiers, EPDM compounds generally only attain a limited tack level, special techniques and compounding skill being necessary to produce adequate building tack.

Some ideas have been proposed on the mechanism of tackification. Elastomeric chain diffusion across the interface may be assisted by similar resin migration causing "inter-lacing" and perhaps involving hydrogen bonding[62]. Tack enhancement has been related to compatibility between elastomeric and resin phases[56], the size and conformation of the alkyl substitution group in phenolic tackifiers being a factor. More significance may be attached to a modified proposal, that of "controlled incompatibility"[64] which is aptly illustrated by the data for a phenolic tackifier in EPDM shown in Table 6. If the tack measurements after increasing ageing periods are successively studied at each tackifier loading, optimum loadings are noted, the optima being reached after shorter ageing periods as loading is increased. The implication is one of tackifier migration to the surface region to enhance tack until an excess of migrated tackifier once again causes local strength deficiencies. The proposal aligns with earlier observations[65] that time is required for Koresin (see Table 5) to bloom to

the surface to increase tack, and that the measured value is diminished by painting the rubber surface with a Koresin solution. The general mechanism can be reasonably applied to other classes of tackifier.

Table 6

The effect of adding different loadings of phenolic tackifier to EPDM compound (after Petersen and Martin[64])

Tackifier loading (phr)	Ageing period (days)	Tack measurements* 0	1	2	3	7
0		3.4	2.7	3.6	3.3	3.0
5		4.0	4.8	4.9	3.0	4.1
12		14.0	19.4	17.4	12.2	0.2
20		22.2	39.1	0.2	0.2	0.2
30		26.2	22.2	0.2	0.2	0.2
40		32.1	19.1	0.2	0.2	0.2

* Contact and separation force of 50N on contact area of 360mm^2: tack is assessed by time (s) to separation in tensile mode.

Using published data, the task of grading the proficiency of tackifiers is made difficult by the different test methods employed, although independent assessments, albeit limited, have been performed[65,54]. A representative collation of results is drawn up in Table 7. The indications are that a substantial tack improvement can occur for non-polar elastomeric compounds with selections from any of the following: modified pine gums and derivatives, terpene polymers, some rosin

Table 7

Collated tack data for the effect of tackifiers on several elastomeric materials *

Tack values as percentages relative to suitable control compounds **

Tackifier loadings (phr)	EPDMg/s	EPDM			Nitrile		SBR			NR
	5.0	2.5	4.0	5.0	2.5	10.0	2.5	4.0	10.0	4.0
Tackifier										
Commercial pine gum		35			183		100			
Modified pine gums and derivatives		74-122			82-217		25-175			
Terpene polymers									533-667	
Rosin and pine tar									166	
Hydrogenated wood rosin esters									100-333	
Rosin esters - aromatic				141						
Ditto - long chain lengths				100-158						
Ditto - short and medium chains		158		175-183						
Hydrocarbon-based ester						115-119				
Aliphatic hydrocarbon resin	219									
Aromatic hydrocarbon resin	142									
C_8 phenolic/aliphatic hydrocarbon	727									
C_8 phenolic/aromatic hydrocarbon	312									
Koresin			92-130					117-150	567	141
C_8 phenolic resin	198		133					188		
C_9 phenolic novolak resin			97-183					114		116
Various phenolic resins		250		58-200						
Reference	63	54	59	54	54	66	54	59	65	59

N.B. Testing modes :- reference 63, peel; all other tests, tensile. Values from the shortest contact times cited. Comparison between tackifiers is best made within each test series as indicated by each reference number.

* One gumstock (g/s), otherwise all blackstocks.

** i.e. Values < 100 indicate a reduction in tack.

esters, and hydrocarbon and phenolic resins. The most effective tackifiers probably exist amongst the terpenic and phenolic groups. Compounds of more polar nitrile elastomers apparently respond to unmodified pine gums and a hydrocarbon-based ester.

In line with the main contribution of the present work, the complex molecular shapes and sizes possessed by the best of these tackifiers may also enhance the distribution of free volume, with a corresponding increase in the number of "sites" into which diffusing chains from the opposite surface can diffuse.

3.1.6 The influence on autohesion of other compounding ingredients and of surface treatments

The advantageous migration of a relatively low molecular weight species through the rubber bulk to the surface region has been noted previously. However, even with tackifiers, excessive migration due to high loadings or incompatibility cause reductions in tack. The reasons may be associated with a weak surface region, but reductions are also caused when some species migrate completely to the surface and inhibit subsequent chain interdiffusion.

Hence diminished tack levels follow the blooming to the surface of compounding ingredients[67] such as sulphur, accelerator, wax, anti-oxidant and stearic acid. The cause of migration is generally associated with solubility and related factors i.e. time of ageing, temperature and loading of ingredient. The eventual surface deposit may be in the form of a fine dust which reduces tack considerably. However, "bloom" and other deleterious surface effects can be inhibited by covering the surface with protective polyethylene sheeting

or fabric liners[20] and by using certain tackifiers[59].

Another general reason for tack reduction is the exposure of elastomeric surfaces to the normal atmospheric environment. For good tack, a dusty atmosphere and excessive water vapour[47] should both be avoided. In addition, the oxidative effect of a mixture of oxygen and ozone on surfaces has been shown[18] to be the formation of a cross-linked non-tacky skin.

These naturally-occurring surface coating phenomena have been utilised by industry in situations where uncured elastomeric articles are required to be non-tacky during storage, but tacky for subsequent assembly. Methods employed include surface treatments by talc or emulsifiers (e.g. 'Teepol', zinc stearate and sodium oleate): Voyutskii[19] has deduced that an oleate layer of thickness 1.75 μm completely destroys tack. Although ozone treatment is probably impractical, a similar oxidative skin can be produced by the action of radiation (especially ultra violet) which has been used to destroy the tack of several elastomeric compounds (not including those of EPDM)[68].

The tack of unmoulded rubber layers can be regained by re-milling so that completely new surfaces are formed. However, for moulded or formed articles, the regeneration of tack after storage is usually performed by heating the rubber surface or wiping it with solvent so that chain segments are mobilised and interdiffusion increased[19,22]: in addition, chemicals deposited on the surface by blooming may dissolve in solvent, to be removed. However, over-heating to ca 60°C can decrease tack again due to skin formation following accelerated

oxidative processes[19]. At higher temperatures (>100°C) the onset of cure would cause the formation of sufficient cross-links at the surface to decrease tack further.

The separate discovery[69-71] by three polymer manufacturers that exposure of EPDM compound surfaces to radiation or ozone can cause enhancements of tack is of special interest. In each case, the presence of certain tackifiers was necessary and one claim[71] required the EPDM to possess a high (80%) ethylene content. In view of the deleterious effect of UV radiation on compounds of elastomers which are normally more tacky than EPDM, these inventions emphasise the complexity which still surrounds autohesive tack.

3.2 The relationship of tack strength and bulk strength of elastomeric materials

On forming a bond between two elastomeric surfaces, subsequent separation forces will be transmitted into the body of the elastomeric material. As the magnitude of autohesive tack is necessarily assessed by destructive test methods (see Chapters 5 and 6), both diffusive and bulk strength characteristics are involved in the assessment. Although both characteristics can be interpreted in terms of molecular weight and of chain flexibility, conformation and packing, the distinction between the characteristics remains valid on the grounds that the diffusive step must precede the development of bulk strength. As the low tack for EP applies across a large molecular weight (M) range, bulk strength is inferentially important to tack measurement only in association with adequate diffusive properties. The ability to form an adequate interpenetrating polymer layer at the interface is the primary

requisite of successful autohesive tack.

Forbes and Mcleod[18] made convenient use of the term relative tack F_R, which is defined as tack strength F divided by bulk strength. For those elastomers which do coalesce readily within the relevant contact time to produce unit relative tack, high bulk strength is desirable, so that F values will also be high: hence a combination of low and high molecular weight fractions is necessary to optimise both diffusive and bulk characteristics. In practice, a value of F_R somewhat less than one can be tolerated provided that the bulk strength is high.

The attainment of unit F_R when the bulk strength is low can lead to erroneous tack test values if excessive contact times are employed, as measurements might reflect bulk rather than diffusive ability. The point has been already made in section 3.1.5 concerning the influence on tack of plasticisers etc: naturally, the addition of oil increases interdiffusion but decreases bulk strength.

The treatment of the compound surface by solvent can promote the diffusional characteristics of the surface whilst retaining an adequate bulk strength. The use of excess solvent, however, weakens the surface region to such an extent that the autohesive bond will be broken even by small separation forces. Liberal use of solvents or rubber solution is more acceptable for applications where separation will not occur (either accidentally or by intent), especially as the contact times during which F_R might increase to unity are great, covering a period from initial contact to the onset of cure.

A particular influence of chain packing which causes enhanced magnitudes of bulk strength at high strains is discussed in the following section.

3.2.1 Stress crystallization and crystallization per se

As the temperature of a polymer in its 'glassy' state is raised from temperatures near to absolute zero, the continuous increase in energy enhances molecular movements to cause an overall increase in volume: the resulting volume/temperature relationship takes the form of a smooth curve which somewhat approaches linearity. A temperature T_G exists at which the polymeric chains are sufficiently separated on a time average basis to allow the onset of fresh molecular movements such as segmental motion. A discontinuity occurs in the volume/temperature curve in the proximity of T_G, the gradient being steeper and more nearly linear in the elastomeric phase above this so-called second-order transition temperature.

For some polymers, additional discontinuities in the same curve can arise at even higher temperatures due to a particular aspect of chain packing. When chain segments of polymers of reasonably regular structure arrange themselves in an ordered state, the polymers exhibit what is termed a first-order transition which is accompanied by an evolution of heat, a contraction of volume and the appearance of characteristic X-ray diffraction patterns. The phenomenon thus resembles the crystallization of simple liquids. Many thermoplastic polymers, such as polyethylene, polypropylene and trans polyisoprene, can possess crystallinity. However, amongst common elastomers, only NR and some other cis IR polymers, very high-cis BR, trans

polychloroprene and perhaps EPDM termonomers possessing high contents of ethylene have the ability to crystallize: for these polymers, effects of both chain packing and chain flexibility can feature prominently at normal temperatures.

Crystallization is never complete in a polymer (e.g. NR never being more than ca 30% crystalline[72]) due to factors such as molecular irregularities and chain entanglements. However, the consequences of any reasonable degree of crystallization in an elastomer are striking, being reflected by considerable changes in properties such as hardness, strength and elasticity: these properties depend on the degree of mobility of the polymer chains. The immobilising effect on chains is noticeable both for vulcanised and unvulcanised elastomeric materials. Several comprehensive reviews[73-77] have been published of the occurrence, growth and effects of crystallization in polymers, and the studies of Bekkedahl and Wood[78] on NR have contributed largely to the subject.

The rate of crystallization in a polymer (and the subsequent melting point of the crystallite regions so formed) is dependent on the temperature of crystallization. NR crystallizes most rapidly at ca -25°C, the rate at zero strain being very slow at normal temperatures. It is therefore to be expected that no initial crystallization exists in NR testpieces moulded under pressure at temperatures of ca 100°C and subsequently either cooled to room temperature (prior to measurements such as tack, green strength, etc.) or subjected to cure at temperatures well above 100°C, cooled and tested (e.g. by tensile measurement, etc.) within one day. Similarly, during storage, NR compounded

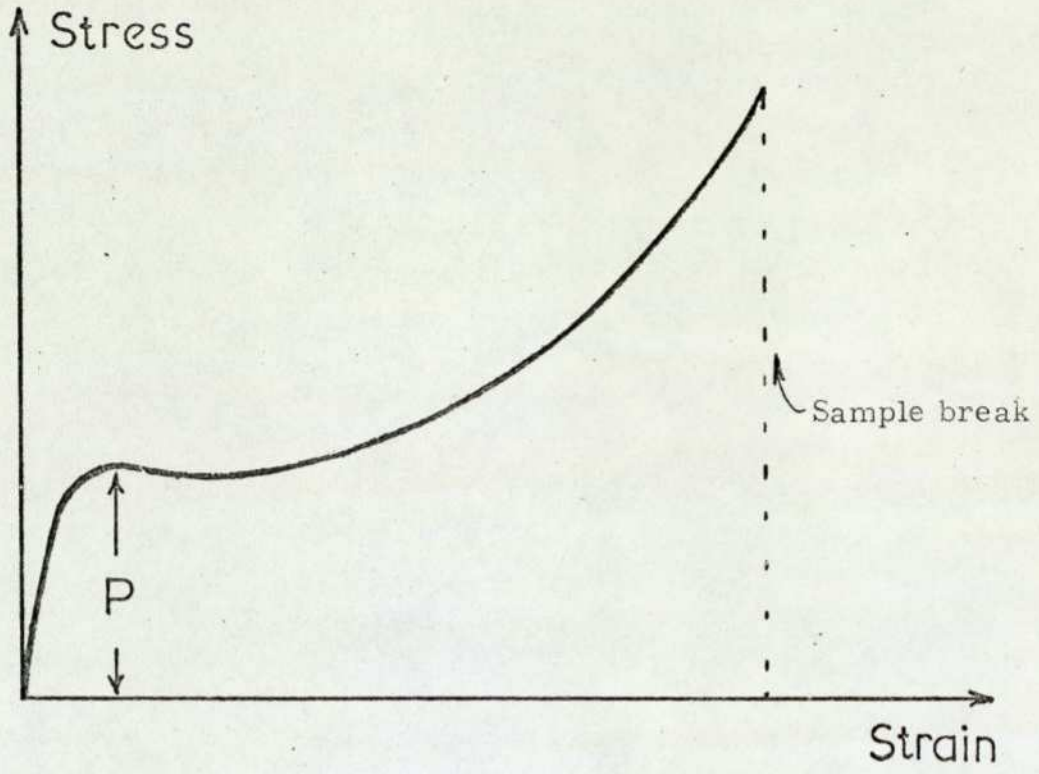

Figure 5 The effect of stress crystallization on the appearance of a stress/strain curve for an elastomer.

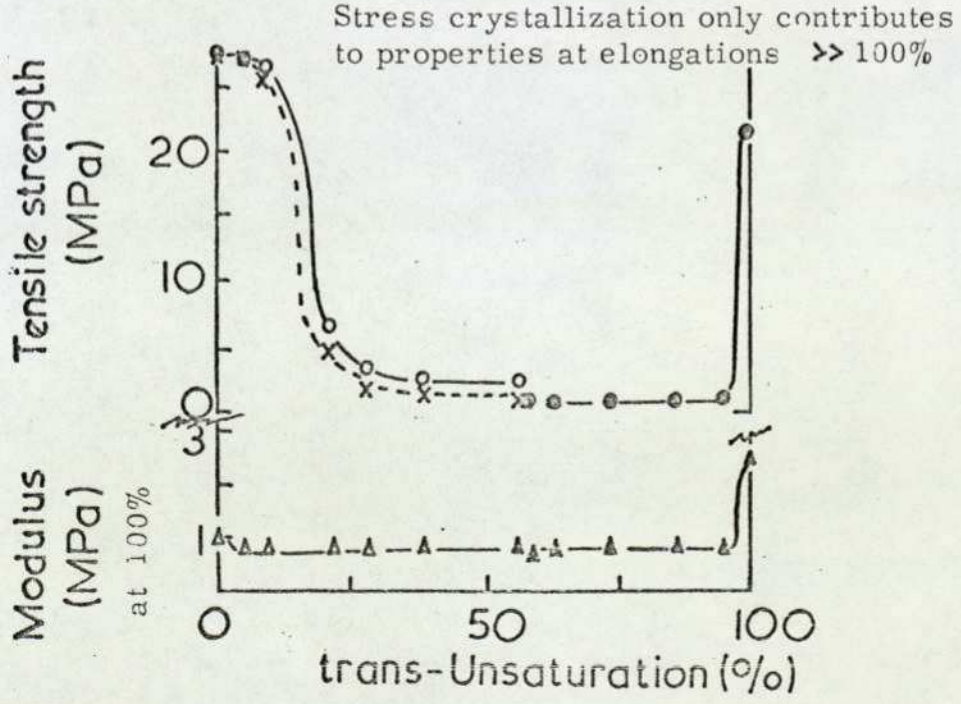

Figure 6 The effects of crystallization and stress crystallization on strength properties of polyisoprene isomers, after Cuneen.

stocks only exhibit signs of crystallinity after extensive periods at low ambient temperatures.

Nevertheless, the proximity of normal temperatures to the crystallization temperatures of NR means that chain energetic and packing considerations are almost suitable for crystallization, and the action of stretching samples to 200-300% elongation provides sufficient orientation to complete the alignment of chains. Physical properties now relate to a polymer possessing crystallinity. Hence the stress/strain curve obtained for NR of moderate to high molecular weight from tensile measurements possesses a tail (Figure 5), the sample often breaking at stresses far greater than the low strain yielding stress P. The relationship between elastomers displaying crystallization, stress crystallization and no crystallization is aptly described by data[79] illustrated in Figure 6 for vulcanised compounds of polyisoprenes at room temperature. Whereas the chain structure of trans IR is sufficiently regular to make the polymer crystalline, that of cis IR (especially NR) will only cause stress crystallization, and intermediate isomeric forms which contain proportions of both cis and trans IR display no crystallization of any form. The point is made in Figure 6 by comparing the curve describing tensile strength behaviour (being associated with elongations of 500-800% at high cis contents) with the curve of modulus measured at only 100% elongation. The necessary isomerisations were performed[79] by chemically treating NR or trans IR with sulphur dioxide for various times at 140°C.

Stress crystallization can be displayed by all of the crystallizable elastomers. For reasons of molecular weight and its distribution,[80]

the stress/strain curves of synthetic IR elastomers can vary from those with no crystallization tail (stress values rapidly decreasing from P to break within an elongation of 300-400%) to those which approach NR in behaviour. Attempts to enhance or supplant the stress crystallization of uncured synthetic cis IR[81] and SBR[82] compounds (to increase strength) have included the incorporation of chemical functionality on to the chains to give some ionic crosslinking with certain compounding ingredients before the main cure.

Because the primary requisite for autohesive tack is reasonably the ability to coalesce (page 45), crystallization reduces tack considerably, as the immobilisation of the orientated well-packed chains inhibits diffusion. Nevertheless, for elastomers such as NR, the separation stage following a successful coalescence can include a contribution by stress crystallization at sufficiently high elongations, to enhance the measured value. Several workers (e.g. Skewis[21]) have considered that stress crystallization is the main cause of the tacky nature of NR. However, the supplementary role of stress crystallization is illustrated by the present author in Chapters 7 and 8.

The occurrence of stress crystallization at relatively low elongations (~50%) in high-ethylene EPDM compounds to give increased bulk strength has been utilised in the approach mentioned in section 3.1.6 of tackifying EPDM compounds by surface irradiation[71].

Coalescent bonds can develop only if

(a) surface energy differences are limited so that intimate interfacial contact can be attained (Chapter 2).

(b) following (a), cohesive energy differences are restricted so that interdiffusion is possible.

The maximum energetic dissimilarity associated with (b) can be roughly quantified. Mixing will occur as a result of a negative free energy change ΔG where

$$\Delta G = \Delta H - T\Delta S.$$

For identical materials there is no enthalpy change and the entropy change will be positive because the removal of an interface by intermixing represents an increase in disorder; hence ΔG will be negative. Whether the equation is satisfied when mixing dissimilar materials is considerably influenced by the ΔH term which in turn depends on $((E_1/V_1)^{\frac{1}{2}} - (E_2/V_2)^{\frac{1}{2}})^2$. $(E/V)^{\frac{1}{2}}$, the square root of the molar cohesive energy, has been termed the solubility parameter[83]. Calculation[84] has suggested that mixing of a liquid with a polymer should take place spontaneously if the difference in solubility parameters is less than ca 1 $(\text{cal. cc.}^{-1})^{\frac{1}{2}}$: however, for the "mixing" of two polymers of $M \sim 10^5$, the value[85] should be less than 0.13 $(\text{cal. cc.}^{-1})^{\frac{1}{2}}$.

Diffusion governs the rate of coalescent bond development for rubbers which satisfy the required degree of energetic similarity.

Various materials as shown.

Picture a shows starting conditions.

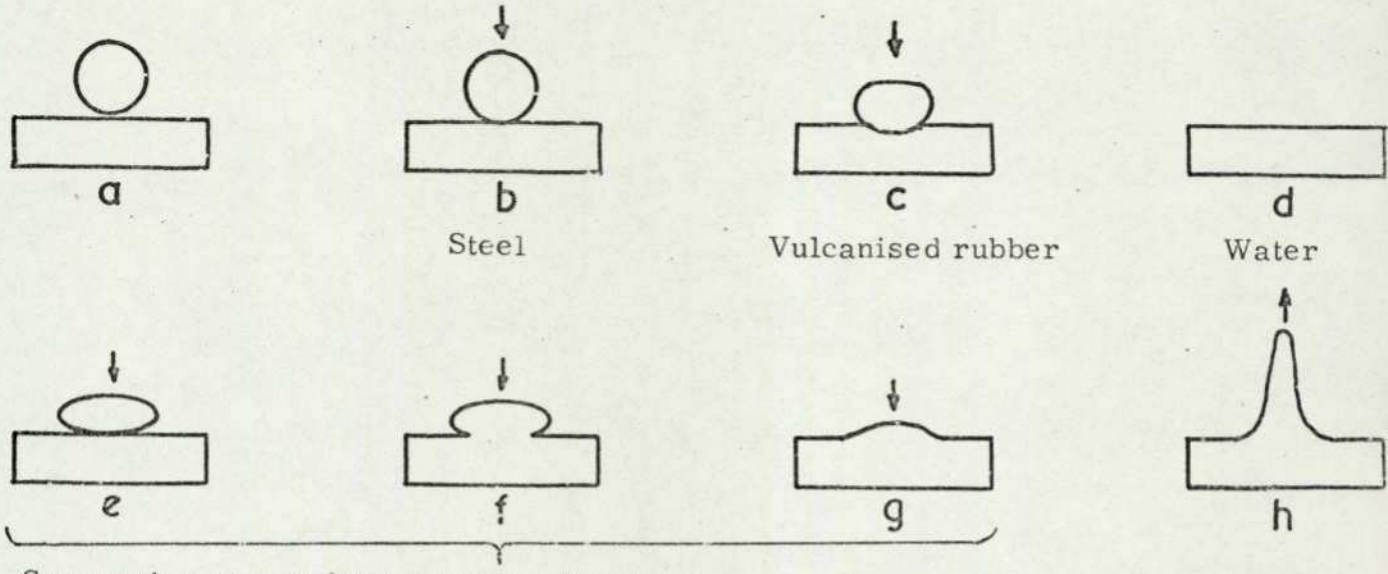

Picture h describes the attempted separation of g.

Figure 7 The addition under convenient pressures of a sphere of a material to a plate of the same material, after Josefowitz and Mark[22].

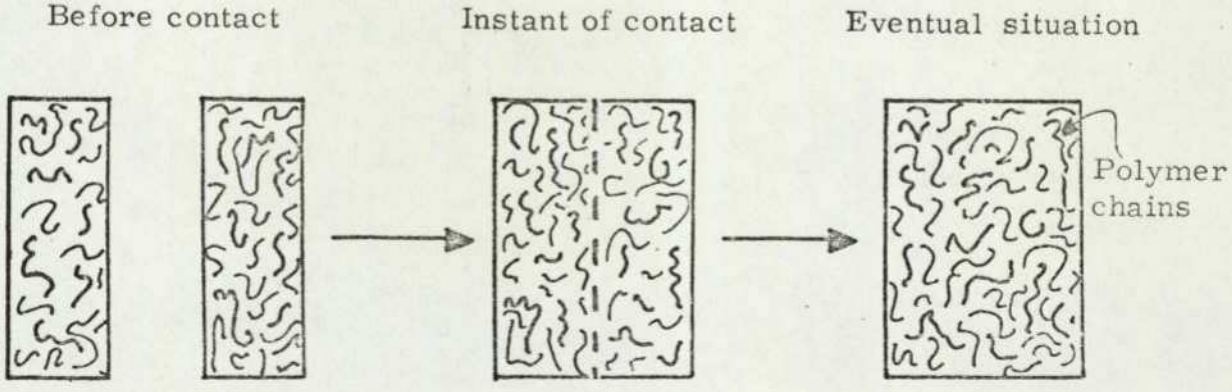

Figure 8 Schematic representation of the coalescence of high polymers, after Voyutskii[19].

4.1 The diffusion theory of autohesion

Discussion so far has frequently referred to autohesive bond development as the diffusion of polymer chain segments across a properly made interface. The hypothesis arose initially from observations on liquids, sticky materials and tacky elastomeric materials by Josefowitz and Mark[22]. A series of situations (reproduced here as Figure 7) arises from the addition at suitably-chosen pressures of a spherical drop of one material to a plate of the same material, the particular conditions applying to each situation (a to h) being included in the figure. Tackiness was visualised as an intermediate between the self-adhesion of liquids and that of solids (in particular, cross-linked polymers). The ability of elastomers to coalesce in the manner of liquids was recognised as the primary requisite for tack, solid-like behaviour only becoming important subsequently for stability (non-flow) or high resistance to separation. However, the explanation of the different autohesive behaviour of various elastomers was solely ascribed to the restriction of chain mobility due to cross-linking. The possibility that each elastomer might possess an unique optimum rate of diffusion was not mentioned.

The greatest proponent of the diffusion theory of autohesion has been Voyutskii[23,19] who developed and rationalised the ideas above. The essential disappearance of the boundary layer is brought about by the diffusive movements largely of individual segments of macromolecules (micro-Brownian motion) due to thermal vibrations (Figure 8). (In a variation to the approach[64], the movements of segments across the interface have been considered to be absorption prior to the inter-

diffusion of whole molecules.) Voyutskii's sentence[19] - "Contact itself is not sufficient for the coalescence of two layers of a high molecular substance" - and other work of his[44] allows the consideration that different rates of diffusion can apply to different elastomers. The bond strength magnitudes after diffusion have been recognised as resulting from intermolecular[22] or mechanical[86] links. The subsequent importance of bulk strength was noted by Voyutskii.

Later sections study the experimental verification of autohesive diffusion, the appraisal of relevant factors and a mathematical quantification for the strength of the developed bond.

4.2. Fundamental diffusion aspects

In all branches of chemistry, the migration of a substance under the action of a difference in chemical potential is called diffusion. According to Gordon[76], the driving force of all diffusion lies in the random thermal motions of molecules, the movements tending to equalise concentrations, or, more accurately, chemical potentials. Although this role of chemical potential is easy to visualise in systems involving the transport of small molecules, the autohesive interdiffusion of segments across an interface between identical elastomeric materials requires the chemical potential of the original surfaces to be in excess of that of the bulk, the equilibrating of potentials occurring by the ultimate disappearance of the interface. Alternatively, from the randomness of molecular motions, the driving force of diffusion might be the compulsion to fill regions of free space, a viewpoint easily covering autohesion as well as other forms of diffusion.

4.2.1 Fick's Laws and subsequent developments

The migration of one species through another is governed by Fick's laws of diffusion[87], whatever the phase of either species. The differences between systems such as gas/liquid, liquid/solid etc. lie in the various boundary conditions, those for autohesion being shown later. If amount dm of substance diffuses across area A in time dt to give a concentration gradient dc/dx, Fick's "First Law" states

$$\frac{1}{A} \cdot \frac{dm}{dt} = -D \frac{dc}{dx} \quad \text{- 4.1.}$$

The term D is the diffusion coefficient (or constant), traditionally possessing the units $cm.^2 s^{-1}$. By considering incremental increases in concentration across the path of the migrating species, one can obtain

$$\left(\frac{\partial c}{\partial t}\right) = D\left(\frac{\partial^2 c}{\partial x^2}\right) \quad \text{- 4.2.}$$

Equation 4.2 (Fick's "Second Law", or the general differential equation of diffusion,) has a more fundamental form:-

$$\left(\frac{\partial c}{\partial t}\right) = D\left[\left(\frac{\partial^2 c}{\partial x^2}\right) + \left(\frac{\partial^2 c}{\partial y^2}\right) + \left(\frac{\partial^2 c}{\partial z^2}\right)\right] \quad \text{- - - - - - - - - - - - 4.3.}$$

These equations assume D to be independent of concentration, which applies when molecules of both species are small. For all molecules, D is influenced by molecular size, and, for a small molecule diffusing in a polymer, D depends on the local concentration so that

$$\left(\frac{\partial c}{\partial t}\right) = \frac{\partial}{\partial x}\left(D\frac{\partial c}{\partial x}\right) + \frac{\partial}{\partial y}\left(D\frac{\partial c}{\partial y}\right) + \frac{\partial}{\partial z}\left(D\frac{\partial c}{\partial z}\right) \quad \text{- - - - - - 4.4.}$$

Mathematical solutions of equation 4.2 to give the concentration at any point must be functions of the product Dt. A particular solution

$$c = (At^{-\frac{1}{2}}) \exp\left(-x^2 (4Dt)^{-1}\right) \quad \text{- 4.5}$$

applies to a plane source. As the total amount m of diffusant is $2A(\pi D)^{\frac{1}{2}}$,

$$c = (m(4\pi Dt)^{-\frac{1}{2}}) \exp\left(-x^2 (4Dt)^{-1}\right) \quad \text{- - - - - - - - - - - - - - - - - - 4.6.}$$

More realistically, an initial distribution would occupy a finite region made up of line elements each acting as a plane source to any point Z at $x>0$. Hence, after time t, the concentration at Z is the summation of expressions analogous to 4.6, the overall summation being of similar form but increased complexity and being portrayed as a concentration/distance curve (e.g. Figure 9). The form coincides with the error function "erf z" of

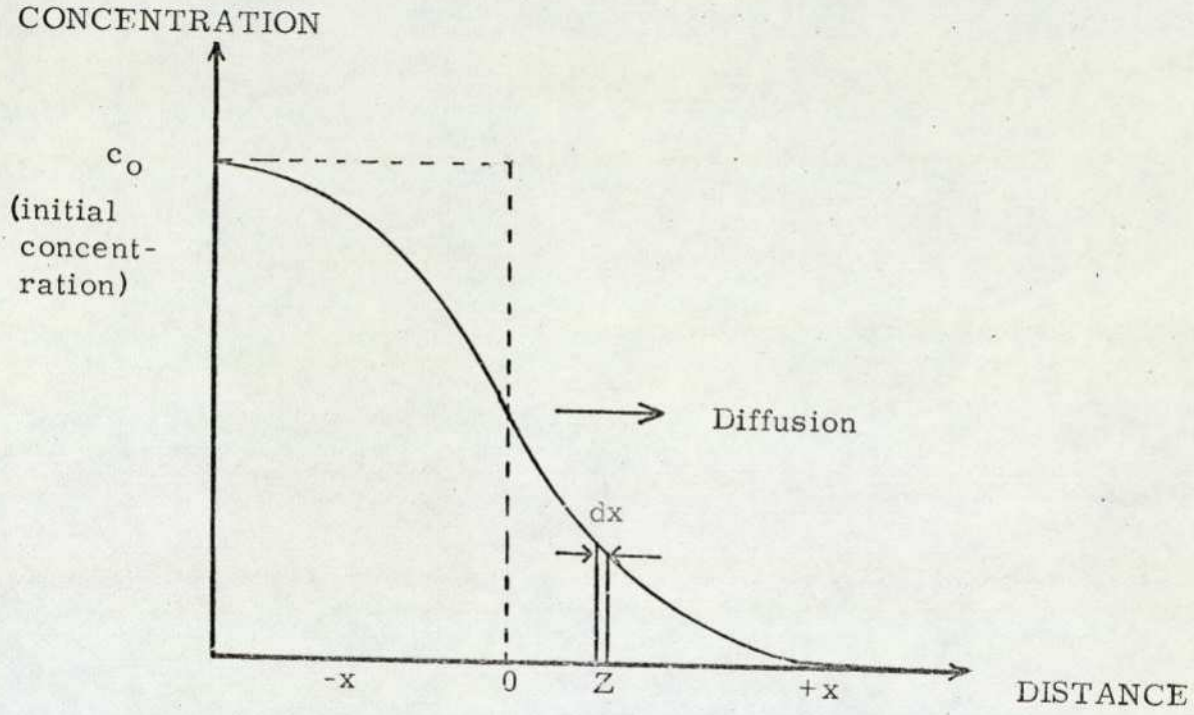

Figure 9 A typical concentration-distance diffusion curve.

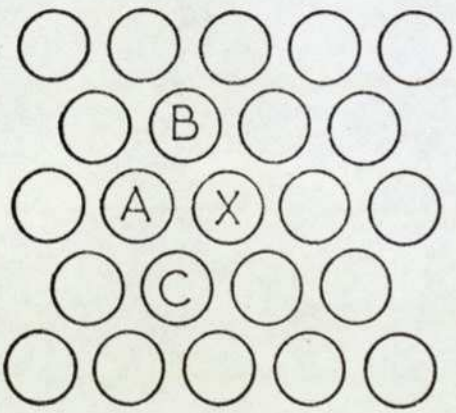

Figure 10 Schematic pattern of liquid molecules, after Bueche[27].

which extensive tables exist. A solution for autohesion is given later.

The average distance travelled from x = 0 by a diffusing particle is given by the mean square displacement $\overline{x}^2$. As the probability p'(x)dx that the particle lies between x and x + dx is proportional to the local concentration[88]

$$\overline{x}^2 = \int_{-\infty}^{\infty} x^2 p'(x)dx = \int_{-\infty}^{\infty} x^2 (4\pi Dt)^{-\frac{1}{2}} (\exp(-x^2(4Dt)^{-1}))dx$$

From this, $\overline{x}^2 = 2Dt$ - 4.7.

Several other diffusion coefficients, proposed[89,90] as being more suitable than D for particular situations, and certain other forms of diffusion which follow non-Fickian guidelines[89], are not relevant to tack.

Miscellaneous relationships involving D:-

a) The Stokes-Einstein equation.

If k is the Boltzmann constant, T is temperature and η is the macroscopic viscosity of solvent streaming past a molecule, radius r, then

$$D = kT/6\pi\eta r \quad - 4.8$$

which is a special case of the more general expression

$$D = kT/\text{molecular friction} \quad - - - - - - - - - - - - - - - 4.9.$$

b) If D_o is a frequency factor correlating with the initial concentration dependence of D, N_A is Avogadro's number and E_d is the activation energy for diffusion, the effect of temperature on diffusion takes the form of an Arrhenius-type relation[91]:-

$$D = D_o \exp(-E_d/N_A kT) \quad - - - - - - - - - - - - - - - - - - 4.10.$$

In general, the stronger the temperature dependence of D, the greater E_d and the slower the expected diffusion. E_d has been discussed in some depth[92] for small molecules diffusing through polymers.

c) The effect of concentration c when $c \rightarrow 0$ has been described as $c \propto D$ and D_o. However, at volume fractions $(\Psi) > 0.2$, a more sophisticated treatment[94] assumes the energies of hole formation to arise from intermolecular attraction and proceeding through probability aspects derives the following expression which covers all concentrations from pure elastomer to pure solvent. If B is a constant and the other subscripts of D refer to the limiting values of Ψ,

$$D_\Psi = D_o(D_1 / D_o)^{1-\exp(1-B\Psi(1-\Psi))} \quad \text{- - - - - - - - - - - 4.11.}$$

4.2.2 Diffusion of a molecule in a liquid

On the basis of Eyring's theory of hole formation[95], E_d derives from kinetic energy, being the energy required to move liquid molecules sufficiently apart plus that necessary to enable the diffusing molecule to transfer or jump into the resulting hole[19]. This energy does not apply to holes which already exist[96], holes being locations of free volume outside the sphere of influence of intermolecular forces. Bueche[27] considered the physical aspects of a random arrangement of interdiffusing liquid molecules (Figure 10) vibrating with frequencies $\sim 10^{12}$ to 10^{13} s^{-1} due to their thermal energy. Local molecules are confined to a rather well-defined cage by the surrounding molecules so that the average position of the mass centre of e.g. molecule A is fairly well fixed. Many vibrations invariably occur before the mass centre traverses a distance of one molecular diameter.

Several translations of the average position of the mass centre of A might occur. Two instances are:-

a) if molecule X is missing from the lattice structure at an instant in time, a hole exists next to A. With sufficient thermal

energy, and with movement in the right direction, A might jump a distance δ_j to the "X-position". The chances are that another molecule will subsequently take the old position of A.

b) Cooperative movements might occur. For example, molecules C, A, B and X could move at the same time in a circular pattern, the displacements being C to A, A to B, etc. Looseness of packing or sufficient local free volume is required for such translations.

An expression for D can be derived from the model. Suppose the jump frequency is Φs^{-1}. In this random situation, the mean square value of the displacement of a molecule occurring in time t is easily shown to be $\Phi t \delta_j^2 / 3$ (the factor 3 performing a reduction from three-dimensions), so that, by analogy with equation 4.7,

$$D = \Phi \delta_j^2 / 6 \quad \text{- 4.12.}$$

4.2.3 Diffusion of a small hydrocarbon through a polymer

Equation 4.12 can also apply to the diffusion of a small molecule through a polymer. Smaller gas molecules, in completely obeying equation 4.10, participate in so-called "Type A" Fickian diffusion[98] in which a plot of ln D versus T^{-1} is linear at temperatures near to ambient. The zone theory of Barrer[97], in which E_d is said to be distributed through many degrees of freedom in the matrix, led to the consideration of cooperative motion of polymer segments in the diffusion mechanism.

An alternative approach[99] employing numerous measurements of the physical size and shape parameters of saturated hydrocarbon diffusants has given the relationship

$$D = KM^{-a'} \text{ - 4.13}$$

where K and a' are constants, a' being ca 1 to 2 for solvent diffusion in rubbers. This expression can be shown to approximate to a particular case of a more rigorous treatment[94] which also assesses unsaturated hydrocarbons.

For penetrants of the size of butane or larger, the plots of ln D vs T^{-1} are no longer linear and display the characteristics of "Type B" Fickian diffusion[98]. The extra chain organisation required to produce critical holes (of sufficient size to accommodate the penetrant molecule) has caused the non-linearity.

4.2.4 Diffusion of a polymer chain segment through a polymer

The application of equation 4.12 to the diffusion through a polymer of other polymeric species relates to chain segments rather than whole chains, and consequently the movement of molecule mass centres is described by

$$D = \Phi \, \delta_j^{\,2} / 6 N_s \text{ - 4.14}$$

where N_s is the number of segments per complete chain. (Chain entanglement effects can be disregarded as they effectively produce combined chains with N_s raised to N_s^*.) Because jumps are essentially of similar magnitudes for all hydrocarbons regardless of diffusant size[99], D is largely influenced by Φ.

If f_o is the segmental friction force, the molecular friction becomes $N_s f_o$ (or $N_s^* f_o$, if appropriate). Hence from equations 4.9 and 4.14

$$f_o = 6kT / \Phi \, \delta_j^{\,2} \text{ - 4.15.}$$

This equation connects two largely complementary ways of observing

segmental motion in diffusion.

The extent of chain cooperation now necessary means that Type B diffusion[98] is well established. Significant changes occur in the terms D_o and E_d in equation 4.10 for relatively small changes in diffusant size. The graph of ln D vs T^{-1} resembles the analogous curve for polymer viscosity. Participating segments are 20-40 C atoms long.[100,96]

Yet another view of segmental diffusion at the interface is provided[25] by applying the particular conditions to Fick's Second Law. As time progresses, the length of polymeric chain which has diffused into the substrate surface from the adherend increases so that diffusion becomes slower than the rate predicted by the law in simple form. Vasenin[25] used a solution[90] which applies when D = f(t) only:-

$$\partial c / \partial t = D(t)\, \partial^2 c / \partial x^2 \quad \text{- - - - - - - - - - - - - - - - -} \quad 4.16.$$

If $\partial\tau$ is defined as $D(t)\,dt$, equation 4.17 reduces to

$$\partial c / \partial \tau = \partial^2 c / \partial x^2 \quad \text{- - - - - - - - - - - - - - - - - - - -} \quad 4.17.$$

The solution of the reduced differential equation took a usual form

$$c = c_o \left(1 - x (\pi\tau)^{-\frac{1}{2}}\right) \quad \text{- - - - - - - - - - - - - - - - - -} \quad 4.18.$$

4.3 The strength of the developed autohesive bond

Autohesive self-diffusion coefficients D of 10^{-11} to 10^{-14} $cm^2.s^{-1}$ have been observed radiometrically (section 4.4) for high molecular weight (10^4 to 10^6) polymers. From equation 4.7, a representative mean path $\bar{x}$ for simple diffusion for the first second is 45 Å. As tracer techniques sensibly consider whole-chain diffusion, the suggestion[101] that $\bar{x}$ for small chain portions (involving higher diffusion rates) depends on a much lower power of t might be speculatively

applied to the initial stages of autohesive contact. (An analogy might be the relationship between dissolution and diffusion during gas permeation through elastomers.) Whatever the case, adequate interdiffusion is clearly possible in the first second of interfacial contact to allow considerable intermingling of chain portions.

The strength of the resulting bond is sensibly proportional to the number of chain segments (conveniently chain ends) and to the depth of their penetration[25]. The number of chain ends per area of $100 mm^2$ has been derived (from Avogadro's number N_A, the polymer density ρ and molecular weight) to be

$$((2+p)N_A \rho M^{-1})^{\frac{2}{3}}$$

for p branchings[25]. The transfer of momentum from ν impacts per second and n_m methylene or methyl molecular groups of mass m' when one molecular chain is torn from the polymeric bulk at velocity u gives $0.5\, m'u\nu n_m$ for the force of resistance. Therefore the analogous force F per $100\, mm^2$ of area will be

$$F = 0.5\, m'u\nu n_m ((2+p)\rho N_A M^{-1})^{\frac{2}{3}} \text{ ---------- -4.19.}$$

The average depth of penetration $\bar{x}$ can be taken as x when $c = c_o/2$. From equation 4.18

$$\bar{x} = 0.5\,(\pi\tau)^{\frac{1}{2}} \text{ ---------- -4.20.}$$

Vasenin derived n_m from molecular dimensions and $\bar{x}$. To eliminate τ from equation 4.20, if b is a constant less than unity, and another constant K_D is equal to D in magnitude (but not dimensionally) when t = 1s, then the expression

$$\tau = K_D t^{1-b} \text{ ---------- 4.21.}$$

suits the original requirement for $\partial\tau$. By substituting for n_m in

equation 4.19 and inserting numerical values for all molecular parameters and standard constants, the expression

$$F = 11.1 \sqrt{\left(\frac{(2+p)\rho}{M}\right)^{\frac{2}{3}}} \; K_D^{\frac{1}{2}} \; ut^{0.5(1-b)} \qquad \text{- - - - - - - - 4.22}$$

was obtained for the strength of the autohesive bond. By assuming[25] b to be 0.5, the power term for t has been taken as 0.25.

A slightly different approach[28] considers that, whilst interdiffusion develops the autohesive bond, the final strength depends on secondary bonds which can slip on the application of stress. The use of Eyring's absolute reaction rate theory gives the jump frequency of the interaction "force centres". As a result, if t_B and f_B are breaking time and force terms specific to the Skewis tackmeter (Chapter 5), then $f_B \propto t_B^{-1}$. Normalised autohesive test data for cis BR agreed with the solution.

4.4 The autohesive diffusion theory - direct experimental evidence

4.4.1 Radiometric evidence

The existence of interdiffusion processes at polymeric interfaces has been proved by the incorporation of a small amount of radioactive isotope into a potential diffusant (thus 'labelling' or 'tagging' the material). As labelled elastomer diffuses into a relatively thick inactive substrate, the intensity of radioactivity emanating from an originally-active surface decreases because of absorption of the radiation by the substrate. Carbon 14, with a half-life of ca 5,700 years and which emits soft beta-rays of energy ca 0.15 Mev, is a radioactive isotope suited to this purpose, as 1 mm rubber will absorb half of the radiation and 7-8 mm will totally absorb the rays. Tritium (H-3) is another

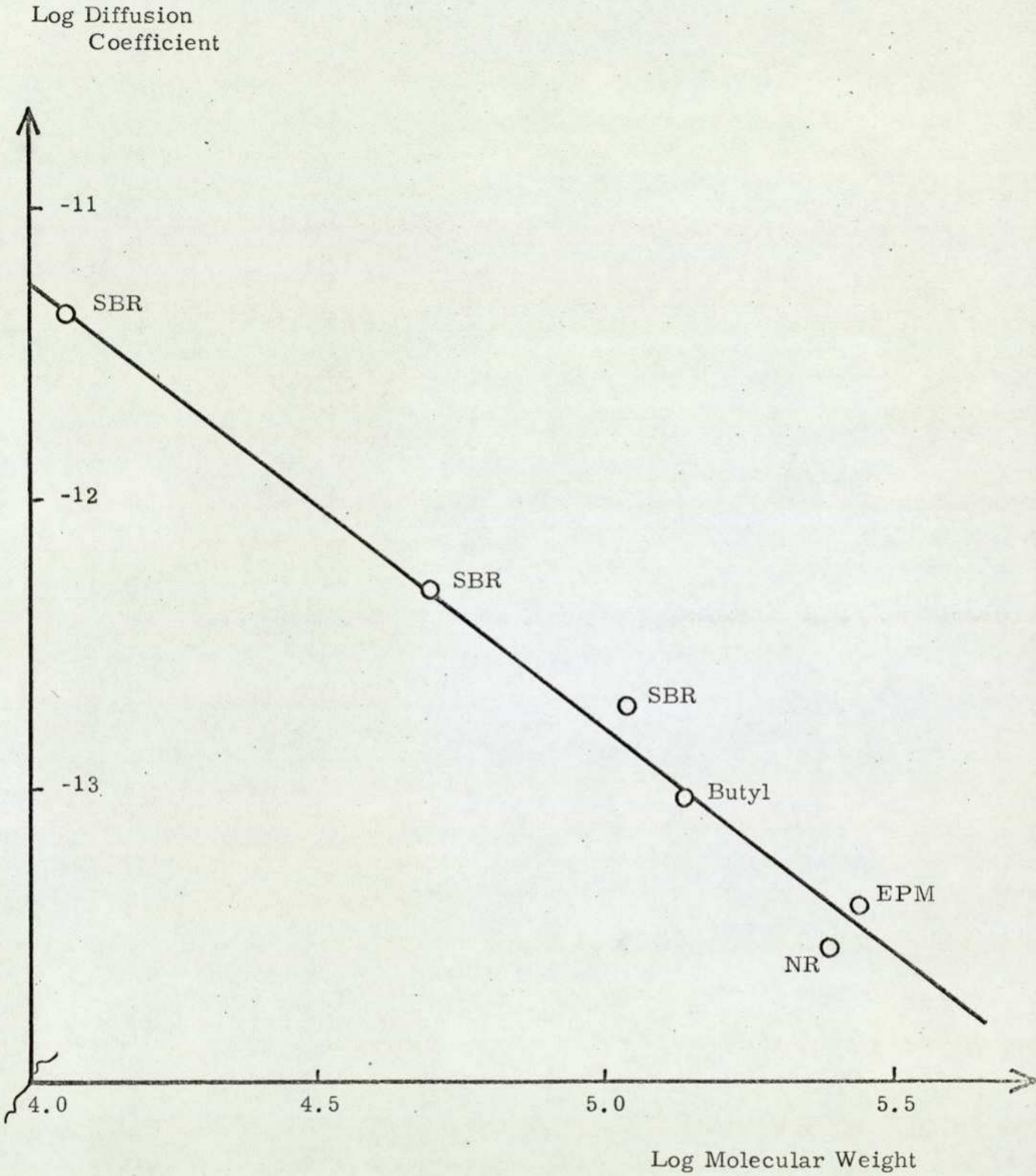

Figure 11 Diffusion coefficients of several elastomers at different molecular weights, after Skewis[21].

suitable isotope.

The elegant experimentation required for radiometric studies has limited the numbers of publications relevant to elastomeric self-diffusion[102,103,21]: other workers have studied radiometrically the diffusion of oils[104] and solvents[99] through polymers, whilst Corish and Palmer[105] have similarly investigated the diffusion of sulphur in rubbers. Studies on self-diffusion[102,103,21] have followed the method of Rayner et al[106] in which a tagged film (5 to 25 μm thick) was cast on to a surface of unlabelled elastomer and a counter measuring the intensity of radiation was positioned normally above the cast film. Equations have been derived to show, for example[21], that Dt was proportional to the radioactive count at time t divided by the initial count: the plotting of count ratio against time gave D directly.

A main conclusion is that, whereas D for sulphur, solvents and oils in polymers is 10^{-6} to 10^{-8} cm.^{2} s^{-1}, the D value for elastomeric self-diffusion is much lower at 10^{-11} to 10^{-14} cm.^{2} s^{-1}. This order of magnitude applied to poly-n-butylacrylate[102], to polyisoprene (M = 1100) diffusing through NR[103] and to several common elastomers[21] where M = 10^4 to 10^6.

Values of D measured for several elastomers[21] of different molecular weight are shown in Figure 11. The overall linear relationship between D and M was taken as indicating, besides the normal effect of chain length, that no major difference of self-diffusion coefficients existed between elastomers of similar values of M. However, inspection of Figure 11 reveals that only SBR elastomer was measured at

radically-different molecular weights. The measured data do not preclude the possibility, discussed later, that at lower values of M diffusion is faster in NR than in synthetic elastomers, especially EPDM. In addition, the experimental difficulties recorded[21] must be at their worst for the lowest orders of D (10^{-13} to 10^{-14} cm.^{2} s^{-1}).

Radiometric evidence has been most important in confirming autohesion as a diffusion phenomenon, in indicating the probable participation of segments and in placing a sensible order of magnitude on D for self-diffusion.

4.4.2 Microscopic evidence

The blurring of elastomeric interfaces when observed by light and ultra-violet microscopy has been considered to reflect interdiffusion aspects[107], although some existence of mass-flow was acknowledged. Electron-microscopy has been used[24] at the polymer/polymer interface to indicate that the change in optical density which occurs when moving the probe from one polymer to the other was gradual, an observation explicable by polymeric interdiffusion.

4.5 Factors which influence autohesive strength

Study of equation 4.22 indicates that the elastomeric variants which affect the magnitude of autohesion are the number of branches p and the molecular weight M, whilst relevant testing conditions are D (being a function of temperature), time of contact t and velocity of separation u of the participating surfaces. The viscoelastic considerations discussed in Chapter 2 demand that force of contact also influences autohesion.

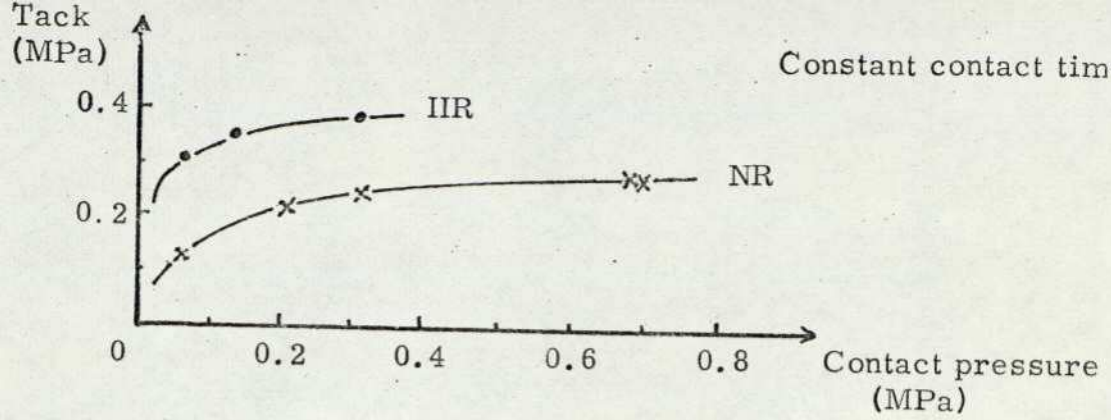

Figure 12 The effect of contact pressure on tack.

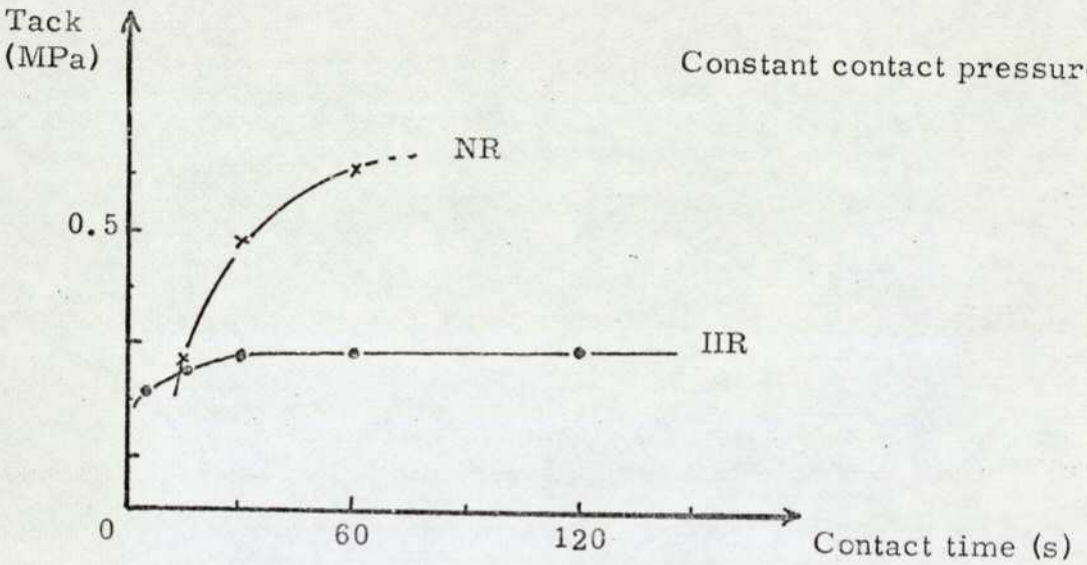

Figure 13 The effect of contact time t on tack.

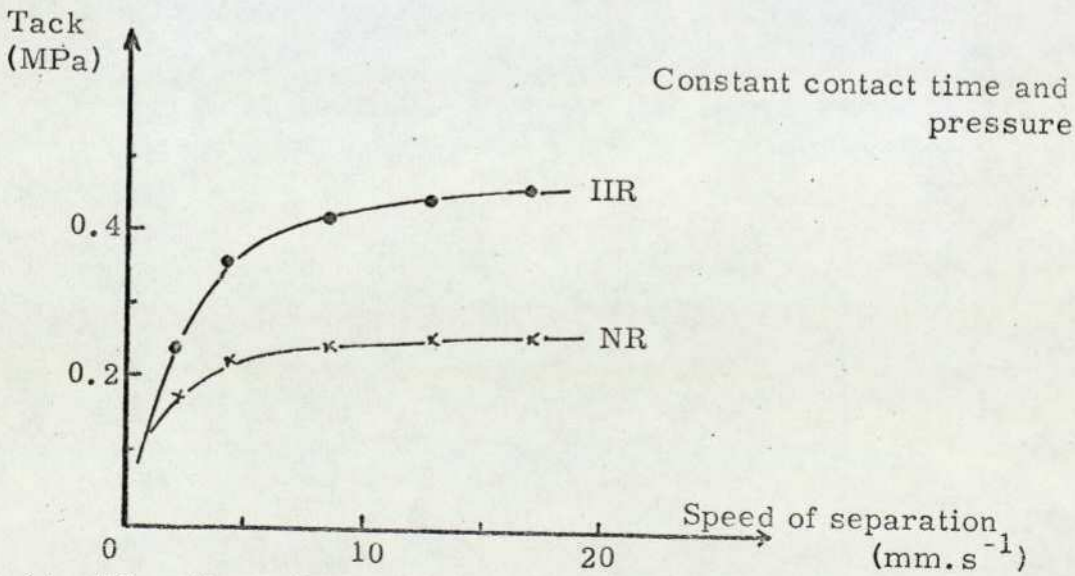

Figure 14 The effect of speed of separation u on tack.

Figures 12-14 are all after Beckwith et al[49] who tested in the tensile mode.

The important influence of the level and distribution of M is discussed separately in section 4.6. The inclusion of p in equation 4.22 is to cover those branches sufficiently long to be capable of following diffusive paths apart from that of the main chain. High autohesion values have been measured by Naunton for polychloroprene possessing molecular chains with widely spaced but long branches[19]: in contrast, the presence of short branches can be a hindrance to the diffusion of the main chain, as indicated by data which compare two polybutadienes[19].

The effects on autohesion of variations in experimental conditions have been frequently discussed[18-21,49,50]. The data of Beckwith et al[49], for autohesion as a function of force of contact, contact time and separation speed (Figures 12 to 14 respectively), are typical. However the effect of the remaining experimental factor, i.e. temperature, is less well-defined. By illustrating, for NR, autohesive tack results which decreased with increasing temperature, Beckwith again demonstrated the dangers of confusing autohesive and bulk strength at conditions of good contact. The data of Voyutskii[19] (Figure 15) for PIB, an elastomer which diffuses more slowly, are more realistic, showing an increase of tack with rising temperature as befits the typical Arrhenius relationship for a diffusion phenomenon.

The effects of force on viscous flow and time on chain interdiffusion reasonably gave[49] curves of similar shape (Figures 12 and 13). The power term arising from the contact time graph for butyl rubber is less than the value 0.25 predicted by equation 4.22, whilst the NR

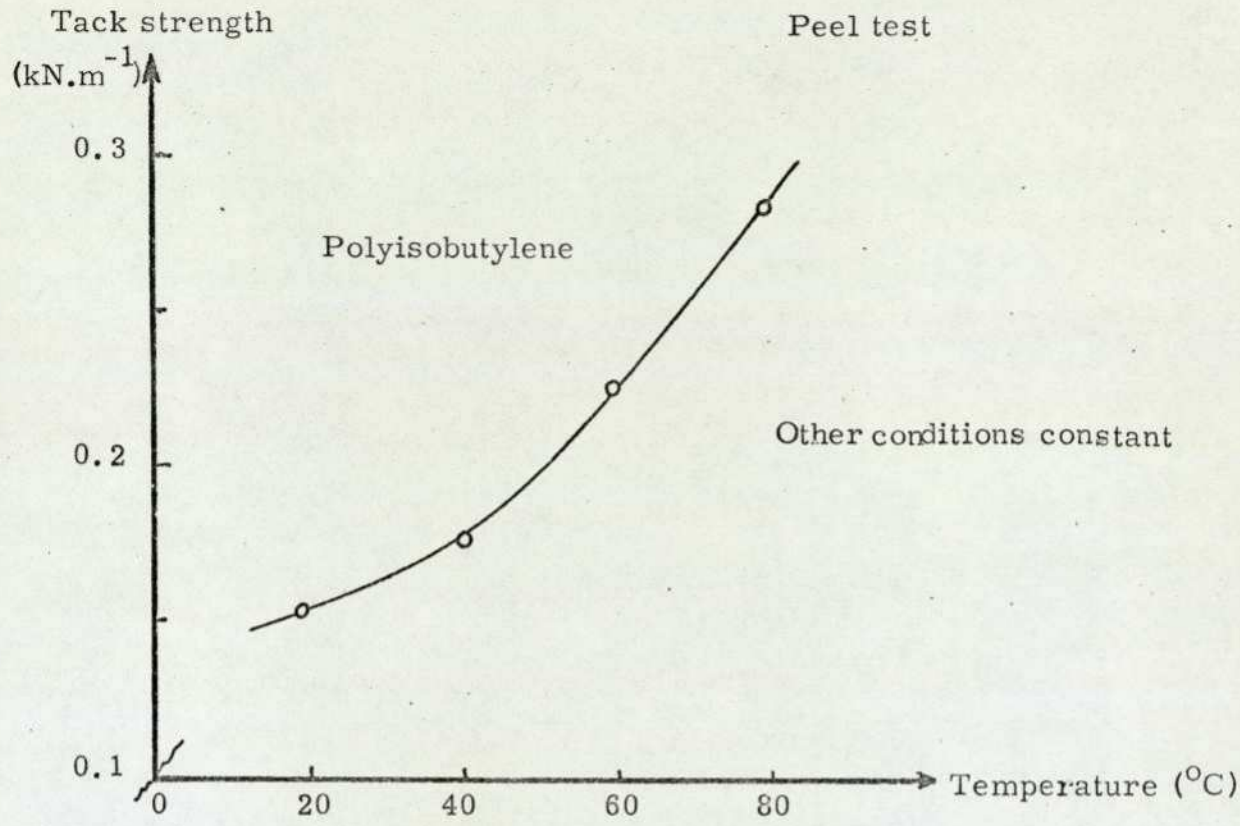

Figure 15 The effect of temperature on tack strength, after Voyutskii[19].

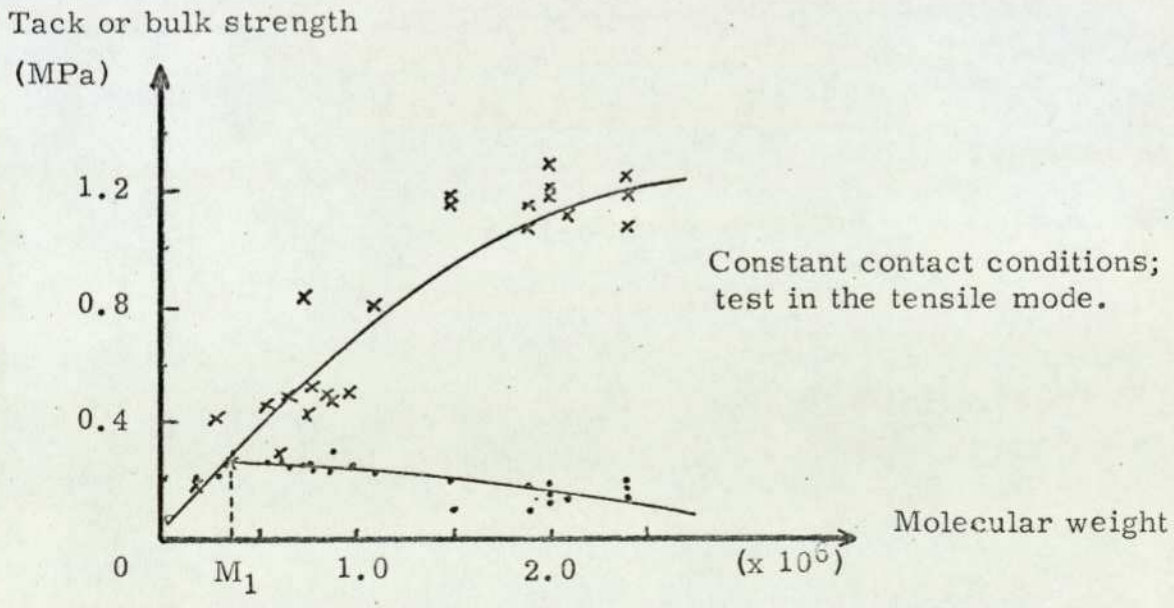

Figure 16 The effect of molecular weight on the tack strength and bulk strength of NR, after Forbes and Mcleod[18].

curve gave a value > 0.25: however other published results fit the equation well[9]. The similar curve which arises when tack is plotted as a function of u (Figure 14 being typical of several publications) does not fit the theory producing equation 4.22. The departure from linearity might reflect initial disentangling of chain segments.

4.6 The influence of molecular weight and related parameters on bond development

4.6.1 The effect on autohesion of molecular weight

When discussing the mastication of rubber compounds during their preparation (section 3.1.3 et seq), a decrease in M was seen to cause an increase in autohesive tack but a decrease in bulk strength. The diffusion coefficient D varies as M is changed according to Bresler[103] who radiometrically measured D for polyisoprene (M = 1100) in NR at 100°C, the empirical solution being

$$D = 6.6 \times 10^{-8} M^{-1.3} \qquad \text{----------4.23.}$$

The increases in F which arise from decreases in M[108] have been checked by Forbes and Mcleod[18] using sharp fractions of NR at different molecular weights. Both tack (contact time t = 30s) and bulk strength measurements were made and represented as functions of M (reproduced in Figure 16). A critical value M_1 of molecular weight was shown below which the relative tack F_R was always unity under the testing conditions used. In practice, the very fact of unit relative tack means considerable difficulties in testing procedures so that M_1 is best considered as a region of molecular weight rather than an

absolute value.

Although the researchers[18] considered that the tack strength curve did not indicate a dependence on M, nevertheless the general level of tack increased from 172 kPa (at $M = 2 \times 10^6$) to 275 kPa when $M = 0.5 \times 10^6$. The present author has repeated the exercise in essence (see Chapter 7) to indicate that a tack increase is particularly noticeable as M (specifically M_V) decreases from ca 7×10^5 to 5×10^5 at the very short contact times and other conditions employed.

4.6.2 The influence of molecular weight distribution

If rubbers possess both low and high molecular weight fractions, that of low M will interdiffuse rapidly to attain locally unit relative tack at very short contact times, whilst the species of high M ensures that adequate bulk strength characteristics are retained. The inextricable entanglements of the two (and intervening) fractions mean that the system should possess an enhanced tack level. The molecular weight distribution (MWD) of various masticated rubbers has been discussed[109].

4.6.3 Autohesion and viscosity

As both viscous behaviour and diffusion are governed by the formation of holes[95], a relationship would be expected between the two phenomena. Eyring[95] derived that $\eta \propto M^{1.3}$ for polymers with unentangled chains, whilst a well-established empirical relationship for normal rubbers[27] is $\eta \propto M^{3.5}$.

Several workers have equated $D\eta$ to KkT where K is constant[110], a solution which can be compared with the Stokes-Einstein equation 4.8.

Bueche[102] has experimentally shown that $D \propto \eta^{-1}$, a solution which also arises from combining the relationships $D \propto M^{-1.3}$ (expression 4.23) and $\eta \propto M^{1.3}$ (Eyring, above).

The inter-relation of viscosity and diffusion has been emphasised for two elastomers by the closeness of the relevant activation energies E_d and E_{vis}[103,111,102]. However, it must be noted that the magnitudes of E_d and E_{vis} quoted do not agree with those of other workers[112,45], the method of measurement being a factor.

On a more practical autohesive footing, relative tack data have indicated[18] that

$$F_R \simeq 3.25 - 0.25 \log \eta_s \qquad \text{----------4.24}$$

where η_s (the shear viscosity) = $10^9 - 10^{13}$ poises so that $F_R \leq 1$.

4.7 Alternative theories of autohesion

The relevance to autohesion of bonding mechanisms involved in other facets of adhesion should be mentioned at this stage. The mechanisms involve the electrostatic, mechanical and adsorption theories (e.g.[9]). However, the basic requirement for electrostatic interaction, that the intimately-contacting bodies are dissimilar, is immediately nullified in self-adhesion. Moreover, the conditions for mechanical bonding are not met, as the provision is required that one participating surface should be higher in modulus by several orders than elastomers to obtain the permanent surface "roughness" (on a microscopic rather than molecular scale) into which the adherent can lock.

4.7.1 An application of the adsorption theory to autohesion

At the most elementary level, adhesion involves the contact of two surfaces on a molecular scale such that adsorption occurs. Studies of continued interest to adhesive scientists include the adsorption of polymer chains on to substrates from dilute solutions[113] and concentrated solutions[114], the existence of chain coils and loops causing only partial surface coverage in the latter case.

The fundamental nature of adsorption has led to an attempted application of the phenomenon to autohesion. Anand et al[115] consider that the typical curves for autohesion versus time or temperature arise for reasons of increasing contact area occurring in two stages of viscous flow. The subsequent bond development takes place instantaneously by intermolecular interactions due to adsorption. Indeed, both diffusive and viscoelastic processes are governed by similar Arrhenius equations, cases of similarity between E_d and E_{vis} having been noted earlier. Anand was mainly interested in highly viscous polymers, performing many experiments on polystyrene at elevated temperatures. The samples possessed surface crenulations of regular form, and bond strengths were measured and compared with theory. Anand accepted the occurrence of diffusion during autohesion, but considered its contribution to bond strength to be insignificant.

4.7.2 Comparison of the diffusion and adsorption/viscous flow theories for autohesion

Much evidence has been cited in favour of the diffusion theory of autohesion. Nevertheless, the similarity of E_d and E_{vis} in the light of

Anand's claims should not be summarily dismissed. For elastomers, the main contention is apparently not whether diffusion occurs, but whether it contributes to the strength of the bond which develops. Intermolecular forces are undeniably involved sooner or later during the development stage. Anand's views[115] of the growth in bond strength being due to increase in contact area and concomitant instantaneous adsorption must be compared with Voyutskii's considerations[24] that the attainment of complete contact is a necessary step automatically performed, that diffusion governs bond strength development and that, ultimately, a chain which has diffused and thus increased the area of molecular surface contact will, only then, experience useful intermolecular interaction.

Contributory factors to the opposing views must be the polymers and conditions employed for experimentation by both parties. Anand used polystyrene (normally a thermoplastic of high viscosity, necessarily employing a contact pressure of ca 50 kPa at elevated temperatures and subsequently testing at room temperature. Voyutskii invariably studied elastomers at considerably lower viscosity and has described[19] how, above a critical contact pressure of only 4 kPa at room temperature, further increases in pressure are not accompanied by increases in autohesive strength for PIB (M = 150,000, t = 5 min), such behaviour being typical (cf Figure 12). For the elastomeric system, data were also shown for the effect of contact time on the autohesion of the same elastomer at a contact pressure of 4 kPa: the increase in test value applies for several hours. Unlike diffusion, viscous flow is force-dependent. Hence, increases in tack

for times greater than 5 mins must have arisen from the occurrence of diffusion.

In addition, the application to autohesion of the adsorption theory suffers a major drawback - how to explain the low autohesive tack of EPDM rubber throughout the complete range of molecular weights applicable to elastomers. The contrast with NR is not easily explicable by molecular interaction on an adsorption basis.

The remainder of this thesis relies on the validity of the diffusion theory for the autohesion of elastomers.

4.8 Definition of the diffusive problem

In the extreme cases of NR and EPDM, optimum autohesive strength data will indicate (Chapter 7) that $F_{NR} \sim 5 \times F_{EP}$ (high tack values developing with 1 s of contact for NR). In Chapter 8, removal of the contribution of stress crystallisation will show that the proportionality factor should be nearer to 3 in more realistic diffusive terms. However, from equation 4.22, for a contact time of 1 second, $F \propto D^{\frac{1}{2}}$ if other conditions are constant. Hence the self-diffusion coefficient for NR should still be an order of magnitude greater than that for EPDM[85]. The radiometric evidence of Skewis[21] does not preclude the possibility due to insufficient experimentation on NR elastomers of different molecular weights.

The problem is now reduced to determining the molecular characteristics which provide for enhanced diffusion in NR.

4.9 Chain parameters influencing autohesive diffusion

Autohesive diffusion is a mutual phenomenon, recipient surfaces also supplying outgoing chain ends or portions. Hence, the apparent difference in self-diffusion coefficient of one order between NR and EPDM might initially appear to arise for reasons connected with either the surface receptivity or outgoing mobility aspects.

Chain mobility is restricted by excessive cross-linking or branching unless the branches, if long, diffuse separately. Crystallinity (packing order involving several monomer units) both inhibits mobility and limits the useful free volume of the recipient surface layer. Whereas whole-chain mobility is governed by magnitude (molecular weight M), segmental motion by definition is largely independent of chain length, as all segments are more or less of the same size. Whether the length of the flow unit is dependent on the ability of smaller chain portions to kink is open to question. In this context, chain flexibility has been described by the equivalent random link q, a statistical term which compares theoretical and experimental values of the optical anisotropy of elastomers: at 20°C q is associated with 5.2 and 10.5 C-C bonds in NR and EPDM respectively[116].

The many publications relevant to the subject have concentrated on the behaviour of the rubber matrix, which in the present case relates to the recipient surface layer. The asymptotic approach of E_d to a limiting value described for the diffusion in rubbers of hydrocarbons[100,96], solvent penetrants[117], larger gas molecules[110] and polyisoprene[103] strongly suggests that the limiting value corresponds to E_d for self-diffusion of the polymer, i.e. indicates the onset of the motion of

segments (of length 20-40 C atoms from the hydrocarbon studies). The point is further made[118] by considering recorded values for E_d of 9.9 and 9.7 k.cal respectively for the diffusion through SBR compound of naphthenic and aromatic oils which are considerably different in molecular character. Further discussion on chain parameters which influence autohesive diffusion will reasonably concentrate on the matrix aspects of the recipient surface layer.

A matter of some relevance is the mode of production of the holes utilised in segmental diffusive jumps (section 4.2). Within the bulk of an elastomer, micro-Brownian thermal motion involving chain elements causes local density fluctuations which continually vary throughout the polymer. Both diffusive and viscoelastic behaviour are influenced by these density changes. Extreme fluctuations of this type within the polymer bulk cause the generation of holes, the hole-formation giving rise at the surface to apertures of commensurate size through which chain portions must pass during autohesive diffusion. The model is effectively that of Bueche[27] but includes an extension to the surface. The initial autohesive mechanism involves the jumps of outgoing segments into these apertures, the segments obviously defining the size of aperture required.

4.10 The formation of holes within an elastomer

Although holes are continuously produced in random positions throughout an elastomer, on a time-average basis (at any constant temperature) the distribution of hole sizes must vary to a certain extent around a consistent mean. Subsequent observations on the formation of critically-sized holes are made within this framework. Estimations

of average hole sizes are most easily made from the free volume of the elastomer.

4.10.1 The free volume of liquids and polymers

The term 'free volume' collectively describes (and frequently quantifies) the free space which exists within a polymer between the molecular chains. The space existing inside the limits of influence (the most probable electron orbitals) of the chemical groups making up the chains is not included in free volume.

Let V_T = observed (bulk) volume at temperature T°K

V_W = summated volume of all contributing molecules from van der Waals dimensions

V_o = volume occupied by these molecules at 0°K in a close-packed crystalline state

notations referring to cc. mole^{-1}. Then[119,120]

Empty volume $V_E = V_T - V_W$ ---------- 5.1

Expansion volume $V_F = V_T - V_o$ ---------- 5.2.

Although V_E is the fundamental form of free volume, V_F is easier to obtain, as V_o can be estimated from appropriate extrapolations of data measured at normal temperatures. Five different approaches for liquids have given V_o values which differ by only 2 - 3%[119]. However, it is more difficult to apply these methods to polymers because of the changes in characteristics which occur during cooling as various transitions are passed. One estimate of V_o (or, more strictly, its specific volume equivalent) has been made for polymers by the extrapolation of plots of the thermal volume expansion coefficient against

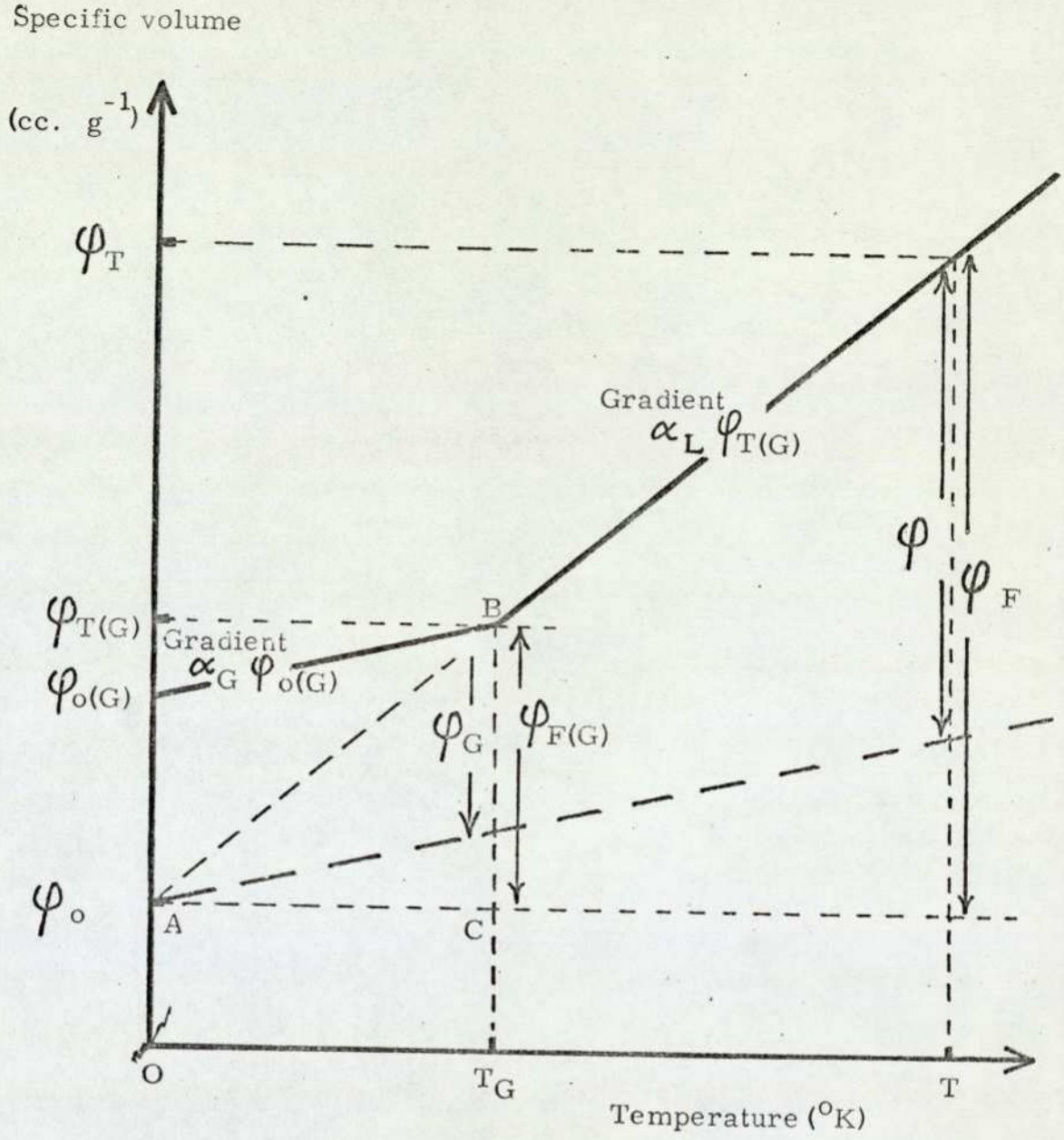

Figure 17 Graphical illustration of Simha-Boyer[121] concept of free volume.

temperature[121]. The concept is illustrated graphically in Figure 17. The expansion coefficients above and below T_G were termed α_L and α_G respectively: to convert to specific volumes per degree, it is necessary to multiply these coefficients by the appropriate reference specific volumes.

If φ(cc.g^{-1}) is substituted for V (cc.mole^{-1}) in equation 5.2, then

$$\varphi_F = \varphi_T - \varphi_o \text{ - 5.3.}$$

Let the "specific expansion volume" at temperature T_G be $\varphi_{F(G)}$. Then

$$\varphi_{F(G)} = \varphi_{T(G)} - \varphi_o = AC \tan B\hat{A}C = \alpha_L \varphi_{T(G)} T_G \text{ - - - - - 5.4.}$$

The ratio $\varphi_{F(G)} / \varphi_{T(G)}$ is the fractional free volume at T_G. Haward[119] has reviewed several publications which indicate from packing considerations that the fractional term is of magnitude ca 0.14, whereas equation 5.4 has given rise to many experimental values well above this level. An alternative system[121] subtracts $\alpha_G \varphi_{o(G)}$ from $\alpha_L \varphi_{T(G)}$ in equation 5.4 so that

$$\varphi_G = (\alpha_L \varphi_{T(G)} - \alpha_G \varphi_{o(G)}) T_G \text{ - - - - - - - - - - - - - - - - - 5.5.}$$

Whatever the physical significance of equation 5.5 (see Figure 17), it gives a fractional free volume of about 0.11 for many polymers (after assuming that $\varphi_{T(G)} \simeq \varphi_{o(G)}$ so that $\varphi_G / \varphi_{T(G)} = (\alpha_L - \alpha_G) T_G$). Haward expressed reservations on the treatment because of the considerable departure from linearity of α_G (especially near 0°K) and α_L. Similar reasoning probably applies to the high values arising from the more basic equation 5.4: Haward suggested that an inequality would be more appropriate, viz

$$\varphi_{F(G)} < \alpha_L \varphi_{T(G)} T_G \text{ - 5.6.}$$

Although $\varphi_G / \varphi_{T(G)}$ has been considered a constant[121], data do not

fully fit the claim, and a case has been presented to the contrary.[119] An alternative treatment of free volume employing viscosity considerations[122,123,1] also proposed an iso-free-volume fraction at T_G, but at the much lower level of 0.025. The difference in magnitude has been ascribed to differences in concepts of the close-packing of chains[119].

Despite the possible drawbacks, equation 5.5 provides the most convenient basis for calculations in Chapter 10 where estimates are made of mean hole sizes for various elastomers. As a gradient-difference is involved, the extrapolation errors of α_L and α_G tend to counteract each other, and any remaining deviations should apply to all elastomers to similar extents so that inter-polymer comparison is permissible. Hence from Figure 17, if the free volume at room temperature T°K is φ, then

$$\varphi = (\alpha_L \varphi_{T(G)} - \alpha_G \varphi_{o(G)}) T \quad \text{- 5.7.}$$

Studies of values of density at various temperatures, and appropriate extrapolations, have indicated that both $\varphi_{T(G)}$ and $\varphi_{o(G)}$ are very near to one for common hydrocarbon elastomers[28a,121a]. Hence

$$\varphi = (\alpha_L - \alpha_G) T \quad \text{- 5.8.}$$

the units of φ still being $cc.g^{-1}$.

4.10.2 The effects of internal pressure and internal rotation

Brandt[92] recognised that, after taking the penetrant size into account, E_d will be a function of chain geometry, chain stiffness and intermolecular forces. The molecular model effectively extended that of Barrer[97]. The repulsive forces existing between those molecular chains bent around a hole were said to be best expressed by the internal pressure P_i. From the chain stiffness viewpoint, the relative permanence of bond distances and angles meant that such a distortion of chains should involve, along the complete segment length, a partial rotation of chain units against the hindering potential of internal rotation.

The optically-derived equivalent random link q (mentioned earlier in the chapter) which relates to the flexibility of chains is apparently associated in general with shorter segments than those participating in diffusive jumps. A sequence of descending magnitudes of internal energy barriers to rotation from estimations[116] is

EPDM > SBR(5%S) > cis BR > SBR(14%S) > NR > SBR(31%S).

Although the sequence bears some resemblance to a reciprocal order of tack magnitude (Table 3), some important discrepancies occur. Besides the obvious misplacement of NR, tack values of SBR copolymers in practice diminish as the styrene content (%S) increases. Butyl rubber was another anomaly, exhibiting a negative value of q when its photoelastic data were treated in the same way by the writer. Nevertheless, chain flexibility might well play some part in autohesion.

If the volume increase due to the activation process is $\Delta V^{\ddagger}$, the work $P_i \Delta V^{\ddagger}$ makes a major contribution to E_d for large penetrant molecules[124]. Hildebrand's definition of P_i has been used to obtain many data for P_i for numerous simple liquids[125], including many hydrocarbons, and some polymers[126]: for the hydrocarbons, the values of P_i were computed at 20°C from literature data for the coefficients of expansion α_L and isothermal compressibility β_T, whilst, for the polymers, direct measurement of the relevant factor $(\partial P_A / \partial T)_V$ enabled P_i to be determined experimentally (P_A being atmospheric pressure). The data showed the P_i values to be independent of methylene branches and chain unsaturation for liquids, limiting values being reached which were only 10 - 15% higher than that for decane, for example.

As a consequence, the internal pressures of all hydrocarbon polymers can be considered similar. The specific energies of chain displacement to overcome van der Waals attractive forces will therefore be of similar magnitudes. Hence the relative facility with which a hole is generated is governed by geometrical considerations. The contribution of chain flexibility cannot fully account for the large differences in tack magnitudes which exist between elastomers: in particular, the spontaneity with which NR can autohere requires further explanation.

F_1 = compressive force F_2 = separative force

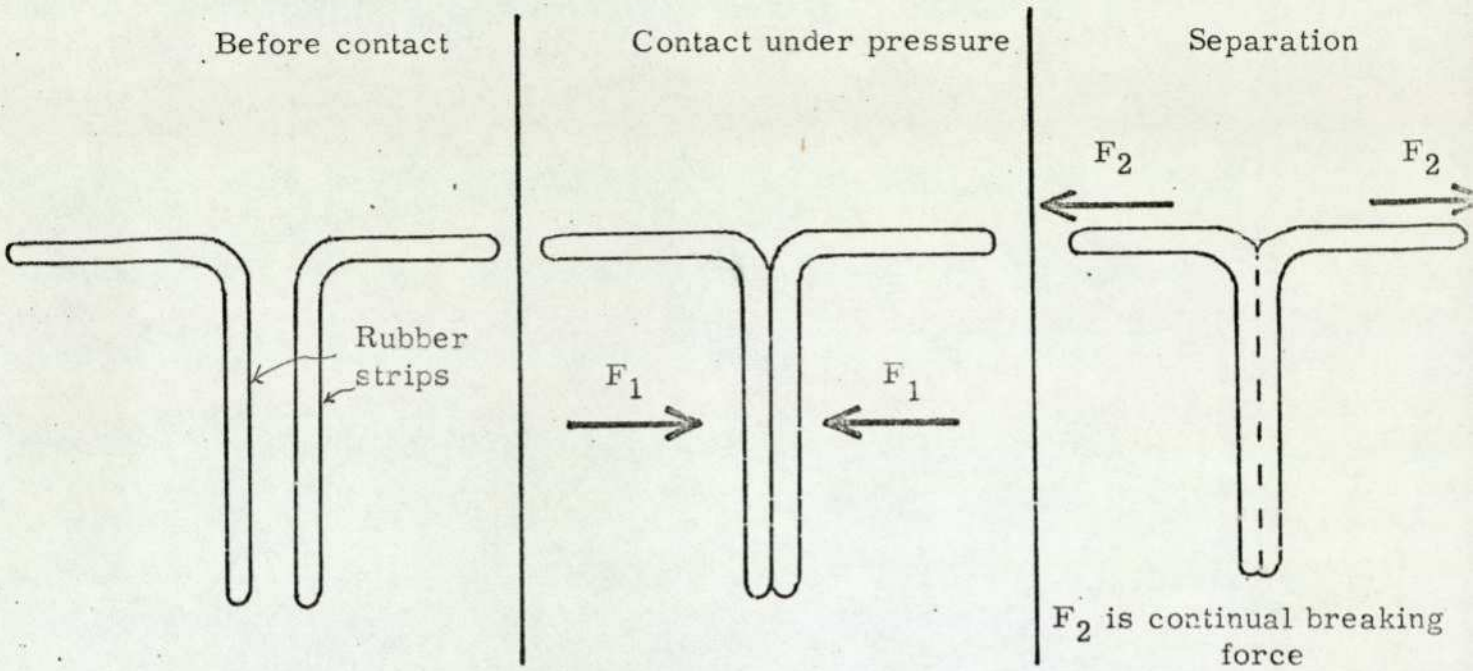

Fig. 18(a) Peel testing.

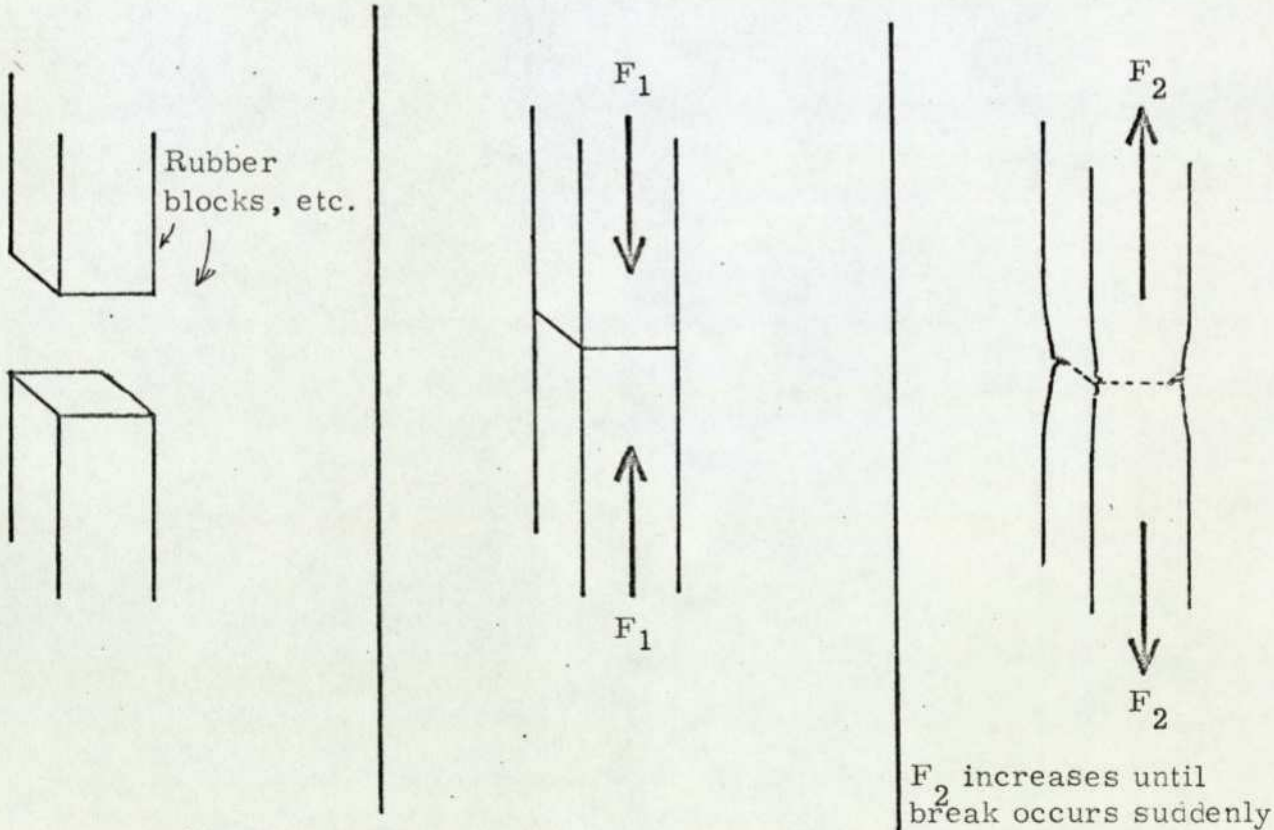

Fig. 18(b) Tests in the tensile mode.

Figure 18 Schematic descriptions of the two main classes of autohesive tack test.

Chapter 5 Methods of measuring magnitudes of autohesive tack

Although the main requirement in technological applications which utilise the autohesive phenomenon is to maintain the bond between the participating surfaces prior to vulcanisation, any assessment of the magnitude of autohesive bonding is necessarily destructive. Ultrasonic radiation has been used to inspect and quantify non-destructively defects in adhesive bond lines[127], but the technique is not yet sufficiently developed for autohesive tack testing.

5.1 Existing methods of test

An early assessment of tack strength was by Griffith and Jones[128], who measured the force required to roll a heavy rubber-covered cylinder over a rubber sheet. The mode of separation during testing of the rubber surfaces was quasi-peeling. Subsequent tests can be largely divided into two classes defined by their mode of separation, although other tests exist (e.g. pendulum tests). The two classes, peel tests and tests in the tensile mode, are illustrated schematically in Figure 18.

Peel testpieces are made by bringing together under pressure two strips of rubber which are fabric-backed for added strength. A narrow non-adhering layer is included between the strips at one end to give two tabs to aid testing. Separation is performed by gripping each end-tab in the jaws of a testing device and applying opposite forces. As peeling occurs, the interface is continuously assessed, the line of separation gradually sweeping the whole contact area. A representative separation force (depending on contact width but not area) is

noted. Decreases in the modulus of the rubber strips cause the angle of separation to become nearer to 180°.

Samples for testing in the tensile mode take a number of forms. However, in principle, two surfaces are brought together normally and, after contact under pressure, are separated in the opposite direction. Separation occurs almost instantaneously to give a representative force for the whole contact area.

Tests in use before 1964 have been admirably reviewed by Bussemaker[20] and later tests have been well-described by the inventors (see references throughout this chapter).

5.1.1 Tack tests in the peeling mode

Results from the early 'rolling' test of Griffith and Jones[128] were noted by Bussemaker as being greatly affected by contact surface deformation, which is presumably the reason for its lack of subsequent popularity. However, a class of tests termed peel tests is now well established generally in adhesion science. For instance, using a system in which a flexible strip is bonded by an adhesive to a rigid substrate, Peel Mechanics have been applied[129] to relate under certain conditions the measured separative force with the angle of peel, and peel testing is frequently used to assess bond strengths between pairs of fabric-backed rubber strips which are uncured at contact but are tested after cure.

Since the early 1950's, Voyutskii and colleagues have performed many peel autohesive tests on a specially-constructed adhesiometer[19]. The strip testpieces were prepared by coating a 6-8%polymer solution

on to a backing fabric and allowing the solvent to evaporate: if necessary, the treatment was repeated several times to obtain, at constant weight, suitably-thick testpieces. The contact between two polymer surfaces was performed by the doubling of single testpieces under prescribed conditions. The test instrument recorded the force required for separation at 180°, a possible variant being the speed of separation. The work of adhesion was derived from the peeling force and an appropriate distance term.

More recently, van Gunst et al[71] have also described the use of a peel-tackmeter for assessing the tack of strips of rubber. A more-publicised instrument which performs a similar function for rubber plies in the factory was constructed by Bussemaker and van Beek[130]. The principle of this rugged tackmeter is still basically that of Figure 18(a), but the three essential stages of testing are carried out automatically to pre-set conditions. The testpieces are again strips of fabric-backed uncured rubber (of approximate size 200 mm x 25 mm). Contact is made through a window, of known contact area, in a thin polyester film, the contact pressure being applied by pneumatically-driven blocks. On removal of the blocks, a powerful motor rotates two wheels on to which the end-tabs of the plies are clamped. The ensuing winding process causes the contacted area to separate immediately after passing between two appropriately-situated rollers. The tack strength is a measure of the torque necessary to drive the collecting-wheels and is obtained on a chart as a trace against time.

The tack strength obtained from any peel test is usually quoted as a

mean value of measured force per unit sample width. However, measurements of the time t_p required to peel apart at constant load two previously-contacted plies are claimed[57] to give better reproducibility than do the usual force assessments, the coefficient of variation depending on $t_p^{-0.5}$.

5.1.2 Tack tests in the tensile mode

Most tests of this type are based on the design of Busse et al[131] or an automated modification[132]. Two rubber samples were pressed normally together under a specified pressure and for a specified time after which they were pulled apart (also normally), the force required being the tack strength per original area of contact. A drawback in design was that contact was made between a cylinder of rubber and a flat rubber sheet.

A similar principle involving the weighted contacting of cylindrical and flat rubber surfaces was used in a robust portable tackmeter constructed by Pickup[133] ostensibly for factory control use. The separative force is applied through a spring, an attached arm indicating the amount of accompanying extension. The arm pushes ahead of itself a slide-fitting ring which runs on a cylindrical calibrated scale. Separation of the rubber surfaces frees the clamped end of the spring. The resulting recoil causes the scale system to jump clear of the moving arm so that the position of the ring, giving the tack force, can be read from the scale. In practice, the tackmeter was easily influenced to varying degrees by individual operators, and although other workers automated the instrument, the small contact area involved meant that reproducibility was not good.

The obvious disadvantages of making contact between a curved and a flat rubber surface have been eliminated[49] by substituting cylindrical samples which were cut sectionally, using a hot knife. The tack was measured endwise between the fresh surfaces. A specially-constructed instrument (although still based on the method of Busse) performed the testing function, extra facilities being added for assessing the effects on tack of temperature and humidity. Forbes and Mcleod[18] carried out similar testing, but on an Instron inertia-less tensile tester . The cylindrical testpieces were elegantly prepared by moulding under evacuated conditions, two test-pieces being formed in one mould by inserting, at the mid-point, a smooth disc made from polytetrafluoroethylene: the tack was assessed between the surfaces which had been pressed against the disc. The preparation of further testpieces from the same elasto-meric material with the omission of the disc meant that bulk strength measurements could be obtained in a manner which was directly com-parable with the tack testing. Thus relative tack values were easily obtained.

Other tests which follow the same principle have been constructed. Voyutskii[19] has described two such instruments, one a modified torsion balance for measuring very small forces, and the second for somewhat larger forces. However, published data of Voyutskii generally refer to the peel test already mentioned. Baranwal and Beatty have described[47] how improved instrumentation allowed the manufacture of a compact portable tackmeter, the 'Tel Tak', which effectively performs the same function as the tackmeter of Forbes and

Mcleod: testing is carried out automatically to pre-set conditions. However, the samples are pellets and the contact area is very small (40 mm^2) so that samples with high tack can distort to large strains before finally breaking. The inventors have attempted to differentiate between tackiness and stickiness by subtracting the measurement from a second test performed between rubber and steel. The resulting value was empirically termed "true tack".

As with peel testing, several workers employing the tensile mode of testing (notably Skewis[134], Petersen and Martin[64]) have chosen to separate contacted testpieces by application of a constant force, so that differences in tackiness are reflected by different times of separation.

5.1.3 Miscellaneous tack tests

Methods of tack measurement other than those belonging to the two main classes are limited in number. The most basic of these is a subjective assessment, made by an operator pressing together by hand the rubber surfaces, which is at best a sorting test only.

Two pendulum tests have been used by separate German workers, one[135] being a modified Schob rebound pendulum: by covering the striker and base by rubber fabric, tackiness causes a decrease in rebound elasticity compared with a control, uncovered result. The effective contact time is obviously extremely short. The contact time is greater, however, in the Bär pendulum tackmeter[136], in which two rubber-covered pendulum bobs are pressed together whilst hanging in a stationary position. One bob is mechanically raised

A modified Pickup tackmeter

for use on an Instron tensile tester

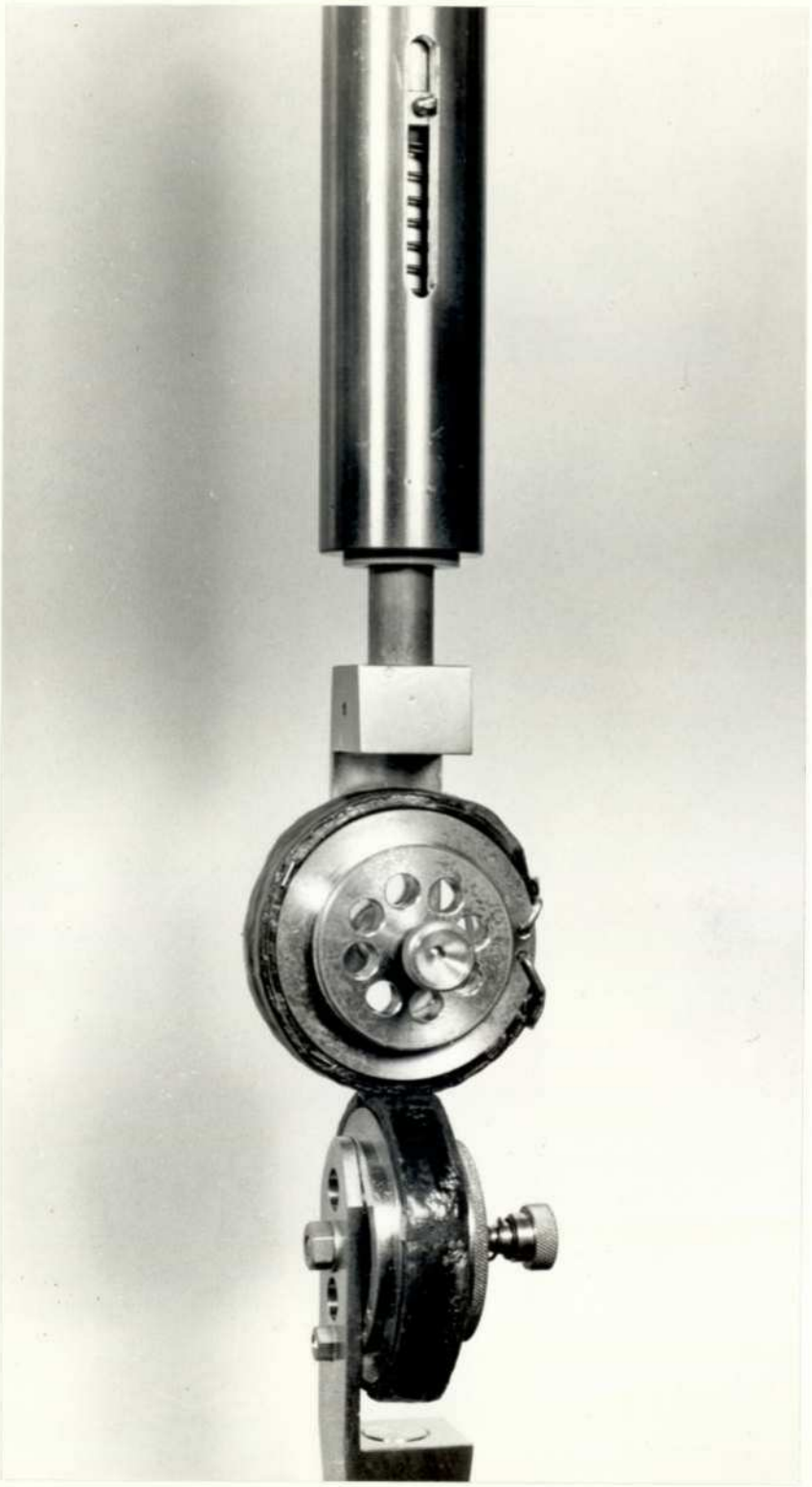

RPU 21456

Plate 2

until the second bob falls away, the height risen being a measure of tackiness.

Because the assessment of adhesive tack (section 1.2) is not of present interest, the very different tests involved[10,11,137] are not described herein.

5.2 Disadvantages of existing tackmeters leading to the requirement of a re-design

The writer began experimentation by specifying modifications made[138] to a Pickup tackmeter for use on an Instron tensile tester, contact during testing being necessarily made between two curved surfaces (Plate 2). Ensuing measurements confirmed indications from the literature that little difference could be shown in this way between the extreme cases of NR and EPDM. One problem in such a tensile tester was apparently that, except when assessing the lowest tack values, the process of measurement was accompanied by considerable distortion, so that doubt often arose as to the actual area of contact. The problem might be less relevant with the cylindrical specimens (tested end-on) of Forbes and Mcleod[18], although testpieces would still experience considerable extension.

In choosing a test to give tack magnitudes which reflect diffusive abilities, tests in the tensile mode are inferior to the peel variety in one important way. Tensile tack tests involve a single separation of the whole contact area so that the representative value will be lowered by local areas of insufficient contact, such decreases being misleading in assessing diffusion aspects. In contrast, peel tack tests,

concerning the separation of previously-contacted surfaces at a line which advances across the contact area, indicate the local regions of poor contact by troughs in the plot of separating force against time. In addition, test magnitudes are such that the final representative value usually applies to a larger area in the peel case. For studies of the viscous flow aspects of tack (perhaps relating to a particular technological process possessing areas of insufficient contact) tensile tack tests would be preferable. However, peel tests should provide information of greater reliability on autohesive diffusion.

A suitable tackmeter should reliably place the tack magnitudes of different rubbers into a sequence agreeing with experience under technologically realistic conditions. High contact pressures are required to produce intimate interfacial contact, and a non-variable contact time for the whole contact area is desirable, the time preferably being short to minimise bulk strength effects. Unfortunately, the contact times during the last stages of peel testing are affected by the times taken for testing, this point being especially important at short contact times. Hence a new design of peel test was required for the present researches.

The solution has been found in a dynamic test, with several attendant advantages. Cheetham[139] has constructed a dynamic rolling ball spectrometer to measure the force required for the circular passage of three steel balls indented under load into a rubber slab. The author of this thesis considered that the replacement of the components by two shallow cylinders of uncured rubber in rolling contact would, with considerable modification, produce the required tackmeter.

PART II - THE CONTRIBUTION OF THE PRESENT WORK, INCLUDING A PROPOSED STRUCTURAL MODEL FOR AUTOHESIVE DIFFUSION

Chapter 6 The testing requirements and the Dunlop Rotary Tackmeter

In previous chapters it has been derived that

(a) an apparent difference of one order exists in the rates of autohesive diffusion between the extreme cases of NR and EPDM

(b) the reason for the difference in ability to self-diffuse reasonably lies within a geometrical theoretical framework.

Before expanding point (b) (Chapter 9 et seq), various experimental stipulations should be met. These are:-

(i) The experimentation giving rise to (a) must be well-substantiated.

(ii) The role of stress crystallization (considered by some workers to cause the high tack of NR) must be ascertained.

(iii) Some tack measurements relevant to a theoretical model to be proposed in Chapter 9 are desirable.

The experimental studies have been performed using the Dunlop Rotary Tackmeter. The principle involved, viz a dynamic peel - type test, was chosen for reasons associated with the technicalities of testing as discussed at the end of the preceding chapter. The new design was ideally required to

(1) function under conditions corresponding to those met during the construction of technological composites such as tyres

(2) place the tack magnitude values of different rubbery materials into a sequence agreeing with technological experience

(3) be suitable for research purposes, i.e. exhibit good statistical reproducibility

(4) assess the diffusive nature of tack rather than viscoelastic or bulk strength effects.

Before describing the Rotary Tackmeter and relevant stages of its development, a personal viewpoint is expressed with regard to these requirements on the relationship of autohesive tack, bulk strength and the ease of handling in practice of uncured elastomeric components.

6.1 The practical handling of uncured rubber layers

From sections 3.1.5 and 3.2, the comparative tack testing of rubbers with unit relative tack F_R (i.e. tack strength F divided by bulk strength) produces measurements of bulk strength rather than autohesive tack. The most suitable condition for both testing and handling is thought to occur when both characteristics are well-developed, but F_R is somewhat less than unity. To justify such an opinion, a typical situation which occurs when constructing composites such as tyres should be considered.

In one traditional manufacturing technique, tyres are built-up from layers of compound or rubberised fabric on a drum or 'former' which is rotated by an operator. Successive sleeves (or 'pockets') of compound are added to the drum by manipulation with a steel rod (or 'poker') as indicated in Figure 19. After the first sleeve has been put on the drum, the addition of subsequent sleeves involves autohesive tack: during the manipulative stage, contact and separation at the

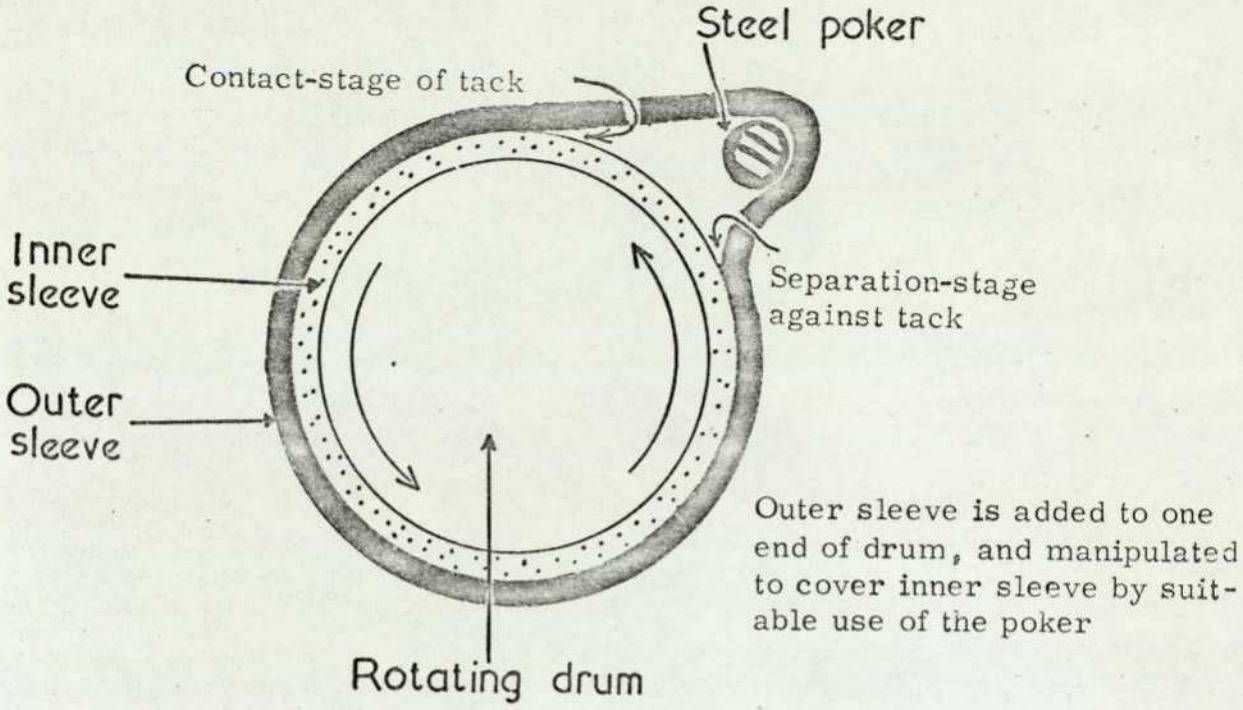

Figure 19 The occurrence of tack during tyre building.

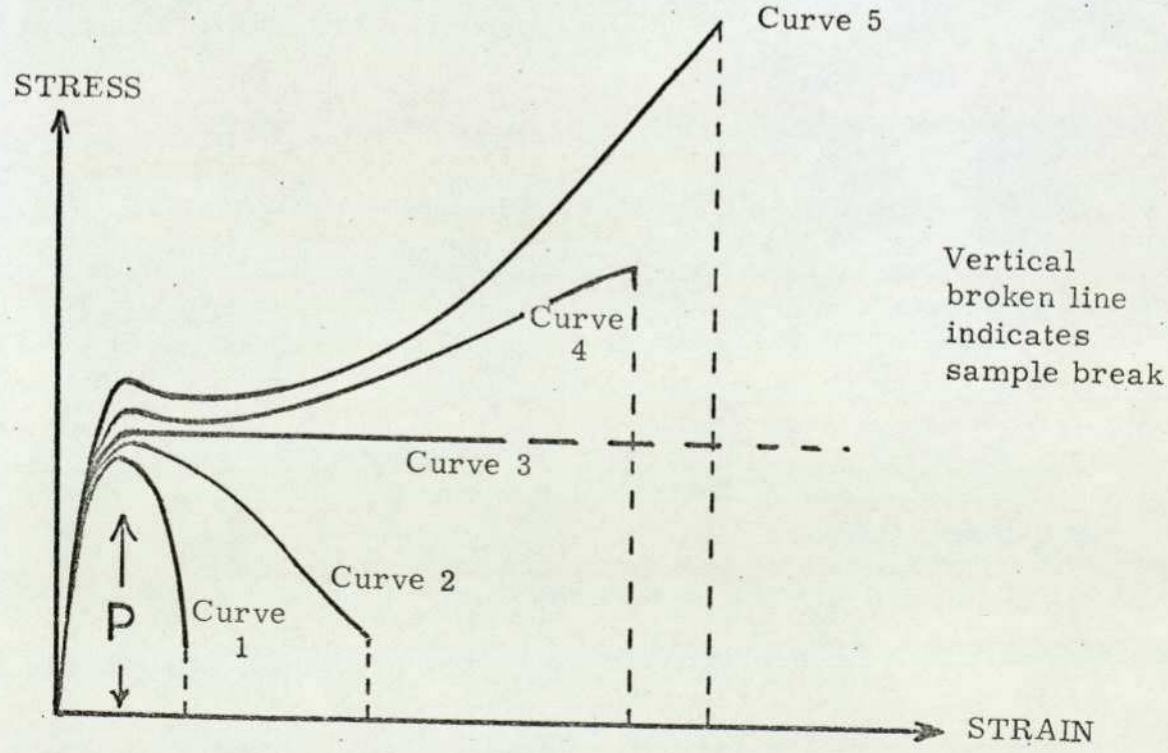

Figure 20 Some typical stress/strain curves for rubber compounds.

poker occurs once per revolution, the contact time being in the order of seconds only.

Whereas insufficient building tack will cause difficulties in keeping a compound sleeve in its allocated position, an excess of tack can cause great problems at the stage of each cycle when separation of the compound layers is required for their re-positioning. Hence an optimum range of tack exists. In addition, it is important that the optimum tack is associated with a magnitude of bulk strength which is sufficiently great (say P_m) to permit only a minimum of permanent stretching of the compound layer during handling. Figure 20 illustrates various hypothetical but typical stress/strain curves of compounds. The behaviour varies from curve 5, which displays a stress crystallization tail, to curve 1, which exhibits extensive post-yield deformation. For curve 3, the yielding stress, of magnitude P, is reached at low strains and is maintained at high strain situations: the minimum requirement for handling is a similar curve with P equal to P_m in magnitude.

The most convenient means of equating P and P_m is by making the molecular weight M sufficiently high, but this action will have retarded the preceding diffusive step. An intuitive and approximate optimum range for F_R during tyre building is 0.25 to 0.75. The apparently superior diffusive ability of NR compounds compared with that of EPDM compounds means that the diffusive requirement can be met at the molecular weight associated with P_m for NR, so that tack strength F can lie within the range $0.25P_m$ to $0.75\ P_m$. This is not the case for EPDM, as $F < 0.25\ P_m$ at such a molecular weight. The

diffusive requirement for EPDM is usually only met at low M values, when $P < P_m$ and the stress/strain curve is of type 1: consequently, the compounds are sticky and unmanageable.

Applying a similar argument to tack testing, a sufficiently large magnitude of bulk strength ($P_{m'}$) is required to prohibit more than a minimum of sample distortion during testing. $P_{m'}$ again largely relates to the yielding stress P (Figure 20) of the test rubber, although for materials displaying stress/strain curves of types 4 and 5, the force applying to local areas of high strain at the interface might be nearer to the breaking strength (which occurs at magnitudes much greater than P).

Hence design-requirement (3) on page 87 involves the attainment for any elastomeric material of a statistical variation which is sufficiently low for the tack comparison between different rubbers to be significant except at conditions of high practical difficulty when F_R approaches unity. In the latter situation, bulk strength measurements alone must suffice.

6.2 Principle and development of the Rotary Tackmeter

6.2.1 Principle

In summary, the Dunlop Rotary Tackmeter uses a "sun and planet" motion for the continuous peel measurement of the tack occurring between the peripheral surfaces of two squat cylindrical rubber specimens. One specimen (the "sun") is attached axially through a spindle to a strong, calibrated leaf spring. During testing, the sun testpiece is in contact with the second "planet" specimen, the two

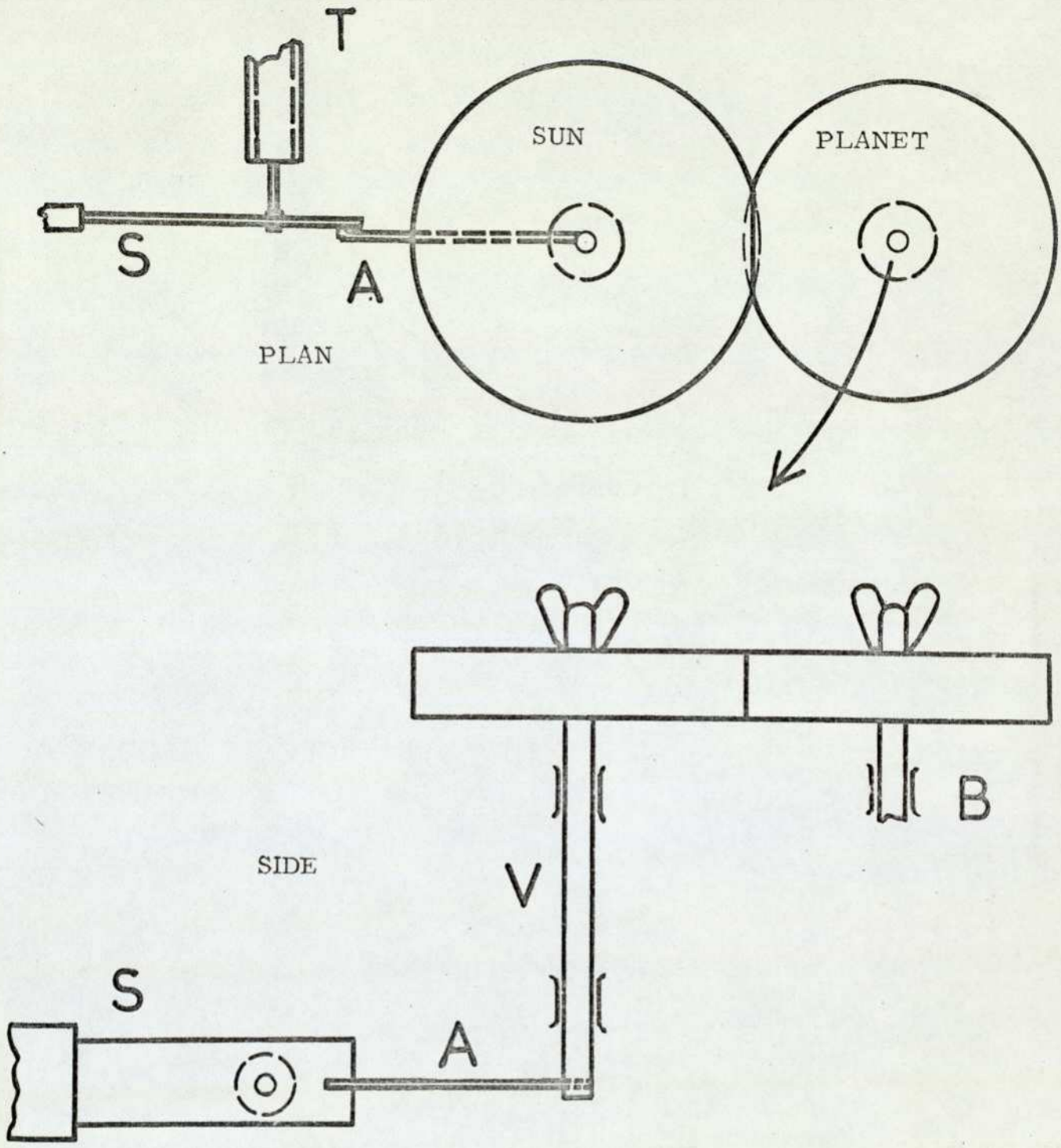

Figure 21 The Principle of the Rotary Tackmeter.

testpieces being held together in the same plane by a calibrated compression spring, and the planet is rotated concentrically around the sun. Hence the planet specimen attempts to drag the sun around with it, the magnitude of this tendency being dependent on the tack between the specimens. The magnitude is represented by the resulting distortion of the calibrated leaf spring, measured with a transducer system. The principle is shown schematically in plan and side-view in Figure 21.

The measured test force also includes a small energy loss (section 1.1) component. Other corrections which are applied to give the final tack strength value involve both the time of contact and the velocity of separation of the two surfaces. These parameters are calculated from the orbiting rate of the planet and the mutual depression of the rubber testpieces, the depression being measured by a Moiré fringe system.

As outlined in section 5.2, a peel test would be overwhelmingly preferable to a test in the tensile mode were it not for the variation in contact time arising from the time taken in testing. In the Rotary Tackmeter:-

(a) The mode of testing is separation by peel. Moreover, the use of rotating cylindrical testpieces means that contact is made at a definite interval before separation, so that, for each test, contact time is constant and short.

(b) The use of small testpieces enables relatively high contact pressures to be applied and means that the separation force is easily measurable.

(c) A dynamic equilibrium occurs between forces from the part of the rubber testpiece being compressed, the trailing edge of the testpiece at which separation occurs and the leaf-spring which is part of the measuring system. As the testpieces are being simultaneously subjected to contact and separation on a continuous basis, this equilibrium condition should be more stable than those conditions imposed suddenly by static tests.

6.2.2 Development

As a first development stage, the present author assembled a crude prototype model mainly from a Meccano construction set and a clock spring to demonstrate the viability of the principle. The testpieces used were normally employed in another form of rubber testing. An approximate reading of magnitude was given by the movement of a pointer around a clock face, corresponding to the degree of torque in the clock spring caused by the tack between the testpieces. The principle was the same as that in Figure 21 with the clock spring and the pointer replacing leaf spring S and transducer system T respectively. The reading caused by natural rubber (NR) testpieces was greater than that for a styrene-butadiene copolymer (SBR) and substantially greater than the level for an ethylene-propylene copolymer (EPM), an overall result agreeing with the observations of personnel handling these materials.

Following the broad success of the crude prototype, the principle and requirements were presented to the Engineering Department, Dunlop Research Centre, and a basic Mark I rotary tackmeter was duly constructed. However, whilst experimenting with this model, the

The Mark I rotary tackmeter

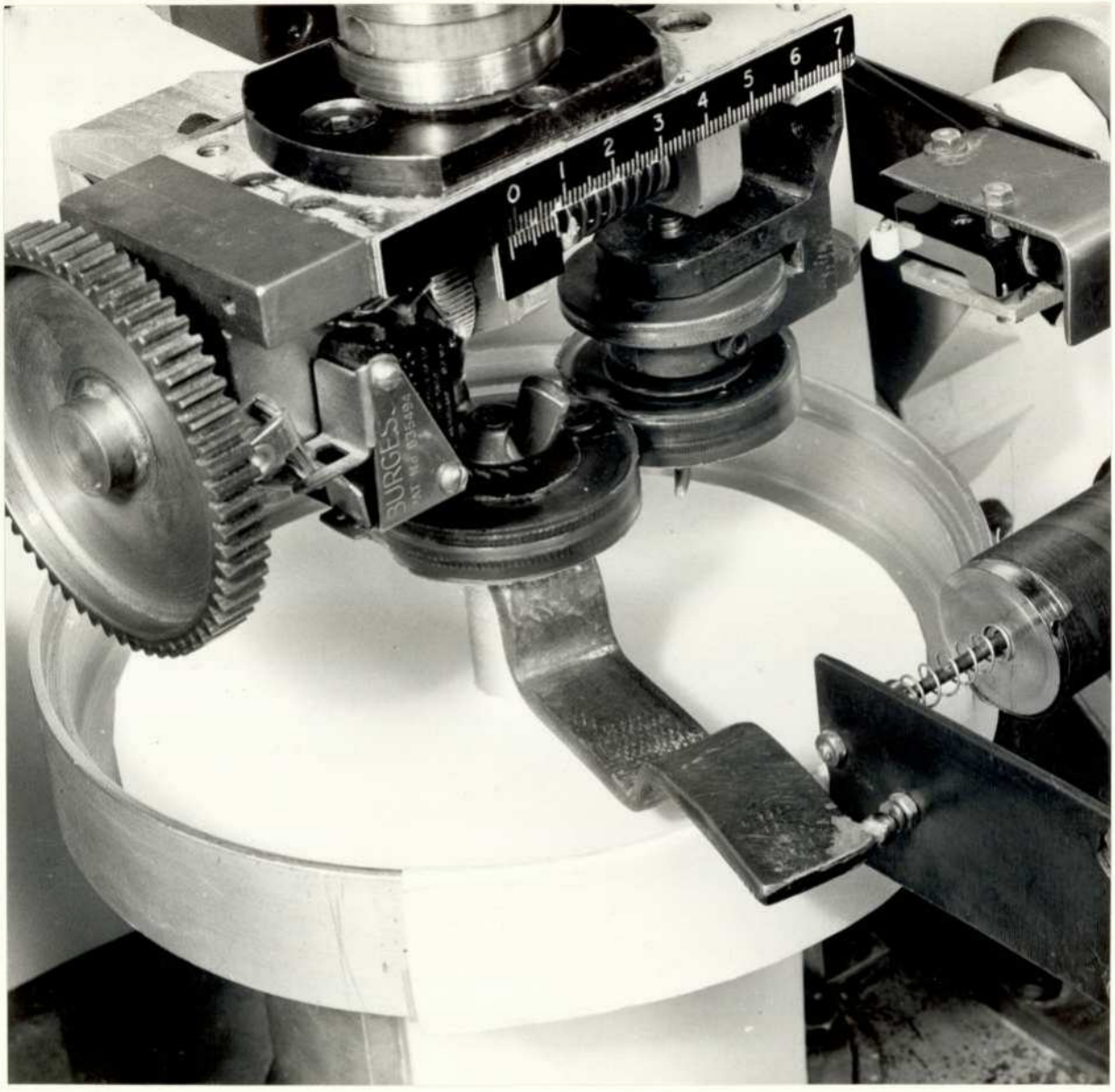

RFU 21456

Plate 3

writer calculated the relationship (see later) of factors such as contact time and velocity of separation with the mutual depression Δ of the rubber testpieces when in contact, and constructed both a simple device for measuring Δ and a leaf spring/transducer system for assessing the tack force. The tackmeter in this form is illustrated during testing in Plate 3. Subsequently the need was established for greater accuracy in the measurement of Δ and, for this and other reasons of improvement, a second model was designed and constructed by Toon, Springer et al[138] to the specifications of, and in frequent consultation with, the present author. This second model is the Dunlop Rotary Tackmeter in its present form.

As the principle of the two models was basically the same, a separate description of Mark I is unnecessary. However, because of the greater simplicity of the first model, an understanding of the description of the present tackmeter may well benefit by some reference to Plate 3 which illustrates Mark I.

6.3 Description and use of the tackmeter

This section is related to Figure 21 and Plate 4. To aid the description, certain labelling letters are used which refer to these two illustrations only.

The cylindrical testpieces of radius ca 20 mm and height 10 mm are described later: they comprise steel centres with peripheral rubber surfaces. The sun testpiece is clamped horizontally to a vertical spindle V, which passes through two bearings in the centre of a large horizontal circular table D. When testing, a 75 watt D.C. electric

The Mark II model

RPU 22728

Plate 4. The present Dunlop Rotary Tackmeter.

motor transmits a drive to the edge of D causing the table to rotate. To carry the planet system, a small rectangular table G is situated on the circular table D by means of a horizontal PTFE slide-bearing which is positioned such that G can move radially. The planet test-piece, positioned in the same horizontal plane as the sun, is supported on a freely-rotating bearing B which is mounted on the sliding table G. A compression spring is mounted on D on a radius through the sliding table G and pushes on G in such a way that the planet test-piece is permanently constrained to move inwards towards the sun testpiece. The two testpieces are held apart against the compression spring by a screw clamp E, this being the situation at all times except when actually testing.

The force of contact due to the compression spring is pre-set before testing by a knurled nut on a screw thread using the previously-calibrated scale C.

To start testing, the electric motor rotates table D to cause the planet testpiece to orbit the sun, the testpieces being not yet in contact. A variable transformer is used to obtain the required revolutions per minute n'(shown on the tachometer). At this point the planet is not revolving around its own axis. With D in motion, a small motor M attached to the underside of D removes the screw clamp E by rotating a large cog attached to E. Hence the planet is already rotating (orbiting) at the required value of n' (normally 4 r.p.m.) as it moves steadily inwards towards the sun at a radial speed of ca 10 mm/min. until contact is eventually made.

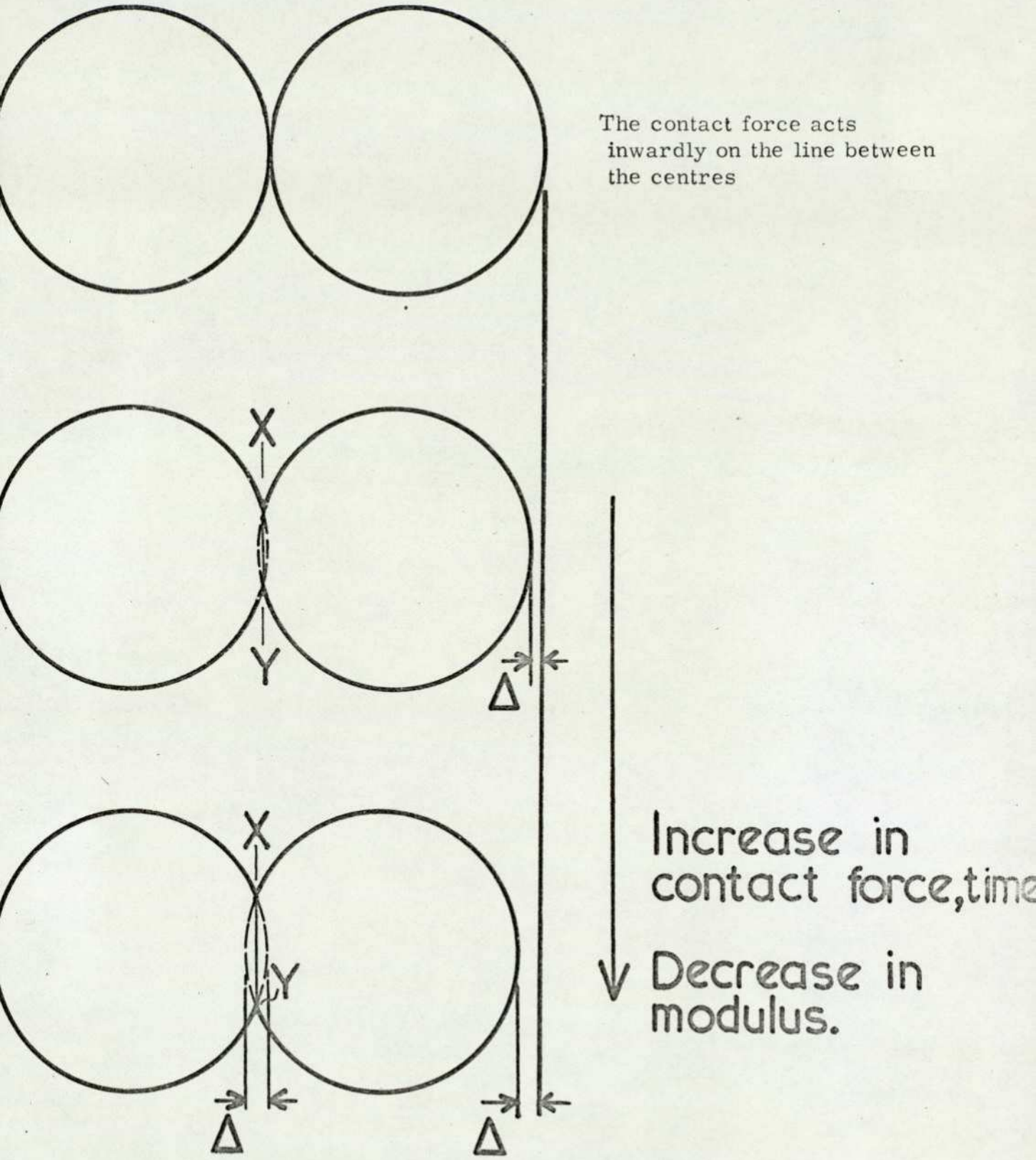

Contact occurs along XY, which increases as Δ increases.

Figure 22 The Mutual Depression Δ of Rotary Tackmeter rubber testpieces.

At the point of initial contact, the sun testpiece takes the place of the screw clamp in acting against the compression spring. The force of contact now relates to the setting on the calibrated scale. The testpiece rubber regions are compressed until, braced by the steel centres, the rubber modulus can resist the contact force. The degree of compression (schematically described in Figure 22) has been termed the mutual depression Δ .

As rotation continues through the contact stage, the planet commences revolving around its own axis on bearing B. The planet testpiece tends to drag the sun testpiece around (largely due to the tack between the testpiece surfaces), the tendency being transmitted to the leaf spring S by the spindle V and steel arm A. (The appearance of typical testpieces during testing is shown in Plate 5.) The distortion of S gives the test magnitude on the Multimeter scale of the transducer system T. The force measured is termed "drag". A dynamic equilibrium is quickly set up between the contacting forces, the drag and the measuring forces.

The term "drag" is necessary because at this stage:-

(1) The forces applied during calibration act in a different direction from that of the tack force during testing. The correction necessary is discussed in section 6.3.2.

(2) A small energy loss component is included.

The energy loss component arises from the compression of the rubber as each region of the testpiece passes through the contact stage. This component of the drag forces is determined by re-testing

Rotary Tackmeter testpieces during testing

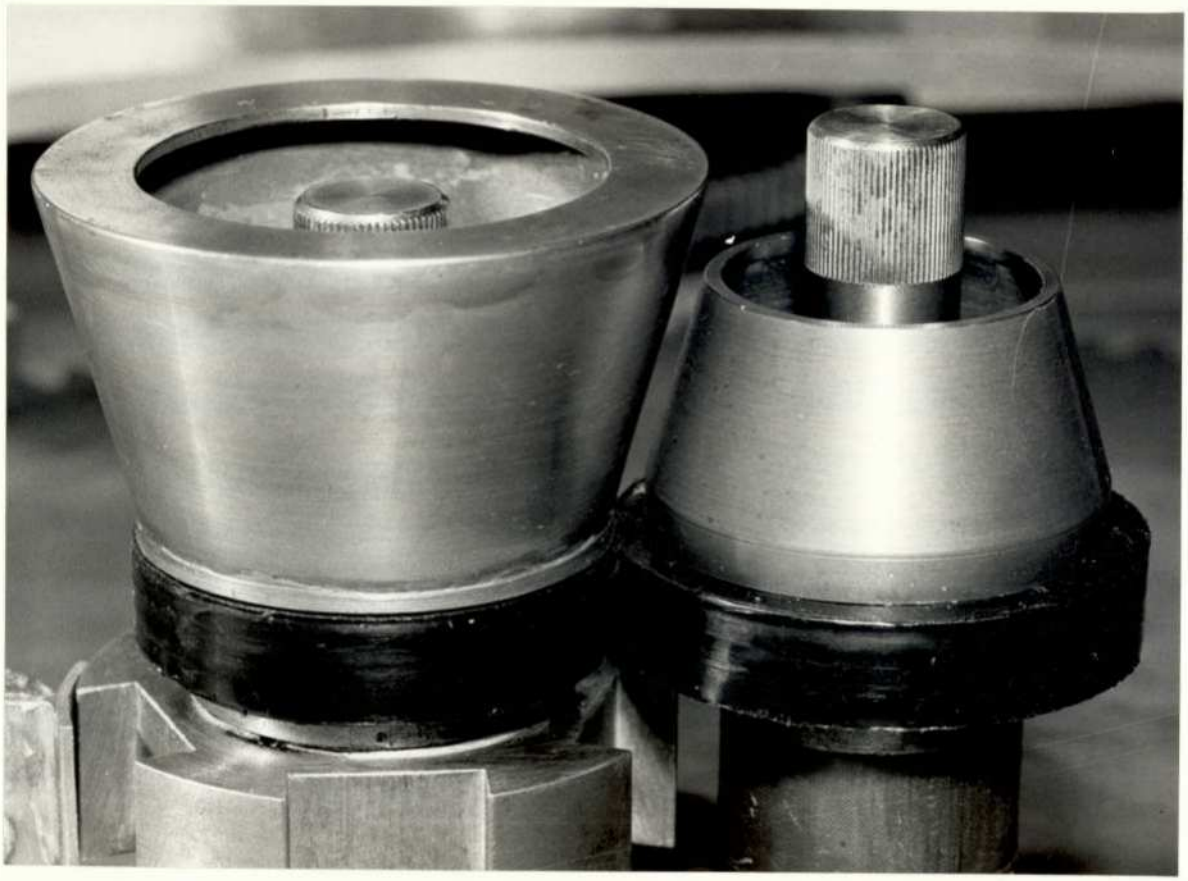

RPU 22925

Plate 5

replicate testpieces which are completely free from tack (a condition brought about by thoroughly dusting the testpiece surfaces with french chalk): the resulting measured value involves both compression and relaxation and is therefore twice the energy loss component associated with tack testing.

The magnitude of Δ is obtained by difference. Before testing commences, the screw clamp E holding the testpieces apart is set to a reference point. By substituting steel "replicates" for the testpieces the constant distance d_o moved by the planet until contacting the sun has been accurately measured by the technique described in the next paragraph. (Alternatively, d_o can be measured using rubber testpieces which only just touch, to allow for shrinkage after moulding.) When replacing the steel "specimens" by rubber testpieces, the planet moves a further distance Δ from the reference point as the rubber regions are compressed.

The distance moved from the reference point is measured directly from the relative motion of two parallel diffraction gratings. One grating is attached to the underside of the sliding table G whilst the second grating is fixed adjacently to the main table D. The gratings are part of a reversible Moiré fringe system, which operates so that any movement radially inwards towards the sun is recorded in cm x 10^{-3} on a three-decade counter. The system was designed and constructed to the necessary fine limits by Hiron and Springer[140]. Hence the value of Δ (generally between ca 0.4 mm and 1 mm) is obtained for any test run by subtracting d_o from the value shown on the counter.

The standard testing practice is to note the drag force and the reading giving rise to Δ during the first revolution of the planet testpiece but after the attainment of equilibrium conditions (i.e. when the value on the three-decade counter is constant). Thus tack measurement occurs on fresh surfaces. However, two exceptions exist to this practice.

(a) When $F_R \sim 1$, considerable distortion of the testpieces occurs, leading ultimately to the transference of all rubber to one testpiece. Hence the writer developed a technique to overcome this difficulty. At the first sign of such distortion, the operator applies an early reading technique by activating a system engineered[140] to hold the value on the counter and notes the Multimeter reading at the same time. As the geometrical considerations described below apply from initial contact onwards, the only departure from the norm is that the force of contact is less than the set value. However, the very fact of unit relative tack means that the critical force of contact has been exceeded.

(b) Further revolutions are permitted in experiments involving different values of the speed of separation u and the contact time t. In this case, use of elastomers of low tack and high strength means that the testpieces will not deteriorate with successive revolutions. A gradual build-up of "high-tack-points" on the surface has been avoided by utilising radii which differ slightly for the two testpieces, viz 22.2 mm (sun) and 20.0 mm (planet).

The experimental determination of tack strength merely requires the multiplication of the tack component force of the drag with a

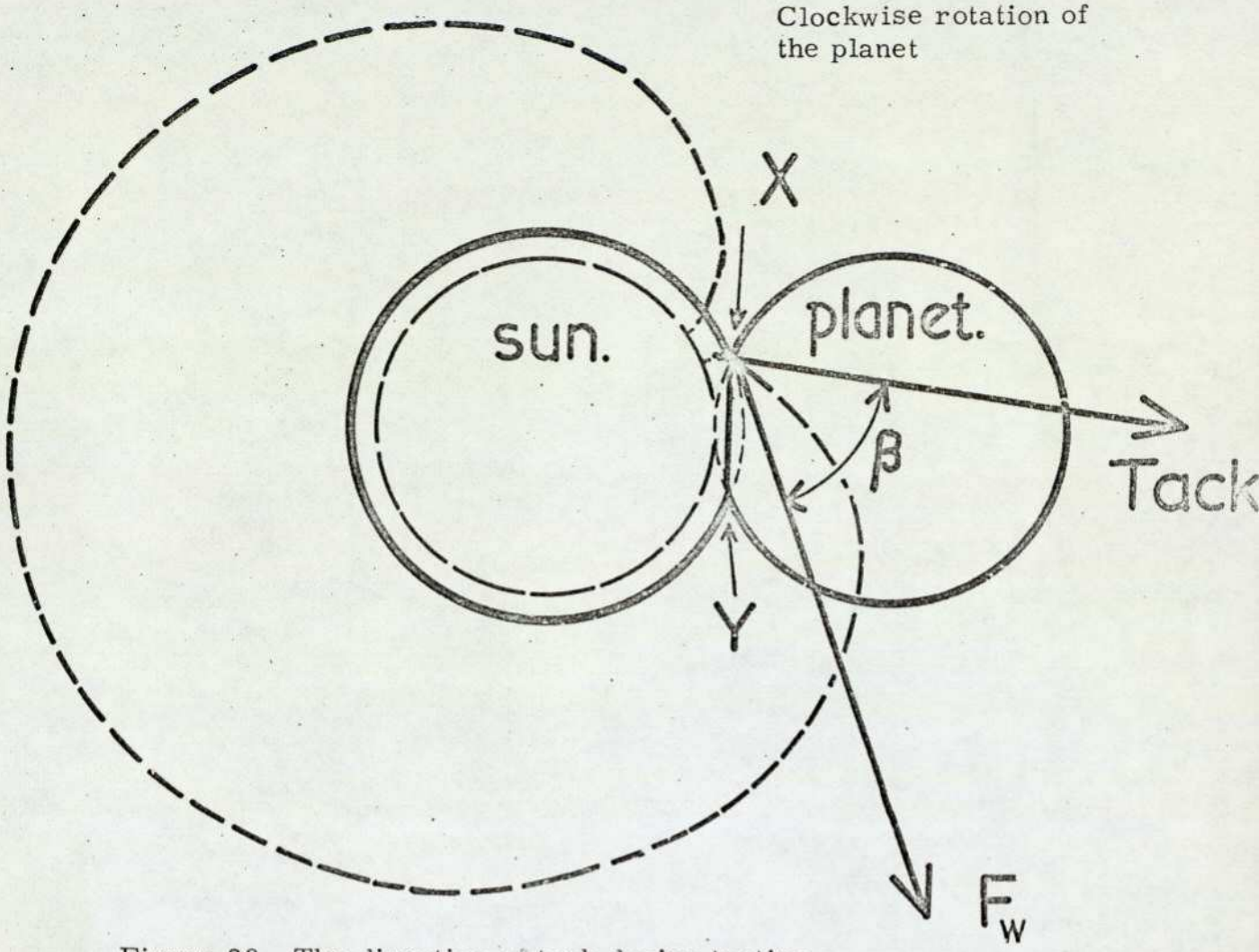

Figure 23 The direction of tack during testing.

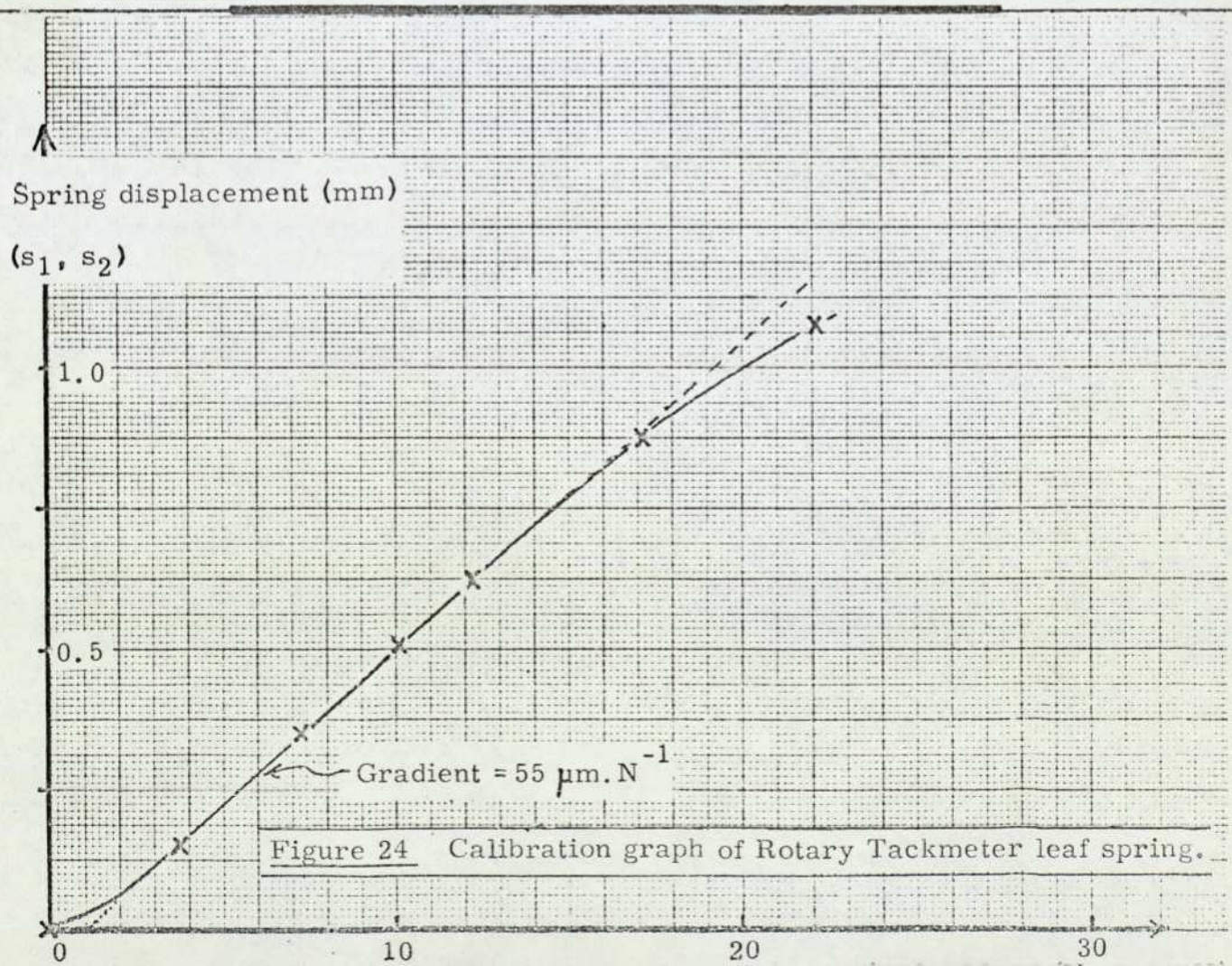

Figure 24 Calibration graph of Rotary Tackmeter leaf spring.

correction factor (Q) which is a function of Δ. The theory behind Q is simple, but rather lengthy, as shown in the following sections. However, the use of a mastergraph of Q versus Δ makes the experimental procedure quick and easy.

6.3.1 The magnitude of the tack component from the measured value of drag

The drag (the force measured during tack testing) is described by:-

Drag = Tack Component F_w + Energy Loss Component H.

The energy loss H acts along the 'chord of contact' XY (Figure 23). It can be shown that $H \propto \Delta^{3/2}$ to a first approximation. On page 95 it was noted that H was directly obtainable by halving the measured value from replicate testpieces rendered non-tacky by coating with french chalk. H is invariably the minor component, being ca 3%of F_w for elastomers of high tack: however, this proportion might increase to ~50% for elastomers which are practically 'non-tacky'.

At the measurement stage, the units on the Multimeter scale represent spring displacements. For later use (in Table 8 and section 7.1), the displacement due to the Drag has been termed s_1 and that from the second run on non-tacky testpieces involving the Energy Loss only (2H) has been designated s_2.

6.3.2 Calibration of the tackmeter

For calibration purposes, a metal "sun" testpiece of normal dimensions was attached to the tackmeter, and using a cord, pulley system and weights, a series of tangiential forces was applied to the sun. The displacement of the leaf spring S (Figure 21) resulting from the application of each weight was noted from the Multimeter scale, the resulting graph (largely of linear gradient 55 $\mu m.N^{-1}$) being shown in

Figure 24. The substitution of displacements s_1 and s_2 into Figure 24 gives respective values for the Drag and '2H'in newtons. Then

$$F_w = \text{Drag} - H$$

However, the direction applicable to tack measurement is not that of F_w. The angle between the direction of the tangiential calibration force and the force of tack has been termed β (Figure 23). Then

$$\text{(Total) tack force} = F_w / \cos\beta \text{ - - - - - - - - - - - - - - - 6.1.}$$

To describe the direction of tack, i.e. the direction of separation of the testpiece surfaces immediately after the contact region, consider two metal (incompressible) testpieces of identical radius and in rolling contact. During one complete orbit of the planet around the sun, the locus of any point on the peripheral surface of the planet takes the form of a cardioid. With two rubber testpieces of identical radius, the locus of a surface point remains cardioidic, but with the cardioid based on a reduced radius ($R - \Delta$) due to the compressibility of the rubber.

The existing situation comprises rubber testpieces of radii which differ by 10%. The locus of a planet surface point when orbiting, but away from the contact region, is described by an epicycloid of similar shape to a cardioid. Consequently, each point on the planet surface passes through the contact region during testing until separation occurs at X whereupon the surface point moves in the direction described by the tangent to the epicycloid at X. The angle between the direction of separation and the tangent at X to the sun testpiece is β, which is now derived in terms of radii a and R (R relating to the sun) and depression Δ.

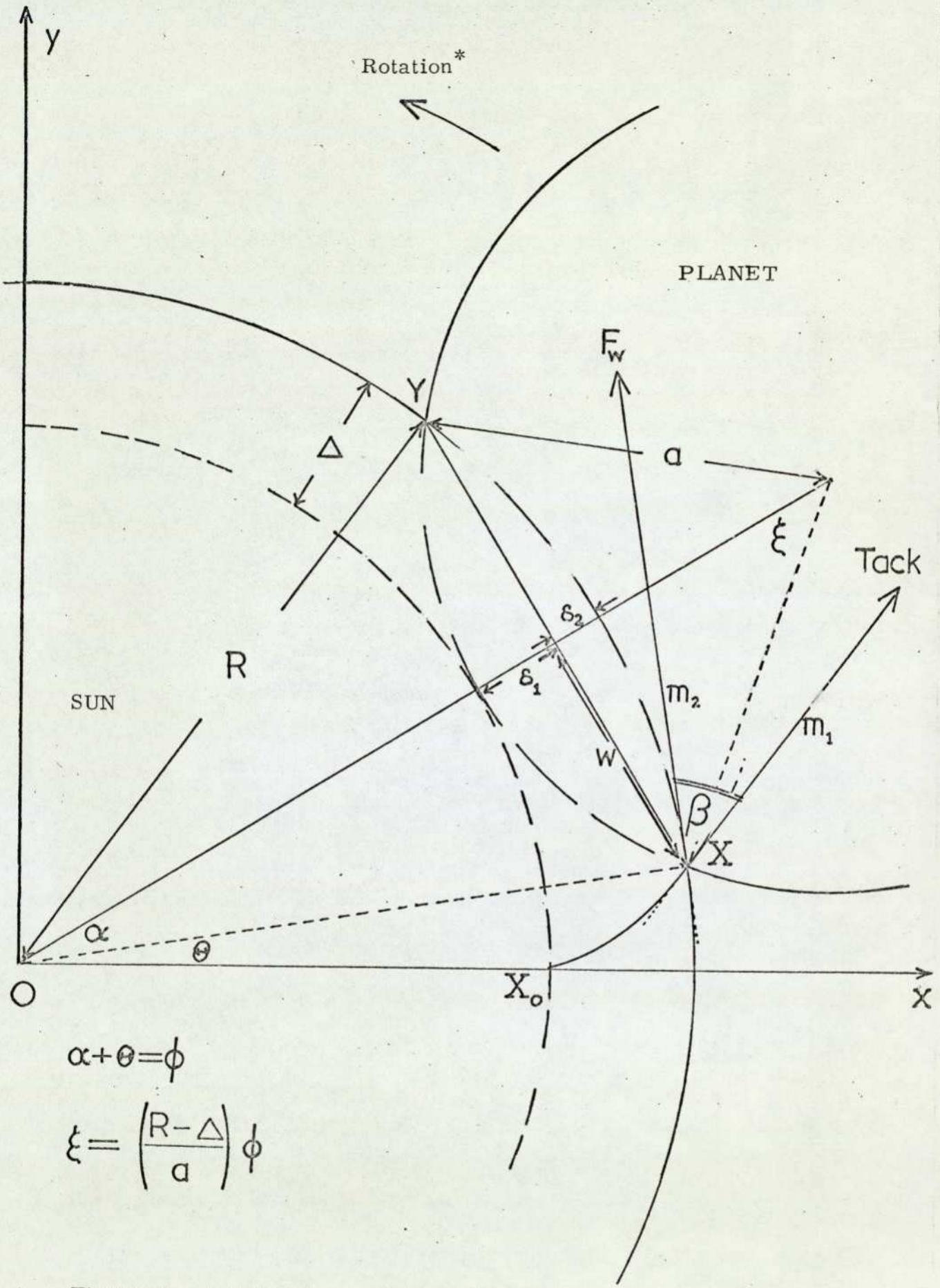

Figure 25 A detailed description of the direction of tack during testing.

* Reversed for convenience so that values of x and y are both positive.

Let the gradient of the tangents at X to the epicycloid and sun test-piece be m_1 and m_2 respectively.

Then $\tan\beta = \dfrac{m_2 - m_1}{1 + m_1 m_2}$ so that the problem is reduced to determining m_1 and m_2. In Figure 25 (a more detailed version of Figure 23) the arc X_oX of the epicycloid subtends angle Θ at the centre O of the sun testpiece, and the semi-width w of contact subtends angle α at O. Whereas m_2 is simply $-\cot\Theta$, the calculation of m_1 is rather more complex. For convenience let $(\alpha + \Theta) = \phi$ so that, as α is constant throughout a test-run, $d\Theta = d\phi$. To describe the epicycloid,

$$x = (a+R-\Delta)\cos\phi - a\cos((a+R-\Delta)\phi/a)$$

$$y = (a+R-\Delta)\sin\phi - a\sin((a+R-\Delta)\phi/a)$$

Thus, after deriving $dy/d\phi$ and $dx/d\phi$,

$$\frac{dy}{dx} = \frac{\cos\phi - \cos((a+R-\Delta)\phi/a)}{\sin((a+R-\Delta)\phi/a) - \sin\phi}$$

$$= \frac{1 - \cos((R-\Delta)\phi/a) + \tan\phi\sin((R-\Delta)\phi/a)}{\tan\phi\cos((R-\Delta)\phi/a) + \sin((R-\Delta)\phi/a) - \tan\phi}$$

At X, $dy/dx = m_1$ and in this unique position

$$\cos((R-\Delta)\phi/a) = (a - \delta_1)/a \quad \text{and} \quad \sin((R-\Delta)\phi/a) = w/a.$$

The ensuing substitutions and simplifications to obtain m_1 are outlined in Appendix 1. The same appendix covers the subsequent determination of $(m_2 - m_1)/(1 + m_1 m_2)$ to give $\tan\beta$, further simplifications being performed to define finally β in its most useful form

$$\cos\beta = \frac{2a + R - \Delta}{2R}\left(\frac{\Delta(2R-\Delta)}{a(a+R-\Delta)}\right)^{\frac{1}{2}}$$

Substituting the values (for convenience in cm rather than mm) of a and R for the testpieces invariably used, viz a = 2.00 cm and R = 2.22 cm, and ignoring powers of Δ greater than one, gives

$$\cos\beta = 1.016\,\Delta^{\frac{1}{2}}(1 - 0.15\Delta) \text{ ---------- } 6.2.$$

6.3.3 Theoretical assessment of testing parameters

An earlier section (4.5) has included a discussion on factors generally considered to influence the magnitude of tack and autohesion. In testing terms, the dominating factors are contact force, contact time and speed of separation. The speed at which the Rotary Tackmeter testpieces initially touch is not a variant, being constant and slow enough to avoid permanent rubber deformation.

CONTACT FORCE

Whereas the time and separation speed factors are concerned with diffusion aspects during the tack process, the contact force was seen earlier to influence the degree of contact occurring between the two participating surfaces. The attainment of intimate contact results from the degree of viscous flow which can occur within the contact time, the phenomenon depending on force. Two series of tack tests using different contact forces have been performed using replicate testpieces of the same elastomer: results are presented in section 7.2.1. The existence was shown of an empirical critical level of force above which further increases in force resulted in negligible increases in tack magnitude, a condition implying that contact is as intimate as can be expected. Rotary Tackmeter testing is normally performed under such a condition of force.

CONTACT TIME AND SPEED OF SEPARATION

Consider Figures 23 and 25 which schematically illustrate the two testpieces being compressed whilst testing. In practice the application of compressive forces necessarily displaces some of the rubber bulk. However, the design of the testpieces is such (section 6.3.5)

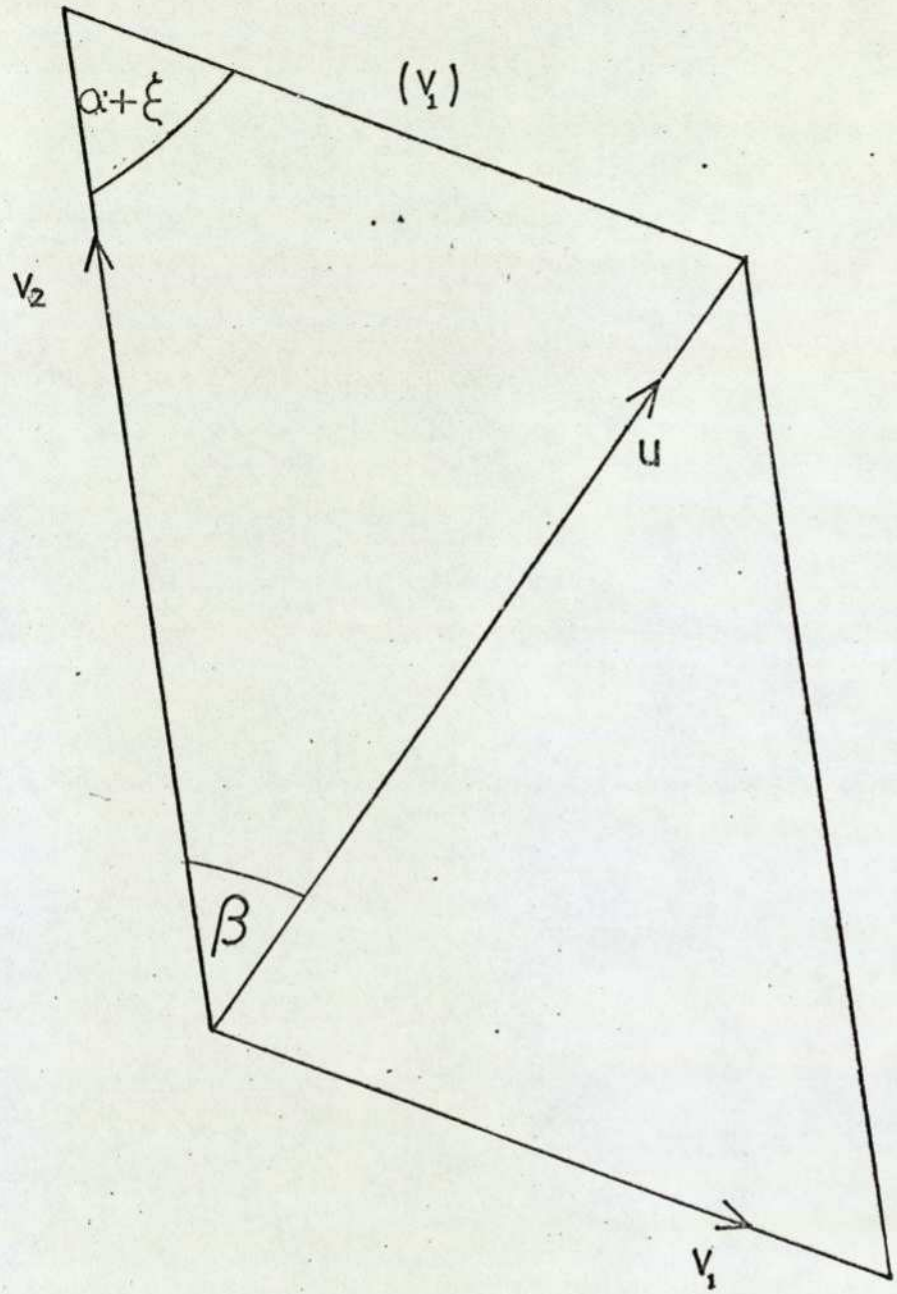

Angles described in Fig. 25

Figure 26 The vector diagram at the point of testpiece separation.

that displacement largely occurs away from the test surface.

To obtain the contact time t, the contact width XY (Figure 25) between the testpieces was compared with the total distance $2\pi R$ travelled per revolution by the peripheral surface of the planet when contacting the sun testpiece, the ensuing ratio being multiplied by the time per revolution, $60/n'$ seconds. The main problem of the accurate assessment of XY (or 2w) can be solved geometrically as outlined in Appendix 2. The solution is

$$2w = 2\left(\frac{2aR}{a+R}\right)^{\frac{1}{2}} \Delta^{\frac{1}{2}} \left(1 - \frac{\Delta(a^2-aR+R^2)}{4aR(a+R)}\right)$$

$$\therefore \quad t = \frac{60}{n'}\left(\frac{2w}{2\pi R}\right) = \frac{60}{n'\pi}\left(\frac{2a}{R(a+R)}\right)^{\frac{1}{2}} \Delta^{\frac{1}{2}} \left(1 - \frac{\Delta(a^2-aR+R^2)}{4aR(a+R)}\right)$$

In practice $R = 2.22$ cm and $a = 2.00$ cm. Hence

$$t = \frac{(12.5)}{n'} \Delta^{\frac{1}{2}} (1 - 0.06\Delta) \text{ - - - - - - - - - - - - - - - - - - } 6.3.$$

To find the magnitude of the speed of separation u, one considers the vector diagram describing the motions at point X in Figure 25. The vector diagram is shown as Figure 26. The term v_2, acting along the tangent to the sun testpiece, represents the velocity (at the instant of time being considered) of the motion of the trailing edge of contact. Velocity v_1 acts tangientially to the planet, being the peripheral velocity of this testpiece.

The angle between v_1 and v_2 can be seen from Figure 25 to be $180^\circ - (\alpha + (R - \Delta)\phi / a)$. The resultant velocity u makes angle β with v_2: if the vector diagram (Figure 26) is considered, the concurrency of this angle and angle β already determined geometrically is confirmed (as outlined in Appendix 1). The calculation based on this

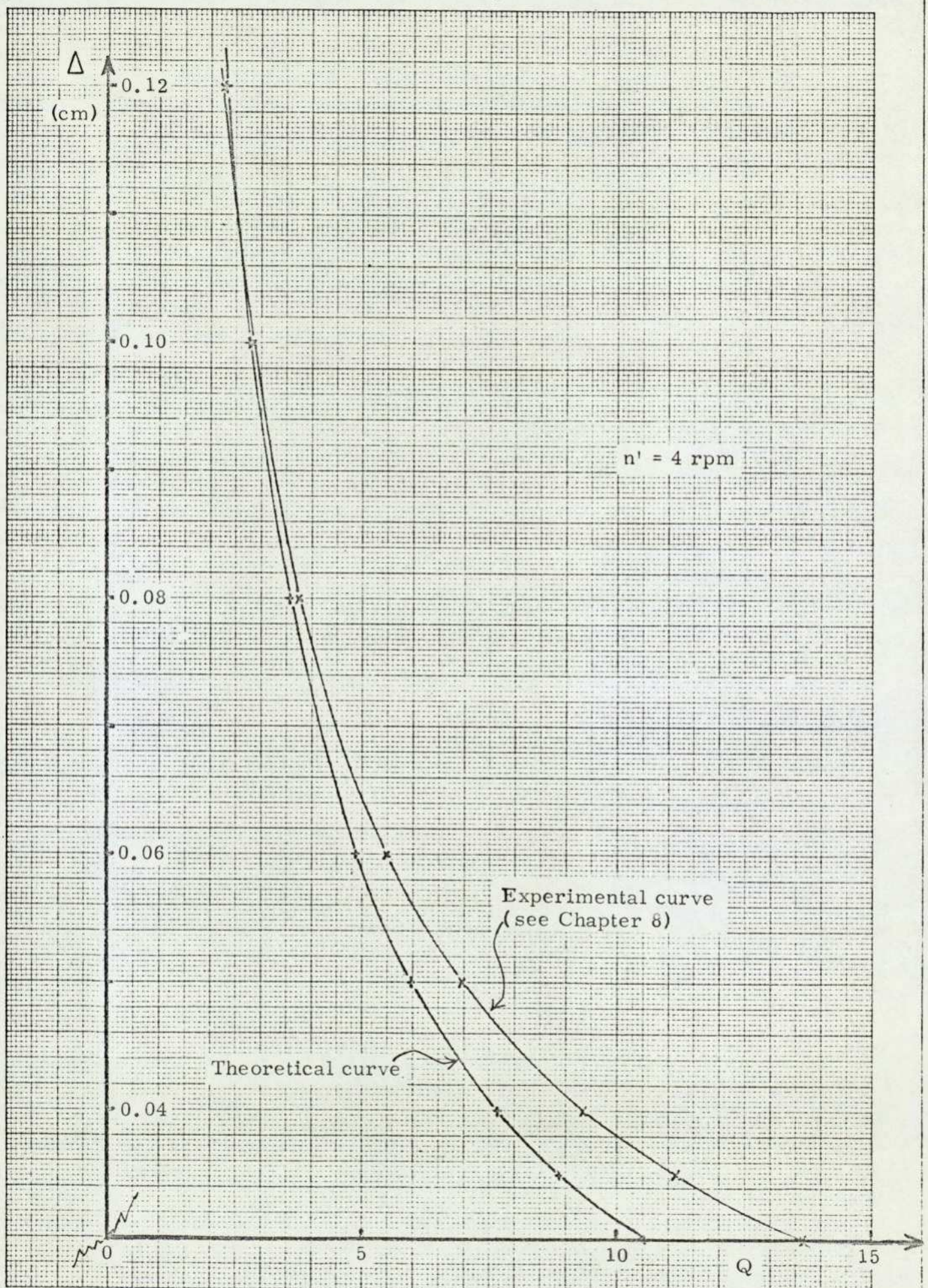

Figure 27 The overall correction term Q plotted as a function of Δ .

vector diagram to find velocity u is given in Appendix 3. The solution is

$$u = 0.32\, n' \Delta^{\frac{1}{2}} (1 - 0.23\Delta) \text{ - - - - - - - - - - - - - - - - - - 6.4.}$$

6.3.4 Tack strength at standard conditions

For most practical purposes, autohesive tack strength values are required at standard conditions of contact time and velocity of separation. From equation 4.22 et seq, for any test

$$\text{Tack force} = K\, ut^{0.25} \text{ where K is a constant - - - - - - - - 6.5.}$$

The performing of a number of test runs and the averaging of the resulting values of u and t gave the following values which have been taken as convenient standards:-

$u_{st} = 0.35 \text{cm.s}^{-1}$, $t_{st} = 1\text{s}$, so that Tack_{st} is F, the tack strength representing the particular elastomer at standard testing conditions. Therefore, if suffix m denotes conditions at measurement, from equations 6.5 and 6.1

$$F = \frac{0.35}{u_m t_m^{0.25}} \times \frac{(F_w)_m}{\cos \beta_m}$$

$$= Q_m (F_w)_m \text{ - 6.6.}$$

The general term $Q = (0.35/ut^{0.25} \cos\beta)$ can be converted to $f(\Delta)$ for normal testing conditions using the expressions 6.2, 6.3 and 6.4 for $\cos\beta$, t and u. Then

$$Q = 0.57 / (n'^{3/4} \Delta^{9/8} (1 - 0.4\Delta)) \text{ - - - - - - - - - - - - - 6.7}$$

(Δ being in cm). Q has been plotted graphically against Δ (Figure 27) for the full range of Δ which has been met for $n' = 4$.

Hence, for a normal tack test, the tack component F_w of the drag is

Table 8

Typical calculations of tack strength at standard conditions from measured data

Elastomer	Multimeter scale readings		Associated forces				Depression readings				Tack strength
	Due to Drag	Due to Energy Loss	Drag+	Energy Loss+							
	s_1	s_2		$(2H)_m$	$(H)_m$	$(F_w)_m$	d_o	$(d_o + \Delta_m)$	Δ_m	Q_m++	$Q_m(F_w)_m$
	(μm)	(μm)	(N)	(N)	(N)	(N)	(cm)	(cm)	(cm)		(N)*
Milled NR	575	25	11.4	0.8	0.4	11.0	0.515	0.549	0.034	9.2	101
SBR 1500	1000	50	20.0	1.6	0.8	19.2	0.478	0.567	0.089	3.2	61
EPDM	250	30	5.5	1.0	0.5	5.0	0.515	0.588	0.073	4.0	20

Tested at 4 r.p.m. Normalised to standard conditions $u = 3.5$ mm.s^{-1}, $t = 1$s.

* More realistically N.(10mm)$^{-1}$, the dimension relating to the height of the testpiece.

\+ Using Figure 24. Energy Loss obtained on replicate testpieces. ++ Using Figure 27.

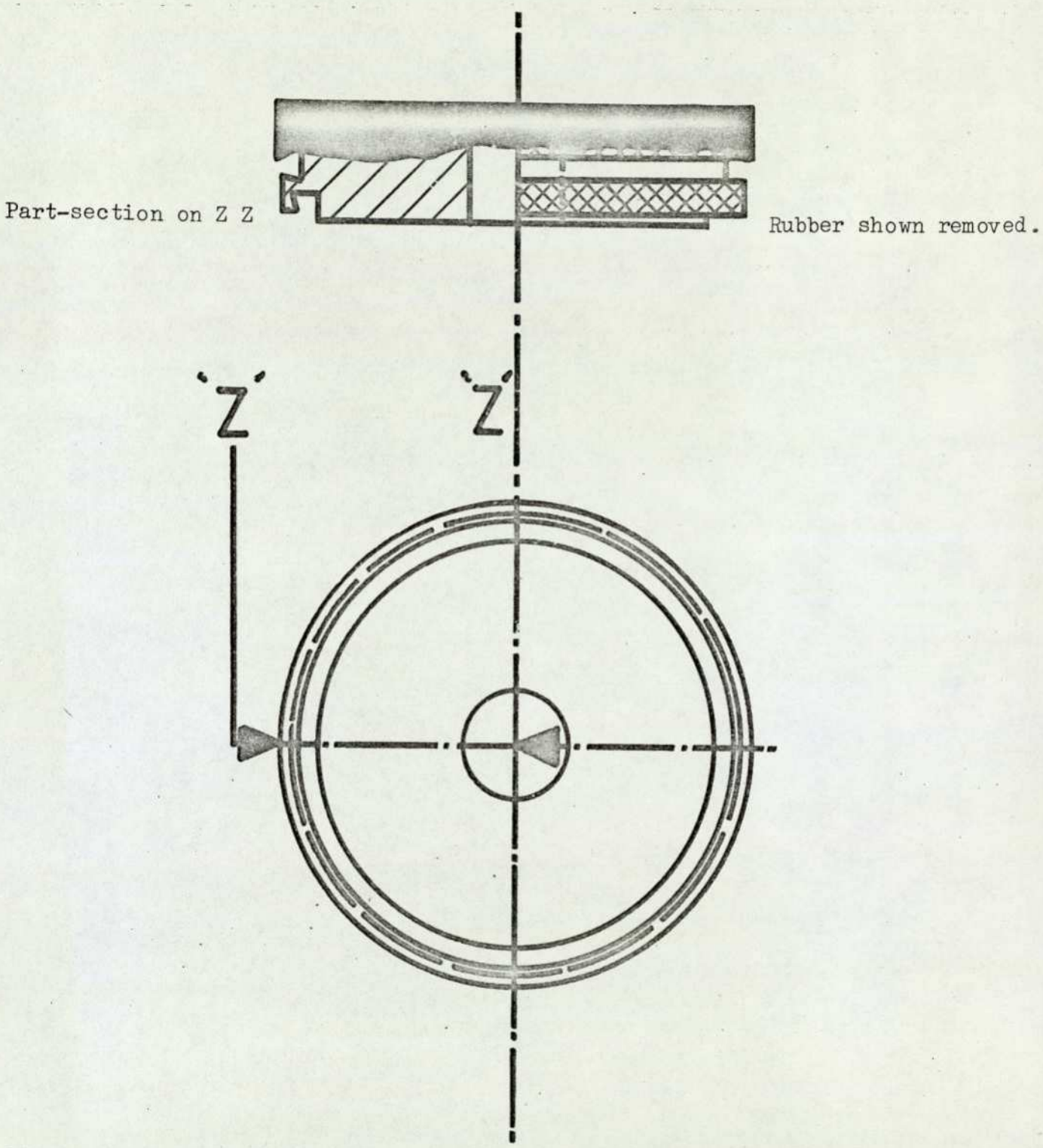

Figure 28 The construction of Rotary Tackmeter testpieces.

obtained by subtracting half the magnitude of the energy loss term measured in a repeat, non-tacky, test run. Multiplication of F_w by that term Q_m which (from Figure 27) applies at the particular depression Δ_m for the test run gives a value of tack strength at the standard conditions, $u = 3.5 mm.s^{-1}$ and $t = 1s$. Typical calculations are shown in Table 8 for three rubbers of widely-differing tack characteristics.

6.3.5 Testpiece preparation

As mentioned previously, Rotary Tackmeter testpieces (Figure 28 and Plate 5) are cylindrical, of radius 20 mm and 22.2 mm and height 10 mm. The testpieces are produced by a transfer-moulding technique under conditions of increased temperature and pressure: the peripheral surfaces of the testpieces are formed against a smooth polyester film ("Melinex").

Although methods of transfer moulding are well-established, the absence of crosslinks after moulding means that more refined techniques are required to retain the moulded shape of the uncured testpieces. Testpiece deformation was limited by the present author by arranging that each testpiece largely comprised a steel centre which was encompassed by a rubber layer of minimum thickness: in addition, high applied pressureswere sustained throughout the process until the moulded testpieces were cooled to ambient temperature.

As the weight of rubber used was only ca 4g, a danger originally existed of the testing force pulling the rubber away from the centres, with subsequent distortion of the rubber. The writer overcame the

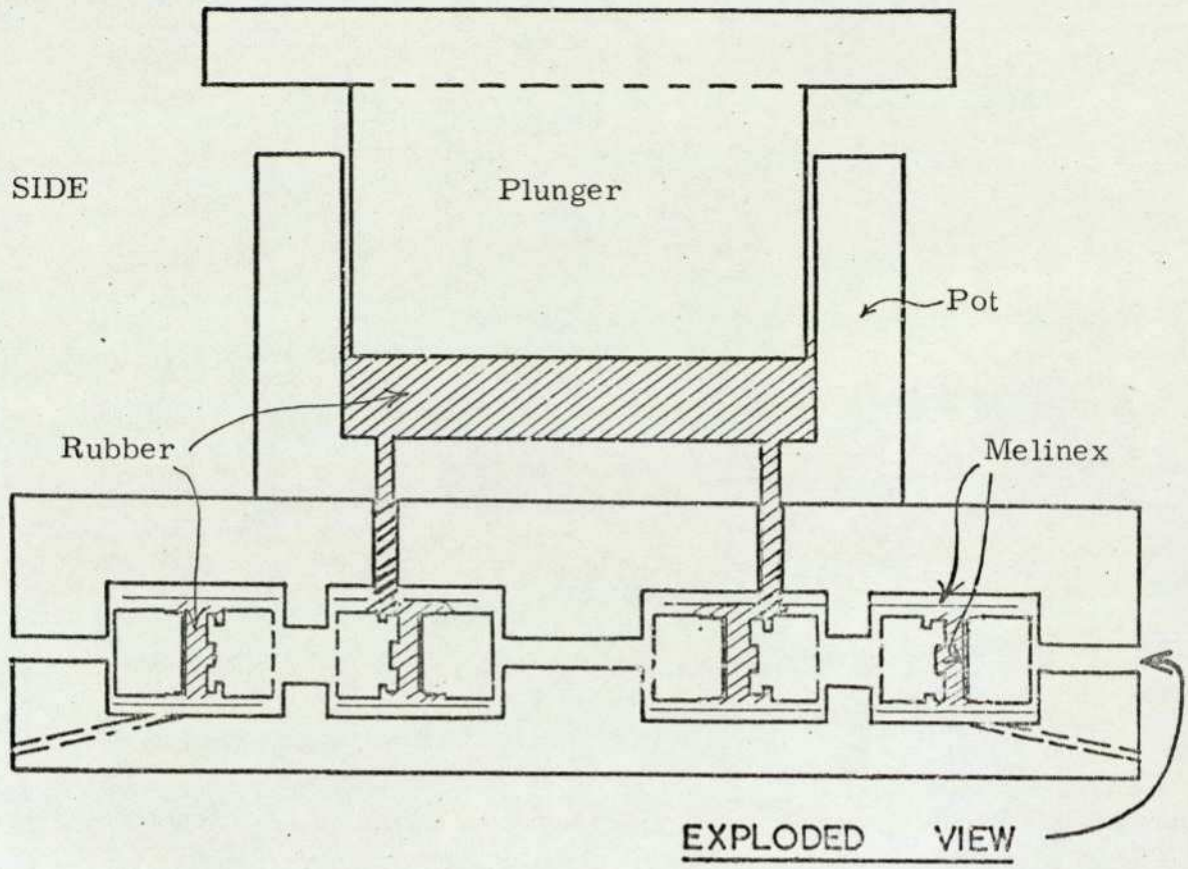

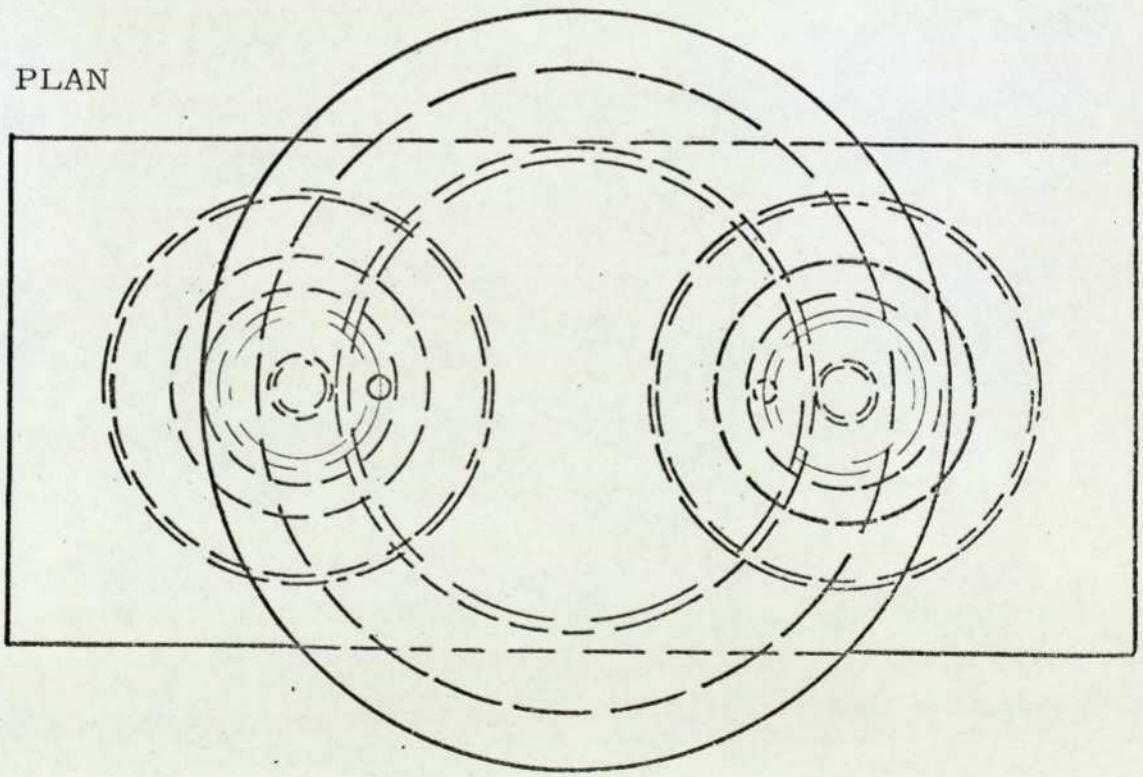

Figure 29 Transfer mould for producing Rotary Tackmeter testpieces.

problem by employing steel centres engineered to the shape shown in Figure 28 in order to enhance mechanical interlocking. This shape and the use of a rough (knurled) steel surface ensured that, during testing, the rubber layer invariably remained in contact with the steel centre.

The transfer-moulding set-up (shown in Figure 29) was constructed[138] to the design of the writer and consists of a steel 'pot-and-plunger' transfer assembly together with a two-chamber assembly in which the testpieces are formed. Each chamber contains a steel centre and has Melinex strips fitted around the peripheral surfaces. Melinex discs are also used to prevent the bases of the moulded testpieces adhering to the mould.

During moulding, the two assemblies rest together, suitable location pins ensuring that the transfer channels (of diameter ca 3 mm) are aligned. Experimentation showed that the channels functioned most efficiently when positioned exactly in the direction of the applied pressure, and that the channels in the chamber assembly should be of a slightly greater diameter. All mould components need to be pre-heated to ca 80°C and the uncured rubber (ca 40g) is similarly hot when fitted as a rough disc into the steel pot. The heat is obtained from the platens of a suitable press, which also applies the load (ca 100 KN) to the plunger as the next stage. The hot rubber is forced through the channels and completely around the steel centres, thus eliminating the formation of voids. The temperature involved and the time of transfer depend on the viscosity of the rubber: for a well-milled sample of natural rubber elastomer, heating for

0.5 minutes at 110°C is sufficient.

After the transfer stage, the mould is completely cooled by the circulation of cold water through the platens whilst the moulding pressure is maintained. On removal from the press, the mould is opened to reveal the testpieces which are then detached. The peripheral Melinex strips are peeled from the testpieces after mounting on the tackmeter, immediately before testing.

Testpieces produced in this way have been found to be consistently uniform and reproducible. Numerous tests have shown that unwanted separation between moulded rubber and steel centre now only occurs with materials for which the magnitudes of tack and bulk strengths are similar.

6.4 Critique of the Rotary Tackmeter

Whilst the Rotary Tackmeter possesses the several advantages already mentioned over more conventional tackmeters, some technical limitations apply in certain areas:-

(a) The time of contact t and rate of separation u cannot be varied independently.

(b) Because the initial stages of rolling contact involve viscous flow, an exact assessment of the contact time applying after reaching the critical contact force is difficult to make.

(c) Test temperatures depend on ambient temperatures which are not necessarily constant.

Limitation (b) applies to all tackmeters, but is only important at low contact times, such as those employed here. Despite this drawback

short contact times are still practically realistic and therefore preferable. Although (a) and (b) indicate that the separate influences on tack strength of t and u are not easily assessed on this tackmeter, good agreement has been found between experimental results and theory, for u especially (sections 7.2.1 and 8.1).

The particular design of the Rotary Tackmeter called for fine tolerances during manufacture to give the testing accuracy required: however, the resulting engineering difficulties have been largely overcome during familiarisation with the instrument. A crude assessment of the order of magnitude of the errors which might arise in readings observed during tack testing is included with other statistical considerations in section 7.1. Such comments become inadequate as F_R approaches unity when, in common with all other tackmeters, testpiece distortion enhances the errors involved: however, the early reading technique (section 6.3) minimises the effect. The final comment on the Rotary Tackmeter must depend on the degree of correlation with practical experience (see Chapters 7 and 8).

6.5 The experimental requirements

Because of the close connection of tack and tyre building and because this branch of the rubber industry invariably utilises non-polar rubbers, no measurements have been made on polar elastomers. Polarity aspects are excluded from considerations of the autohesive mechanism. (This restriction is not intended to suggest that the tack property does not apply to polar materials when employed in appropriate branches of the industry.)

The particular experimentation necessary to indicate the reliability of the tackmeter and to satisfy the experimental requirements listed at the beginning of the chapter is largely self-evident. However, experimental requirements (ii) and (iii) (page 86) do require further explanation.

Requirement (ii)

Cuneen[79] has shown that isomerised NR containing > 21% trans polyisoprene does not exhibit stress crystallization (Figure 6). Hence, if the optimum tack magnitudes of sufficiently-isomerised polyisoprenes are greater than those of all other elastomers, the explanation can only lie in enhanced self-diffusion characteristics.

Requirement (iii)

By measuring the uncured adhesion between two different elastomers which nevertheless are of similar critical surface tension γ_c, and selectively producing a unilateral diffusive flow by the use of suitable-different molecular weights, comment is intended on the microstructural model to be proposed later.

All measured test data are recorded in the following chapter and most are discussed in Chapter 8.

Chapter 7 Measured values of autohesive tack strength

All results of tack measurements made by the writer are recorded in this chapter. Test data refer to a contact force greater than the critical value (the force frequently relating to a mean contact pressure ~1MPa), and have been normalised (section 6.3.4) to a contact time of 1s and a separation speed of 3.5mm.s^{-1}, except when these factors are variants (section 7.2.1): similarly, the planet testpiece is invariably rotated at 4 r.p.m. around the sun. A single set of data measured by a colleague, but of considerable relevance, is included in section 7.1.

7.1 Statistical considerations

An irony of tack-testing is that the testing process itself can cause deformation and deterioration of the testpieces. It is, therefore, not surprising that the reproducibility between different test runs has been observed as being best for rubbers of low tack: however, their impractical nature does not warrant statistical studies. In a separate investigation[85], Kirkham of these laboratories statistically assessed Rotary Tackmeter results from ten pairs of testpieces moulded from a single milled piece of natural rubber (NR): the data are shown in Table 9.

Because the size of the 'statistical sample' in Table 9 is small, comment on the mean is best provided by 95% confidence limits[141].

If L_s is the 95% limit on either side of the mean,

n_s is the 'statistical sample', the number of testpiece pairs,

σ_s is the standard deviation,

t_s is obtained from a "student's t" table for $(n_s - 1)$ degrees of freedom to give a confidence of 95%,

then $$\pm L_s = \pm t_s \sigma_s n_s^{-\frac{1}{2}}$$

Table 9

85

Rotary Tackmeter test data for 10 replicate pairs of milled NR elastomer

Specimen No.	Autohesive strength $(N(10mm)^{-1})$
1	125
2	97
3	108
4	136
5	127
6	101
7	138
8	104
9	119
10	90
Mean	114.5
σ_s	16.8
L_s	12.0

There is a 95% statistical probability that the mean from any other such series of testpiece pairs taken from this piece of milled NR would exist within the limits $114.5 \pm 12.0\ N(10mm)^{-1}$. Hence the mean is apparently a genuine representation of the general magnitude of autohesion for the milled NR.

An alternative assessment of the errors involved in tack determination arises from reasonable uncertainties in the various measurements. To obtain an expression suitable for such an assessment, an approximate

solution for the tack strength F can be derived in terms of the original spring displacements s_1 and s_2 which apply to the Drag and Energy Loss (2H) respectively. The linear portion of the leaf-spring calibration graph in Figure 24 is of gradient 55 $\mu m.N^{-1}$ and, when extrapolated, intercepts the load axis at 1 newton. Hence

$$\text{Drag} = ((s_1/55)+1) = 0.0182\,(s_1+55)$$

Similarly $\quad 2H = 0.0182\,(s_2+55)$

$\therefore$ Tack Component F_w = Drag - H = $0.0091\,(2s_1 - s_2 + 55)$.

Combining expressions 6.6 and 6.7:-

$$F = 0.57\,F_w\,n'^{-3/4}\,\Delta^{-9/8}$$

to a good approximation, where Δ is the mutual depression of the testpieces and rotational rate n' is 4 r.p.m. for normal testing. Therefore

$$F = 0.00183\,(2s_1 - s_2 + 55)\,\Delta^{-9/8}$$

If the uncertainties associated with measured results can be indicated by using the prefix ∂, the uncertainty in F is given by:-

$$\%\,\text{Error} = \pm 100\left(\frac{\partial s_1 + \partial s_2}{2s_1 - s_2} + \frac{1.125.\,\partial\Delta}{\Delta}\right) \text{- - - - - - - - 7.1.}$$

Reasonable values for the uncertainties are 25 μm, 6 μm and 0.002 cm respectively, the difference in the two uncertainties read on the Multimeter scale arising from the different full-range settings employed. Insertion into expression 7.1 of the appropriate data from Table 8 for milled NR, SBR 1500 and EPDM gives errors of $\pm$ 9.4, 4.1 and 9.7% respectively: the percentage error is minimised when values of $(2s_1 - s_2)$ and Δ are both relatively high. The tack strengths calculated in Table 8 would therefore be better represented as 101 ± 9.5, 61 ± 2.5 and 20 ± 1.9 respectively for the three samples:

hence the autohesive differences between the samples are considerably greater than the experimental uncertainties.

Autohesive values under optimum conditions fall conveniently into definite regions within the numerically extensive range between high and low tack. Therefore, because the level of tack strength required for technological acceptance is quite well-defined (section 7.4), representative values for rubbers are obtained from two, three or four test runs only.

7.2 Factors influencing autohesive tack strengths

7.2.1 Experimental factors

CONTACT FORCE

(The contact force is applied non-uniformly over a contact area $\sim 65 mm^2$: its relationship with contact pressure is discussed in Chapter 8.)

Eight replicate pairs of testpieces were moulded from a simple elastomeric compound comprising SBR 1500 rubber and HAF carbon black (of particle size ca 25nm) added at a loading of 40 parts by weight per hundred parts of rubber (40 phr). Tack measurements were performed at different forces of contact, the results being given in Table 10.

Table 10

The influence of contact force on the tack strength of SBR 1500/HAF

Contact force (N)	20	30	45	52	55	70
Tack strength ($N(10mm)^{-1}$)	45	72 82	79	84 71	95	90

A similar exercise was performed on an EPDM elastomer of relatively low molecular weight, but substantial stiffness, caused by the presence of blocks of polyethylene due to a high ethylene content of 80%. The results are expressed in Table 11.

Table 11

The influence of contact force on the autohesive strength of high ethylene EPDM

Contact force (N)	22	36	45	53	58	64	67
Autohesive strength $(N(10mm)^{-1})$	15.0	12.0	14.0	20.5	20.5	20.5	21.0

In both instances, initially raising the contact force from low values increased the tack until a limiting level was reached. Above a critical contact force, the tack became largely independent of further increases in force. The critical contact forces were ~30N for the SBR compound and ~50N for the EPDM elastomer.

CONTACT TIME t AND SPEED OF SEPARATION u

These two terms are inter-connected. If Tack strength $\propto u^y t^z$ and $(F_w)_1$ etc. represent tack components measured at appropriate conditions, then (as will be shown in section 8.1)

at constant Δ,

$$(y - z) = (\log_{10}(F_w)_1/(F_w)_2)/\log_{10}(n'_1/n'_2) \quad \text{- - - - - - - - - - - - 7.1}$$

at constant n',

$$(y + z) = \{((2 \log_{10}(F_w)_3/(F_w)_4)/\log_{10}(\Delta_1/\Delta_2)) - 1\} \quad \text{- - - - - - - 7.2.}$$

The testpiece depression Δ is altered by varying the contact force at values above critical. The measurements recorded in Table 12 were obtained at rates of rotation (n') of 1 and 4 r.p.m. on an EPDM

elastomer. A low-tack elastomer was intentionally used so that one pair of testpieces could be used throughout (the first measurement being checked by a re-test after the completion of test runs 2 and 3).

Table 12

The measurement of the tack component of an EPDM pair of samples at two values of n' and Δ

Test run	Contact force (N)	n' (r.p.m.)	Δ (cm)	F_w (N)
1	67	4	0.083	3.35
2	61	4	0.065	2.40
3	67	1	0.081	2.05

The values of Δ were effectively the same in test runs 1 and 3. Hence the data could be substituted into equations 7.1 and 7.2. The resulting expressions simplified to

$$y - z = 0.354$$

$$y + z = 1.664$$

so that $y = 1.01$ and $z = 0.66$. The empirical solution

$$\text{Tack strength} \propto u^{1.01} t^{0.66}$$

is discussed in detail in section 8.1.

7.2.2 Molecular weight variations

NR and other cispolyisoprenes

The molecular chains of cis polyisoprenes such as NR are broken down by mastication on a mill (section 3.1.3). A single piece of NR elastomer was banded around a mill and continuously masticated at 90°C, samples being removed at regular intervals. The viscosity of

solutions in benzene of each sample (1 to 9) were measured and the molecular weight calculated using the expression[142]

$$[\eta]_{benz} = 1.85 \times 10^{-4} (M_V)^{0.74}$$

Measurements from a simple indentation plasticity test were also obtained. Bulk strength was measured in the tensile mode by testing "die C dumbells"[143] cut out of a flat moulded slab of each sample, and the most appropriate shape(s) of stress/strain curve (see Figure 20) noted.

Relevant details are given in Table 13.

Table 13

Experimental details of milled NR samples

Sample No.	Molecular weight M_V x 10^5	Wallace plasticity (units)	Bulk strength		
			Type of curve *	Mean yield strength P (kPa)	Breaking strength if >P (kPa)
1	8.4	51	5	290	558
2	7.8	47	4/5	145	240
3	7.0	42	4	110	140
4	6.5	38	3/4	143	150
5	5.6	31	2	120	-
6	4.6	24	2	135	-
7	3.8	17	1/2	111	-
8	3.6	16	1	104	-
9	3.1	12	1	66	-

* As described in Figure 20.

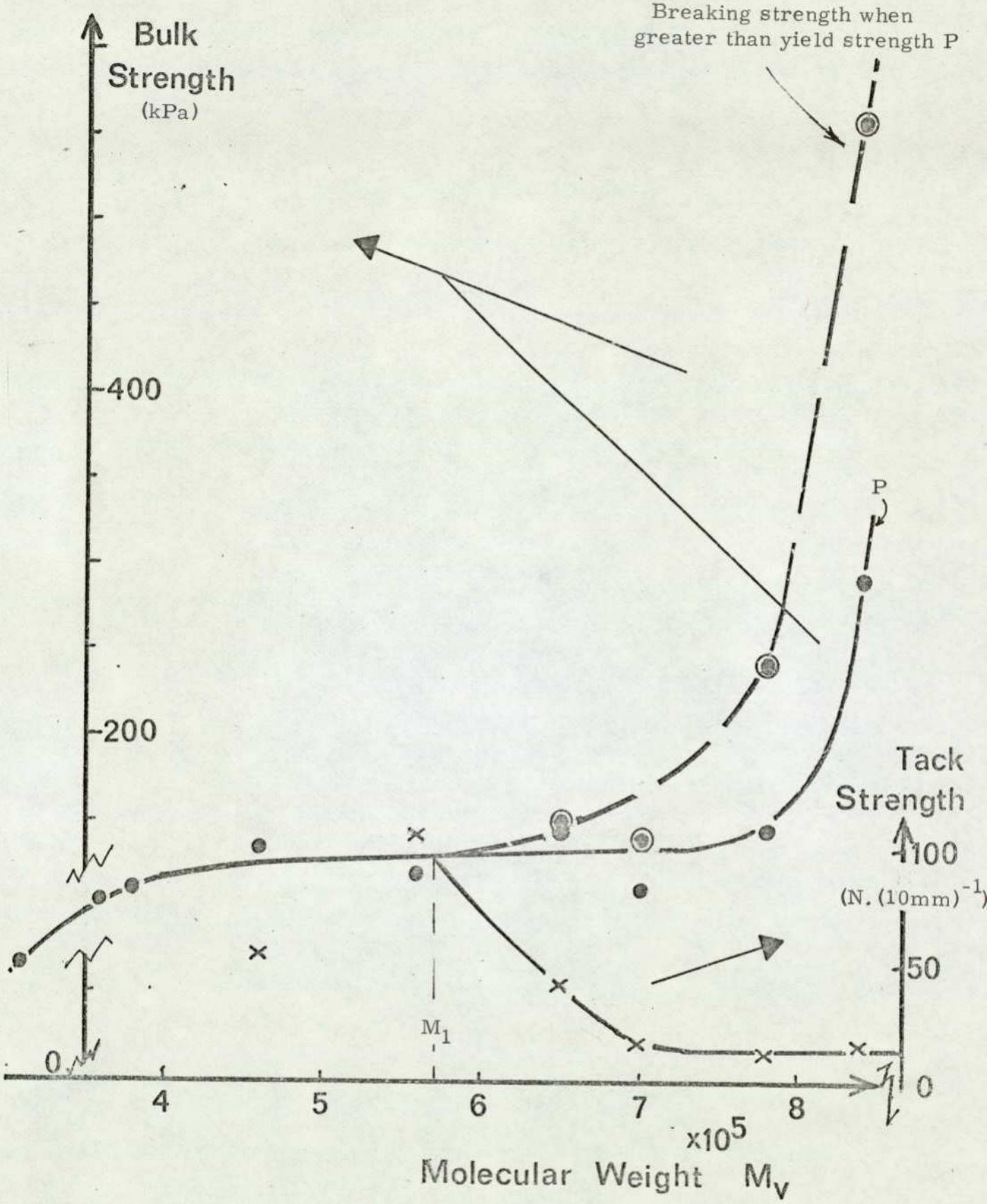

Figure 30 Plots of autohesive tack and bulk strength test data against molecular weight

Tack measurements were also made under standard testing conditions on samples 1 to 6, and are shown in Figure 30 as a function of molecular weight. The early reading technique (section 6.3) was necessarily applied to samples 5 and 6, great testing difficulties being experienced due to the similarity of bulk and tack strength (i.e. relative tack $F_R \sim 1$): not unnaturally, the tack-testing of samples 7 to 9 (of lowest molecular weight) proved to be impossible due to strength deficiencies. The results from samples 5 and 6 were used to equate empirically the units of test data from the Rotary Tackmeter and from standard tensile strength testing. Bulk strength values from Table 13 (both for yield point P and breaking strength when greater than P) are also included at a suitable scale in Figure 30. Decreasing the molecular weight M_V generally decreased bulk strength (especially when $M_V > 700,000$), the extra strength due to stress crystallization apparently disappearing when $M_V < 500,000$. (The variability which exists between some bulk strength measurements arose because post-moulding shrinkage gave rise to difficulties in assessing the cross-section of the die C dumbell.) In contrast, decreases in M_V increased the autohesive strength F, particularly when M_V was between 550,000 and 700,000

In a separate exercise, three tack tests were performed on another sample of NR elastomer which had been extensively milled so that $F_R \sim 1$. The average measured tack strength was 127 $N(10mm)^{-1}$.

Natsyn 2200, a synthetic cis polyisoprene ex Goodyear Rubber Co. polymerised with a Ziegler catalyst (a Ti/Al alkyl complex) has also been subjected to mastication at 90°C. Brief details of tack

measurements are given in Table 14. The increase in autohesive strength with decreasing molecular weight (i.e. with increasing milling time) is similar to that found with NR. The molecular weight of Natsyn 2200 ex bale was somewhat less than that of NR ex bale.

Table 14

Autohesive data from milled samples of synthetic IR

Milling time at 90°C (min)	Wallace plasticity (units)	Rotary Tackmeter autohesive strength (N.(10mm)$^{-1}$)
5	34	7
10	29	14
20	23	45
25	21	103 +

+ Samples ripped whilst testing i.e F_R is ~1.

A limited exercise under the same testing conditions also indicates the increase in tack strength which occurs on masticating a simple compound of NR and HAF carbon black (50phr). When just mixed, F was 21 N.(10mm)$^{-1}$, the value becoming 133 N.(10mm)$^{-1}$ after substantial milling.

IIR and EPM elastomers

For synthetic elastomers other than cis polyisoprenes, mastication alone does not significantly reduce molecular weight M. However, a reduction does occur if chemically-induced during mastication by the addition of certain organic peroxides, and a sample of IIR (with

unsaturation of 0.7% mole) has been subjected to this type of treatment. Brief mastication details and tack results are shown in Table 15. Although values for M and plasticity were not obtained, the physical state of the masticated elastomer confirmed that a full range of M had been covered.

Table 15

Autohesive data from milled samples of IIR, some containing 2% dicumyl peroxide

Mastication time at 100°C (min)	Physical appearance	Mean autohesive strength (N (10mm)$^{-1}$)
0	Rubbery and firm	13
Substantial time	Still rubbery	17
5, plus 60 in oven+	Quite sticky - less bulk strength	35
125+	Sticky - low bulk strength	38.5

+ Containing peroxide

The data in Table 15 indicate that the tack of butyl rubber (IIR) does increase with decreasing molecular weight, but the effect is small compared with that for cis polyisoprenes.

A similar exercise was performed on a single piece of EPM (initial M_V = 220,000), mill-mastication being at 150°C in the presence of a small amount of a ketone peroxide: the Wallace plasticity covered the range ca 25 to 5 units. Tack and bulk strength measurements were obtained from samples removed at regular intervals

during the mastication: the bulk strength values all refer to yield points as the stress/strain curves were of types 1 and 2 (Figure 20). The test data and brief mastication details are shown in Table 16. A possible decrease in the autohesive strength of EPM occurred as molecular weight was reduced.

Table 16

Autohesive and bulk strength data from milled samples of EPM containing a small amount of ketone peroxide

Milling time at 150°C (min)	Wallace plasticity (units)	Comparative autohesive strength (%)	Bulk strength (kPa)
0	23.5	23.5	252
6	11.5	18.2	140
12	8.5	16.4	112
20	5.0	17.0	84 +

+ Inadequate strength for handling.

Measurements made on the Mark I rotary tackmeter and hence expressed by comparison with a single NR control compound.

7.2.3 The effect of tackifiers

NR

A compound containing NR and HAF carbon black has been compared with a similar compound which contained, in addition, a hydrocarbon tackifying resin (2 phr). The compounds were prepared by normal mixing techniques and then each subjected to a further controlled milling experiment performed with cold water running through the mill rolls. Samples for tack testing were removed at regular

intervals, the test data being given in Table 17.

Table 17

The effect on tack strength of a hydrocarbon tackifier in a compound of NR and HAF

Cold milling time (s)	Autohesive tack strength	
	Without tackifier (N.(10mm)$^{-1}$)	With tackifier (2phr) (N.(10mm)$^{-1}$)
0	33	51
75	35	70
150	67	48
225	53	56
300	62	85*
600	47*	54*

The cold milling time excludes the time for initially mixing the compound.
* From observation, $F_R \sim 1$.

A further comment on the effect of tackifiers and processing oils is provided for NR compounds in section 7.4 (Table 21).

A series of three EPDM compounds in which the one variant was the type of tackifier has been compared with a control compound containing no tackifier. The general formulation comprised a 50/50 blend of two EPDM elastomers of different ethylene content and high loadings of carbon black and processing oil. Details of the ensuing tack strength, bulk strength (necessarily the yield point P) and Wallace plasticity data are given in Table 18.

Table 18

The effect of various tackifiers on levels of autohesive tack, yield point P and plasticity for a typical EPDM blackstock

Tackifier present (10 phr)	Mean autohesive tack strength ($N\ (10mm)^{-1}$)	P (kPa)	Wallace plasticity (units)
None - control	62	360	26
A	68	340	23
B	63	330	23
C	65	350	23

The composition of C was a phenolic/PIB mixture; those of A and B were unspecified by the manufacturers.

It is unlikely that the increases in tack strength arising from tackifiers B and C are significant, whereas that from tackifier A was probably just so. The addition of any of the three tackifiers caused a small decrease in bulk strength.

7.2.4 The addition of carbon black

Different amounts of HAF carbon black were mechanically incorporated into samples of one lump of SBR elastomer. The milling time was kept similar in each case (including the control). Tack measurements from the resulting blackstocks are shown in Table 19.

Table 19

The effect on tack strength of adding different amounts of HAF black to a sample of SBR elastomer

HAF loading (phr)	0	20	40	50	60	80
Tack strength ($N(10mm)^{-1}$)	16.5	39.0	47.5	50.5	70.0	53.5

A different sample of SBR from those of Table 20.

The magnitude of tack strength passed through a maximum region as black loading was increased. The highest tack values occurred between loadings of 40 and 80 phr and especially in the region of 60 phr.

7.3 Assessment of the autohesive strengths of different elastomers

The test data appropriate to a comparison between elastomers are naturally those measured at optimum conditions of molecular weight. Hence some values have already been given in section 7.2. Results obtained for several common elastomers are shown in Table 20: the value for an experimental ethylene butene -1 copolymer (EBM) is also included in the table.

Table 20

Measured autohesive data for several elastomers at optimum molecular weight conditions

Elastomer	Rotary tackmeter autohesive strength			
	F_1	F_2	F_3	$\overline{F}$
	$(N(10mm)^{-1})$	$(N(10mm)^{-1})$	$(N(10mm)^{-1})$	$(N(10mm)^{-1})$
NR	136	122	123	127
Synthetic cis IR	103	-	-	(103)
SBR 1500	56	60	56	57
Cis BR	50	59.5	53	54
EBM	42	38.5	35.5	39
IIR	35	38.5	-	37
EPDM	21	22	-	21.5

A clear sequence of autohesive magnitude is indicated, with

cispolyisoprenes displaying by far the greatest values. Ethylene propylene terpolymers are truly non-tacky.

More autohesive data for polyisoprene elastomers containing proportions of both cis and trans isomers are given in section 7.5.

7.4 Assessment of the tack strengths of various elastomeric compounds

A selection of test data which have been measured for rubber compounds is given in Table 21.

Table 21

Measured tack data for a variety of rubber compounds

Rubber compound	Rotary tackmeter mean tack strength ($N.(10mm)^{-1}$)
Typical factory NR blackstock+, excessively milled	156
NR plus HAF black (50phr) only, ditto	133
Typical factory blackstock+ of NR and synthetic cis IR	132
Typical factory blackstock+ of NR, cis IR and SBR 1500	101
SBR 1500 plus HAF black (40phr) only	93
Typical EPDM blackstock+ with stress/strain curve type 1*	83
Typical EPDM blackstock with stress/strain curve type 5*	48

+ Including processing oil and tackifier.

* See Figure 20.

The cis polyisoprene compounds and the blend of NR, cis IR and

SBR 1500 can be handled easily in the factory, whereas compounds of lower tack values can give rise to practical difficulties. Thus a minimum requirement to give a suitable degree of tack in practice can be conveniently taken as 100 N $(10mm)^{-1}$. The EPDM black-stocks do not reach the critical tack value.

The highest value in Table 21 was produced by masticating a typical NR blackstock for times much longer than normal to assess the tack potential of the compound. In practice, for time-saving purposes, mastication is stopped when the tack level of this compound is much nearer to the minimum requirement level. Comparison with the simple NR/HAF compound, also milled to optimum conditions, indicates the contribution to tack enhancement of tackifier and processing oil.

7.5 Tack measurements on isomerised polyisoprenes

Initial autohesive measurements were performed on two isomerised samples of de-proteinised NR generously supplied by Cuneen of MRPRA. The details of the samples and subsequent tack results are listed in Table 22.

The appearance of the samples indicated the presence of highly crosslinked polymer, a condition confirmed by the insolubility values in Table 22 and shown for similar isomers elsewhere[79]. The occurrence of such crosslinking can be easily rationalised (section 8.3). Hence the low levels for autohesive strength are to be expected. To obtain optimum autohesive values for polyisoprenes which can display no stress crystallization, the present author prepared a series of

Table 22

The autohesive strengths and some relevant details of isomerised polyisoprenes ex MRPRA

	Sample 1	Sample 2
Degree of isomerisation (% cis content)*	17	40
Autohesive strength (N $(10mm)^{-1}$)	14+	13
Insolubility in benzene (%)	9.8	39.1

* According to Cuneen (by NMR)

\+ Becomes 27 N $(10mm)^{-1}$ after substantial milling.

---

isomerised polyisoprenes by modifying the approach of Cuneen[79], the series continuing until the required conditions were achieved.

7.5.1 Isomerisation details

Suitable methods of isomerisation[79] involve the treatment of NR with sulphur dioxide, the latter being either applied directly or by heating butadiene sulphone ($\overline{CH_2CHCHCH_2SO_2}$) in a vessel with the NR. (The isomerisation mechanism is discussed in section 8.3.1). However, for the present purpose, preliminary experiments indicated that the mechanical incorporation of the sulphone (BS) into NR was experimentally more convenient and still allowed the isomerisation to occur.

Initial experiments also confirmed that treatment with BS, if sufficiently intense to give rise to > 20% trans polymer, additionally caused excessive crosslinking. Consequently, tertiary butyl catechol (TBC), a well-known inhibitor by radical absorption of unwanted crosslinking during polymerisation reactions, was also

Table 23

Brief details of various isomerisation experiments

Expt. No.	State of original NR: No. of mill passes	State of original NR: Wallace plasticity (units)	Loadings: BS (phr)	Loadings: TBC (phr)	Isomerisation time at 160°C (min)	Isomerisation time at 170°C (min)	Type of reaction vessel	Trans content (NMR) (%)	Observations
I	100	30	3	1	90	-	Open	12	< 21%trans*: quite tacky.
II	30	50	4	2	-	105	Open	17	
III	15	61	4	2	60	-	Closed	26	Crosslinked; non-tacky.
IV	15	61	4	2	-	150	Closed	63	Highly crosslinked.
V	15	61	4	2	120	-	(i) Closed	61	Highly crosslinked.
							(ii) Open	16	Not crosslinked; tacky but weak ($F_R \sim 1$).
VI	0	74	5	1.5	180	-	Largely closed+	23	Not crosslinked; tacky and suitable trans content.

* Critical value for avoiding stress crystallization[79].
+ See text.

The NMR values were also generally confirmed by infra-red spectroscopic measurements. These analysis results were obtained by [redacted] of Dunlop Research Centre.

incorporated into isomerisation mixes. However, the incorporation on a mill could only be performed with care under cool conditions, and, at first, the use of sufficient TBC to prevent excessive cross-linking also inhibited the process of isomerisation. Experimental conditions needed to be closely monitored to reach the required compromise.

Brief details of selected experiments and appropriate data are shown in Table 23. In the final experiment (no. VI) to obtain isomerised polyisoprene at a suitable molecular weight for tack, the original NR was high molecular weight ribbed smoked sheet. The incorporation into the NR (100g) of BS (5g) and TBC (1.5g) was performed on a cold mill with a minimum of mechanical working: in this way, little TBC was lost and the NR was still of high molecular weight. The isomerisation was carried out in the steel pot (capacity ca 500 ml) of the tack mould pot-and-plunger assembly (Figure 29), so that, after the removal of small specimens for analysis, the isomerised rubber could be immediately formed into tack testpieces. The isomerisation, requiring 3 hours at 160°C, was performed in a press in such a way that the platens sealed off the reaction vessel, which was therefore closed to the atmosphere but contained some air.

7.5.2 X ray diffraction data

A portion of the polyisoprene produced by isomerisation experiment VI was moulded conventionally into a slab so that tensile 'die C dumbells'[143] could be stamped out. A normal procedure for bulk strength assessment was performed so that the percentage by which the uncured testpieces had elongated at break ($\%EB_u$) could be measured: the average

value was 500%. The mean Wallace plasticity of these samples was 15 units.

A further sample of the isomerised polyisoprene was mill-mixed with tetramethyl thiuram disulphide (3phr), stearic acid (2phr) and zinc oxide (5phr), ingredients which give crosslinks on the application of sufficient heat. The compound was moulded into a slab of thickness 4 mm and cured for 60 min. at a temperature of 134°C. A reference distance was marked on the cured slab which was then clamped to a special jig designed to apply considerable extension to attached samples. Measurement of the extended reference distance showed the elongation to be 525%, i.e. a higher strain than EB_u.

Analogous compounds were also made from NR and from a synthetic polyisoprene, Cariflex IR 305 (ex Shell Chemical Co.) which contains 92% cis polyisoprene. After masticating to a Wallace plasticity of 15 units for matching purposes, the respective values of EB_u were measured as 450% and 350%. A similar curing process was performed on these two compounds, the resulting slabs both being attached in turn to the special jig and elongated to 500%.

The clamping jig was additionally designed for incorporation into an X-ray diffraction apparatus situated in Analytical Section, Dunlop Research Centre, and X-ray diffraction patterns for all of the samples were obtained. The X-ray results are summarised in Table 24.

Table 24

The X-ray diffraction patterns of various polyisoprene gumstocks; performed by Tarrant

	Gumstock			
	Unstretched	Stretched		
	NR	NR	IR 305	Isomerised polyisoprene
Sharp peaks	None	Two*, spacings 6.27Å and 4.23Å	None	None
Broad peaks	One, spacing 4.72Å	One, spacing 4.72Å	One, spacing 4.72Å	One, spacing 4.72Å

* Superimposed on broad peak

The broad peaks are due to polymer of very low crystallinity, whilst the sharp peaks for stretched NR are attributable to crystalline cis 1,4-polyisoprene. In addition:

a) (For any of the polymers) a peak as small as 1/30th of the height of the 4.23Å peak found for stretched NR compound would have been positively identifiable against the background trace.

b) The ratio of the crystalline peak area to the total peak area, although not an absolute measure, is used to arrange similar polymers in order of crystalline content: the ratio was 58% for the stretched NR.

Clearly the technique was well-capable of detecting stress crystallization as evidenced in the case of NR: hence the absence of any appropriate peak for both stretched IR 305 and isomerised polyisoprene

strongly indicated that no stress crystallization occurred in these polymers at strains up to E_u and above.

7.5.3 Autohesive measurements

Autohesive measurements made on three samples of the isomerised polyisoprene from experiment VI (Table 23) gave the values 66.5, 63.0 and 61.0 $N(10mm)^{-1}$, the mean result being 63.5 $N(10mm)^{-1}$. The average value for Cariflex IR 305 (92% cis) polyisoprene at the same Wallace plasticity (15 units) was 77 $N(10mm)^{-1}$.

7.6 The adhesion between different uncured elastomers at various molecular weights

The adhesion has been measured between Intene NF 45 (ex ISR Co.), a low-cis polybutadiene elastomer at a molecular weight suitable for processing, and high molecular weight natural rubber. Similarly, the adhesion level between the Intene elastomer and high molecular weight cis BR has been obtained. The high molecular weight elastomers were obtained by ageing standard samples in the open atmosphere until substantial gelling had occurred. Four 'planet' testpieces of Intene NF 45 and two 'sun' testpieces of each of the high molecular weight elastomers were prepared so that two tests could be performed on the Rotary Tackmeter in each case. The test results are shown in Table 25 together with some details of the elastomers.

Table 25

Measurements on the Rotary Tackmeter for the adhesion of Intene NF 45 to two high mol.wt.elastomers

Elastomer	Wallace Plasticity	Adhesion level to Intene NF 45		
		F_1	F_2	$\bar{F}$
	(units)	$(N(10mm)^{-1})$	$(N(10mm)^{-1})$	$(N(10mm)^{-1})$
NR (high mol.wt.)	96.5	13.1	13.1	13.1
Cis BR (high mol.wt.)	100 approx.	11.9	11.9	11.9
Intene NF45 polybutadiene*	30	-	-	-

The autohesion of Intene NF 45 is irrelevant and was therefore not measured.

* Cis 1,4 isomer, 37%; trans 1,4, 52%; vinyl 1,2, 11%.

The implications of these data are discussed in section 10.6.

Chapter 8 A discussion of test results and a re-appraisal of certain factors which influence autohesive tack

The statistical assessments in the previous chapter have indicated that the processes of moulding and testing produce data of acceptable significance. The correlation with technological experience of the tack strength magnitudes for rubber compounds (Table 21), in particular the practical difficulties indicated for EPDM compounds, provides further comment on the validity of the data obtained on the Rotary Tackmeter. The sequence of autohesive levels obtained for a range of elastomers (Table 20) similarly agrees with practical experience, magnitudes being somewhat less than those of the corresponding compounds.

The present work has confirmed the previously-noted existence (section 3.1.4) of a loading of filler associated with maximum tack magnitudes: for HAF black, such a loading conveniently coincides with the loadings which produce optimum levels of many post-cure properties. The measurements have also confirmed the existence of critical values of contact force or pressure above which further increases in force did not radically increase tack strength. The critical force phenomenon has already been attributed to viscous flow. Other measurements in Chapter 7 employed contact forces above the critical value. It should be noted that average values of the contact pressures utilised have been up to 1 MPa and that pressures in the region of maximum rubber compression will be even higher. These average pressure levels represent an increase of one order over those used by other workers[18,28]. The higher pressures should give rise

to tack measurements which represent the diffusive aspects of autohesion.

8.1 The influence on autohesion of contact time t and speed of separation u

Let Tack strength $\propto u^y t^z$. Then from equation 6.1

$$\text{Tack component } (F_w) \propto (\cos\beta\, u^y t^z).$$

$\cos\beta$, u and t are all functions of Δ, the mutual depression of the testpieces. Substitution from the appropriate equations 6.2, 6.3, and 6.4, and simplification, gives

$$F_w \propto (1.016)(0.32^y)(12.5^z)(n'^{y-z})(\Delta^{(y+z+1)/2})(1-(0.15+0.23y+0.06z)\Delta) \text{ - - - } 8.1.$$

Expression 8.1 gives equations 7.1 and 7.2 (recorded earlier) by considering the following special conditions which can be employed for testing. If Δ is kept constant by manipulation of the contact force above the critical value, let values $(F_w)_1$ and $(F_w)_2$ be associated with rates of rotation n'_1 and n'_2 respectively.

Then

$$(F_w)_1/(F_w)_2 = (n'_1/n'_2)^{y-z} \qquad \text{so that}$$

$$(y-z) = (\log_{10}((F_w)_1/(F_w)_2))/\log_{10}(n'_1/n'_2) \text{ - - - - - - - - } 7.1.$$

By further manipulation of the contact force, if n' is kept constant and values $(F_w)_3$ and $(F_w)_4$ relate (at super-critical contact forces) to Δ_1 and Δ_2, then to a good approximation

$$(F_w)_3/(F_w)_4 = (\Delta_1/\Delta_2)^{(y+z+1)/2} \qquad \text{so that}$$

$$(y+z) = ((2\log_{10}((F_w)_3/(F_w)_4))/\log_{10}(\Delta_1/\Delta_2)) - 1 \text{ - - } 7.2.$$

As noted in section 7.2.1, the solution of these simultaneous equations from the experimental data has resulted in the expression

$$\text{Tack strength} \propto u^{1.01}\, t^{0.66} \text{ - - - - - - - - - - - - - } 8.2.$$

The appropriate theoretical relationship has already been expressed as

$$\text{Tack force} \propto ut^{0.25} \quad \text{----------6.5.}$$

Hence the power term for the speed of separation u has been well-substantiated by the measurements described in Chapter 7. At first sight, less agreement has been found between the theoretical and practically-derived powers of t. However, the geometrical portrayal of tack testing (Figure 25, section 6.3.2), which contributes through expression 6.3 to expressions 7.1 and 7.2, does not allow for the time taken during the initial stages of rolling contact for each element to experience viscous flow until reaching the critical force: in diffusive terms the true contact time is less than that predicted by expression 6.3. The proportion of actual contact time involved in viscous flow will be less as n' is decreased and Δ increased, so that, from considerations of equations 7.1 and 7.2, one can speculate that expression 8.2 would be expressed more accurately by

$$\text{Tack strength} \propto u_{ca}^{1.01} t^{<0.66} \quad \text{----------8.3.}$$

The reasonable correlation found between theory and practice at the very low contact times employed by the Rotary Tackmeter supplements the similar agreement found at much longer contact times with other tackmeters (section 4.5): indeed the correlation with speed of separation is perhaps better in the present case.

The experimentally-derived equation 8.2 could be considered as more relevant to Rotary Tackmeter testing than expression 6.5, and therefore more suitable for the purposes of normalising to standard conditions (section 6.3.4). The correction term Q arising from expression 6.5 is

$$Q = 0.57 / (n'^{3/4} \Delta^{9/8} (1 - 0.4\Delta)) \text{ - - - - - - - - - - - - - - - - 6.7.}$$

The analogous expression derived in a similar manner but from expression 8.2 is

$$Q = 0.203 / (n'^{0.35} \Delta^{1.335} (1 - 0.42\Delta)) \text{ - - - - - - - - - - - 8.4.}$$

The plots against Δ of Q derived from both equations when n' = 4 r.p.m. are included in Figure 27 (section 6.3.4). At this commonly-used rate of rotation the plots are fortuitously similar for the values of Δ normally measured. Hence the present system of using the theoretically-derived correction factor can be continued.

8.2 The role of molecular weight in optimising both autohesive and bulk strengths

As already discussed, the autohesive strength F is increased as molecular weight M decreases from ca 10^6 to 5×10^5 until F reaches the bulk strength at a particular molecular weight M_1. The graphical portrayal of the present data (Figure 30, section 7.2.2) for a contact time of 1 s exaggerates the effect shown by Forbes and Mcleod[18] (Figure 16, section 4.6.1) for a contact time of 30 s, possibly because of the enhanced contact force. Thus the influence of M on F applies to short and longer contact times. An additional comment arising from the present results is that, at realistic practical contact times, stress crystallization was apparently absent in the M_1 region.

Patterns such as those exhibited by Figures 16 and 30 can be used to assess the practical suitability of experimental changes which might be made to a rubber compound. Consider the schematic representation for NR shown in Figure 31. Provided that the contact force is above the critical level, a series of tack curves can be obtained for

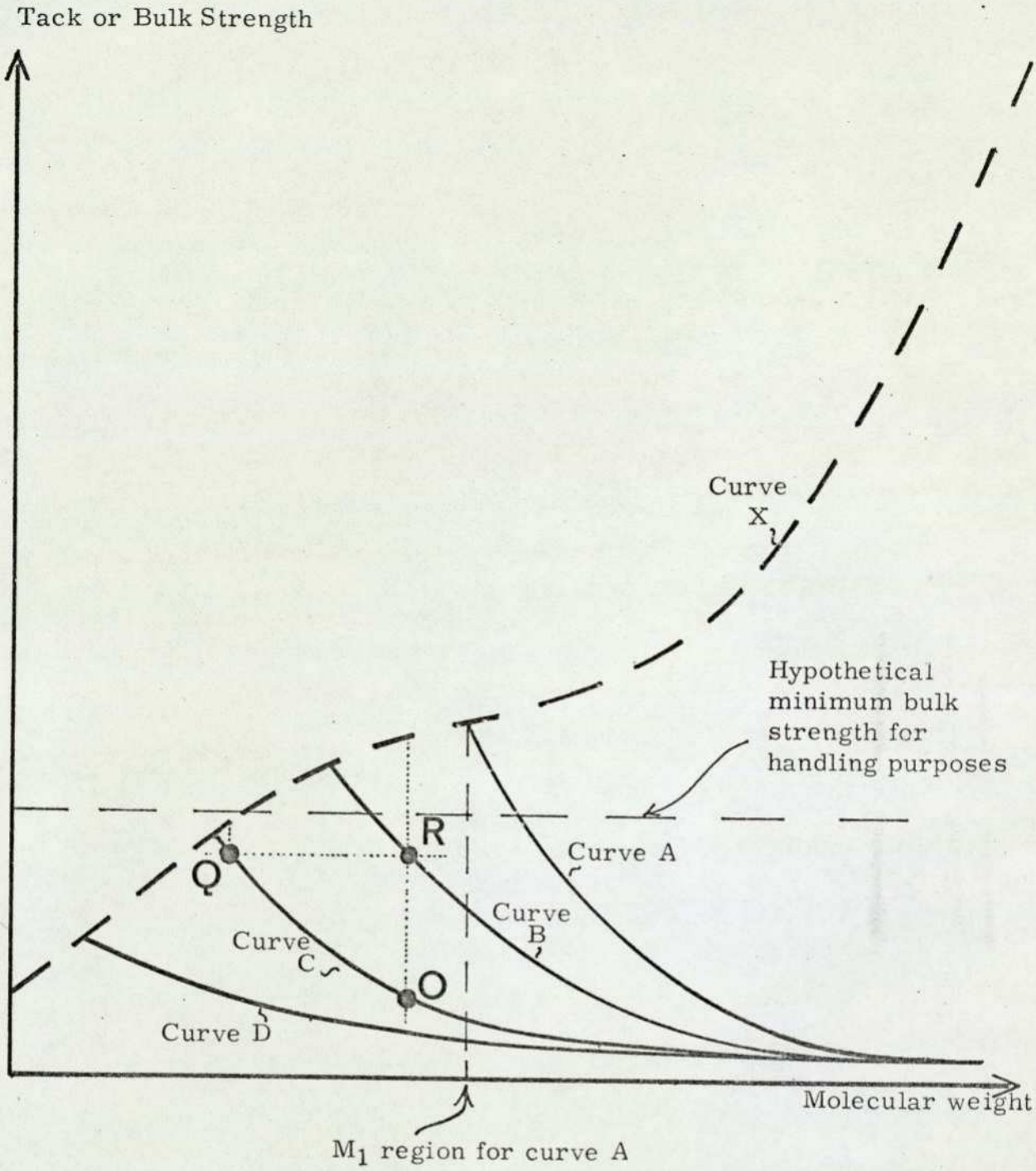

At R, Tack ~ 0.7 Bulk Strength
which is acceptable (section 6.1), whereas the same level of tack at Q is associated with a bulk strength below the minimum handling value.

Figure 31 Various hypothetical curves of autohesive tack and bulk strength as functions of molecular weight.

a variety of reasons. For instance, successive reductions in contact times give the series of curves A, B and C, the reduced diffusion causing a shift of the M_1 region to lower levels of M. The bulk strength curve X is considered to apply throughout at constant temperature and jaw separation speeds for viscoelastic reasons.

The same curves can be used to demonstrate other experimental effects which alter the extent of diffusion. Suppose an elastomeric material possesses at suitable conditions a value of tack such that it lies on curve C at position O. Suppose also that a second material exists, identical with the first except for the addition of a small loading of tackifier. If the tackifier merely acts by decreasing M (or, more strictly, $\overline{M}$) for the system, its behaviour could be described by point Q, still on curve C but nearer to the M_1 region and consequently associated with a lower bulk strength. However, if the tackifier truly enhances diffusive aspects, the system might be represented by point R on curve B: here, the gain in autohesive tack has not been made at the expense of bulk strength. Figure 31 also indicates a hypothetical case when the yielding stresses are such that, at the appropriate contact times, adequate magnitudes for both tack and bulk (handling) strengths could only arise with the genuine tackifier.

In these terms, the tackifier which when incorporated into a NR/HAF compound gave the data shown in Table 17 genuinely increased tack, as unit relative tack F_R was reached at a much higher level of tack than the best reached by a control compound.

Extending the argument, elastomers of low tack such as EPDM might follow curve D (Figure 31), for which M_1 lies well below the minimum M value associated with adequate magnitudes of bulk strength (ca 5×10^5 from Figure 30). To reach curve B or A the contact time is so long as to be completely impractical. Hence, curves A - D represent as a function of M the degree of diffusion which can be varied by technological means, (e.g. tackifiers, solvent wipes), by choice of experimental condition (contact time, temperature), or fundamentally (by choice of elastomer).

8.3. The useful, but supplementary, role of stress crystallization

8.3.1 The polyisoprene isomerisation mechanism

The logic behind experimental requirement (ii) (Chapter 6) required the formation by isomerisation of polyisoprenes possessing > 21% trans polymer. Cuneen[79] proposed the following "on-off" mechanism for such an isomerisation by thiol acids:-

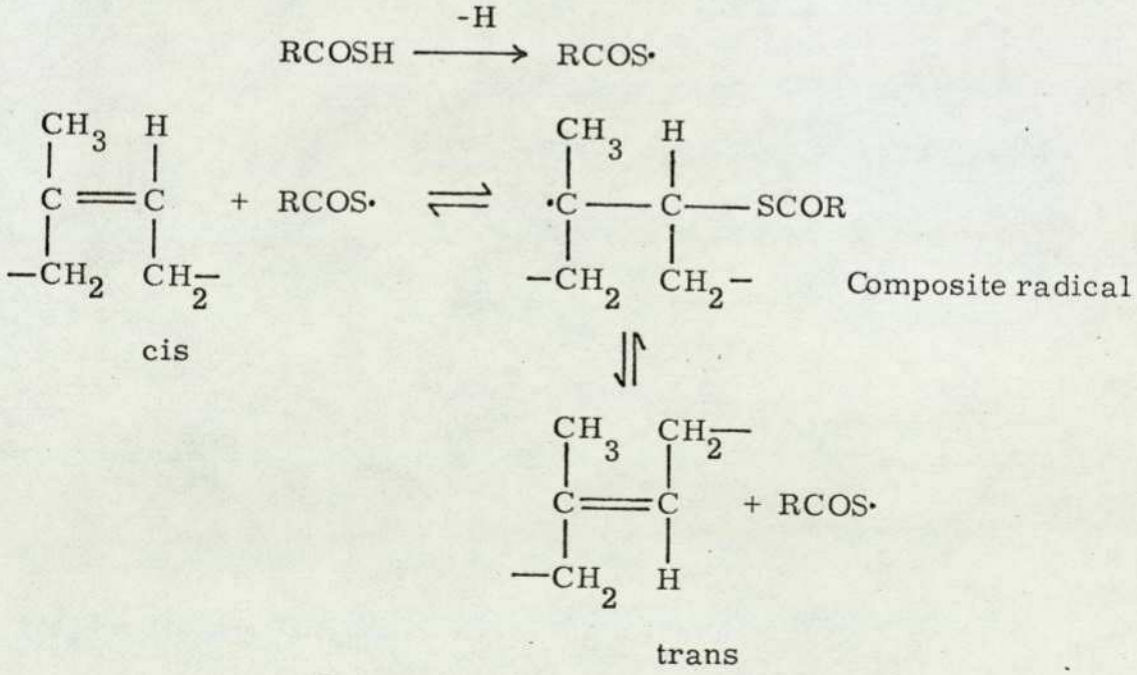

The isomerisation proceeds to a 50/50 cis/trans situation providing

that an additional step, in which the composite radical reacts with more thiol acid to form an adduct, is inhibited by the conditions employed. Cuneen also suggested that isomerisation by sulphur dioxide presumably occurs via a similar "on-off" reaction at the double bond, but claimed that free radicals are not involved since the rate of isomerisation appears to be insensitive to free radical catalysts and inhibitors. However, sulphur dioxide is known to participate in copolymerisation reactions with olefin monomers by means of free-radical initiation[144], the overall reactions being given by the general equation

$$CH_2{=}CHR + SO_2 \longrightarrow \text{-}(CH_2\ CHR - SO_2)\text{-}$$

Sulphur dioxide also forms 1:1 complexes with olefins, the complex then reacting as a unit with a radical. Hence the isomerisations herein employing butadiene sulphone, $\overline{CH_2\ CH\ CH\ CH_2\ SO_2}$ (or possibly $CH_2\ CH{=}\underset{\displaystyle SO_2}{\overset{\displaystyle |}{=}}CH\ CH_2$) reasonably proceed by free radical reactions.

With many of these types of reaction, the possibility of crosslinking exists due to the juxta-position of monomer units from neighbouring chains at the instant that the units become radicals. From the practical experience of the author, excessive crosslinking occurs in the present isomerisation unless inhibited by tertiary butyl catechol. TBC absorbs free radicals quite readily, presumably due to the formation of new radicals which are stabilised by resonance with the appropriate quinonoid structure.

The conditions found necessary to obtain a sufficiently-isomerised polyisoprene which was apparently free from crosslinks and of

suitable molecular weight (Table 23, experiment no. VI) arose from a compromise of the isomerisation, crosslinking and radical absorption reactions together with a normal (at high temperatures) chemically-induced chain breakdown involving the oxygen of the air, such as[145]

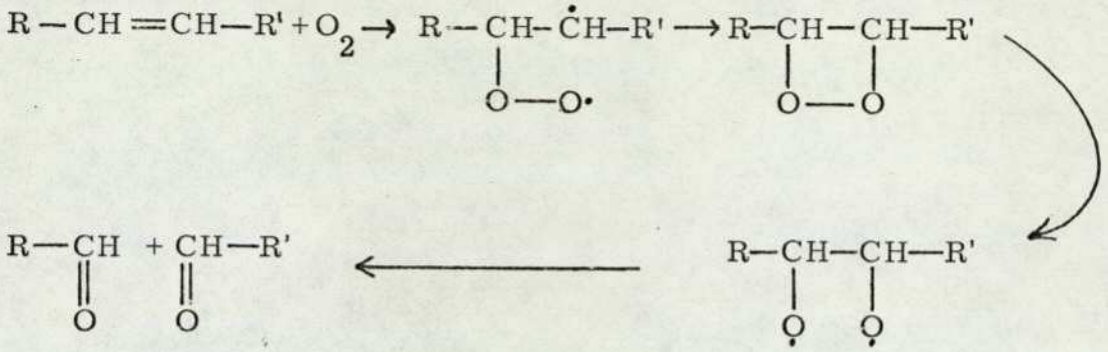

8.3.2 Implications from the autohesive measurements of isomerised polyisoprenes

The X-ray diffraction evidence showing a complete absence of stress crystallization in polyisoprene sample VI containing 23% trans isomer (Table 23) has confirmed the previous findings[79]. The autohesive strength magnitude quoted in section 7.5.3 for sample VI is ca 11% greater than that of SBR 1500, the most tacky non-isoprenic elastomer (Table 20).

The onset of stress crystallization is inhibited by increasing packing disorder and by decreases in molecular weight. Table 24 shows that no stress crystallization was evident in a cured sample of extensively-milled Cariflex IR 305 elongated to 45% greater than EB_u, even though this elastomer only possesses 8%trans polyisoprene. Although high local strain might be met at the uncured interface during the separation stage of tack testing, they are unlikely to be much greater than EB_u. Hence no stress crystallization should occur during the tack assessment of this elastomer. The autohesive value of the

IR 305 sample (section 7.5.3) was 35% better than the SBR 1500 level (Table 20). For the purposes of section 4.8, autohesive magnitudes of the non-crystallizing polyisoprenes were greater than the EPDM level (Table 20) by a factor of ca 3.

It is also noted that, at the relatively low average molecular weights associated with the very high optimum autohesive strength for NR (Figure 30), the stress/strain curves during bulk strength measurements display no sign of the crystallization property: any effect which may exist locally due to high molecular weight regions is unlikely to be a major influence. Although for the present purposes a measurement of autohesive strength was necessary for a polyisoprene under conditions (> 2 1% trans) at which the absence of stress crystallization was without question, a case exists indicating that stress crystallization does not contribute in any way to the optimum autohesive strength of even the 100% cis isomer. The usefulness of the stress phenomenon for compounds, involving polymer of higher molecular weight, is not being questioned - merely the validity of its application at the relatively low molecular weights associated with optimum autohesion levels of the unfilled elastomer.

Whatever the case, the exercise performed substantiated the approach of sections 3.2 and 3.3: the primary requisite for tack is the ability to form an adequate interpenetrating polymer layer at the interface. Stress crystallization is undoubtedly useful, but only for handling purposes at the post-coalescence stage, in common with other bulk strength properties. The crystallization phenomenon by itself does not satisfactorily explain the high magnitudes of autohesion which can be

obtained for cispolyisoprenes.

8.4 General

Of the experimental factors reviewed in section 4.5, only temperature has not been studied herein. Such an investigation was not considered relevant to the assessment of the tackmeter or to the experimental requirements of the present work.

Having first indicated practically the viability of the tackmeter, the data presented and discussed in the last two chapters have satisfied the experimental requirements. The estimation of an apparent difference in diffusion rate of one order for polyisoprenes and EPDM, based on a comparison of autohesive test data, is reasonable. The following chapters deal with a proposed geometrical model to explain the difference in diffusive ability between the elastomers.

Chapter 9 A proposed microstructural model for resolving the autohesive problem

A microstructural model is now proposed which relates geometrical features to autohesive diffusion rates. It arises from the observations that elastomers possessing unsaturation, especially if associated with side-group substitution, are more tacky than saturated rubbers. The striking geometrical factor is the comparative permanency, during normal chain movements, of the relative positions of those carbon atoms linked by unsaturated bonds. A characteristic such as this, which at one scale of organisation can influence the crystallographic repeat distance of an elastomer[73a], is associated at a smaller scale with local surface features which can enhance autohesion.

The approach has been facilitated by studying Stuart molecular models, considered[146] to represent accurately the van der Waals and atomic dimensions of molecular systems. Indeed, the existence of "permanent" regions of free space associated with certain chain characteristics was strongly supported by adhering plasticine to appropriate Stuart models and noting that some plasticine could not be removed either by reasonable rotations of all the model components or by sensible movements of neighbouring "chains". Stuart models were also employed to choose representative configurations for quantification purposes.

The influence of local microstructural regions on the generation of holes is understood more clearly by classifying free space to accommodate the space finely-distributed around the chain surface microstructure.

9.1 The 'classification' of free space into interchain and intrachain components

Whilst recognising the unique pervasive nature of free space, a distinction is proposed between interchain free volume and space elements (collectively defined herein as intrachain free volume) which are localised in conjunction with certain chain structural features. All polymers contain interchain free space, whereas intrachain free space is more evident in some rubbers than in others.

Quantitatively, intrachain free volume is the minor component. However, the proposal is that, at any instant, these local space elements may possess extra usefulness from the point of view of potential 'filling' (displacement by matter). An analogy from the macro-scale in which we live is demonstrated by an empty cup. Regarding the general atmosphere as space for convenience, the space within the cup is no different from, and is a continuum with, the vast regions of surrounding space: yet only the space within the cup can be usefully displaced by fluid.

The structural features causing intrachain free space are visualised as 'containing' cavities of space between themselves, such cavities having one end open to the proximate interchain free space. Whereas interchain free space (that is, all free space which cannot be classed as intrachain) may be displaced by any haphazard movements of neighbouring chains, intrachain cavities can only be occupied by a largely determinate approach from another chain portion.

The type of structural features considered to provide intrachain free space cavities are now exemplified.

NATURAL RUBBER

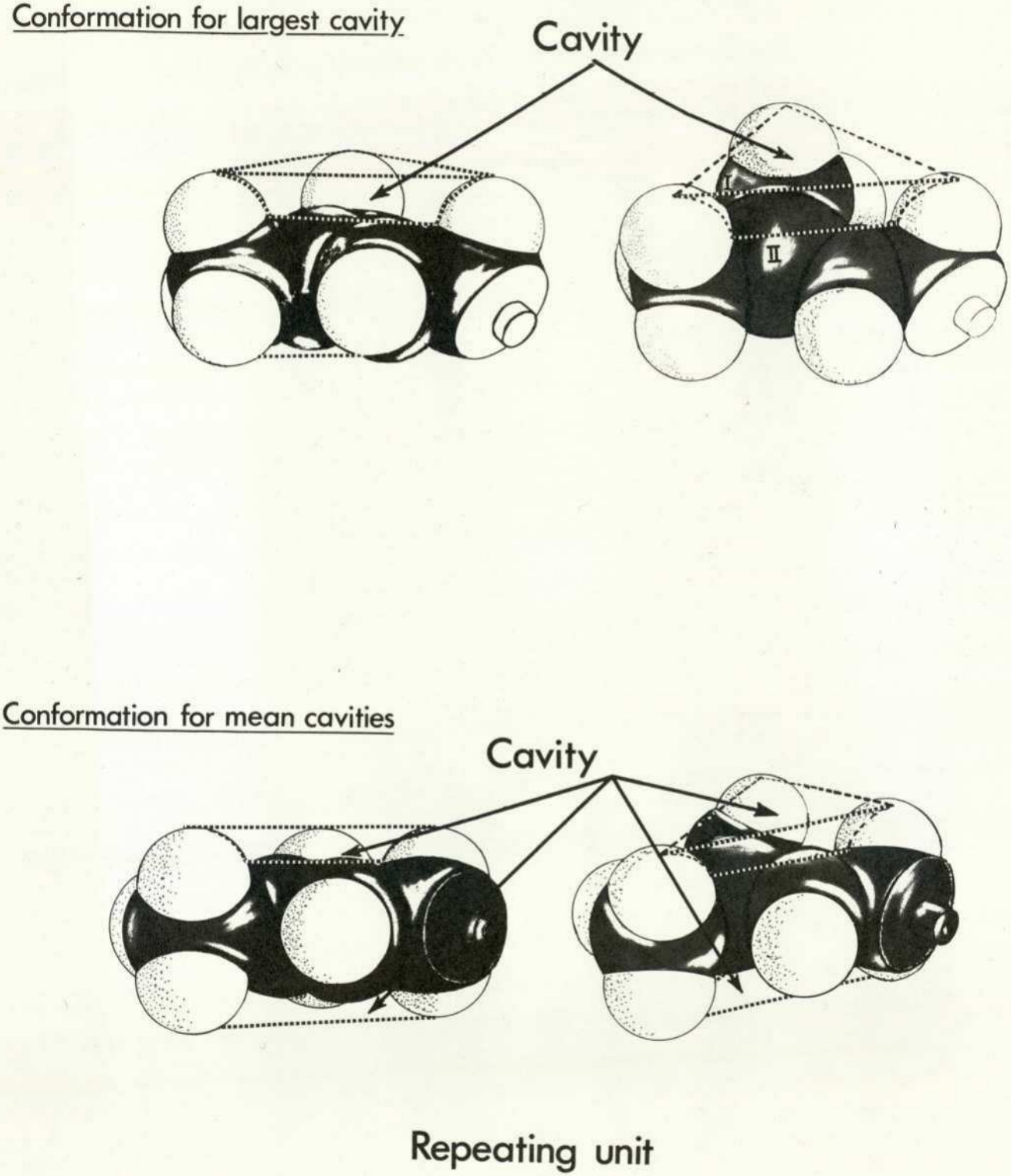

Figure 32 Stuart Models showing permanent, but flexible, cavities associated with a pi-bond and substituted grouping.

9.2 The illustration of intrachain free space cavities

The cavities are well-demonstrated by studying the configurations of chain monomer units of NR and IIR (or PIB) elastomers. For the general purpose hydrocarbon elastomers, the second case will be seen to be the smallest cavity which can reasonably be considered as such, whilst the cavities of NR and other cis polyisoprenes are apparently amongst the largest cavities occurring in abundance throughout a polymer. Larger cavities can be associated with polymers possessing bulky side-groups but such polymers are invariably of high T_G and not elastomeric at normal temperatures: large cavities of this type are met in copolymers such as SBR, but in limited numbers only.

9.2.1 Permanent molecular features associated with pi-bonds and substitution

A monomer unit (i.e. a repeating unit originally derived from one molecule of monomer) of cis polyisoprene possesses both unsaturation and a substituted olefinic carbon atom. Consequently the five carbon atoms in the unit exist permanently in the same relative positions (due to the rigid pi-bond) independently of chain rotations and of thermal vibrations of the chain as a whole. Rotating the peripheral carbon-carbon sigma-bonds gives many conformations of the monomer unit, two of which are illustrated in Figure 32. However, whatever the conformation, a region of space (indicated in Figure 32 by broken lines) exists permanently between the limits of influence of the chemical groups based on the five carbon atoms, both above and below the pi-bond. These cavities, which can vary according to conformation between a substantial and a minimal volume, are easily accessible to

POLYISOBUTYLENE / IIR

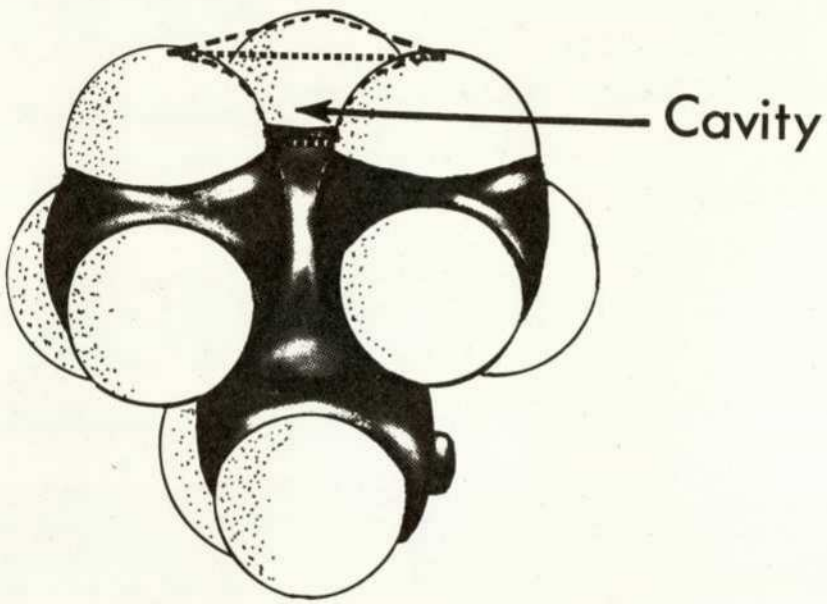

Repeating unit + $-CH_2-$

Figure 33 Stuart Model showing a temporary cavity associated with substituted groupings in the absence of pi-bonds.

a determinate approach by another chain portion. A mean or representative cavity size has been considered to apply when equal intrachain cavity volumes exist above and below the pi-bond (Figure 32 b).

For the same reasons, the chain carbon atoms of a cis polybutadiene (cis BR) monomer unit possess a permanency of structure. However, the absence of any substituted side-group means that the cavity has little depth , no grouping of the size of the two cis methylene groups existing in the monomer (repeating) unit on the opposite side of the chain axis. Although a cavity volume can be calculated, the value is small.

9.2.2 Permanent molecular features associated with sigma-bonds

For saturated polymers with no substituted groupings the only permanent chain feature is the carbon-carbon sigma-bond, next nearest-neighbour atoms adopting variable positions on the rotational cone about the preceding sigma-bond. In EPDM elastomers (i.e. ethylene propylene terpolymers), the $-(CH_2)-$ units therefore have no intrachain space. The presence of the substituted grouping in the propylene moiety of EPDM causes permanent features which give cavities of "medium" volume but of limited access in terms of cross-sectional area. Similar cavities exist in other copolymers of ethylene and higher alkenes, and in greater numbers in butyl rubber (IIR) or polyisobutylene.

Figure 33 illustrates for IIR (or PIB) one monomer unit plus a methylene unit in such a conformation that a cavity exists between the

peripheries of three hydrogen atoms, each hydrogen being bonded to a different carbon atom. The limited accessibility of the cavity is obvious, such a cavity defining the smallest free space allocation considered relevant, as these cavities could only each accommodate a small spherical segment of an incoming hydrogen atom.

Further study of PIB in Figure 33 reveals that a second similar cavity exists on the 'face' of the chain portion. The construction of a Stuart model involving several monomer units reveals the existence of two cavities per unit: the conformational variations which destroy one cavity simultaneously produce a replacement elsewhere on the monomer unit.

The substitution of a hydrogen atom for one methyl group belonging to the PIB monomer unit illustrates a portion of polypropylene. It can be clearly visualised from Figure 33 that the same type of cavities occur in the two polymers: however, only one cavity exists per unit of polypropylene. Obviously the number X of these cavities per monomer unit of a typical EPDM elastomer relates to the mole fraction present of propylene.

9.2.3 General comments on the permanent features

Whilst the existence of cavities is a permanent feature of appropriate polymer chains, rotation of groupings causes the continual size change of those individual cavities associated with pi-bonds, and axial rotation of chain portions plus rotation of groupings alters the location (but generally not the numbers) of cavities in substituted saturated elastomers. The largest cavities which can exist in high

numbers are associated with both unsaturation and substitution: the loss of either quality considerably diminishes the size of the intra-chain space cavity. The point is emphasised by the following estimations of cavity volumes and cross-sectional areas.

9.3 The estimation of cavity volumes c'' and cross-sectional areas a''

Just as the existence on a time average basis of a consistent pattern of generated holes has been accepted (section 4.10), so the variations due to bond rotations of molecular conformations give rise to cavities of continually-varying size which can be described by representative values.

The shapes of the cavities for each of several general purpose elastomers have been studied using Stuart models. A laboratory-produced elastomer, ethylene butene-1 copolymer (EBM), was also assessed for interest. By approximating each cavity to a simple geometric figure and calculating the volume using atomic dimensions (Table 26)

Table 26

Useful atomic dimensions, largely after Pauling[147]

Atomic radii (Å)	van der Waal's radii (Å)	Atomic bond angles
C-C; 1.544	H; 1.200	Tetrahedral (sp^3); 109.5°
C-H; 1.085	C; 1.650 *	Trigonal planar (sp^2); 120° +
Aliphatic C=C; 1.334		
Aromatic C=C; 1.397		

1 Angstrom unit (Å) = 0.1 nm.
* After extrapolation.
\+ Preferred[116] to Pauling's 125°.

Table 27
Details of Monomer Units

Elastomer	Mol. wt. M_M of monomer unit	Copolymer moiety	Molar proportion	Volume of cavity c'' $(Å)^3$	Cross-sectional area of cavity a'' $(Å)^2$	Length of monomer unit L (Å)	No. of cavities per monomer unit X
NR and cis IR	68.1			3.25	1.19	4.40	2.00
SBR 1500	60.8	Styrene	2	5.34	2.11	4.23	1
				2.13	0.68		1.70
		Butadiene	13	1.85	0.56		1.81
Cis BR	54.1			1.00	0.40	4.40	1.99
IIR	56.1			1.47	0.67	2.52	2.00
EBM	42.1	Ethylene	1	0	0	2.52	0
				1.47	0.67		1.00
		Butene-1	1	1.47	0.67		2
EPDM	32.7	Ethylene	2	0	0	2.52	0
				1.47	0.67		0.33
		Propylene	1	1.47	0.67		1
Emulsion BR	54.1			1.71	0.54	4.46	1.83

For copolymers and isomers, average values are shown for M_M, L and X.

Butadiene isomers:-				
	Cis BR elastomer	96% cis 1,4;	1% 1,2;	3%trans 1,4
	Emulsion BR (typical)	19%	17%	64%
	Emulsion BR in SBR	6%	19%	75%

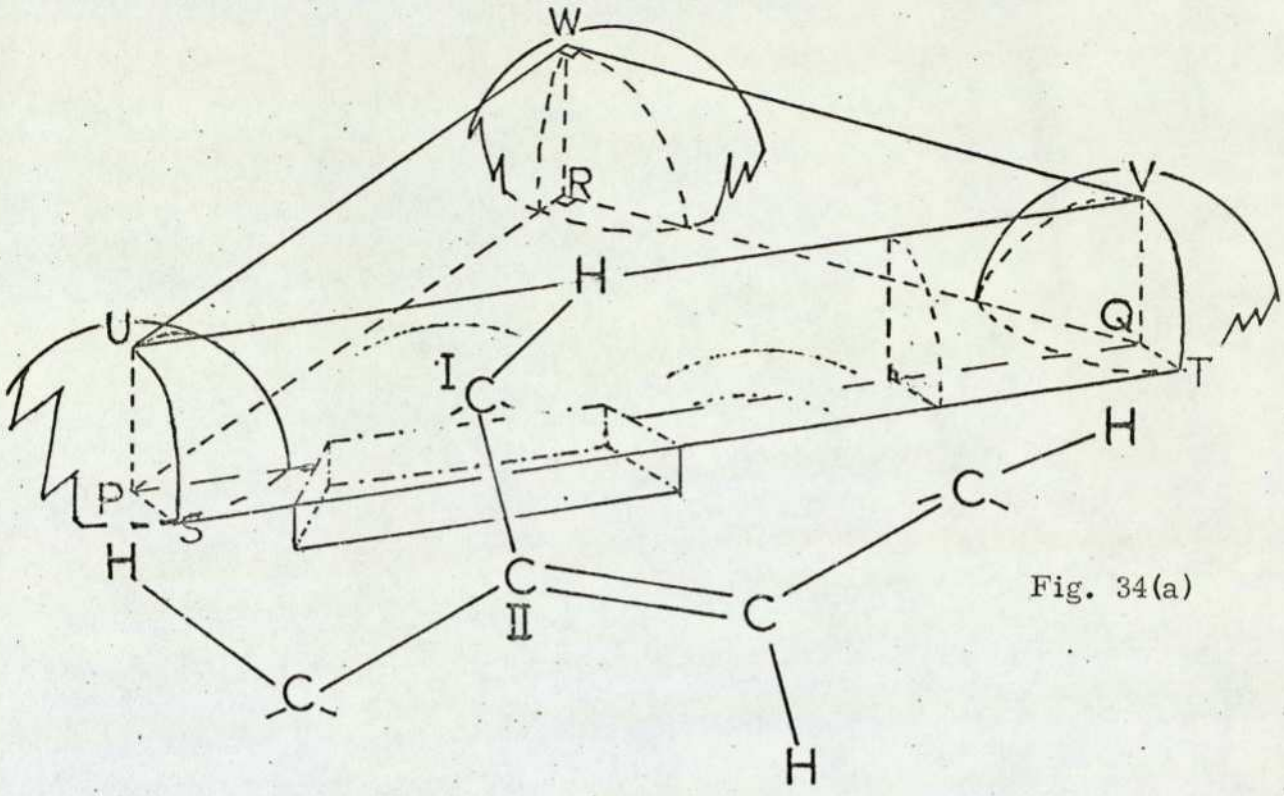

Fig. 34(a)

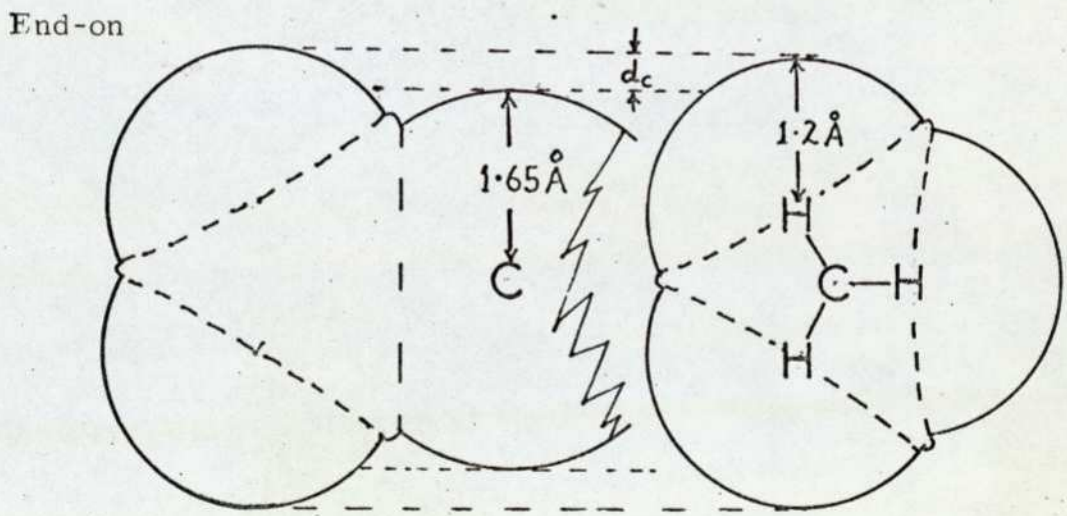

Fig. 34(b)

Figure 34 A breakdown of the NR cavity.

largely as quoted by Pauling[147], estimates of the mean cavity volume c'' and the typical cavity cross-sectional area a'' have been obtained. The results are given in Table 27 together with details for each monomer unit of the number of cavities X, the molecular weight M_M and the length L (the latter relating to a fully-extended monomer). For copolymers (including isomers), the appropriate molar proportions are included so that the representative molecular parameters could be derived from the contributing moieties,

i.e. $c'' = \frac{\overline{\Sigma X_i c_i''}}{X}$ and $a'' = \frac{\overline{\Sigma X_i a_i''}}{X}$.

9.3.1 The calculation of c'' values

For most elastomers, the calculations have involved the subtraction from a Euclidean shape of a volume arising from intruding portions of hydrogen atoms, the heights of the portions giving the representative depth d_c of the cavity. The Stuart models have indicated that, in each of these instances, the total intruding volume v_H is one half of a spherical segment.

Hence $v_H = (1/6)\,\pi d_c^{\,2}(3r_H - d_c)$ ---------- 9.1

where r_H is the radius of a hydrogen atom.

Cis Polyisoprenes (including NR).

Study of the Stuart model illustrated by Figure 32 indicated that the mean cavity size was best represented by the broken lines shown plus an extra region of space which is shielded by two vertically protruding hydrogen atoms. The cavity is suitably broken down in Figure 34(a) for estimation purposes. Figure 34(b) indicates the mean depth d_c of the cavity, which is equal to $(1.2 + (1.085 \cos 19.5^{\circ}) \cos 30^{\circ} - 1.65)\text{Å} = 0.436\text{Å}$.

End-on

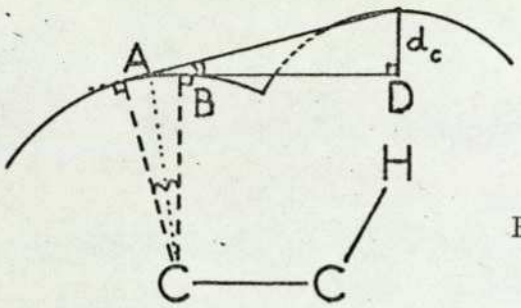

BD taken as $\frac{x+y}{2}$,

see below.

Plan

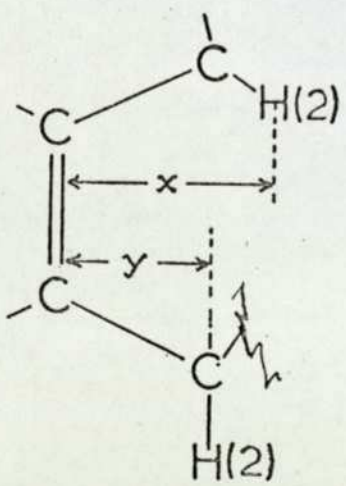

Figure 35 A breakdown of the cis BR cavity.

Then:-

$$c''_{NR} = c''_1 + c''_2 + c''_3$$

where c''_1 = (volume of right triangular prism UVWPQR) minus v_H

c''_2 = (volume of cylindrical segment UPSVQT) minus v_H

c''_3 = minor component below the plane of the general cavity base.

To find c''_1:

$WV = 1.334 + 2(\sin 30^\circ(1.544 + 1.085 \sin 19.5^\circ))\,\mathring{A} = 3.240\,\mathring{A}$

$UW = 2(\cos 30^\circ(1.544 + 1.085 \sin 19.5))\,\mathring{A}$

$\therefore c''_1 = (0.5 \times 3.240 \times 3.302 \times 0.436) - (\pi(0.436)^2((3 \times 1.2) - 0.436)/6)$

$= 2.332 - 0.315 = 2.017\,(\mathring{A})^3$.

To find c''_2:

$UV = 4.626\,\mathring{A}$ (Pythagoras). Area of circular segment UPS

(where $UP = d_c$) $= 0.2805(\mathring{A})^2$ by standard trigonometry.

$\therefore c''_2 = (4.626 \times 0.2805) - 0.315 = 0.983\,(\mathring{A})^3$.

To find c''_3:

Study of the Stuart model indicates that the extra depression is of depth ca $0.085\,\mathring{A}$ by standard trigonometry, of length $\sim$ the diameter of the chain-substituted hydrogen atom, and width approximately half the length.

$\therefore c''_3 = 0.085 \times 2.4 \times 1.2 = 0.245\,(\mathring{A})^3$

$\therefore c''_{NR} = 3.25\,(\mathring{A})^3$.

Cis Polybutadienes and isomers.

The replacement of the substituted methyl group by a hydrogen atom considerably reduces the size of cavity, the cross-section now being that of a wedge decreasing from height d_c, as shown in Figure 35. The length of cavity remains WV (Figure 34(a)) and v_H is again $0.315\,(\mathring{A})^3$.

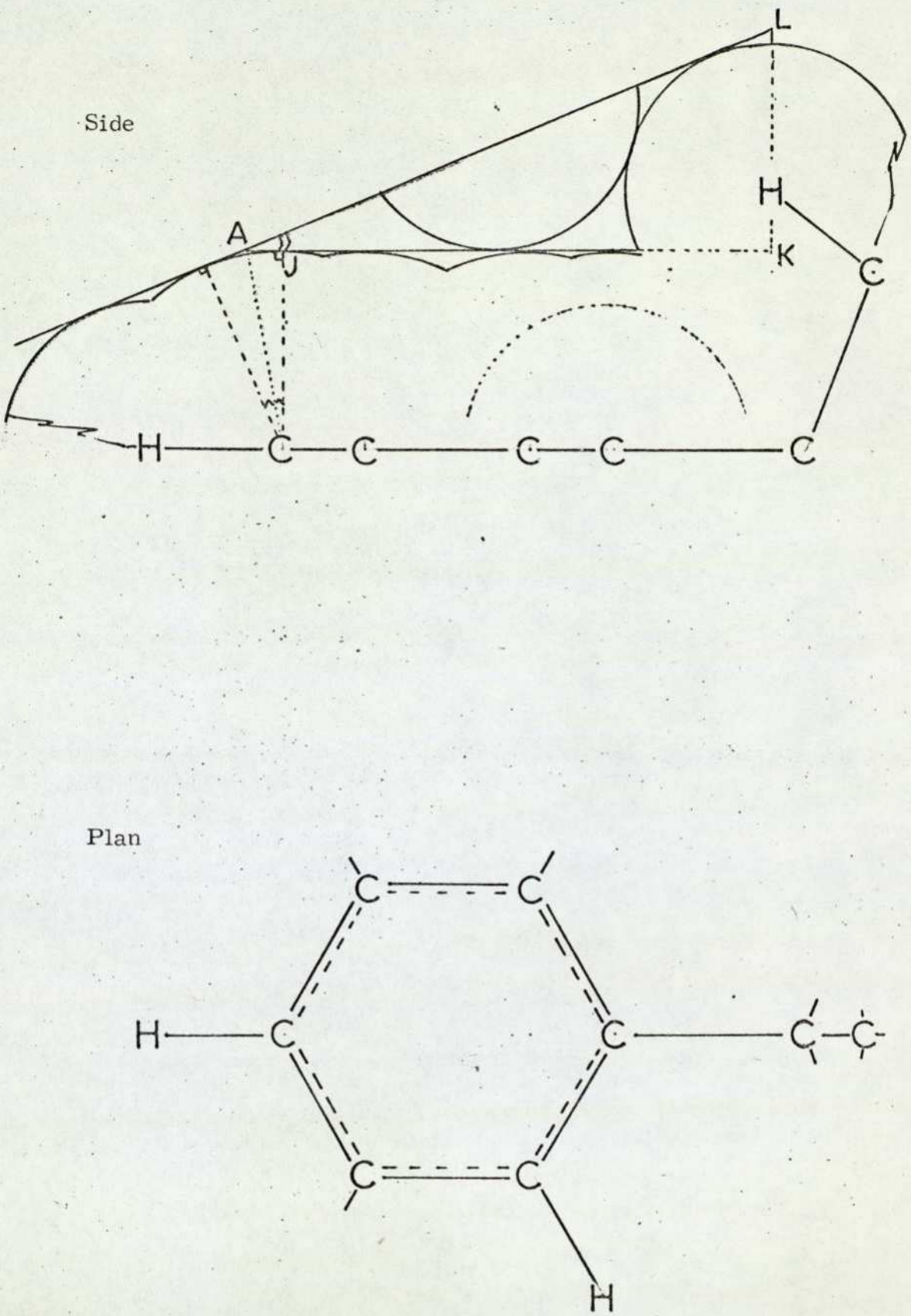

Figure 36 A breakdown of the styrene moiety cavity.

The distance BD (Figure 35) differs for the two extreme conformations of the chain methylene groups: the mean distance is

$0.5((1.544\cos 30^{o}+(1.085\cos 54.75^{o})\cos 24.75^{o})+1.544\cos 30^{o}) = 1.621\ \mathring{A}$.

From standard trigonometry AB = $0.195\ \mathring{A}$ so that AD = $1.816\ \mathring{A}$.

$\therefore c''_{cBR} = (0.5 \times 1.816 \times 0.436 \times 3.240) - 0.315 = 0.97\ (\mathring{A})^3$.

The value of $1.00\ (\mathring{A})^3$ recorded in Table 27 arises because the molecular chains of the elastomer quoted as cis BR in that table also contain minor proportions of monomer units of trans BR and vinyl (1,2) BR. The Stuart model of trans BR indicated the cavity to be equivalent to twice the component c''_2 of c''_{NR}, so that $c''_{tBR} = 1.97\ (\mathring{A})^3$. The cavity of vinyl BR visually relates to the cavities of PIB, which will shortly be estimated to be of magnitude $1.47\ (\mathring{A})^3$.

Styrene moiety

The styrene cavity formed between the benzene ring and adjacent methylene group is reasonably represented in Figure 36: a contribution v_H again applies. The dimension not visible is given by the breadth of the carbon atoms of the benzene ring, $2 \times 1.397 \sin 60^{o}$, ($2.420\ \mathring{A}$). Trigonometric treatment of the atomic dimensions produces $4.010\ \mathring{A}$ for base JK and $1.688\ \mathring{A}$ for maximum cavity depth KL. Applying the last dimension to expression 9.1 produces $2.853\ (\mathring{A})^3$ for v_H. Hence

$c''_S = (0.5 \times 4.010 \times 1.688 \times 2.420) - 2.853 = 5.34\ (\mathring{A})^3$.

PIB and other substituted saturated elastomers.

The shape of the cavity shown in Figure 33 approximates well to a

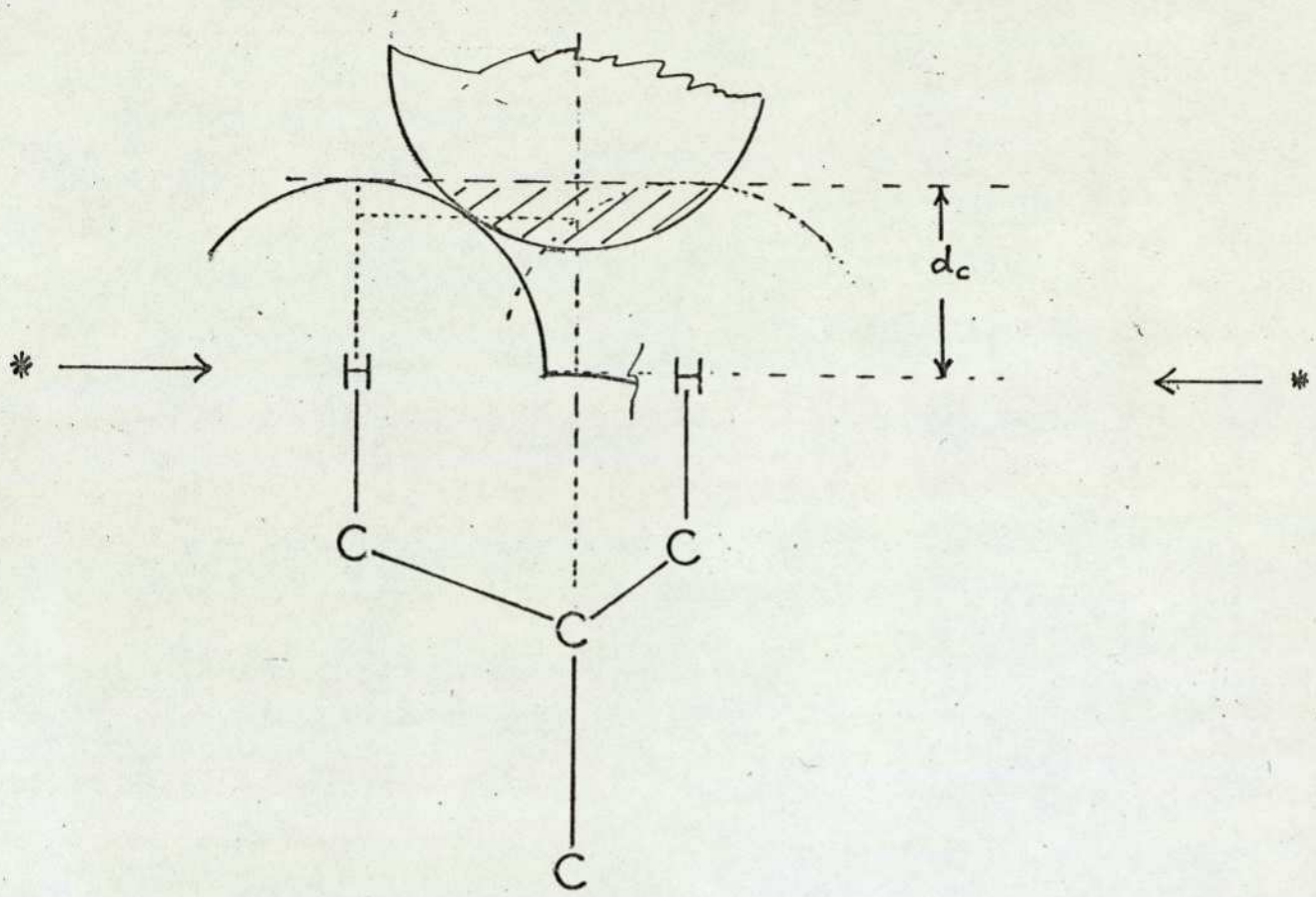

Hydrogen atoms form vertices of equilateral triangle across section marked * * .

Figure 37 A breakdown of the PIB cavity.

regular triangular prism from which are removed three spherical segments of intruding hydrogen atoms. The prism length is d_c, calculable as $(1.544 \sin 19.5^{o} + 1.085 + 1.2 - 1.65) = 1.150\,\mathring{A}$ (see Figure 37). The area of the triangular base formed by the hydrogen atoms is calculated as $2.752\,(\mathring{A})^2$ so that the prism volume is $3.165(\mathring{A})^3$. From expression 9.1, v_H is $1.697\,(\mathring{A})^3$.

$\therefore\ c''_{PIB} = 1.47\,(\mathring{A})^3$.

9.3.2 The calculation of a" values

For many elastomers, the calculation of a" follows from that of c". The purpose of estimating a" is to assess the effectiveness of the different cavities in assisting the formation of holes to enhance autohesive diffusion. Hence the cross-section of interest is perpendicular both to the tangent plane between the intrachain cavity and the adjacent interchain space, and to the most probable direction of approach by an incoming diffusant. Consequently, the section applicable to a" for cis polyisoprene lies on the extension through the cavity of the direction given by carbon atoms I and II in Figures 32 and 34 (a). For styrene moieties, the relevant section traverses the pendant benzene ring whilst, for all other elastomers considered, the plane acting across the cavity at 90^{o} to the chain direction is employed.

In elastomers such as NR, Stuart models show that cavities are easily accessible to the correct approach from another chain and that the incoming chain can, under the right conditions, fully fill the cavity: a" should then properly relate to the complete cavity. However, for cavities which can only accommodate a partial segment of the smallest

component of an incoming chain, namely a hydrogen atom, the above treatment should not apply. Cavities of this type (e.g. as shown in Figure 33) reasonably give rise to a'' values derived from the degree of penetration reached by an incoming hydrogen atom.

Cis Polyisoprenes including NR.

$$a''_{NR} = a''_1 + a''_2 + a''_3$$

where a''_1, a''_2 and a''_3 are the area components respectively relating to the volume components c''_1, c''_2 and c''_3 employed earlier in the section.

To find a''_1

The cavity width (i.e. in the direction defined above) strongly depends on conformation, whilst the depth d_c is as before (Figure 34). Representative widths for the two conformations have been calculated by standard trigonometry to be 2.006 Å and 1.647 Å. Hence a''_1 is best given by $0.5\,(2.006 + 1.647) \times 0.436 = 0.796\,(\text{Å})^2$.

To find a''_2

Previously the area of circular segment UPS was calculated to be $0.2805\,(\text{Å})^2$. The direction of section UPS can be shown to differ from the line of carbon atoms I and II by $15^\circ 32'$. Therefore

$a''_2 = 0.2805 \sec 15^\circ 32' = 0.291\,(\text{Å})^2$.

To find a''_3

From the calculation of c''_3, $a''_3 = 0.085 \times 1.2 = 0.102\,(\text{Å})^2$.

$\therefore\ a''_{NR} = 1.19\,(\text{Å})^2$.

cis Polybutadienes and isomers

From Figure 35 and the calculation of c''_{cBR}, a''_{cBR} is simply

$(0.5 \times 1.816 \times 0.436)$.

$\therefore\ a''_{cBR} = 0.396\ (\mathring{A})^2$.

a''_{tBR} is twice the area of circular segment UPS in the NR model (Figure 34) $= 2 \times 0.2805 = 0.56\ (\mathring{A})^2$, and $a''_{vBR} = a''_{PIB}$, which will be seen to be $0.67\ (\mathring{A})^2$.

The values of a'' are suitably proportionated for the BR isomers recorded in Table 27.

Styrene moiety

The most representative section for a'' reasonably incorporates the breadth of the benzene ring (which experiences no steric restrictions) whilst the second dimension arises from an incoming hydrogen atom (see Figure 36). By a series of geometrical and trigonometric considerations the axial length of hydrogen atom inserted as far as possible into the cavity can be estimated as $0.872\ \mathring{A}$.

$\therefore\ a''_S = 2.420 \times 0.872 = 2.11\ (\mathring{A})^2$.

PIB and other substituted saturated elastomers

a''_{PIB} arises completely from the degree of penetration possible by a hydrogen atom (Figure 37), a value calculable by twice employing the theorem of intersecting chords and applying the standard formula for the area of a circular segment.

Then $a''_{PIB} = 0.67\ (\mathring{A})^2$.

9.4 The role of cavities in hole formation

Within the hole-distribution framework discussed previously, hole formation is facilitated in appropriate elastomers when several neighbouring segments, which may or may not belong to different

Chain cross-sections in an ideal packing arrangement: n = 4.

At C: cavities occupied by part of an incoming chain.

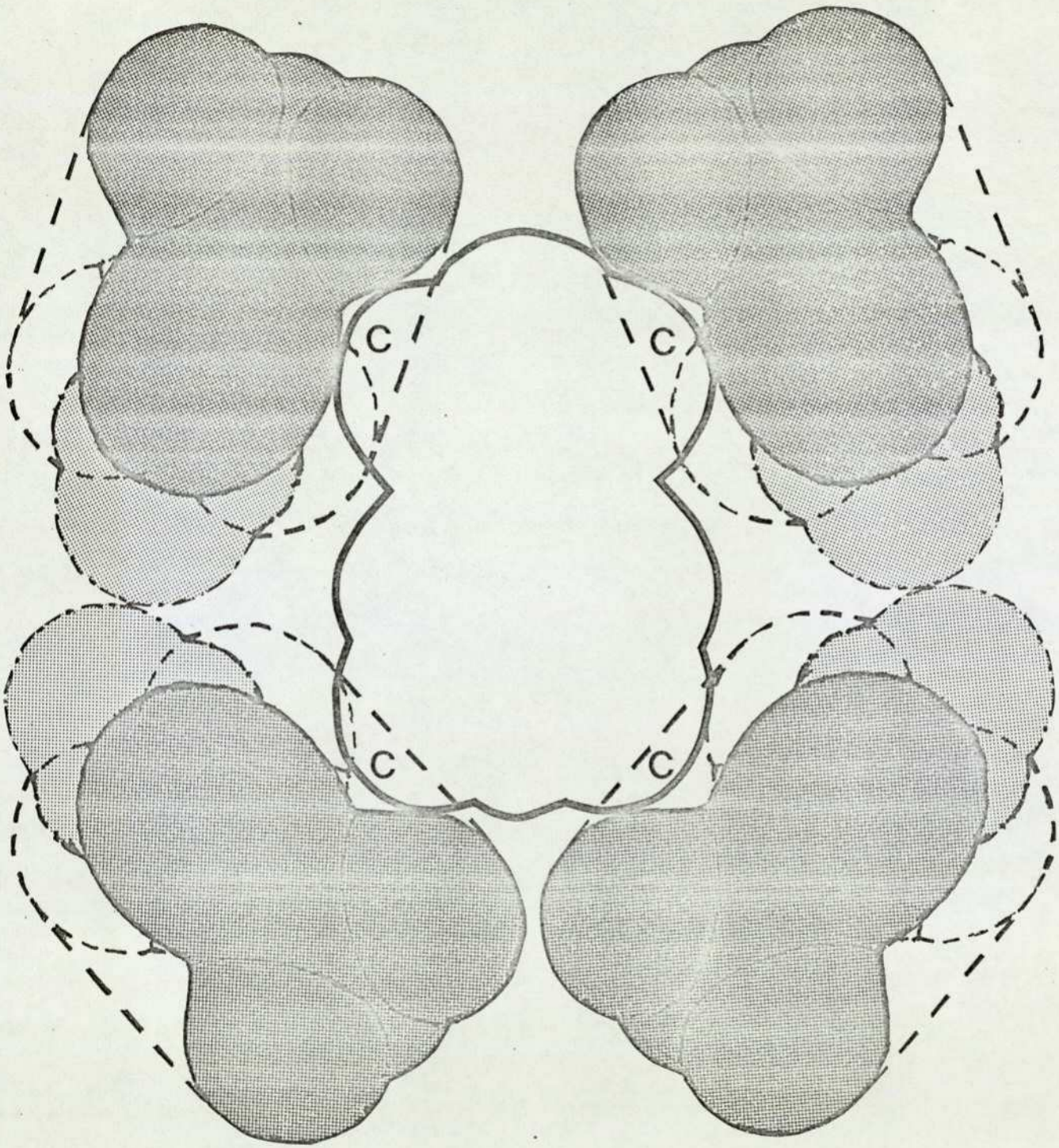

Figure 38 Hole formation involving the participation of large accessible cavities (NR-type).

Ideal packing, n = 4.

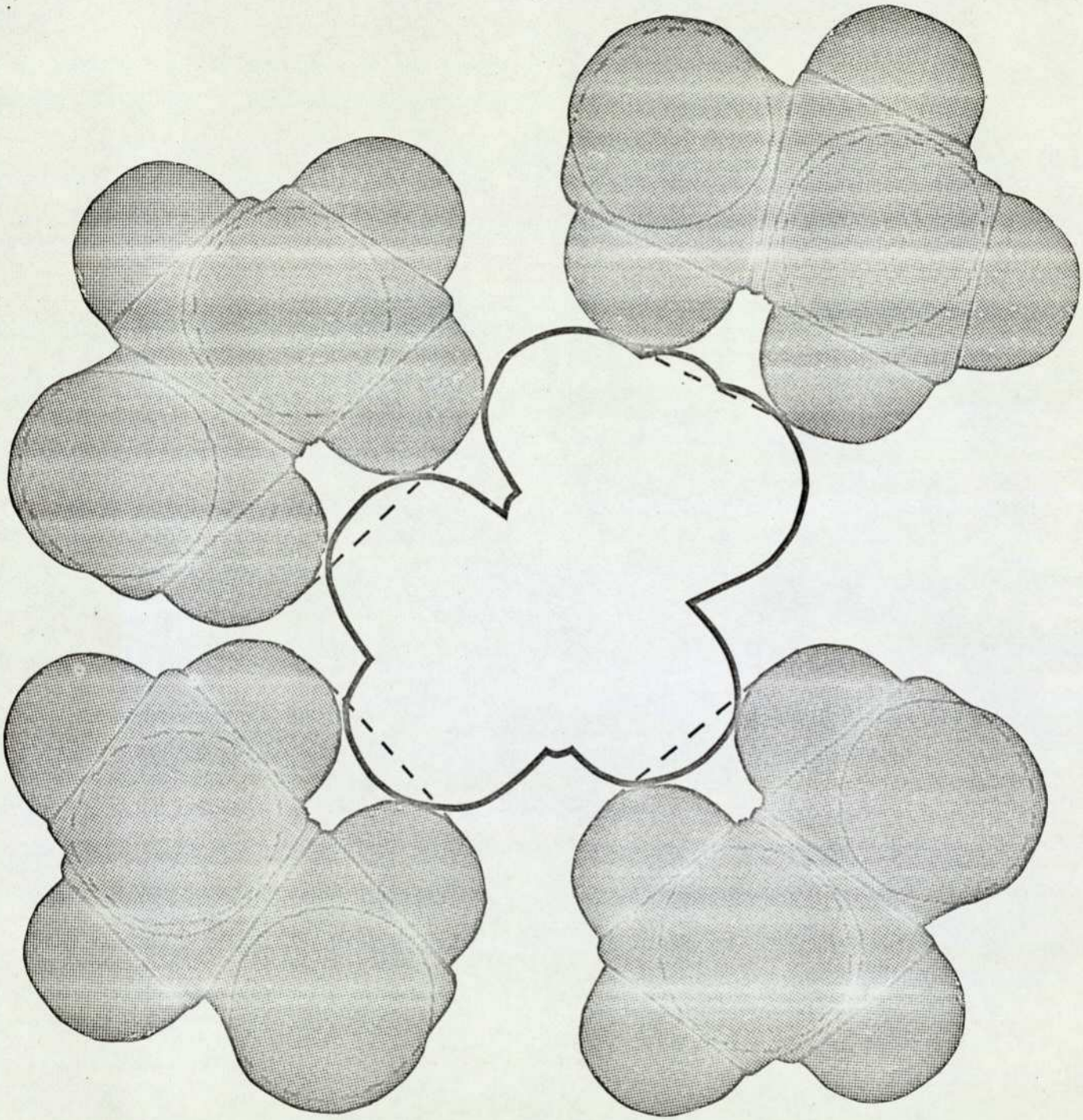

Figure 39 Hole formation involving negligible contribution from cavities of limited accessibility.

The particular sections shown are of EPDM.

chains, are positioned momentarily in such a way that intrachain cavities coincide. The space contributions of these cavities and that of the intervening free space combine to form a hole of critical size in situations of chain proximity close enough to prohibit critical hole formation for those other elastomers which possess no cavities.

The concept is illustrated in Figures 38 and 39 for an ideal packing arrangement conveniently comprising four chains: a system of NR chain sections (Figure 38) is compared with an analogous situation for EPDM (Figure 39). The chains are represented by photographic reproductions of sections of Stuart models which were manipulated in both cases to obtain no more than the critical hole size. Measurements taken both with the sections closely-packed and in the positions shown in the figures indicated that the increases necessary in root mean square distance between chains to attain the critical hole sizes are only ca 15% for NR but ca 27%for EPDM.

Naturally, chains involved in hole formation during random thermal fluctuations are rarely positioned in the ideal manner shown in Figure 38. The following situations are more probable:-

a) When the local surface region of NR participating in the formation of a hole is that of the methyl or methylene groups, the neighbouring cavities are not presented to the hole. Viewed in perspective, however, it seems reasonable that the cavities will, at the same instant or very soon afterwards, assist the formation of another hole.

b) Numerous variations occur in the number of participating chains and their positioning or direction relative to each other.

Nevertheless, when comparing polymers, the point made by Figures 38 and 39 reasonably applies for all analogous situations: the presence of cavities means that critical holes can be attained after relatively less outward movement of each participating chain portion.

From the considerations above, critical hole formation is clearly enhanced by the total number of available cavities. In the calculations performed in Chapter 10, the number X of cavities per monomer unit is related to that per gramme (N_o).

9.5 The resulting effect on the numbers of available critical holes

Arising from the comments of section 9.4, the activation energy of diffusion and the molecular friction should be minimised by the presence of cavities which contribute to the formation of critical holes. Hence, the number of holes attaining the critical size for diffusion during normal chain fluctuations must be considerably greater for elastomers containing intrachain cavities than that for elastomers with negligible intrachain free space. The effect is tentatively related to E_d, jump frequency and diffusion constant in Chapter 11.

Chapter 10 Mathematical treatment of a simple model and the proposed alternative

10.1 Free volume data for several elastomers

The case is made in section 4.10.1 for employing the Simha-Boyer[121] concept of free volume to compare the representative hole sizes of various elastomers. Writing again equation 5.8,

$$\varphi = (\alpha_L - \alpha_G)T \qquad 10.1$$

where φ is the free volume (cc. g^{-1}) and α_L and α_G are the....(cont.)

Table 28

The total free volume and other data for several elastomers

$T = 294^{o}K$

Elastomer	$(\alpha_L - \alpha_G)$ (cc. g^{-1} deg.$^{-1}$) x 10^{-4}	φ (cc. g^{-1})	General reference
NR	4.7	0.138	148
SBR 1500	4.5	0.132	149
Cis BR	5.8	0.171	149
IIR	4.9	0.144	1
EBM+	-	0.153	150
EPDM	5.55	0.163	149
Emulsion BR	4.85*	0.143	149

The data used for IIR were quoted for polyisobutylene.
+ $T_G = 217^{o}K$.
* From extrapolated SBR data.
The units of $(\alpha_L - \alpha_G)$ are discussed in section 4.10.1.

The degree of packing n is the number of chains packed around a space.

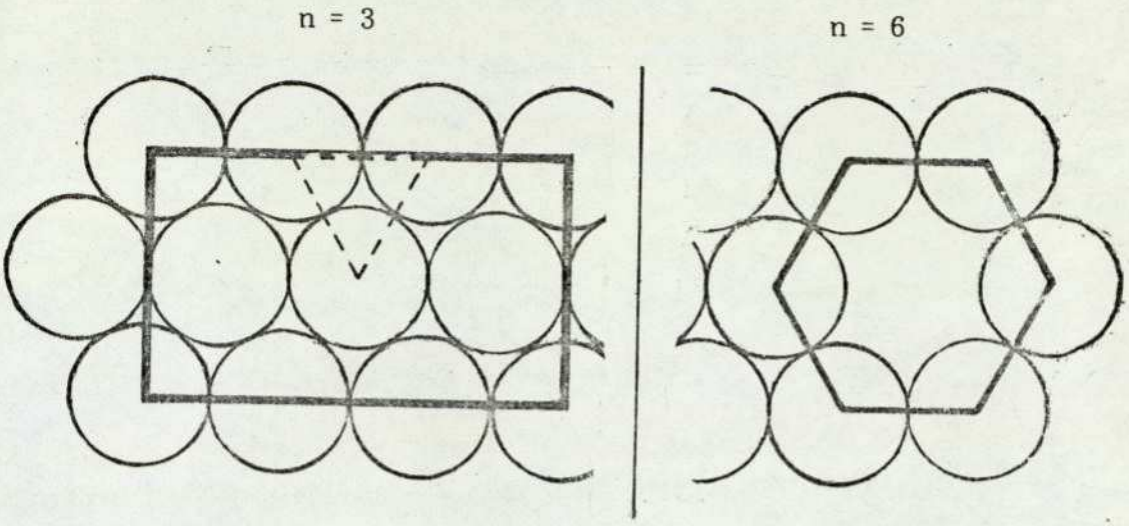

In any polygon joining the circle centre points, the ratio of number of circles to number of spaces is constant. i.e. When n = 3, the triangle contains one space and 3 sectors of total area one semi-circle whilst the rectangle contains a total of 12 spaces and 6 full circles. The number of spaces per circle $S_n = 2$.

When n = 6, the hexagon contains one space and 6 sectors of total area 2 circles. $\therefore S_n = 0.5$.

Similarly when n = 4, $S_n = 1$ and when n = 5, $S_n = 0.67$.

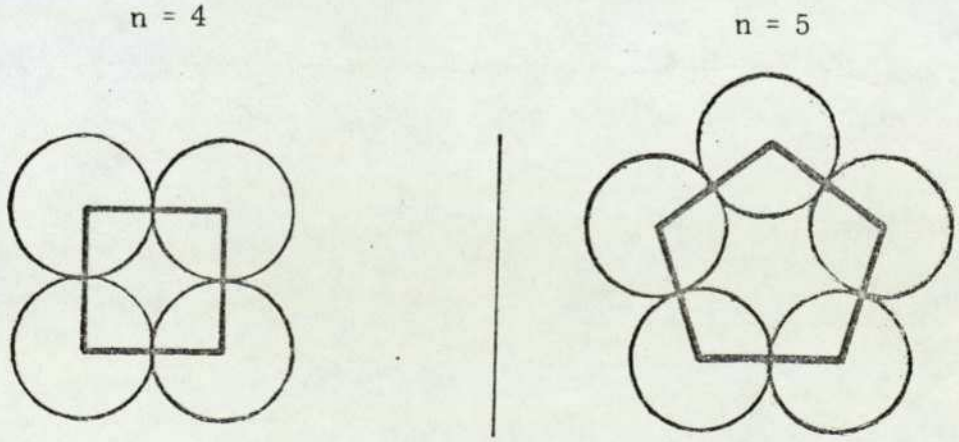

Figure 40 The two-dimensional packing of circles in ideal systems.

respective volume expansion coefficients above and below T_G. A single source for data of α_L and α_G could not be found for the seven elastomers described previously in Table 27. Hence values of φ for these elastomers have been obtained (Table 28) from collated α_L and α_G measurements which are apparently representative by comparison with other data. In the absence of a value of $(\alpha_L - \alpha_G)$ for EBM, the approximation of an iso-free-volume fraction of 0.113 at T_G [121] (see section 4.10.1) has been employed, φ being obtained by proportionation.

10.2 The distribution of free volume amongst monomer units

10.2.1 The mean hole cross-section for a simple model

A simple exercise is first required for subsequent comparison with the proposed model. To distribute the free volume φ amongst the monomer units in the most simple model (where all space is taken to be interchain), the close and semi-close packing of circles (or ellipses) representing ideal polymer chain cross-sections is considered. The space between circles is concentrated in interstices, the number of interstitial spaces per circle (S_n) depending on the degree of packing n: when n is 3, 4, 5 or 6, S_n is 2, 1, 0.67 or 0.5 respectively (Figure 40).

Polymer chain packing will tend towards these ideal conditions, the degree of packing continually fluctuating about a mean value $\bar{n}$. Hence a calculated average volume of free space for each monomer unit is shared between S_n regions of space. The mean cross-sectional area A of such a space region is given for the simple model by

$$A = \frac{\varphi M_M}{S_n N_A L} \quad \text{for any degree of packing n, } ----- 10.2$$

where N_A is Avogadro's number (6×10^{23}) and M_M and L are the molecular weight and the length of a monomer unit: values of M_M and L were given in Table 27.

10.2.2 The mean hole cross-section for the proposed model

For the proposed model, φ is shared between the total interchain free space φ' and the total intrachain free volume C'' where

$$C'' = \Sigma c'' = Xc''N_A / M_M :$$

values of X (the number of cavities per monomer unit) and c'' are given with M_M in Table 27. The estimates of C'' and φ' (obtained by subtraction) are shown in Table 29.

By analogy with the simple model, the average contribution A' of interchain free space to the area A of a hole formed by the coinciding cavities plus the intervening interchain space (Figure 38) is given by $\varphi' M_M / S_n N_A L$: the contribution from the participating cavities, depending on the number of chains involved, is na'', so that

$$A = na'' + \frac{\varphi' M_M}{S_n N_A L} \quad ---------- 10.3$$

Values of A for both models when n is conveniently 4 are shown in Table 29.

Table 29

Calculations of the specific intrachain (C'') and interchain (φ') free volumes, and typical hole cross-sections

			If n = 4 (S_n = 1)		
			Simple model	Proposed model	
Elastomer	C''	φ'	A	A'	A=na''+A'
	(cc. g^{-1})	(cc. g^{-1})	$(\text{Å})^2$	$(\text{Å})^2$	$(\text{Å})^2$
cis IR*	0.057	0.081	3.56	2.09	6.85
SBR 1500	0.036	0.097	3.17	2.31	5.03
cis BR	0.022	0.148	3.49	3.04	4.64
IIR	0.031	0.113	5.35	4.18	6.86
EBM	0.021	0.132	4.26	3.68	6.36
EPDM	0.009	0.154	3.53	3.33	6.01
Emulsion BR	0.035	0.108	2.88	2.18	4.34

* Including NR.
For the proposed model, the magnitude of A is irrespective of the number of holes which exist.
φ' is calculated from $\varphi - C''$.

10.3 The effect of the distributed free volume on the number of critical holes

A diffusing chain end involved in the autohesive phenomenon varies between polymers in shape and dimensions. For the simple model, the number of areas of interchain free space attaining the critical cross-sectional area A_o (to provide access to an incoming chain end) during normal thermal movements must proportionate to the average interchain space area A for any chosen polymer. If A_o were the same for all polymers, the most tacky polymer should possess the greatest A value. As A_o varies between polymers, the ratio A/A_o is more

applicable to autohesion.

For the proposed model, the autohesive properties of any polymer, sensibly relating to the number of critical holes formed, will depend on both A/A_o and the actual number of cavities per gramme (N_o) where

$$N_o = XN_A/M_M, (X = \Sigma X_i \text{ for copolymers}). \quad \text{- - - - - - - - 10.4.}$$

N_o is not an absolute factor, as each cavity would not participate in hole formation after every chain movement. For convenience, rationalised values f representing N_o for the various polymers, using N_o for cis BR as the normalising factor, are presented in Table 30.

Table 30

Normalised factor f relating to the number of cavities per gramme

Elastomer	N_o	$f = 100\left(\frac{N_o}{N_{o(cisBR)}}\right)$
	$\times 10^{21}$	(%)
cis IR	17.62	79.8
SBR 1500	16.78	76.0
cis BR	22.07	100.0
IIR	21.39	96.9
EBM	14.25	64.6
EPDM	6.12	27.7
Emulsion BR	20.30	92.0

At this stage, the calculations of A/A_o and $f(A/A_o)$ for the simple and proposed models require only the determinations of A_o, which are now performed.

10.3.1 Estimations of elastomeric chain cross-sectional areas

In the absence of a direct method, representative cross-sections would ideally relate to measurements from model hydrocarbons. However, no comprehensive range of measured A_o data utilising molecular sieves is available for such hydrocarbons. For consistency, all A_o values were therefore estimated: where possible, certain sequences of A_o data involving molecular sieves are also provided for comparison.

Stuart models were used to determine the most representative regular chain aspect for A_o: an arbitrary length of ca. 5 Å was considered, hopefully to relate to the initial autohesive jump across the interface. The most bulky cross-section was assumed to be circular or elliptical (as appropriate to each polymer) and radii (semi-axes) were calculated trigonometrically from the atomic dimensions of Table 26.

Estimated data are shown in Table 31, each cross-section being taken in the same plane as a" (section 9.3.2) for that elastomer. Values were proportionated for copolymers and isomeric polymers, molar ratios being in Table 27. The additional possibility of "end-on" diffusion of the styrene moiety (during initial diffusion) gives rise to a second A_o value for SBR. A comment on the validity of the A_o values is made by the following model measurements made[151-153] employing molecular sieves:-

(i) A sieve of representative pore size 19.6 $(Å)^2$ selectively absorbed 1-butene from a mixture with 2-methylpropene[151]. In Table 31, the cross-section for cis IR is greater than 19.6 $(Å)^2$ whilst the BR values are less than 19.6 $(Å)^2$.

Table 31

Estimated A_o values for the seven elastomers

Elastomer	Copolymer Moiety	Estimated elastomeric cross-section A_o $(\text{Å})^2$	
cis IR (including NR)			19.8
SBR 1500	Styrene	17.4, 41.6	18.0, 21.3
	Butadiene	18.1	
cis BR			18.0
IIR			35.5
EBM	Ethylene	21.1	25.1
	Butene-1	29.1	
EPDM	Ethylene	21.1	23.2
	Propylene	27.4	
Emulsion BR			18.2

The proportions of cis 1,4 , trans 1,4 , and 1,2 isomers in the various polybutadienes are given in Table 27. The values shown for A_o were computed from the following estimations for the 100% isomers:- cis 1,4 = 18.0$(\text{Å})^2$; trans 1,4 = 16.6$(\text{Å})^2$; 1,2 = 24.3$(\text{Å})^2$. The minor (ca 1%) moieties in IIR and EPDM have not been considered.

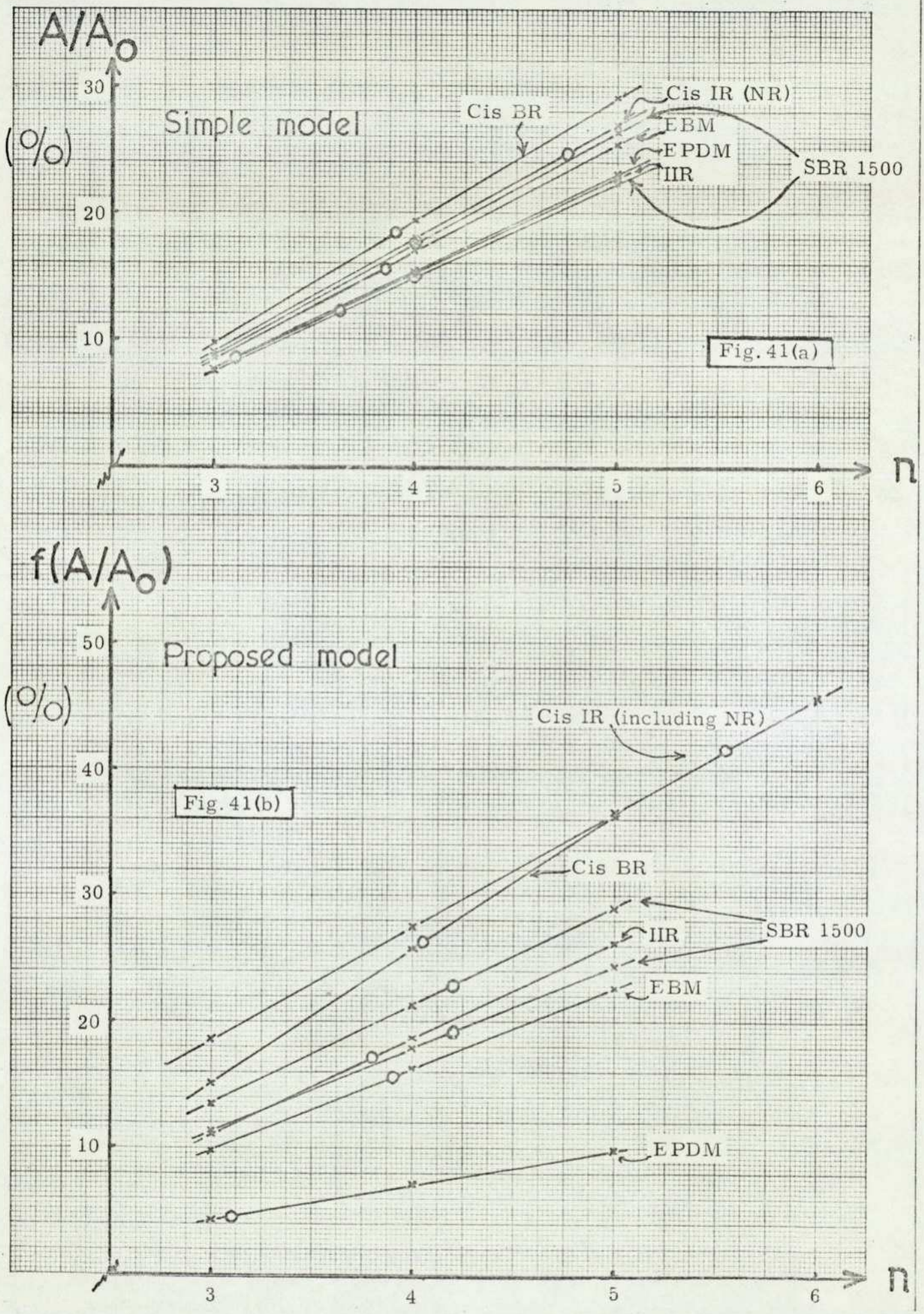

Figure 41 Mean ratio proportionating to the number of critical holes formed at different levels of packing for the two free volume models

(ii) Sieve measurements have indicated[152] cross-sectional areas of the higher n-paraffins (up to ca C_{16}), the isoparaffins and 2,2,4-trimethylpentane to be ca 19.0, 24.5 and 28.5 $(\text{Å})^2$ respectively. Some agreement is shown with the A_o data in Table 31 for the ethylene moiety, EPDM and IIR respectively: it should be noted that an appropriate unit of IIR possesses more side-groups than 2,2,4-trimethylpentane.

(iii) The selective absorption of propene from a mixture with propane has shown[153] that A_o for a saturated material is greater than the equivalent unsaturated value (cf in Table 31 values for the ethylene and butadiene moieties).

More details of some of the trigonometric calculations are provided in Appendix 4.

10.4 The correlation of autohesive strength measurements with $f(A/A_o)$ at reasonable levels of chain packing n

Sufficient data are now available to compute factors $f(A/A_o)$ and (A/A_o) at several degrees of packing n for the elastomers being studied. Graphs of the appropriate factor plotted against n for both the simple and proposed models are shown in Figures 41 (a) and (b) respectively: the two SBR 1500 plots for each figure arise from the two possible values of A_o for styrene (see preceding section). For the simple model at any value of n, no correlation of A/A_o with autohesive magnitude data (Table 20) is exhibited, the main discrepancy involving NR. In contrast, Figure 41 (b) shows for the proposed model that at any value of n which might reasonably be met during normal chain fluctuations, the factor $f(A/A_o)$ is greatest for cis IR and least for EPDM, the

intervening elastomers being placed in a sequence which generally correlates with autohesive magnitudes.

As discussed in section 10.3, the magnitude of $f(A/A_o)$ reasonably relates to the number of critical holes available as potential tack sites. Hence the mathematical appraisal provides general support for the proposed model. A slight reservation arises from the necessity to employ more than one source for the original free volume data. However the representative nature of the values chosen suggests that any resulting deviations should not be large.

Because A is a mean area term, the magnitudes of A/A_o (simple model) and $f(A/A_o)$ at the mean packing level $\bar{n}$ for each elastomer should be obtained for comparison purposes.

10.5 The correlation of autohesive strength measurements with $f(A/A_o)$ at the most probable ideal mean chain packing level $\bar{n}$

The estimation of values of $\bar{n}$ has necessarily been made by a method based on ideal, static packing situations.

10.5.1 Calculation of values of $\bar{n}$

In a hypothetical form of packing, the molecular chains of a polymer can be visualised as parallel cylinders lying only between two opposite faces of a cube. The diagrams already used in section 10.2.1 to obtain S_n (Figure 40) represent chain cross-sections (radius r) contact-packed in this ideal way for various values of n. The sections are better represented by ellipses for some elastomers: however, the general argument is not thus affected.

As discussed at intervals throughout this work, micro-Brownian

thermal movements of chain elements provide continually-varying local density fluctuations around a consistent mean on a time average basis. The mean is associated with an average value $\bar{n}$ which is specific to each polymer. The determination of $\bar{n}$ for a polymer involves the comparison of (i) a packing ratio estimated from measured data with (ii) a graphical representation of the equivalent ratio estimated geometrically for several values of n.

(i) For the plane given by Figure 40,

$$\text{let Ratio } R_A = \frac{\Sigma \text{ chain cross-sectional areas}}{\Sigma \text{ interstitial space areas}}$$

For a cube, side l_c, containing 1g of a polymer, the number of ideal parallel chains is $N_A L/M_M l_c$. Hence the total volume occupied by polymeric matter is $(N_A L/M_M l_c)A_o l_c = N_A LA_o/M_M$, and the total volume of free space in the cube $= l_c^3 - (N_A LA_o/M_M)$, so that

$$R_A = \frac{(N_A LA_o/M_M)/l_c}{(l_c^3 - (N_A LA_o/M_M))/l_c} = \frac{N_A LA_o}{M_M l_c^3 - N_A LA_o}$$

At the mean packing level $\bar{n}$, by the definition of l_c,

$$\text{density } \rho = l_c^{-3} \text{ g.cm}^{-3} \text{ (or Mg.m}^{-3})$$

$$\therefore \quad R_A = \frac{N_A LA_o \rho}{M_M - N_A LA_o \rho} \qquad \text{----------10.5}$$

(ii) In this case $R_A = \dfrac{\Sigma \text{ circle (or sector) areas}}{\Sigma \text{ interstitial space areas}}$

A study of Figure 40 shows that, whatever the packing, R_A is represented for N space areas within a defined boundary by

$$R_A = \frac{N\pi r^2 \frac{(n-2)}{2}}{N nr^2 \tan\left(\frac{90(n-2)}{n}\right)^\circ - N\pi r^2 \frac{(n-2)}{2}}$$

$$= \frac{\pi(n-2)}{2n \tan\left(\frac{90(n-2)}{n}\right)^\circ - \pi(n-2)} \qquad \text{----------10.6}$$

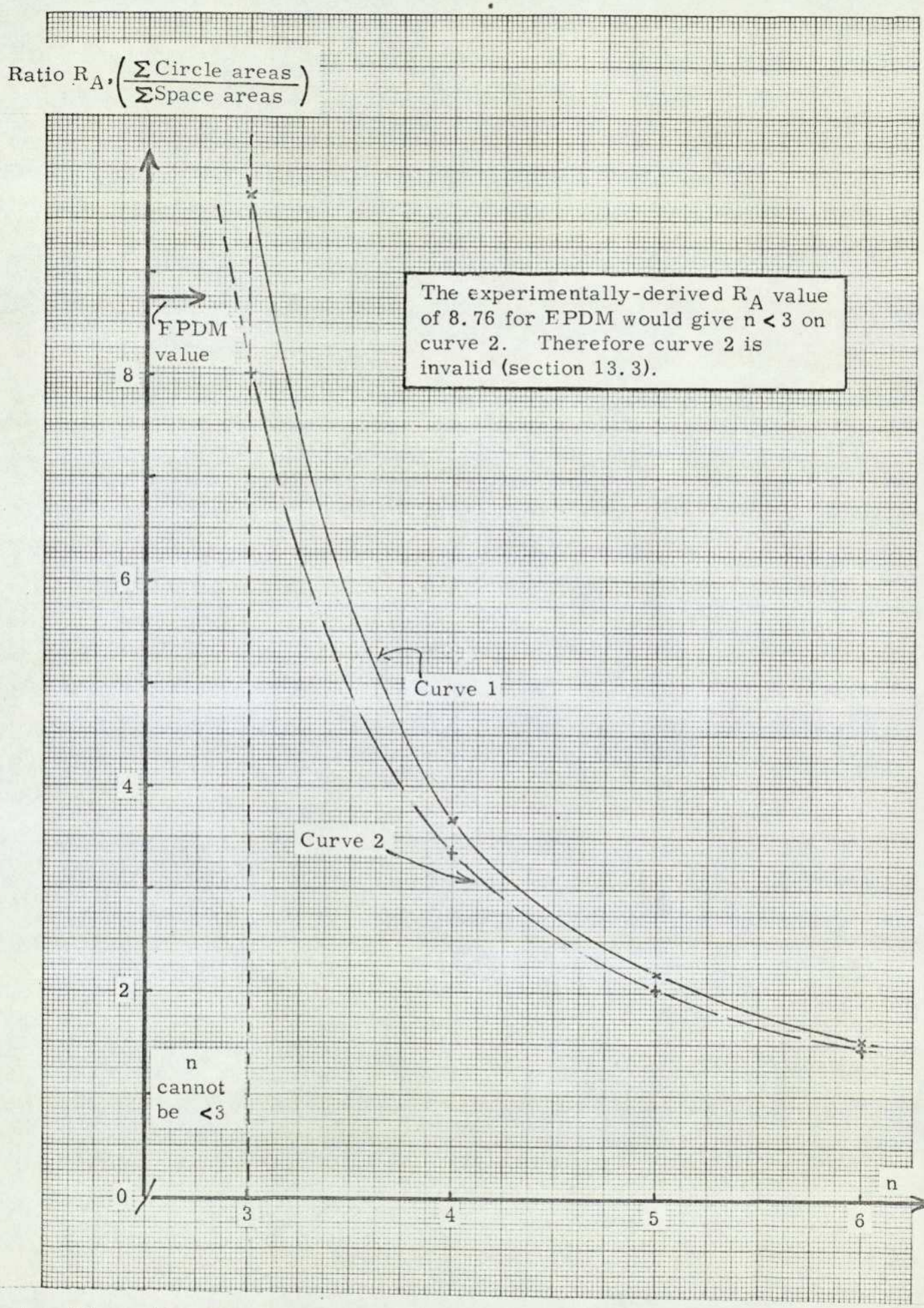

Figure 42 The change in the ratio of occupied area to space area as the degree of packing is altered.

Hence R_A can easily be plotted against n, the resulting graph being given in Figure 42 (curve 1).

For each elastomer, the substitution of data for N_A, L, A_o, M_M and ρ into equation 10.5 provides a value of R_A associated with $\bar{n}$. The substitution of the value of R_A into Figure 42 (the graphical form of equation 10.6) gives $\bar{n}$ as a result. As magnitudes of N_A, L, A_o and M_M are known from the preceding sections, the only measurements necessary involved ρ. The test data measured at 21°C on a gravitometer against anhydrous ethanol ($\rho = 0.789$) are included in Table 32 for the elastomers described earlier in Table 27: after the assessments in air, samples were steeped in the ethanol until (after 48 to 68 hours) consecutive readings of the density were constant.

The estimated values of $\bar{n}$ at 21°C for the elastomers are also shown in Table 32.

Table 32

Estimated ideal mean levels of packing $\bar{n}$ for the two models

Elastomer	Measured density ρ (Mg. m^{-3})	Simple model $\bar{n}$	Proposed model $\bar{n}$
cis IR*	0.91	4.75	5.55
SBR 1500	0.89	4.00	4.20
cis BR	0.91	3.90	4.05
IIR	0.88	3.65	3.80
EBM	0.90	3.85	3.90
EPDM	0.84	3.10	3.10
Emulsion BR	0.89	3.90	4.05

* Including NR

Two sets of results are given because, for the proposed model, the level of chain packing in the vicinity of cavities should be estimated by the replacement in equation 10.6 of A_o by $(A_o - xa'')$: to allow for all regions along the chain, $\bar{n}$ was weighted for each elastomer on a length basis between the modified and unmodified equation 10.6 according to the length of the particular cavities. Although the estimations of $\bar{n}$ are based on a hypothetical model, for comparable elastomers the greater values of $\bar{n}$ apparently relate to the bulkier polymers or those with relatively-large side groups.

10.5.2 The correlation with autohesive strength

The estimates of $\bar{n}$ from Table 32 have been indicated for each elastomer on the graphs in Figures 41 (a) and (b) by the insertion of a circle. The associated readings for (A/A_o) or $f(A/A_o)$ as appropriate have been collated into Table 33, together with the autohesive test data already recorded earlier in Table 20. Comparison of the columns in Table 33 indicates that, at mean levels of chain packing, both models correlate reasonably with autohesive properties in order of magnitude. However, in terms of actual magnitude, the proposed model can explain more realistically the superiority of the autohesion of cis polyisoprenes over that of the other five elastomers. The further advantages for the proposed model at values of n other than $\bar{n}$ were noted in section 10.4.

Table 33

Calculated factors to monitor autohesion for the two models at mean levels of chain packing $\bar{n}$

Elastomer	Simple model A/A_o (%)	Proposed model $f(A/A_o)$ (%)	Measured autohesive strength $(N(10mm)^{-1})$
NR*	24.8	41.6	127
SBR 1500	(a) 17.6 (b) 14.9	(a) 22.8 (b) 19.3	57
cis BR	18.4	26.5	54
IIR	12.4	17.3	37
EBM	15.7	15.7	39
EPDM	8.4	4.7	21.5

* Also other cis polyisoprenes
The estimation of A_o for SBR includes (a) the "end-on" cross-section of styrene units (b) "face-on" styrene.
$\bar{n}$ is given in Table 32 and applies at 21°C.

Comparison of the results of Figures 41 (a) and (b) suggests that IIR, although not a tacky rubber, possesses a higher magnitude of autohesion than the EPDM value for reasons due to the presence of cavities and to its higher value of $\bar{n}$. The relatively high rating of cis BR arises mainly from total free volume aspects only, whilst the presence of a few, very large, cavities in SBR 1500 probably contributes somewhat to the appropriate level of autohesion. The numerous, large, cavities of NR cause a higher autohesion magnitude than that of cis BR in spite of the smaller total free volume of the former.

10.6 The experimental comparison of recipient surfaces employing unilateral diffusion

The semi-quantitative estimations just performed have indicated that NR might reasonably possess more critical holes than cis BR, despite the greater total free volume of the latter, because of larger contributions by NR intrachain cavities. Although autohesion levels have been rationalized by the proposed model, a more direct experimental comment on the model can be made if the elastomers being compared are compelled by the use of very high molecular weights to provide only recipient surfaces. Unilateral diffusive flow can then occur by applying a suitable, third, low mol.wt.elastomer, so that differences in bond strengths reflect differences in the recipient surfaces.

Naturally, this approach is only valid if the thermodynamic requirements of making contact and intermingling are both satisfied. Table 25 (section 7.6) gives the appropriate results for the bonding of Intene NF 45 low-cis polybutadiene to high mol.wt.samples of either cis BR or NR. Because the contact force will cause Intene NF 45 to flow rather than the high mol.wt.rubber, good contact should follow if the surface energies allow the Intene elastomer to wet the other rubber. As γ_{lv} is similar to γ_c for hydrocarbon polymers[9], Intene NF 45 will wet either of the high mol.wt.rubbers according to the values of γ_c shown in Table 2 (section 2.1). With regard to the requirements for intermixing, the solubility parameters of the two polybutadienes are identical and the NR value is 0.3 $(\text{cal.cc.}^{-1})^{\frac{1}{2}}$ lower[34]. For unilateral diffusive mixing, the proportion of high molecular weight species will be dominant in the interfacial region, and, under these conditions, such a difference in solubility parameters can be reasonably tolerated.

From the experimental data of Table 25, the bond strength of Intene NF 45 to the high mol.wt. sample of NR was 10% higher than that to high mol.wt. cis BR. The implication is that the NR recipient surface possesses more critical holes than the cis BR surface.

PART III - THE PROPOSED MODEL RELATED TO VARIOUS FORMS OF DIFFUSION AND TO OTHER PHENOMENA WHICH DEPEND ON CHAIN PARAMETERS

Chapter 11 Autohesive diffusion and its relation to the proposed model and chain flexibility

A strong case now exists that differences in autohesion largely occur for geometrical reasons arising from chain structural and packing considerations. Hence the relationship between chain flexibility and the proposed microstructural model should be discussed. However, as the microstructural model (unlike flexibility) is not an established concept, a brief discussion is first appropriate on other situations where the fine-scale distribution of free volume around local geometrical features has apparently influenced measured properties.

11.1 Other instances of the application of microstructural geometrical shapes

After considering the molecular structure, submolecular motion and mechanical behaviour of amorphous polyolefins, Martin and Gillham[154] have concluded that the shape of the free volume contributes to the relation of free volume and the glass transition temperature T_G. The geometrical effects which could influence the shape of interstitial space regions might contribute to deviations from a proposed[121] iso-free volume state at T_G (section 4.10.1).

Another suggested partitioning of free volume[155] has followed a disagreement between experimental observations of the internal pressure P_i and the theoretical assessment of P_i arising from reasonable magnitudes of the fractional free volume. A considered explanation was that only part of the total free volume is available for configurational changes. Wake[96] had already suggested that some free volume is employed in 'loosening' processes, functioning within the influence of

the sixth power law of intermolecular forces, whilst other free volume outside this influence always exists as holes (albeit in ever-changing positions). Allen[155] contemplated that the free volume might be dispersed in pockets smaller than the volume occupied by a segment of the polymer chain so that a configurational change could only occur when a sufficiently large amount of free volume had been collected in the appropriate region.

After an extensive study of the diffusion rates of various penetrants (of size C_{18} or C_{36}) into several elastomers, Auerbach et al[99] noted that the removal of double bonds from the elastomeric molecular chains tended to decrease the diffusivity of octadecane through the elastomer. A 47 - 61% decrease in diffusivity was measured upon saturating (i.e. hydrogenating) three elastomers, namely BR, SBR and IR. Chain unsaturation was considered to increase the possibility of hole formation due to the localised rigidity at the double bonds and a subsequent hindrance to close packing.

11.2 An apparent explanation of the extremes in tack behaviour in terms of the proposed model and chain flexibility

The proposed model has demonstrated semi-quantitatively (in terms of high opportunities for hole formation) the order of autohesive strength obtained for six elastomers. Comparison of the calculated data for two models has shown that the main role of the proposed model is to offer an explanation for the high tack of NR rather than to grade the tack of all elastomers. Cis polyisoprenes are unique amongst common rubbery polymers in containing numerous cavities of substantial size and high accessibility to incoming chains.

The spontaneity with which the most tacky elastomers adhere possibly suggests a rapid initial diffusion, from each surface, of short chain ends or portions into the opposite recipient surface, utilising the relatively numerous critical holes formed by the coincidence of cavities in these polymers. This possibility might relate to the Type A diffusion of Frisch[98] (section 4.2 et seq).

The subsequent development of bond strength depends on the diffusion of statistical chain segments of length 20 to 40 carbon atoms[100,96] (or Type B diffusion[98]). Such diffusion requires a high degree of cooperative segmental organisation within the polymer bulk to form critically-sized holes. From an established viewpoint, saturated systems are generally associated with high internal energy barriers to rotation[116]: unsaturation is desirable for cooperative organisation. Furthermore, the effective size of saturated diffusive units will be high. From the viewpoint proposed herein, the microstructural model can also be applied to this scale of segmental organisation. The presence of cavities should facilitate the cooperative alignment of discrete holes, thus enabling the critical segmental hole size to be attained with less chain cooperation: consequently, critical segmental holes will again occur in greater numbers. The structure of cis polyisoprenes is such that these elastomers derive benefit from both viewpoints.

The factors which govern the diffusion constant D have been seen

(Chapter 4) to be the activation energy E_d, the frequency factor D_o, the molecular friction (the product of the segmental friction f_o and the number of segments per chain N_s), the jump frequency Φ and the jump distance δ_j. The apparent difference of one order in rate of diffusion between NR and EPDM arises from differences in those factors which in turn are influenced by the geometrical considerations discussed above.

To reiterate briefly

$$D = kT/N_s f_o \quad \text{- - - - - - - - - - - - - - - - from 4.9}$$

and $$D = \Phi \delta_j^2 / 6N_s \quad \text{- 4.15}$$

so that $$f_o = 6kT/\Phi \delta_j^2 \quad \text{- 4.16}$$

(T being temperature and k being Boltzmann's constant)

whilst $$D = D_o \exp(-E_d/(N_A kT)) \quad \text{- - - - - - - - - - - - 4.10}$$

where N_A is Avogadro's number.

D_o exists at quite different magnitudes for different systems of diffusion in polymers, the magnitude depending on the dimensions of the penetrating molecule[89], and has been considered to be an entropy term[99]. D_o is not relevant to hole formation in the matrix (or recipient surface for autohesion) and consequently not relevant to the present proposals. According to equation 4.10, diffusion is naturally enhanced by a decrease in the magnitude of the activation energy. Wake[96] has pointed out that holes already in existence within a polymer, if participating in the formation of a larger critically-sized hole, do not require a contribution from E_d. A similar logic reasonably applies to intrachain cavities which can be classed as holes (albeit small) already in existence. In the particular chain packing

arrangement shown in Figure 38, for example, the formation of critically-sized holes only required chains to move outwards by a root-mean-square distance of 15% for NR chains (possessing intra-chain cavities), whereas the outward movement required by EPDM was 27%. Clearly, E_d will be lower in the first case, as the degree of chain rotation required against the hindering potential of internal rotation[92] is smaller.

Referring to equations 4.9 and 4.15, the only parameters which might be influenced by the presence of cavities according to the proposed model are f_o and Φ (all jumps for hydrocarbon polymers being of similar magnitude). Indeed, at constant temperature, $f_o \propto \Phi^{-1}$ from equation 4.16. The segmental friction factor, the force f_o required to pull a single freely-orientating segment through its surroundings at unit speed[27], is almost completely required to push chains sufficiently apart to allow the passage of the segment[1]. As such, f_o should be the force associated with activation energy E_d, after correction for the number of segments involved, and is reasonably smaller if the presence of cavities means that the cooperative chain movement required is decreased. In such a case, the concomitant frequency Φ is suitably increased. Hence for the simple model of distributed free space considered herein, one might assume

$$\Phi \propto f_o^{-1} \propto A/A_o$$

and for the proposed model

$$\Phi \propto f_o^{-1} \propto f(A/A_o)$$

where f is the normalising factor for the number of cavities existing in an elastomer (section 10.3). The sum total of these considerations is

that, during normal chain fluctuations, the number of critical holes, which act as potential tack sites, is increased by the presence of cavities.

In short, the effects of chain structure on both flexibility and the provision of intrachain cavities are largely complementary. The chain flexibility sequence shown in section 4.10.2 relates reasonably, although not absolutely, with an order of autohesive strength, and the proposed model can well explain the discrepancies. The explanation in structure terms of the apparent difference of an order of magnitude between the diffusion coefficients for NR and EPDM is feasible under such considerations.

TABLE 34

Collated Data for Diffusion of Gases and Solvents in Several Polymers

Diffusion Constant D Values, $cm^2/s \times 10^7$

Polymer	Diffusion Temp. (°C)	Diffusion of Gases[158]				Diffusion of Solvents		Diffusion of Long-chain Hydrocarbon Solvents				
		H_2	N_2	O_2	CO_2	Benzene[159]	1,1-Diphenylethane[160]	Dodecane[157]	Hexadecane[157]	Octadecane[99]	**Oil[118] (~24 -C- atoms)	Octadecyl[99] stearate
NR	25	102.0	11.0	15.8	11.0	1.4	0.55	1.02	0.76	-	-	-
	40	-	-	-	-	-	1.86 (45°C)	-	-	1.69	-	1.02
	50	222.0	34.2	47.0	35.0	-	-	-	-	2.85	-	1.40
	60	-	-	-	-	-	-	-	-	3.94	-	1.94
	100	-	-	-	-	-	-	-	-	-	~3.5	-
SBR 1500	25	-	-	-	-	-	0.21	0.40	0.27	-	-	-
	40	-	-	-	-	-	-	-	-	1.38*	-	-
	50	-	-	-	-	-	0.96 (48°C)	-	-	2.29*	-	-
	60	-	-	-	-	-	-	-	-	3.22*	-	-
	100	-	-	-	-	-	-	-	-	-	~1.9	-
cis BR	25	-	-	-	-	-	4.41	5.75	4.57	-	-	-
	100	-	-	-	-	-	-	-	-	-	~6.4	-
Emulsion BR	25	96.0	11.0	15.0	10.5	-	0.83	-	0.83	-	-	-
	40	-	-	-	-	-	-	-	-	2.78	-	0.95
	50	180.0	29.0	37.0	28.0	-	-	-	-	3.62	-	1.41
	60	-	-	-	-	-	-	-	-	6.19	-	1.80
IIR	25	15.2	0.45	0.81	0.58	-	0.004+	0.007+	0.006+	-	-	-
	40	-	-	-	-	0.047+	-	-	-	-	-	-
	50	43.8	2.2	3.84	2.76	-	0.03+ (48°C)	-	-	-	-	-
EPM (31-33 mole % P)	23	-	-	-	-	1.05	-	-	-	-	-	-
	40	-	-	-	-	2.7	-	-	-	-	-	-
	100	-	-	-	-	-	-	-	-	-	~2.6	-

*GRS 1006.

** Filled compounds.

+Polyisobutylene.

Typical microstructure of emulsion BR: cis 19%, trans 64%, vinyl 17%.

Chapter 12 Correlation of the proposed model with diffusion through elastomers of gases and solvents

Whereas the diffusing chain portion in autohesive diffusion varies in size between elastomers, gaseous and solvent diffusion permits comparison of the same diffusant in a range of polymers. Thus any relationship of diffusion and distributed free volume might be studied. The absence of matrix-penetrant interaction found[156] for several solvent/polymer systems allows such a comparison.

Various workers have measured values of the diffusion coefficient D for different systems. Typical data have been collated in Table 34. Values of D are sensibly decreased by the presence of side-groups and with increasing diffusant size and molecular weight, the nature of the rubber matrix being the major factor in diffusion[118]. The rates of diffusion involved ($D \sim 10^{-5} - 10^{-7}$ cm.^{2} s^{-1}) are high relative to those for autohesion. Gaseous diffusion (for the smaller molecules especially) involves Type A Fickian diffusion, whereas, for larger penetrants, Type B becomes the dominating influence.[98] A more detailed appraisal of the data in Table 34 now follows.

A general relationship of solvent diffusion and total free volume[157] cannot be applied to gaseous diffusion according to the data of van Amerongen[158]. However, the situation is apparently rationalised by studying in particular two elastomers, NR and emulsion BR, assuming once again the presence of intrachain cavities.

12.1 Natural rubber and emulsion polybutadiene

In summary, for the smallest penetrants, especially hydrogen, and

for the largest diffusant (octadecyl stearate), $D_{NR} > D_{eBR}$, whereas for diffusants of intermediate size $D_{NR} < D_{eBR}$. These apparently paradoxical comparative data may be resolved by the proposed concept: the discussion refers to diffusion at near-room temperatures, higher temperature diffusion data facilitating certain comparisons.

12.1.1 The diffusion of molecules of comparable size to polymer segments

With the bulkiest diffusant (octadecyl stearate) the sequence of diffusion rates is NR > emulsion BR. This diffusant is roughly as big as a polymer chain segment (20 - 40 chain carbon atoms). Critical hole formation reasonably requires considerable cooperative chain organisation, the role of chain flexibility being important, as with autohesion. Hence, as discussed in Chapter 11, the presence of cavities should minimise the chain cooperation necessary so that many more critical holes can form, especially in the case of NR: the total number of cavities, N_o, is again a relevant factor.

The appropriate diffusion coefficients are $\sim 10^{-7}$ cm.^{2} s^{-1}. It might therefore be speculated that D is also ca 10^{-7} cm.^{2}s^{-1} for the initial stages of autohesive diffusion (section 4.3), the much lower values ($\leq 10^{-11}$ cm. s^{-1}) actually recorded by tracer techniques relating to whole-chain movements.

12.1.2 The diffusion of solvents and the larger gases

As the other solvent penetrants in Table 34 are considerably less bulky than octadecyl stearate, they can pass easily through the holes discussed in section 12.1.1. Moreover, additional diffusion occurs through smaller holes (being part of the thermally-driven local

density fluctuations which continually vary throughout any polymer), varying in dimensions down to the critical sizes which now apply. The formation of these critical holes requires less chain cooperation, with lower activation energies, than before.

From Table 34, these penetrants (unlike octadecyl stearate) diffuse more quickly through emulsion BR than through NR (the rate being even greater in cis BR). Comparison with Table 28 (Chapter 10) shows that the same sequence also applies to the magnitude of total free volume for these three elastomers, a relationship[157] between free volume and solvent diffusion already having been noted. It is therefore reasonable to assume that, in elastomers, the general magnitude of kinetic energy at normal ambient temperatures is highly likely to produce many holes which, whilst of super-critical size for solvent penetrants, do not require excessive amounts of activation energy (or associated chain cooperation). The presence of cavities would not be expected to influence significantly the numbers of critical holes for these penetrants.

The diffusion of gases cited in Table 34 (other than hydrogen) involves all holes discussed above plus the relevant critical holes (and all intermediates). The formation of these critical holes requires a minimum cooperation estimated at four or five $-CH_2-$ units[124,146]. D values in the two elastomers are similar, to mark the onset of another trend which is emphasised by the relative rates of diffusion of hydrogen in these rubbers.

12.1.3 Hydrogen diffusion

A single $-CH_2-$ unit probably possesses enough associated free volume

to permit the occurrence of a diffusive step of a hydrogen molecule[124] and its jump frequency is sufficiently rapid to utilise fully every hole of sufficient size[156]. As hydrogen easily passes through all holes discussed so far in this chapter, differences in the diffusion rates between elastomers should arise from the efficiency of its transport through the tightest-packing situations. To obtain a hole between close-packed chains by reducing a larger hole requires chain movements which combine a decrease in the level of packing n and a moving-together of chains at constant n. In either case, the proportion of intrachain free space increases with decreasing hole size: the influence of cavities becomes a major factor once again.

Hydrogen diffuses more quickly through NR than through emulsion BR. (A hydrogen molecule is only of circular cross-section 4.5 $\mathring{A}^2$ and elliptical cross-section 5.9 $\mathring{A}^2$ if estimated from atomic dimensions as before (Chapters 9 and 10)). During normal chain fluctuations, continually-changing regions of close-packing occur, and holes of minimum cross-section A_c for any level of packing n may exist by the coincidence of cavities plus the closest-packing interchain free space relevant to n. Whereas equation 10.3 described a mean hole area A, the interchain component of A_c may be estimated by ideal close-packing geometry. From section 10.5.1 (by consideration of equation 10.6),

$$A_c = na'' + A_o\left(\frac{n}{\pi}\tan\left(\frac{90(n-2)}{n}\right)^o - \frac{(n-2)}{2}\right) \quad ----- 12.1$$

Although both elastomers possess numerous cavities, the large NR cavities cause A_c values of magnitude equal to the critical cross-sections for a hydrogen molecule to occur when n is as low as 3.0 - 3.3,

whereas the equivalent packing for emulsion BR is 3.55 - 3.8. Clearly NR can offer critical holes for hydrogen diffusion even when tightly packed whereas emulsion BR only provides large enough holes at n values quite near to its mean packing level $\bar{n}$ of 4.1. BR must possess many holes of insufficient size, the free volume being utilised much more fully in NR for hydrogen diffusion.

12.2 Elastomers in general

A complete comparison of the diffusion rates of the full range of penetrants in elastomers in general has not been possible due to insufficient data (Table 34). However, those values of D which are provided support the arguments of section 12.1 for all elastomers considered except butyl rubber (IIR). The comparison is limited to the diffusion of solvents and an oil, the latter possessing on average 24 carbon atoms per molecule and hence being of similar size to a polymer segment.

For the smallest diffusant which can be considered (benzene), the effect of NR cavities on diffusion through closely-packed chains is still apparent, as EPM possesses the higher total free volume, but $D_{NR} > D_{EPM}$. With other solvent diffusants, the values of D in NR, SBR 1500, cis BR and emulsion BR follow the sequence of appropriate free volume magnitudes (Table 28). At the scale of chain organisation required for oil diffusion through NR, SBR 1500, cis BR and EPM, although the amount of free volume still largely dominates, the participation by NR cavities improves D_{NR} to a value which is once again greater than D_{EPM}, thus upsetting slightly the correlation with total free volume.

12.2.1 The relatively low diffusion rates in butyl rubber (IIR)

D values for all diffusants considered are very low in IIR (or PIB). Although a Stuart model of the elastomer shows two accessible cavities per monomer unit (X = 2), other shielded free volume cavities exist at any micro-Brownian segmental conformation. In addition, although the cavities are of moderate size, their shape precludes more than partial ingress, even by a hydrogen atom (Figure 33, section 9.2.2). Free volume data derived from the combined expansivity behaviour of all chains (i.e. an energetic source) should reasonably include shielded free volume regions. Hence, the useful free volume for IIR may be considerably less than initially expected, to explain at least in part the low values of its diffusion coefficients. The existence in benzene-swollen IIR of many holes of insufficient size to accept further diffusing benzene molecules has already been indicated[156].

Further support for such a picture arises by studying Table 34 to compare, for every possible penetrant, the diffusion coefficient through IIR with that through NR by means of the ratio D_{IIR}/D_{NR}. The ratios are shown as percentages in Table 35.

Table 35

A comparison of values of D for several diffusants in IIR and NR

	$100\ D_{IIR}/D_{NR}$ (%)						
Diffusant / Temperature (°C)	H_2	N_2	O_2	CO_2	1,1-diph.-C_2	C_{12}	C_{16}
25	14.9	4.1	5.1	5.3	0.7	0.7	0.8
50	19.7	6.4	8.2	7.9	-	-	-

Although the overall rate of diffusion through NR is by far the greater, the extent of its superiority varies with size of penetrant: the general trend is one of decreasing ratio with increasing diffusant size. As indicated in section 12.1, diffusion through NR is apparently efficient, because a network of critical holes for hydrogen diffusion exists throughout the elastomer even at the closest conditions of packing and the high mean packing level $\bar{n}$ of 5.6 suggests that ample space will be available for the passage of larger penetrants. Therefore the variations of the ratio in Table 35 are reasonably influenced by characteristics of the butyl elastomer. As a consequence, the high value of the ratio for hydrogen diffusion compared with the other ratios quoted suggests that many more holes exist of magnitude similar to that of a hydrogen molecule than exist of larger magnitude: a proportion of the smaller holes should exist permanently in such a way that they cannot contribute to a larger hole in the event of the appropriate local chain fluctuations. The shielded cavities discussed earlier conform with such a conclusion.

From Table 34, $D_{IIR} < D_{EPM}$ for benzene diffusion, whereas, for autohesion, $D_{IIR} > D_{EPM}$ from tack test results. Hence, although the collated data in Table 34 do not cover the point, a reversal of the trend shown in Table 35 might be expected for large diffusants. Comparison of other[99] values of D at elevated temperatures for IIR and NR suggests that the reversal in trend might have started for octadecane as diffusant.

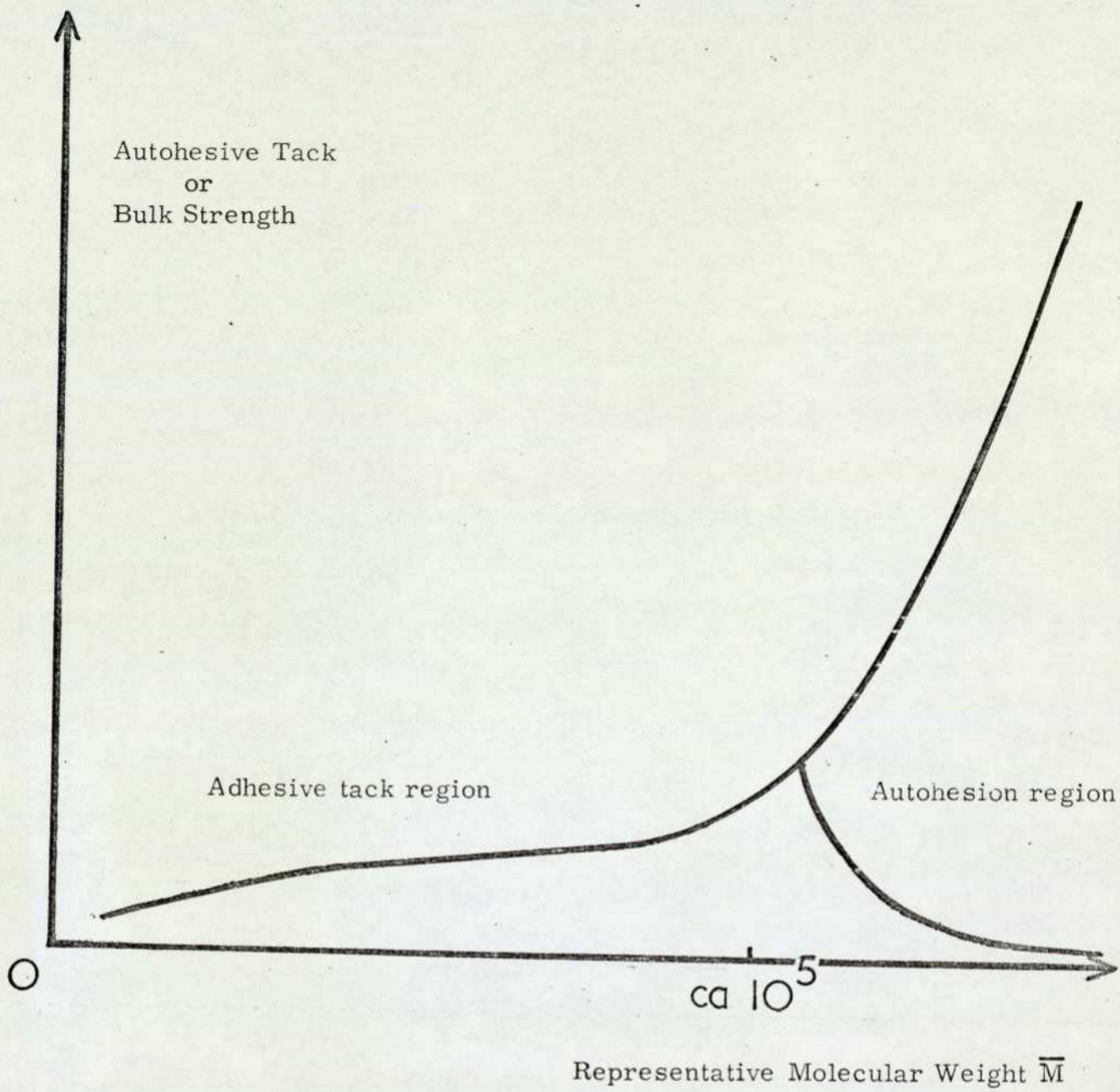

Figure 43 Schematic representation of the use of molecular weight to compare autohesion and adhesive tack.

Chapter 13 Implications arising from the present work on autohesion

Before discussing implications which arise if the existence of intrachain cavities is accepted for certain elastomers, the relationship of autohesion and the bonding of two adhesive coatings (section 1.2) can be viewed perspectively according to the approach used herein regarding the role of molecular weight M. Whilst accepting that M has been long-established as a factor in these processes, the approach of using short (and realistic) contact times, so that diffusive and bulk strength characteristics can be largely differentiated, is less common.

13.1 The relationship of autohesion and the rubber/rubber aspect of adhesive tack

Figure 43 shows a schematic portrayal of Figure 30 (section 7.2.2) with the curve suitably extrapolated so that the molecular weight scale extends down to values associated with viscous liquids. The term $\bar{M}$ relates to a representative value of molecular weight with contributions from elastomer, plasticiser, tackifier and, where appropriate, solvent.

When adhesive coatings are brought together, several workers have shown (section 1.2) that considerations of viscoelasticity[27,1] and mass flow are of greater importance to bonding than is diffusion: in the terms of Figure 43, the relative tack F_R is unity essentially as soon as the surfaces touch. The contribution of diffusion is now only minor. An applied constant stress causes segments to move despite the retarding influence of the product of the segmental friction force f_o and the velocity of the segments. At constant temperature, the relative movement per unit stress is given by a complex expression which includes:-

(i) a constant governing static and dynamic molecular considerations

(ii) summations of exponentials raised to power terms governed by the magnitude of time.

The high bond strengths which follow contact and viscoelastic fusion are enhanced for contact adhesives by evaporation of any residual solvent and by the support given by the proximate rigid substrates: the bond strength applies to the composite as a whole. Other adhesives increase $\overline{M}$ after contact by chemical crosslinking to give strong bonds.

In contrast, autohesion requires sufficient bulk strength for the practical handling of rubber compounds (sections 6.1 and 8.2) so that molecular weights must be much greater (ca 250,000 to 500,000). Usually $\overline{M} > M_1$ (Figure 43), and the times of viscoelastic and mass flow response to the contact force are longer than the appropriate contact times applicable to the thermodynamically-driven diffusion phenomenon.

13.2 Conclusions regarding rubber tack

The theoretical justification which the proposed model gives to the sequence of autohesive strengths for different elastomers at optimum molecular weights (section 7.3) also emphasises the practical problems facing technologists when handling the compounds of certain elastomers. Compounding techniques, at least by conventional means, only improve the optimum autohesive magnitudes of elastomers by a relatively small amount (section 7.4) Consequently, if the chain structure of an elastomer means that its magnitude of autohesion cannot be high, the tack strength of its conventionally-mixed compounds will also be inadequate.

For the greatest autohesion, the minimum requirement for the structure of a repeating unit combines the associated presence of both restricted rotation and one or more bulky side group, in a form of sufficient disorder to avoid substantial crystallization at room temperatures. Such a structure will probably possess a significant amount of free volume besides possessing cavities of considerable size.

13.2.1 The particular implications concerning the tack of EPDM compounds

The theory described in Chapters 9 and 10 totally opposes the possession of a high degree of autohesion by EPDM and, consequently, conventionally-mixed EPDM compounds could never be expected to be sufficiently tacky for technological purposes. The balance between sticky, unmanageable compounds and non-tacky compounds of high strength (the choice resting mainly with the representative molecular weight of the system, section 6.1) is unlikely to be overcome by conventional compounding means.

A common technological method of overcoming processing difficulties or deficiencies in property level associated with a particular elastimer is to blend the elastomer in suitable proportions with another polymer which separately satisfies the particular requirement. Thus a compound-blend of NR and EPDM can be obtained at an acceptable level of tack. However, certain advantages associated with EPDM, such as resistance to post-cure atmospheric ageing, are partially removed by the dilution with NR: the compromise can rarely be restricted to the area of interest only.

A similar argument would presumably apply to an alternative approach,

that of chemically-modifying the EPDM chains during polymerisation. Although resulting alterations in chain packing might enhance autohesive abilities, the change in structure could again reduce the oxidative ageing resistance. Additionally, after excessive chemical modification, the elastomer ceases to be EPDM.

If a solution exists to the tack problem of EPDM compounds, it lies most probably in novel approaches which may not wholly involve diffusive properties. A substantial advance has been claimed[71] by employing the following procedure. The diffusive/bulk strength requirements are both optimised by utilising an EPDM elastomer of molecular weight probably no more than 250,000 but with a high ethylene content of 80% to produce stress crystallization readily: in addition, the termonomer of the EPDM should be specifically ethylidene norbornene which when polymerised into the rubber chains is of structure:-

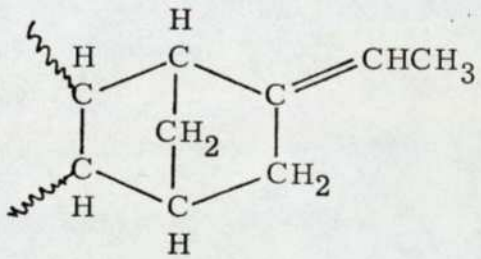

The approach concerns compounds and not the EPDM elastomer alone. These compounds comprise a mixture of the elastomer and compounding ingredients which, although standard, must include phenolic tackifier and aromatic oil: in addition, a sensitiser for photochemical reactions (e.g. tetraphenyl-porphirin) should be incorporated. These materials must be included in both components to be adhered. The surfaces of the uncured rubber compounds are next irradiated by visible light, using fluorescent tubes as sources. The resulting

The existence of cavities in a tackifier molecule.

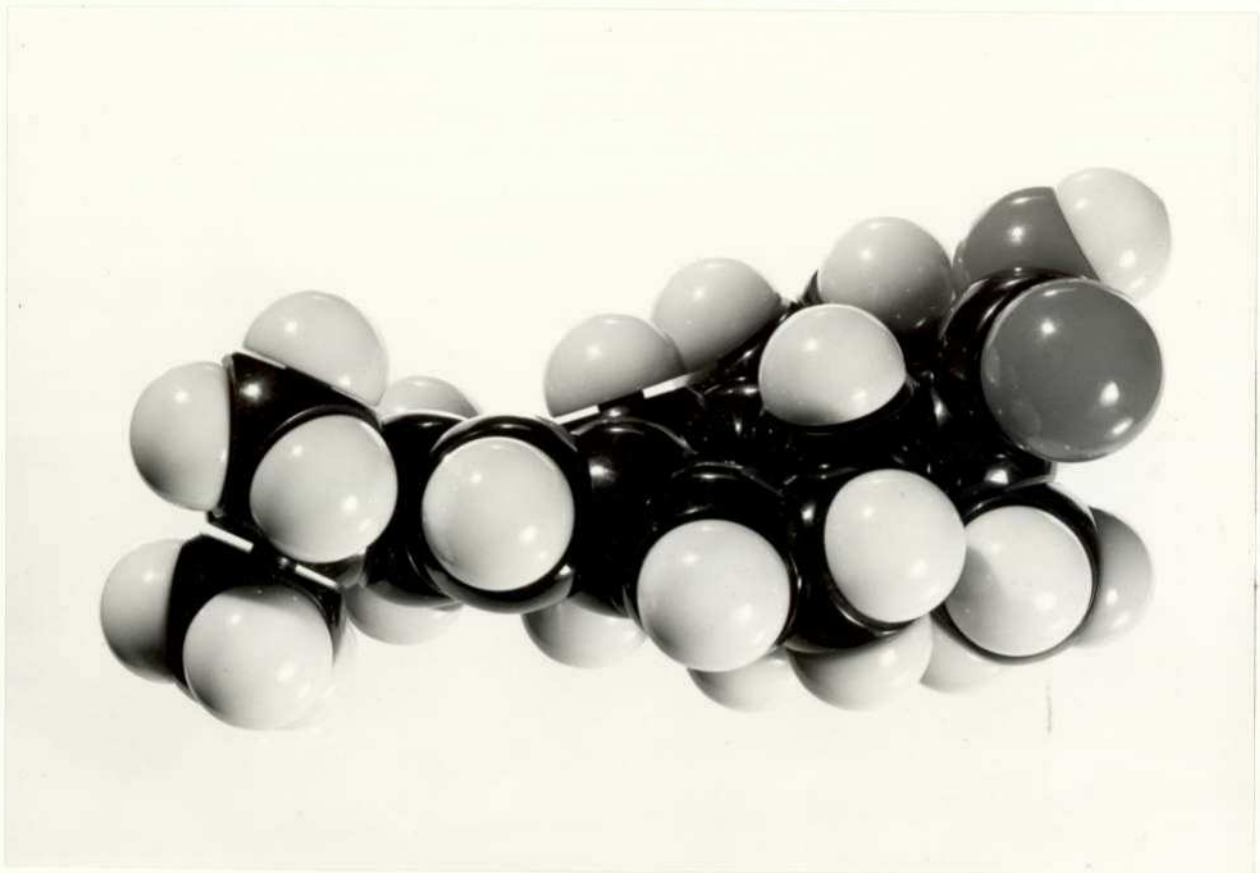

RPU 24499

Plate 6. Stuart model of a molecule of abietic acid (wood rosin)

surfaces are claimed to possess sufficient tack for the subsequent construction of articles such as tyres. Work at Dunlop Research Centre[68] has confirmed an increase in tack for a similar EPDM compound when irradiated by UV.

The mechanism of such an approach or that of other studies involving irradiation (see section 3.1.6) is not clear. The effect of the radiation on the ethylidene norbornene termonomer has been shown by van Gunst[71] to be the formation of hydroperoxides: in addition, a two-phase system at the surface has been observed, the second phase being rich in tackifier. Whatever the case, novel compounding techniques such as these are apparently required to obtain EPDM compounds possessing adequate tack: the answer theoretically cannot lie with the polymer itself.

13.2.2 Possible implications concerning tackifiers

As detailed in section 3.1.5, the main function of tackifiers is to migrate to the surface sufficiently to improve diffusive aspects, excessive migration being avoided so that no weak boundary layer is formed: the term "controlled incompatibility" thus arises. However, the pre-occupation of the present work with chain structural and packing details leads to a further tentative suggestion concerning the role of tackifier molecules.

Plate 6 illustrates a Stuart model of a molecule of abietic acid, this being the main constituent of wood rosin, a common tackifier. It is apparent that several "intrachain" cavities of a substantial size exist over the surface of the molecule. Hence, although the tackifier cannot

reasonably contribute to the strength of the system, the passage of a diffusing chain portion into the recipient surface might be facilitated by the formation of extra critical holes which are made possible by contributions from the cavities of tackifier molecules. Consequently, the tackifier which has migrated to surface regions can be visualised as not only enhancing the fluidity of outgoing chain portions, but also improving the efficiency of the recipient surface.

13.3 General comments on the packing of elastomeric chains

The speculative model which has been proposed has indicated the influence of particular regions of finely distributed free space on those characteristics of an elastomer which regulate an incoming diffusing species. These characteristics can also be monitored by factors at a higher scale of organisation such as chain structural symmetry (causing crystallinity), chain magnitude (or molecular weight) and free volume when crudely distributed throughout the polymer. NR possesses a high degree of autohesion because of the local supplementation of space distributed on a relatively massive scale amongst the dynamic thermal movements of long molecular chains by specific void features from a lower scale of organisation.

The phenomenon is considered to be an example of a more general hierarchical viewpoint held by Wilson[161] and others concerning the structure and construction of polymeric materials, and the relationship of these forms to various properties. Briefly, solid polymeric materials need not exclusively be considered as the result of infinitely ordered (crystalline) or limitedly disordered (glassy) cohesions of fine particles. According to Wilson, a valid alternative lies in

agglomerating the fine particles into larger particles to produce a coarser-scale complementary geometry between the agglomerated units and free space. The process can again be performed on a yet larger scale, although the complementary species may now be two components rather than one component and space. A succession of such formal jumps in scales of organisation, each scale eclipsing its finer predecessor, offers a concomitant number of approaches which can be attempted in order to influence a property of interest.

In the present case, the magnitude of the autohesive property can be influenced at several levels of organisation. For instance, an exposed tacky surface can be rendered non-tacky on progressively finer scales by the application of talc, soap solution and UV irradiation. Bulk effects which lessen autohesion are, in order of diminishing scales of organisation, filler particles (excessive loadings decreasing autohesive strength (section 3.1.4)), the blooming of curing ingredients or oils (section 3.1.6) and the immobilisation of polymer chains (high molecular weight or crystallization). However, if these effects are absent, the production of high autohesion relies only on three scales of sub-colloidal organisation:-

(i) the scale of chain organisation involved in producing cooperative movements of segments and statistical segments

(ii) the scale of chain organisation and agitation giving rise to the general distribution of free space through the polymer

(iii) the geometrical details of the molecular chain providing the local structural features giving rise to cavities.

On a complementary basis, the production of autohesion can be considered as being due to the free volume (associated with (i) to (iii)

above) also existing in hierarchical classes, viz that resulting from chain cooperation of such a magnitude to provide a critical hole for a segment, that which is distributed more or less evenly amongst the polymer chains and that contained by cavities (i.e. c''). A sub-cavity scale apparently exists in polymers such as IIR, effectively using up some free volume and inhibiting the diffusion even of hydrogen molecules. (In addition, finer scales of organised space occur within the environs of atoms themselves, but these are outside the definition of free volume given in section 4.10.1).

The scales of organisation which are apparently relevant to autohesion (and to forms of viscoelasticity such as those monitoring adhesive tack) do not necessarily apply to other properties, or to systems comprising more than one elastomeric component. The present work may, however, suggest one possible approach when studying such problems. Indeed, earlier work by Pechold[77] describes in detail for polyethylene the effect of rotational isomerism on molecular order and mobility (that is organisation at the microcrystallization scale) by correlating many conformations with plots of the complex shear compliance versus frequency and/or temperature.

Although the free volume of a polymer has been seen as greatly influencing certain properties, a part of the present work has drawn attention to its relative sparseness. The estimation of the average packing level $\bar{n}$ for elastomers (section 10.5.1) assumed an ideal situation (Figure 40) comprising parallel contact-packed chains with thermal fluctuations effectively being restricted to the highly organised cooperative motion of all chains within the relevant cube. Suppose

A typical representation [162] of the molecular chains in rubber using a wire model

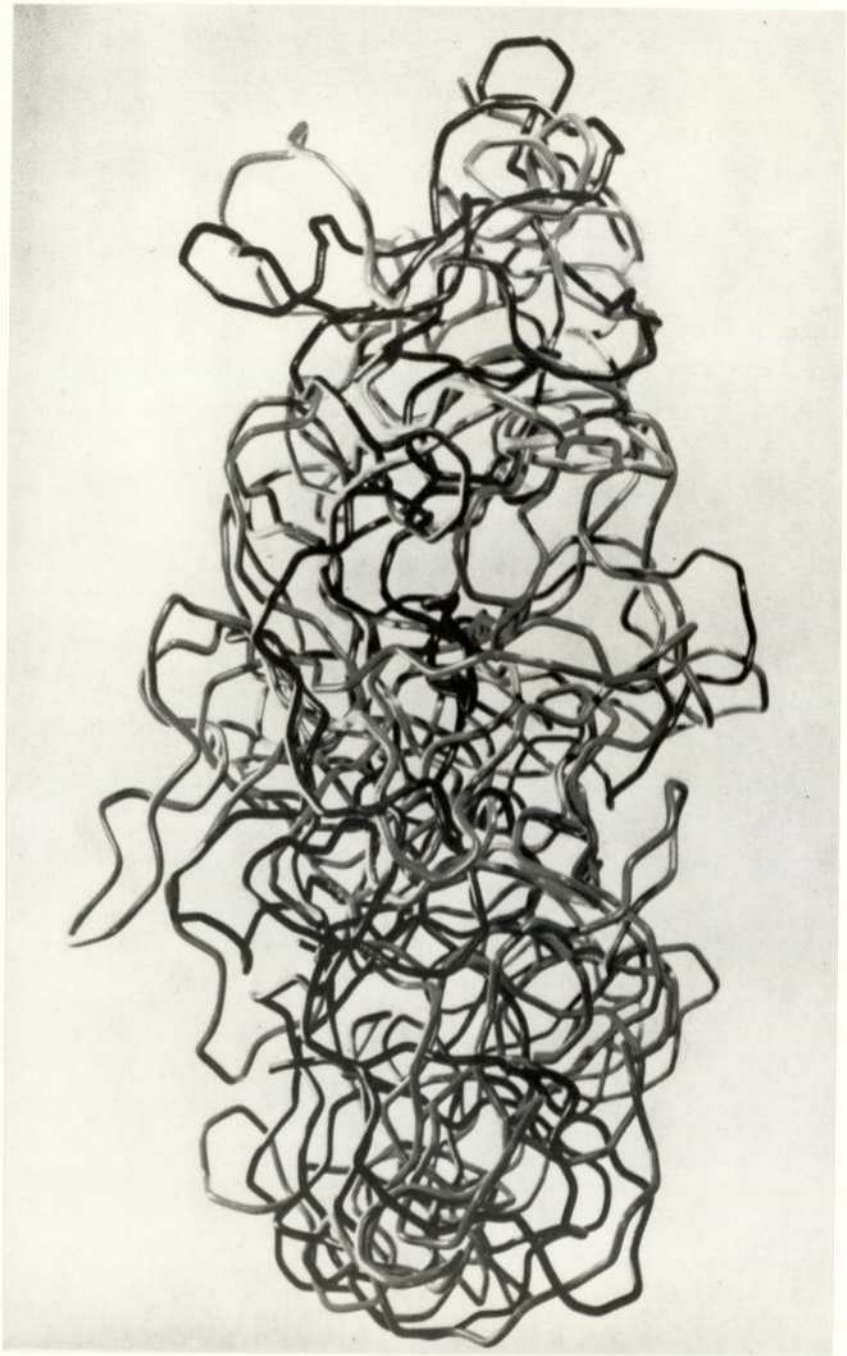

RPU 24498

Plate 7

instead that the chains were considered to be separated from nearest neighbours by a small distance 2s. The ratio R_A of area occupied by matter to that occupied by space now depends on a modified form of expression 10.6, with the term nr^2 substituted by $n(r+s)^2$. A value of s (namely 0.01r) has been arbitrarily considered, the subsequent estimations being plotted against n and shown in Figure 42 as a broken line (curve 2). The alternative experimentally-derived ratio R_A (obtained for any elastomer utilising expression 10.5) is 8.76 for EPDM at 21°C, the ensuing values of n from curves 1 (s = 0) and 2 in Figure 42 being 3.1 and 2.9 respectively.

Clearly, a packing level < 3 is meaningless for the model being considered. Hence, by inference, curve 2 does not apply and s < 0.01r, i.e. the average distance between the chains is less than 1% of the chain diameter. As real polymer matrices must contain a large distribution of chain crossover points (presumably involving bigger free volume interstitial regions) s must actually be considerably less than 0.01r. Consequently the influence of s was disregarded when estimating $\bar{n}$ in section 10.5.1. But, more to the present point, chains exist in a state of continual flux at situations of proximity much closer than the popular representation (e.g. [162]) illustrated by Plate 7. Whereas such models are helpful visually when discussing the random nature of intertwined, fluctuating chains, or the development and response of networks, a more realistic picture is of holes dispersed throughout a closely-knit system with considerable contact invariably being maintained during segmental movements. The importance of molecular friction and activation energy is thus emphasised. The

point has been separately made[77] with regard to microcrystalline effects.

13.4 The way for future developments

Following previous points of discussion, possible areas for further work are:-

1) For established elastomers which lack basic autohesion, further studies of novel compounding techniques.

2) The chemical modifications of elastomers (possibly during polymerisation) to introduce intrachain cavities as structural features (remembering the reservations expressed in section 13.2.1).

3) For the production of new tackifiers, geometrical as well as compatibility considerations: the possibility of incorporating extra cavities as molecular surface features.

4) The production of new elastomers with geometrical features specifically designed to produce high tack when at optimum molecular weight.

(a) Unsaturated polymers would undoubtedly be modelled on NR, hopefully to attain large cavities but with sufficient disorder to minimise crystallization: elastomers possessing five chain carbon atoms per monomer unit might be of interest.

(b) Saturated polymers would presumably require the incorporation of bulky side-groups, possibly producing steric hindrance to enhance the size of cavities.

It is, however, unlikely that polymers which might evolve would find commercial outlets due to the competition of existing elastomers and for cost considerations.

5) The utilization of a hierarchical approach: the possibilities could be considered of the bonding of elastomeric materials by mechanisms which function at higher scales of organisation.

6) The use of packing considerations to increase further the impermeability of rubbers by causing a decrease in rates of gaseous diffusion.

7) Radiochemical studies of the self-diffusion of NR and EPDM over a range of molecular weights.

8) Corish[163] has pointed out that tack testing and other work in the following areas could provide further information on the understanding of autohesive tack:-

(a) The extension of the proposed model to other non-polar elastomers such as the polypentenamers and poly-2,3-dimethylbutadiene, and certain low-polarity non-hydrocarbons (e.g. polypropylene oxide). Free volume data would be required.

(b) Similarly applying the proposed model to polar elastomers such as acrylonitrile-butadiene copolymers and polychloroprene.

(c) Studies on the effects of molecular weight distribution (M.W.D.): comparison could be made between different cis BR elastomers which are produced with similar average molecular weights, but different values of M.W.D.[163]

As a point of general relevance, the measurement in one laboratory of free volume data for many common polymers would facilitate comparisons such as those performed in Chapter 10. The approach (cf section 4.10.1) might be a fundamental summation of the appropriate van der Waals radii or the accurate assessment of expansion coefficients α_L and α_G for all of the polymers on a single dilatometer.

Chapter 14 Concluding appraisal

The early chapters have considered the areas of established science relevant to autohesion, a bonding phenomenon applying to polymers which, for reasons of chain packing and magnitude of molecular weight (M), exhibit elasticity and other rubbery qualities. The analogous bonding property associated with rubber compounds (i.e. elastomers with additives incorporated for practical reasons) is autohesive tack. The coalescence of two similar elastomeric surfaces satisfies appropriate thermodynamic requirements, but, when M is high, constraints due to viscoelasticity are only overcome by the application of a sufficiently large contact force. When contact conditions are acceptable, a sequence of autohesive strengths exists for elastomers, ranging from high magnitudes for NR and other cis polyisoprenes through the levels of other synthetic elastomers to low values for EPDM polymers. The explanation has been found in a fine study of the bonding mechanism of the coalescence, which is broadly the interdiffusion of polymer chains across the interface.

The general bonding mechanism must also apply to the more frequently-met autohesive tack. An analogous sequence of tack strengths exists for different elastomeric compounds. Certain technological problems caused by low tack can often be overcome by improving chain mobility to enhance the rate of interdiffusion. Examples are:

(i) (for cis polyisoprenes) the mechanical reduction of M, a major factor influencing autohesion. This process can be enhanced by the presence of fillers in compounds, due to increased shear forces.

(ii) the addition to compounds of processing oils and tackifiers,

the latter now being chemically-designed to migrate to the surface region for maximum effectiveness.

In contrast, autohesive ability can be diminished by effects of radiation, surface contaminants and excessive filler loadings.

The relationship between tack strength and bulk strength influences both the construction of composites and tack testing. The use of excessively-long contact times can lead unintentionally to the assessment of bulk strength when tack testing, the confusion broadly arising because tack strength $\propto M^{-1}$ whilst bulk strength $\propto M$. The distinction exists between the terms on the grounds that the diffusive step must precede the development of bulk strength. The ability to form an adequate interpenetrating interfacial layer is the primary requisite of autohesive tack. Consequently, other characteristics which increase bulk strength, such as stress crystallization, reasonably influence tack strength in a supplementary fashion: whereas permanent crystallization inhibits the initial diffusive step to destroy tack, the following of a successful coalescence by the onset of stress crystallization increases the resistance to separation.

Existing methods of tack testing fall largely into two groups, peel tests and those in the tensile mode. A case can probably be made for preferring peel tests, despite the variable contact times involved. Both groups of test provide useful evidence concerning the effects of experimental conditions on autohesion, but generally fail in differentiating between the test magnitudes obtained from different elastomers. The sequence of tack strengths mentioned earlier in the chapter, known to exist from the practical experience of handling elastomeric materials,

was obtained using the Dunlop Rotary Tackmeter. This tackmeter (designed and constructed during the study described herein) is a dynamic test in the peel mode but with constant time of contact during any one test due to the sun-and-planet motion employed. The contact time is realistically short, as in technological handling. A necessary theoretical appraisal has been performed so that tack strength at standard conditions can be obtained from two direct readings followed by the elimination of a small energy loss contribution and treatment with a normalising factor. Many test measurements have been made to confirm known trends arising from variations in experimental conditions and other influencing factors (viz molecular weight, the addition of fillers and tackifiers etc.), to relate the autohesive tack sequence arising from elastomers and their compounds, to indicate the supplementary role of stress crystallization by studying isomerised polyisoprenes and to assess briefly adhesion between different elastomers.

As indicated above, the explanation of the elastomeric tack sequence (now experimentally substantiated) rests in the bonding mechanism. The mutual diffusion of chain portions across the interface between the participating surfaces has received firm experimental support by radiometric techniques (especially) and by microscopy. The diffusion can be treated as Fickian, but the application of the general differential equation of diffusion includes a compensation for the increasing size of diffusant with time. An alternative approach relates the self-diffusion coefficient D to the jump frequency and distance, where a "jump", by analogy with liquid diffusion, is a determinate movement which fills a suitable hole. A third treatment links D

with viscosity or molecular friction, a certain inter-relation between the different approaches being possible. The diffusing chain segments have been shown by activation energy studies elsewhere to contain 20 to 40 carbon atoms: however, the initial step during the autohesive process might involve smaller chain portions diffusing very rapidly into suitable apertures in the recipient surface.

The extension of the Fickian approach gives a theoretical expression for the strength of a developed autohesive bond. Experimental studies of factors in the expression agree well with the theory. From a comparison of optimum autohesive magnitudes of the extreme cases cis IR and EPDM (under conditions such that the single variant of the theoretical expression is polymer type), the rate of autohesive diffusion of cis IR is apparently an order of ten greater than that of EPDM, thus defining the autohesive problem. A detailed study of the relevant chain parameters indicates that the cause of the problem lies in the ease with which critical holes form in the elastomeric recipient surfaces. Estimations of the hole sizes, made around a time-average representative distribution, conveniently utilise a quantification of free volume, the space existing within a polymer between chains. A breakdown of the factors governing hole formation shows that the enhanced diffusion in NR arises for geometrical reasons concerning the packing and motion of chains.

The main contribution of the present work is the proposal of a geometrical model which apparently explains the autohesive problem. NR and other cis IR elastomers possess microstructural geometric features which cause the existence within each monomer unit of

permanent "cavities", albeit of continually-varying sizes, the cavities indenting the cylindrical aspects more usually visualised as describing polymer chains. During normal chain fluctuations, holes form between participating chain portions: the coincidence of cavities in the chains with the intervening free space causes a critical hole to form in situations of chain proximity close enough to prohibit critical hole formation for other elastomers not possessing cavities. Clearly, the number of holes formed is greater for cis IR elastomers for the same expenditure of energy per unit mass: the appropriate self-diffusive properties should therefore be considerably enhanced. Certain other elastomers also possess cavities, but either of smaller size or in less numbers than in NR. Estimates have been made of cavity sizes and cross-sections.

The free space collectively associated with cavities has been classed as "intrachain" free volume, the remaining space being "interchain" free volume. In a mathematical treatment of the model, the subtraction of the intrachain free volume estimates (the sum of the cavity sizes per unit weight) from literature free volume data has given values of the interchain free space which can be distributed to give in each case a representative interchain cross-section of a hole. The complete hole area requires the addition of a cavity cross-section from each surrounding chain. The ease of hole formation (and the numbers of holes which should form per unit expenditure of energy) depends for each elastomer on the product of the number of cavities and the ratio of the representative hole area divided by the chain cross-sectional area. The solutions varied with the degree of chain packing,

but plots against packing indicated a polymer sequence correlating with that of tack strength. The point has been emphasised by employing mean packing levels for each polymer (estimated specifically for the purpose). An analogous treatment of a simple alternative which did not recognise the existence of cavities gave a less convincing solution.

The argument can be extended to cover chain segmental movements. The presence of cavities can still facilitate critical hole formation at this scale. Activation energy and molecular friction aspects are thus minimised so that an increased number of segments can participate in diffusion per unit energy. An additional geometrical factor controlling cooperative movements during hole formation arises from the increased chain flexibility associated with unsaturated systems: this factor, whilst unable to explain the full tack sequence in its own right, largely complements the proposed model so that the apparent difference of one order between the self-diffusion of cis IR and EPDM is feasible. Further justification of the proposed model arises from its application to the diffusion through elastomers of gases and liquids, to resolve the apparently paradoxical diffusive behaviour of diffusants through NR and emulsion BR.

The implications from the present work centre around the microstructural requirements of polymers and tackifiers for high magnitudes of autohesive tack, the resulting problems regarding EPDM and possible novel practical solutions, and comments on the overall influence on rubber properties caused by chain packing aspects. The usefulness of a hierarchical scale of semi-organised matter is noted.

Appendix 1

Calculations involved in obtaining testing parameter Cos β (section 6.3.2)

From section 6.3.2 and referring to Figure 31, $m_2 = -\cot\Theta$ and m_1 is dy/dx of the epicycloid at X. In this unique position,

$\cos((R-\Delta)\phi/a) = (a-\delta_1)/a$ and $\sin((R-\Delta)\phi/a) = w/a$,

so that
$$m_1 = \frac{(1-((a-\delta_1)/a) + (\tan\phi)(w/a))}{(\tan\phi)(a-\delta_1)/a + (w/a) - \tan\phi}$$

$$= (\delta_1 + w\tan\phi)/(w - \delta_1\tan\phi)$$

Hence
$$\tan\beta = ((m_2 - m_1)/(1 + m_1 m_2))$$

$$= \frac{-\cot\Theta - (\delta_1 + w\tan\phi)/(w - \delta_1\tan\phi)}{1 - \cot\Theta(\delta_1 + w\tan\phi)/(w - \delta_1\tan\phi)}$$

From Figure 31, $\phi = \alpha + \Theta$ so that $\tan\phi = (\tan\alpha + \tan\Theta)/(1 - \tan\alpha\tan\Theta)$.

After substituting for $\tan\phi$ and rearranging conveniently, a further substitution is made, as

$$\tan\alpha = w/(R - (\Delta - \delta_1))$$

The expression for $\tan\beta$ can now be reduced to

$$\tan\beta = w(R-\Delta)/(\delta_1(R-\Delta+\delta_1) + w^2$$

w^2 can be written as $\delta_1(2a - \delta_1)$ (theorem of intersecting cords).

From this
$$\underline{\tan\beta = w(R-\Delta)/(\delta_1(2a+R-\Delta))} \text{ - - - - - - - - - - - - A.1}$$

$$\therefore \cos\beta = \frac{\delta_1(2a + R - \Delta)}{(w^2(R-\Delta)^2 + \delta_1^2(2a + R - \Delta)^2)^{\frac{1}{2}}}$$

As $\delta_1(2a - \delta_1)$ $(=w^2)$ $= \delta_2(2R - \delta_2)$ and $\delta_2 = \Delta - \delta_1$ we can obtain

$$\delta_1 = \Delta(2R - \Delta)/2(a + R - \Delta)$$

Substituting for w^2 and δ_1 gives an expression which reduces to

$$\underline{\cos\beta = \frac{2a + R - \Delta}{2R} \sqrt{\frac{\Delta(2R-\Delta)}{a(a+R-\Delta)}}}$$

App. 1 (cont.)

The use of a vector diagram (Figure 32) can also be used to derive expression A. 1 above.

In Figure 32, $\tan\beta = \dfrac{v_1 \sin(\alpha+((R-\Delta)\,\phi/a))}{v_2 - v_1 \cos(\alpha+((R-\Delta)\,\phi/a))}$

In the time t which would be required for point X_o (Figure 31) to progress to X, the trailing edge of contact moves through angle ϕ whilst the planet rotates through $(R-\Delta)\,\phi/a$.

Hence $v_2 = R\phi/t$ and $v_1 = a((R-\Delta)\,\phi/a)/t$ so that $v_2/v_1 = R/(R-\Delta)$

$$\therefore \tan\beta = \frac{\sin(\alpha+((R-\Delta)\,\phi/a))}{R/(R-\Delta) - \cos(\alpha+((R-\Delta)\,\phi/a))}$$

Expanding, substituting for $\sin\alpha$, (w/R), $\cos\alpha$, $((R-\Delta+\delta_1)/R)$, and as above for $\sin(R-\Delta)\,\phi/a)$, $\cos((R-\Delta)\,\phi/a)$ and δ_1, and collecting the terms gives once again equation A. 1:-

$$\underline{\tan\beta = w(R-\Delta)/(\delta_1\,(2a+R-\Delta))}.$$

Appendix 2

Calculation of the width of contact (2w)

(For use in estimating the contact time, section 6.3.3).

In Figure 31, $\Delta = \delta_1 + \delta_2$,

δ_1 and δ_2 being the contributions to the depression from the planet and sun testpieces respectively.

From Appendix 1,

$$w^2 = \delta_1 (2a - \delta_1)$$

and $$\delta_1 = \Delta(2R - \Delta)/2(a + R - \Delta)$$

Substituting in the first expression and taking the square root

$$w = (a\Delta(2R - \Delta)/(a + R - \Delta))^{\frac{1}{2}} \left(1 - \frac{\Delta(2R - \Delta)}{4a(a + R - \Delta)}\right)^{\frac{1}{2}}$$

Expanding binomially, and as Δ^2 terms and above are negligible for reasonable values of a, R and Δ,

$$w = (a\Delta)^{\frac{1}{2}} \left(\frac{2R - \Delta}{a + R - \Delta}\right)^{\frac{1}{2}} \left(1 - \frac{\Delta(2R - \Delta)}{8a(a + R - \Delta)}\right)$$

$$= \left(\frac{2aR\Delta}{a + R}\right)^{\frac{1}{2}} \left(1 - \frac{\Delta}{2R}\right)^{\frac{1}{2}} \left(1 - \frac{\Delta}{a + R}\right)^{-\frac{1}{2}} \left(1 - \left(\frac{\Delta(2R - \Delta)}{8a(a + R)}\right)\right) \left(1 - \frac{\Delta}{a + R}\right)^{-1}$$

Again expanding and neglecting terms of $\Delta \geqslant 2$,

$$\therefore w = \left(\frac{2aR\Delta}{a + R}\right)^{\frac{1}{2}} \left(1 - \frac{\Delta}{4R}\right) \left(1 + \frac{\Delta}{2(a + R)}\right) \left(1 - \left(\frac{\Delta(2R - \Delta)}{8a(a + R)}\right)\right)$$

$$= \left(\frac{2aR\Delta}{a + R}\right)^{\frac{1}{2}} \left(1 - \Delta\left(\frac{1}{4R} - \frac{1}{2(a + R)} + \frac{2R}{8a(a + R)}\right)\right)$$

$$\therefore w = \left(\frac{2aR}{a + R}\right)^{\frac{1}{2}} \Delta^{\frac{1}{2}} \left(1 - \Delta\left(\frac{(a^2 - aR + R^2)}{4aR(a + R)}\right)\right)$$

Appendix 3

Vector calculations for section 6.3.3

In Figure 32,

$$u^2 = v_1^2 + v_2^2 - 2v_1 v_2 \cos(\alpha + (R - \Delta)\phi/a)$$

$$v_2 = R\phi/t \text{ and } v_1 = a((R - \Delta)\phi/a)/t = (R - \Delta)\phi/t$$

$$\therefore u_2^2 = (\phi/t)^2((R - \Delta)^2 + R^2 - 2R(R - \Delta)(\cos\alpha \cos(R - \Delta)\phi/a - \sin\alpha \sin(R - \Delta)\phi/a))$$

Specific values for $\cos\alpha$, etc., have all been described in Appendix 1.

Substitution, collection of terms as before and reduction gives

$$u = (\phi/t)(\Delta(2R - \Delta)(a + R - \Delta)/a)^{\frac{1}{2}}$$

As the planet revolves at n' revolutions per minute

$$\phi/t = 2\pi n'/60 \quad \text{to give}$$

$$u = (\pi n'/30)(\Delta(2R - \Delta)(a + R - \Delta)/a)^{\frac{1}{2}} \text{ cm.s.}^{-1}$$

As before, in practice R = 2.22 cm and a = 2.00 cm

so that

$$u = 0.32\, n' \Delta^{\frac{1}{2}} (1 - 0.23\Delta)$$

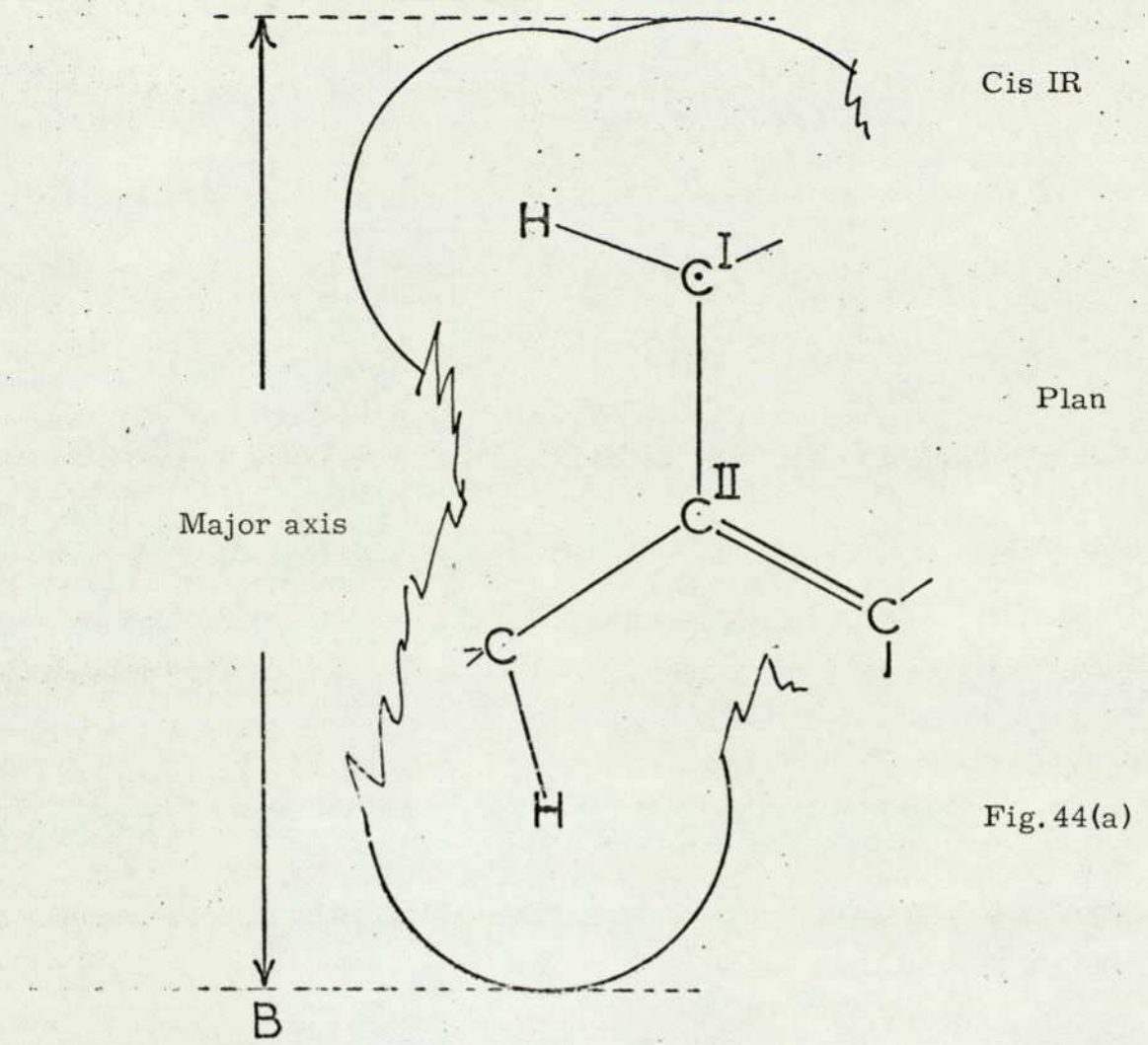

Fig. 44(a)

IIR (or PIB)

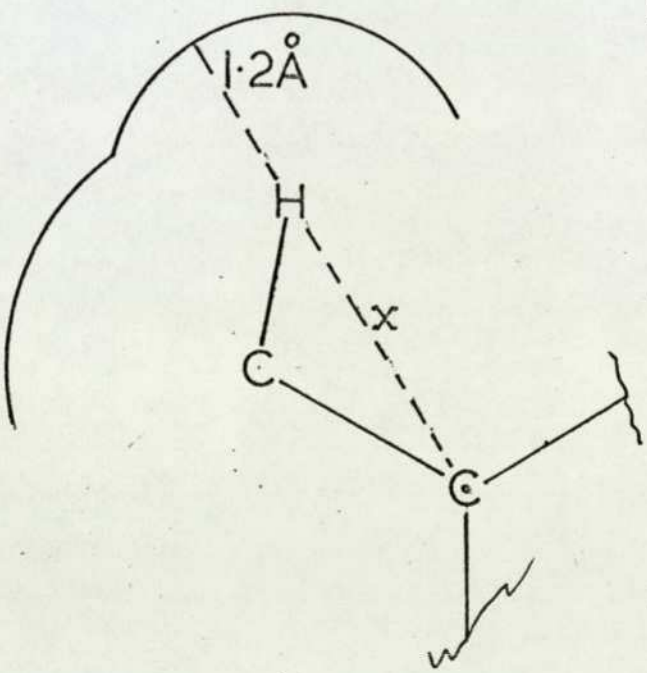

Fig. 44(b)

Figure 44 Typical conformations used to estimate chain cross-sectional areas A_o.

Appendix 4

Some details of the trigonometric estimations of chain cross-sections (A_o) for three typical cases

Natural rubber.

The most representative regular chain cross-section for NR, lying in the direction given by carbon atoms I and II in Figures 32 and 34(a), is shown in Figure 44(a) which is a suitable projection of Figure 32. The chain when viewed end-on resembles an ellipse of major axis AB, its minor axis being the mean distance across the methyl or methylene units (Figure 34(b)). Using the atomic dimension of Table 26:-

Major axis $= 1.65 + 1.544(1+\sin 30^\circ) + 1.085\sin(109.5^\circ - 30^\circ) + 1.2 = 6.23\text{Å}$

Minor axis $= 0.5((2.4 + 1.085(\cos 19.5^\circ + \cos 54.75^\circ \cos 35.25^\circ)) + 2(1.2 + 1.085\sin 54.75^\circ))$

$= 4.05\text{Å}$

$\therefore \quad A_o$ = area of ellipse $= 19.8\ (\text{Å})^2$

Cis BR

The best section is perpendicular to the axis of the double bonds. Then

major axis $= 2.4 + 1.085(\sin 60^\circ + \sin(109.5^\circ - 60^\circ)) + 1.544\sin 60^\circ = 5.50\text{Å}$

Best minor axis is given by $2(1.2 + 1.085\sin 54.75^\circ) = 4.17\text{Å}$

$\therefore \quad A_o = 18.03\ (\text{Å})^2$

IIR

The chain construction is cylindrical in form and well-packed, so that the cross-section is effectively circular. The most representative radius (Figure 44(b)) is given by $(1.2 + x)$ which is 3.36Å, as $x = 2.16\text{Å}$ by the Cosine Rule. $\therefore \quad A_o = 35.5\ (\text{Å})^2$.

Other A_o values (Table 31) were estimated similarly.

References

1. J. D. Ferry, Viscoelastic Properties of Polymers (John Wiley & Sons, New York, 2nd ed., 1970).
2. A. V. Tobolsky, Properties and Structure of Polymers (John Wiley & Sons, New York, 1960).
3. A. V. Tobolsky and J. R. McLoughlin, J. Polym. Sci. 8,543 (1952).
4. K. Schmieder and K. Wolf, Kolloid-Z. 134,149 (1953).
5. I. I. Zhukov and S. L. Talmud, Kolloid-Z. 1,5 (1935).
6. P. J. Counsell, Aspects of Adhesion 7 (Transcripta, London, Eds. Alner & Allen, 1973) page 202.
7. C. A. Dahlquist, Adhesives Age 2,25 (1959).
8. W.C.Wake, Adhesion (Oxford Univ.Press, Ed Eley, London, 1961) page 191.
9. W. C. Wake, Adhesion and the Formulation of Adhesives (Applied Science, London, 1976) esp. Chaps. 2-5 and 7.
10. F. H. Wetzel, Rubb. Age 82,291 (1957).
11. R. F. Bull, C. N. Martin and R. L. Vale, Adhesives Age 11(5) 20(1968).
12. C. A. Dahlquist, Adhesion: Fundamentals and Practice (Maclaren, London, Ed. Ministry Tech., 1969) page 143.
13. C. Marco, 13th Annual Conference on Adhesion and Adhesives, City University (1975).
14. R. Bates, Ph. D. Thesis, City University (1974).
15. R. Bates, J. Appl. Polym. Sci. 20,2941 (1976).
16. H. Green, Industrial Rheology and Rheological Structures (Wiley, New York, 1949).
17. N. Priklonskaya, Kauch. i. Rez. 5,49 (1937) or see ref. 19.
18. W. G. Forbes and L. A. Mcleod, Trans. Inst. Rubb. Ind. 34,154 (1958).
19. S. S. Voyutskii, Autohesion and Adhesion of High Polymers (trans S. Kaganoff) (Interscience, New York, 1963) esp. Chaps. I-III.
20. O. K. F. Bussemaker, Rubb. Chem. Tech. 37,1178 (1964).
21. J. D. Skewis, Rubb. Chem. Tech. 39,217 (1966).
22. D. Josefowitz and H. Mark, Ind. Rubb. World 106,33 (1942).
23. S. S. Voyutskii and Yu. L. Margolina, Rubb. Chem. Tech. 30,531 (1957).
24. S. S. Voyutskii, J. Adhesion 3,69 (1971).
25. R. M. Vasenin, Vys. Soed. 3,679 (1961). English Translation: RAPRA Translation 1010.
26. W. C. Wake, J. Inst. Rubb. Ind. 7,242 (1973).
27. F. Bueche, Physical Properties of Polymers (Interscience, New York, 1962).
28. R. F. Bauer, J. Polym. Sci. (A. 2) 10,541 (1972).

28a. R. F. Bauer, Dunlop Research Centre (North America) Internal Report.

29. D. O. Baumbach, J. Appl. Polym. Sci. 11,1755 (1967).
30. D. D. Eley, Adhesion (Oxford Univ. Press, Ed. Eley, London, 1961) Chap. 3.
31. G. J. Crocker, Rubb. Chem. Tech. 42,30 (1969).
32. R. Good, Aspects of Adhesion 7 (Transcripta, London, Eds. Alner & Allen, 1973) page 182.
33. W. A. Zisman, Contact Angle, Wettability and Adhesion (Ed. Gould, Publ. A. C. S., Washington, 1964) page 1.
34. L-H Lee, J. Polym. Sci. (A. 2) 5,1103 (1967).
35. L-H Lee, J. Appl. Polym. Sci. 12,719 (1968).
36. Brit. Patents 119,242; 119,241; 115,234; 147,960; (filed 1916 to 1918).
37. N. Tokita and I. Pliskin, Rubb. Chem. Tech. 46,1166 (1973).

38. H. Palmgren, Eur. Rubb. J. 156 (5) 30 (1974); 156 (6) 70 (1974).
39. E. S. Dizon, Rubb. Chem. Tech. 49, 12 (1976).
40. M. L. Studebaker and J. R. Beatty, Rubb. Age 108 (5) 21 (1976); 108 (6) 21 (1976).
41. G. R. Cotten, Rubb. Chem. Tech. 48, 548 (1975).
42. N. Tokita and J. L. White, J. Appl. Polym. Sci. 10, 1011 (1966).
43. A. S. Craig, Dictionary of Rubber Technology (Newnes-Butterworth, London, 1969) pages 26-28.
44. V. G. Raevskii, Yu. S. Maloshchuk, D. M. Treiger and S. S. Voyutskii, Sov. Rubber Tech. 25(2) 23 (1966).
45. S. S. Voyutskii and V. M. Zamazii, Rubb. Chem. Tech. 30, 544 (1957).
46. L. P. Stogova, V. G. Raevskii and S. S. Voyutskii, Sov. Rubb. Tech. 29 (11) 18 (1970).
47. K. Baranwal and J. R. Beatty, International Rubb. Conf., Paris, Sessions 3 and 4 (Adhesion of Flastomers) page 79 (1970).
48. T. E. Jermyn, Cabot Corp., Internal Report for Dunlop Co., (1968).
49. R. K. Beckwith, L. M. Welch, J. F. Nelson, A. L. Chaney and E. A. McCracken, Ind. and Eng. Chem. 41, 2247 (1949).
50. K. Baranwal, Rubber Age 102 (2) 52 (1970).
51. Yu. S. Maloshchuk, V. Ya. Kiselev and S. S. Voyutskii, Sov. Rubb. Tech. 30 (9) 12 (1971).
52. U. S. Patents 3,873,482 (1975) and 3,929,755 (1975).
53. U. S. Patent 3,880,807 (1975).
54. W. J. Mueller, B. Bennett, P. B. Stickney, N. J. Halbrook, W. H. Schuller and R. V. Lawrence, Rubb. Age 100 (6) 59 (1968); 101 (7) 43 (1969).
55. U. S. Patent 3,709,924 (1973) and Brit. Patent 1,279,868 (1972).
56. A. S. Burhans and A. C. Soldatos, Rubb. Age 92, 745 (1963); also U. S. Patent 1,271,830 (1972).
57. Th. Kempermann, DKG Sectional Spring Meeting, Cologne, W. Germany (June 1976).
58. L. E. Gwin and E. J. Weaver, ACS (Rubb. Div'n.), Minneapolis, USA (1976).
59. A. Giller, DKG Sectional Spring Meeting, Würzburg, W. Germany (May 1976).
60. e.g. F. M. Musser, Adhesives Age 19 (7) 38 (1976).
61. G. G. Hamilton and A. J. Simpson, Eur. Rubb. J. 154 (4) 25 (1972).
62. A. G. Belorossova, M. I. Farberov and V. G. Fpstein; English review in reference 19.
63. U. S. Patent 3,708,554 (1973).
64. K. C. Petersen and R. A. Martin, ACS (Rubb. Div'n.), Cleveland, USA (1968).
65. A. van Rossem and J. M. Vercruysse, ACS (Rubb. Div'n.), Cleveland, USA (1950).
66. U. S. Patent 3,647,759 (1972).
67. B. A. Dogadkin; English review in reference 19.
68. J. P. Davies, Dunlop Research Centre Internal Reports.
69. Brit. Patent 1,286,668 (1972).
70. Brit. Patent 1,321,151 (1973).
71. C. A. van Gunst, H. J. G. Paulen and E. Wolters, Adhesion 1 (Applied Science Publ., Ed. K. W. Allen, London, 1977) pages 85-106.
72. S. C. Nyburg, Brit. J. Appl. Phys. 5, 321 (1954); Acta Crystall. 7, 385 (1954).

73. L. A. Wood, Advances in Colloid Science, Vol. II (Interscience, New York, 1946) page 57.
73a. C. W. Bunn, Chemical Crystallography (Oxford University Press, London, 1945); Chem. in Brit. 11, 171 (1975).
74. P. J. Flory, J. Chem. Phys. 15, 397 (1947); 17, 223 (1949).
75. E. H. Andrews and A. N. Gent, The Chemistry and Physics of Rubber-like Substances (Maclaren & Sons, London, Ed. Bateman, 1963) Chap. 9.
76. M. Gordon, High Polymers, Structure and Physical Properties (Iliffe Books, London, 2nd ed., 1963) Chaps. 6-8.
77. W. Pechhold, 23rd IUPAC meeting, Boston, USA (1971): Macromolecular Preprint II, page 786.
78. N. Bekkedahl and L. A. Wood, Ind. Eng. Chem. 33, 381 (1941); J. Appl. Phys. 17, 362 (1946).
79. J. I. Cuneen, Rubb. Chem. Tech. 33, 445 (1960).
80. Y. Inukai, S. Minatono, T. Kageyama and H. Harima, Nipp. Gomu. Kyok. 49, 251 (1976).
81. P. Luijk and J. M. Rellage, Annual DKG meeting, Wiesbaden, W. Germany (1971).
82. E. J. Buckler, G. J. Briggs, J. F. Henderson and E. Lasis, Eur. Rubb. J. 159 (7/8) 21 (1977).
83. J. Hildebrand and R. Scott, The Solubility of Nonelectrolytes (Reinhold, New York, 3rd ed., 1949).
84. J. A. Brydson, Materials, page 107 (Dec. 1961).
85. M. C. Kirkham, Dunlop Research Centre, private communication and Dunlop Research Centre Internal reports.
86. W. S. Penn, Rubb. Age 25, 146 (1944).
87. A. Fick, Annln. Phys. 94, 59 (1855).
88. W. J. Moore, Physical Chemistry (Longmans, Green & Co., London, 3rd ed., 1957) page 449.
89. J. Crank and G. S. Park (Eds.), Diffusion in Polymers (Academic Press, London, 1968) Chap. 1.
90. J. Crank, The Mathematics of Diffusion (Oxford Clarendon Press, London, 1956) page 147.
91. R. M. Barrer, Nature, Lond. 140, 106 (1937).
92. W. W. Brandt, J. Phys. Chem. 63, 1080 (1959).
93. A. Aitken and R. M. Barrer, Trans. Farad. Soc. 51, 116 (1955).
94. R. M. Vasenin, Vys. Soed. 2, 851 (1960); 2, 857 (1960). English Translations: RAPRA Translations 1005 and 1006.
95. H. Eyring, J. Chem. Phys. 4, 283 (1936).
96. W. C. Wake, Trans. Farad. Soc. 43, 708 (1947).
97. R. M. Barrer, J. Phys. Chem. 61, 178 (1957).
98. H. L. Frisch, Polym. Letters 3, 13 (1965).
99. I. Auerbach, W. R. Miller, W. C. Kuryla and S. D. Gehman, J. Polym. Sci. 28, 129 (1958).
100. W. Kauzmann and H. Eyring, J. Am. Chem. Soc. 62, 3113 (1940).
101. S. F. Edwards, Cavendish Laboratory, Cambridge University. Private communication.
102. F. Bueche, W. M. Cashin and P. Debye, J. Chem. Phys. 20, 1956 (1952).
103. S. E. Bresler, G. M. Zakharov and S. V. Kirillov, Polym. Sci. USSR 3, 832 (1962).
104. J. E. Lewis and M. L. Deviney, Rubb. Chem. Tech. 40, 1570 (1967).

105. P. J. Corish and M. J. Palmer, IRI Conf:- Advances in Polymer Blends and Reinforcement, Loughborough Univ., (1969).
106. C. L. Rayner, L. Thomassen and L. I. Rouse, Trans. Am. Soc. Metals 30,313 (1942).
107. L. P. Morozova and N. A. Krotova, Kolloid-Z. 20,59 (1958).
108. S. S. Voyutskii and V. L. Vakula, Rubb. Chem. Tech. 37,1153 (1964).
109. T. Homma, N. Tagata and K. Hibino, JSR News Bulletin 6,1 (Aug. 1968).
110. G. J. van Amerongen, Rubb. Chem. Tech. 37,1065 (1964).
111. D. W. Saunders and L. R. G. Treloar, Trans. Inst. Rubb. Ind. 24,92 (1948).
112. J. L. White and N. Tokita, J. Appl. Polym. Sci. 9,1929 (1965).
113. A. Baszkin, M. Nishino and L. Ter-Minassian-Saraga, Adhesion 1 (Applied Science Publ., Ed. K. W. Allen, London, 1977) pages 181-206.
114. Y. Lipatov, Adhesion 2 (Applied Science Publ., Ed. K. W. Allen, London, 1978 (in press)) pages 197-218.
115. J. N. Anand, H. J. Karam, R. Z. Balwinski and L. Dipzinski, J. Adhesion 1, 16,24 and 31 (1969); 2,16 (1970).
116. R. J. Morgan and L. R. G. Treloar, J. Polym. Sci. (A. 2) 10,51 (1972).
117. R. J. Kokes and F. A. Long, J. Am. Chem. Soc. 75,6142 (1953).
118. B. G. Corman, M. L. Deviney and L. E. Whittington, Rubb. Chem. Tech. 43,1349 (1970).
119. R. N. Haward, J. Macromol. Sci.-Revs. Macromol. Chem. C4(2), 191 (1970).
120. A. Bondi, J. Phys. Chem. 58,929 (1954).
121. R. Simha and R. F. Boyer, J. Chem. Phys. 37, 1003 (1962).
121a. R. Simha and R. F. Boyer, J. Polym. Sci. (Letters) 11,33 (1973).
122. M. L. Williams, R. F. Landel and J. D. Ferry, J. Am. Chem. Soc. 77,3701 (1955).
123. M. L. Williams, J. Phys. Chem. 59,95 (1955).
124. C. A. Kumins and T. K. Kwei, Diffusion in Polymers (Academic Press, Eds. Crank and Park, London, 1968) Chap. 4.
125. G. Allen, G. Gee and G. J. Wilson, Polymer, Lond. 1, 456 (1960).
126. G. Allen, G. Gee, D. Mangaraj, D. Sims and G. J. Wilson, Polymer, Lond. 1, 467 (1960).
127. P. A. Meyer and J. L. Rose, J. Adhesion 8, 107 (1976).
128. R. W. Griffiths and M. Jones, Trans. Inst. Rubb. Ind. 4, 235 (1928).
129. A. N. Gent and G. R. Hamed, J. Adhesion 7,91 (1975).
130. O. K. F. Bussemaker and W. V. C. van Beek, Rubb. Chem. Tech. 37,28 (1964).
131. W. F. Busse, J. M. Lambert and R. B. Verdery, J. Appl. Phys. 17,376 (1946).
132. F. W. J. Beaven, P. G. Croft-White, P. J. Garner and G. Rooney, Proc. 2nd Rubb. Tech. Conf., London, 224 (1948).
133. B. A. Pickup, Trans. Inst. Rubb. Ind. 33,58 (1957).
134. J. D. Skewis, Rubb. Chem. Tech. 38,689 (1965).
135. E. Schmitt, J. Rubb. Res. 17,195 (1948).
136. W. Breuers and H. Luttropp, Buna Herstellung-Prüfung Eigenschaften, VEB Verlag Technik, East Berlin (1954) page 174.
137. Pressure-Sensitive Tape Council test - 18.
138. E. B. Toon, F. S. Springer et al, Dunlop Research Centre; private communication.
139. I. C. Cheetham, Trans. Inst. Rubb. Ind. 40(4) T 156 (1965).
140. A. C. Hiron and F. S. Springer, Dunlop Research Centre; private communication.

141. K. A. Brownlee, Industrial Experimentation (H. M. Stationery Office, London, 4th ed., 1949) page 33.
142. J. Brandrup and E. H. Immergut (Eds.), Polymer Handbook (Interscience, New York, 1966) page IV-30.
143. ASTM Standards Designation D412-75.
144. R. W. Lenz, Organic Chemistry of Synthetic High Polymers (Interscience, New York, 1967) Chap. 12.
145. N. Grassie, Chemistry of High Polymer Degradation Processes (Butterworths Sci. Publ'ns., London, 1956) page 208.
146. A. S. Michaels and H. J. Bixler, J. Polym. Sci. 50,413 (1961).
147. L. Pauling, The Nature of the Chemical Bond (Cornell Univ. Press, New York, 3rd ed., 6th imp., 1967).
148. N. Bekkedahl, Rubb. Chem. Tech. 8, 5 (1935).
149. G. M. Bartenev and M. V. Voevodskaya, Sov. Rubb. Tech. 25(3) 20 (1966).
150. Elastomer prepared and T_G measured (dilatometer, DSC) at Dunlop Research Centre.
151. P. B. Weisz and V. J. Frilette, J. Phys. Chem. 64,382 (1960).
152. K. H. Nelson, M. D. Grimes and B. J. Heinrich, Anal. Chem. 29, 1026 (1957).
153. Union Carbide Molecular Sieves for Selective Adsorption, BDH Chemicals Information Booklet, 3rd ed., 3rd imp. (rev.), page 14.
154. J. R. Martin and J. K. Gillham, ACS Polym. Preprints, 12,554 (Sept. 1971).
155. C. Allen, D. Sims and G. J. Wilson, Polym. Lond. 2,375 (1961).
156. B. G. Corman, M. L. Deviney and L. E. Whittington, Rubb. Chem. Tech. 45,278 (1972).
157. S. P. Chen and J. D. Ferry, Macromolecules 1, 270 (1968).
158. G. J. van Amerongen, J. Polym. Sci. 5, 307 (1950).
159. H. K. Frensdorff, J. Polym. Sci. (A) 2,341 (1964).
160. C-P. Wong, J. L. Schrag and J. D. Ferry, J. Polym. Sci. (A. 2) 8,991 (1970).
161. P. I. Wilson, Dunlop Research Centre Internal Reports and private communication.
162. P. H. Williams, The Science of Rubber (Publ. for Dunlop Ltd. 1975).
163. P. J. Corish, Dunlop Research Centre, private communication; also, with B. D. W. Powell, Rubb. Chem. Tech. 47,481 (1974).